TAMPEREEN TEKNILLINEN YLIOPISTO
TAMPERE UNIVERSITY OF TECHNOLOGY

Ontrei Raipala

Novel Methods for Loss of Mains Protection

Julkaisu 1535 • Publication 1535

Tampere 2018

Tampereen teknillinen yliopisto. Julkaisu 1535
Tampere University of Technology. Publication 1535

Ontrei Raipala

Novel Methods for Loss of Mains Protection

Thesis for the degree of Doctor of Science in Technology to be presented with due permission for public examination and criticism in Tietotalo Building, Auditorium TB104, at Tampere University of Technology, on the 16th of March 2018, at 12 noon.

Tampereen teknillinen yliopisto - Tampere University of Technology
Tampere 2018

Doctoral candidate: Ontrei Raipala
Laboratory of Electrical Energy Engineering
Faculty of Computing and Electrical Engineering
Tampere University of Technology
Finland

Supervisor: Sami Repo, Professor
Laboratory of Electrical Energy Engineering
Faculty of Computing and Electrical Engineering
Tampere University of Technology
Finland

Instructors: Sami Repo, Professor
Laboratory of Electrical Energy Engineering
Faculty of Computing and Electrical Engineering
Tampere University of Technology
Finland

Pertti Järventausta, Professor
Laboratory of Electrical Energy Engineering
Faculty of Computing and Electrical Engineering
Tampere University of Technology
Finland

Pre-examiners: Kimmo Kauhaniemi, Professor
Department of Electrical Engineering and Energy Technology
University of Vaasa
Finland

Hjörtur Jóhansson, Senior Scientific Consultant
Department of Electrical Engineering
Technical University of Denmark
Denmark

Opponents: Kimmo Kauhaniemi, Professor
Department of Electrical Engineering and Energy Technology
University of Vaasa
Finland

Seppo Hänninen, Senior Scientist
VTT Technical Research Centre of Finland LTD
Finland

ISBN 978-952-15-4104-9 (printed)
ISBN 978-952-15-4113-1 (PDF)
ISSN 1459-2045

Abstract

Small-scale generation connected to distribution networks has increased significantly in recent years. This trend is driven by developments in distributed generation (DG) technologies, environmental concerns and economic reasons. The diffusion of generation into the distribution network level has many potential benefits, but it also raises challenges, such as unintentional islanding, which is hazardous to the safety of both personnel and equipment. Due to the safety risks, all DG units need to be equipped with a loss of mains (LOM) protection scheme capable of rapidly detecting and stopping islanding. LOM protection methods can be divided into passive, active and communication-based methods. Passive methods rely on detecting islanding by monitoring chosen system quantities. These methods are affordable and applicable to all types of DG units, but their performance is highly dependent on the local power imbalances between the production and consumption in the islanded zone. Most, if not all, passive methods, fail to detect islanding if the local production closely matches the local consumption. The set of power imbalance combinations that lead to non-detected islanding is referred to as the non-detection zone (NDZ). Active methods are based on deliberately injecting small perturbations to the grid and monitoring the response of the system. These methods generally have smaller NDZ than passive methods. However, this comes at the cost of degraded power quality. Communication-based methods rely on other means than the local monitoring of system quantities, which makes them immune to the NDZ problem. However, these methods tend to be costly.

The performance of passive and active methods can be improved by applying more sensitive LOM protection settings. However, if the LOM protection settings are too sensitive, voltage dips caused by faults in the transmission grid may result in a cascading disconnection of DG. In order to avoid such risks, which threaten the system's stability, many grid codes include fault-ride-through (FRT) requirements, which specify the depth and duration of voltage dips which DG units need to be able to withstand. FRT requirements often also require the DG units to feed reactive current to the grid during the voltage dip in order to support the system voltages. The work conducted for this thesis indicates that FRT requirements significantly degrade the performance of LOM protection. This thesis also studies how the type of the protected DG unit affects LOM protection. The frequency of an islanded circuit sustained by a directly-coupled synchronous generator is determined by the local active power imbalance, whereas the frequency of an islanded circuit sustained by a converter-coupled DG unit is determined by the local reactive power imbalance. However, when there are both directly-coupled synchronous generators and converter-coupled DG units in an islanded circuit, the synchronous generator seems to dominate these relationships. This has significant implications on the performance of active LOM protection schemes.

One of the main issues distribution system operators face when they are evaluating the adequacy of LOM protection for DG installations is the lack of suitable analysis tools. This thesis proposes

a novel LOM risk management procedure which utilizes the existing analysis tools embedded in a modern network information system (NIS). This NIS-based procedure analyzes what kind of power imbalance combinations are possible in the studied network sections. Based on the possible combinations of power imbalances and predefined NDZ mappings of optional LOM protection schemes, the procedure tells protection engineers if there are any risks of non-detected islanding in the analyzed network sections and proposes which LOM protection schemes would be most suitable for each DG installation. Although the proposed LOM risk management tool is presented at the concept level only here, it is clearly a promising area for future research.

Two active LOM protection methods and one communication-based protection automation concept were also developed during this thesis work. The first of the active LOM protection methods is based on forcing the frequency of an islanded circuit out of the utilized frequency thresholds by constant injection of reactive power pulses and a dedicated reactive power versus frequency droop. The knowledge gained during the development of this method resulted in a second, significantly more advanced, active LOM protection scheme. This is based on forcing the rate-of-change-of-frequency of an islanded circuit to a desired value by applying a dedicated reactive power versus frequency droop. This method is able to detect islanding rapidly and reliably even if the local power imbalances are negligible. Moreover, this can be achieved with a very modest injection of reactive power. The communication-based protection automation concept is designed to solve typical DG related protection challenges and to automatically change the feeding path of the protected DG unit in case if the original feeding route becomes faulted. However, the successfulness of the automatic feeding path changing depends on many factors such as DG unit type, network parameters and the momentary input power provided by the primary energy source.

The methods developed in this thesis have slightly different purposes. The proposed NIS-based LOM risk assessment procedure is useful for evaluating the adequacy of existing LOM protection as well as for choosing optimal LOM protection schemes for new DG installations. If the LOM risk assessment procedure indicates that the local power imbalances will always be very large, then passive LOM protection schemes are a sensible choice. However, should the LOM risk assessment procedure reveal that the local power imbalances could be so small that reliable LOM protection cannot be ensured with passive LOM protection schemes, then active or communication-based LOM protection schemes are preferable. Active LOM protection schemes are suitable if the ratio of converter-coupled to directly-coupled generator capacity in the analyzed zone is large. This is because certain active LOM schemes, such as the one proposed in this thesis, are able to detect islanding reliably and rapidly even if the local active- and reactive power imbalances would be negligible, provided that the ratio between converter coupled to directly coupled synchronous generator capacity is large. However, if a significant proportion of the generation capacity in the analyzed network section is synchronous generator based, then sensitive and rapid LOM protection cannot always be guaranteed. In such cases, it is advisable to utilize advanced communication-based LOM protection schemes which are immune to the NDZ problem.

Preface

The thesis work was done at the department of Electrical Engineering at Tampere University of Technology (TUT) during the years 2010-2017. The work was primarily funded by TUT. The extra funding provided by the scholarships from the Fortum foundation, Ulla Tuominen Foundation and KAUTE foundation is greatly appreciated.

Firstly, I would like to express my sincere gratitude to my supervisors, Prof. Sami Repo and Prof. Pertti Järventausta for their guidance and insightful comments throughout my thesis work, as well as for providing me an inspiring workplace. I am also grateful to the preliminary examiners of this thesis, Prof. Kimmo Kauhaniemi from the University of Vaasa and Dr. Hjörtur Jóhansson from the Technical University of Denmark, for their constructive comments.

I want to thank all my colleagues at the department of Electrical Engineering for the great working atmosphere. I especially want to thank Dr. Anssi Mäkinen for his valuable help during the research work, for friendship and for all the fun that we had along this journey. I also want to thank Dr. Kari Mäki for helping me in the beginning of my thesis process with all his valuable advices, and Dr. Ari Nikander, for the interesting discussions and collaboration in many projects. Special thanks also go to Dr. Anna Kulmala, Mr. Bashir Siddiqui, Ms. Heidi Krohns-Välimäki and Mr. Peyman Jafary for good collaboration and for all the enjoyable moments that we had during this time. I am also grateful to Ms. Terhi Salminen, Ms. Mirva Seppänen, Ms. Nitta Laitinen and Ms. Merja Teimonen for their valuable assistance in practical matters.

I also want to thank Mr. Kai Hiitelä from ABB for helping me in configuring IEDs used in the studies, and Mr. Adrian Benfield, for proofreading my thesis.

I consider myself very fortunate to have so many good friends. A big thank you to you all. I also want to express my sincere gratitude to my girlfriend Enni for always cheering me up. Finally, I am deeply grateful to my parents, Mirja and Markku, and to my sister Iiris, for all the support and caring throughout my life.

Tampere 15.1.2018

Ontrei Raipala

Contents

LIST OF PUBLICATIONS

This thesis is based on the following publications:

[P1] O. Raipala, S. Repo, K. Mäki and P. Järventausta, "Studying the effects of distributed generation on autoreclosing", *in Proc. 9th Nordic Electricity Distribution and Asset Management Conference (NORDAC)*, Aalborg, Denmark, September 2010

[P2] O. Raipala, A. S. Mäkinen, S. Repo and P. Järventausta, "The effect of different control modes and mixed types of DG on the non-detection zones of islanding detection", *in Proc. International Conference on Electricity Distribution (CIRED) Workshop 2012*, Lisbon, Portugal, May 2012

[P3] O. Raipala, A. S. Mäkinen, S. Repo and P. Järventausta, "Interaction of fault ride through requirements and loss of mains protection", *in Proc. International Conference on Renewable Energies and Power Quality (ICREPQ'13)*, Bilbao, Spain, March 2013

[P4] O. Raipala, S. Repo and P. Järventausta, "Network information system based loss of mains risk management", *in Proc. 22nd International Conference on Electricity Distribution (CIRED)*, Stockholm, Sweden, June 2013

[P5] O. Raipala, A. S. Mäkinen, S. Repo and P. Järventausta, "A novel anti-islanding method based on the combination of a Q-f droop and RPV", *in Proc. 5th IEEE PES Innovative Smart Grid Technologies Conference (ISGT) Europe*, Istanbul, Turkey, October 2014

[P6] O. Raipala, S. Repo and P. Järventausta, "A communication based protection system for solving DG related protection challenges", *in Proc. 23rd International Conference on Electricity Distribution (CIRED)*, Lyon, France, June 2015

[P7] O. Raipala, A. S. Mäkinen, S. Repo and P. Järventausta, "Performance analysis of Q-f droop anti-islanding protection in the presence of mixed types of DG", *in Proc. 2015 IEEE Innovative Smart Grid Technologies Conference (ISGT) Asia*, Bangkok, Thailand, November 2015

[P8] O. Raipala, A. S. Mäkinen, S. Repo and P. Järventausta, "An anti-islanding protection method based on reactive power injection and ROCOF" *IEEE Trans. Power Delivery*, vol. 32, pp. 401-410, February 2017

LIST OF ABBREVIATIONS

AFD	Active frequency drift
AIP	Anti-islanding protection
APS	Automatic phase shift
DG	Distributed generation
DMS	Distribution management system
DSO	Distribution system operator
ENTSO-E	European network of transmission system operators for electricity
FRT	Fault ride through
GOOSE	Generic object oriented substation event
IED	Intelligent electronic device
LOM	Loss of mains
LVRT	Low voltage ride through
LV	Low voltage
MV	Medium voltage
NDZ	Non-detection zone
NIS	Network information system
OFP	Overfrequency protection
OVP	Overvoltage protection
PCC	Point of common coupling
P-f droop	Active power versus frequency droop
PLC	Power line carrier
pu	Per unit
Q-V droop	Reactive power versus frequency droop
RfG	Requirements for generators
ROCOF	Rate of change of frequency
ROCOP	Rate of change of power
ROCOV	Rate of change of voltage
Q-f droop	Reactive power versus frequency droop
RTDS	Real time digital simulator
SCADA	Supervisory control and data acquisition
THD	Total harmonic distortion
TSO	Transmission system operator
UCTE	Union for the Coordination of the Transmission of electricity
UFP	Underfrequency protection
UVP	Undervoltage protection

LIST OF SYMBOLS

C	Capacitance
cf	Chopping fraction
cf_0	Chopping fraction when no frequency error exists
f	Frequency
f_{CCP}	frequency at the connection point of the DG unit
f_{Grid}	frequency of the main power grid
f_m	The frequency at which the maximum phase shift Θ_m occurs
f_{nom}	Nominal frequency
f_r	Resonant frequency
$f_{tar,high}$	Higher frequency checking criterion threshold
$f_{tar,low}$	Lower frequency checking criterion threshold
G	Nominal power of the generator
H	Inertia constant
K	Gain
L	Inductance
P_e	Electrical power output of the generator
P_{INV}	Real power fed by the inverter
P_{Load}	Real power consumption of the load
P_m	Mechanical power input to the generator
Q_C	Capacitive reactive power
Q_f	Quality factor
Q_{INV}	Reactive power fed by the inverter
Q_L	Inductive reactive power
Q_{Load}	Reactive power consumption of the load
R	Resistance
T_{Vutil}	Period of the main grid voltage
t_z	The period during which the current fed by the inverter equals to zero
V	Line-to-line voltage
δ	rotor angular displacement from the synchronously rotating reference
Θ	Phase shift between voltage and output current
Θ_m	Maximum phase shift between voltage and output current

1 Introduction

Carbon dioxide emissions, city-smog and other types of environmental pollution are driving the energy sector towards more eco-friendly methods of energy production. This change is also driven by concerns over the dwindling reserves of fossil fuels, internationally ratified agreements such as the Kyoto Protocol, government policies such as the EU 2030 climate and energy framework [1]. Although such initiatives have similar aims, they differ somewhat in terms of their specific objectives. The Kyoto Protocol aims to reduce greenhouse gas emissions to a defined level, whereas, the EU-2030 framework has specific and binding aims for all its member states which are based on their current levels of greenhouse gas emissions. For instance, EU 2030 aims to reduce greenhouse gas emissions in the EU member states by 40 % from their 1990 levels, to increase the proportion of renewable energy to at least to 27% of total energy consumption, and to improve energy efficiency by 27 % by 2030 [1], [2]. In order to accelerate change, many countries have introduced a range of subsidies for power production based on renewable energy sources. These subsidies have led to the rapid growth of such power generating modules, for instance, wind and solar power generators. The surge in demand for these types of generating units has led to significant advances in renewable energy-based technologies and reductions in cost, which is in turn leads to increased demand.

Whereas large, conventional power plants are connected to the grid at the transmission network level, many of the renewable energy-based generating units are relatively small and are connected to the grid at the distribution network level, as this is more cost-effective. Another reason for the growth in distributed generation (DG) is that renewable energy-based generating units are often situated in rural areas, where the only feasible way of connection to the grid is via a distribution network. [3] Thus, significant numbers of small-scale power generating units are now being connected to distribution networks, which have traditionally handled very little, if any, generation capacity. Nevertheless, it should be noted that DG is not limited to renewable energy-based generating units but covers all types of small-scale generation connected to distribution networks.

This rapid growth of DG has precipitated significant changes in electric power systems. Traditionally, electric power was produced in large power plants which fed power through the transmission grids to distribution networks which delivered the power to the end users. Thus, the power flows and currents have been unidirectional in radial distribution networks. This has enabled simple voltage control and protection principles in distribution networks. However, when DG units are added to distribution networks, it can no longer be assumed that power flows and currents are unidirectional [3]. The addition of DG units brings many potential benefits to the operation of distribution

networks but it also introduces a number of challenges, such as problems with the protection systems, voltage management and increased fault levels [3]-[5].

1.1 The protection impacts of DG

The traditional way of establishing feeder protection in radial distribution networks is to use non-directional overcurrent relays for feeder protection [6]. This is sufficient as long as the protected feeders do not include generation, that is, if the fault currents are always unidirectional. In isolated neutral and neutral compensated networks, suitable earth fault protection schemes are also needed for reliable feeder protection [7]. However, when the feeders contain DG, the assumption of unidirectional power flow is no longer valid, and this may render non-directional overcurrent protection insufficient. This is because DG units contribute to fault currents and can thereby disturb the operation of overcurrent protection [8], [9]. Firstly, DG units can back-feed fault currents via the substation bus to faults located on adjacent feeders. This can cause unwanted tripping of the feeder overcurrent relay protecting the non-faulted feeder where the DG is situated [3], [9]. Another problem for feeder overcurrent protection caused by DG is referred to as protection blinding, or protection under-reach [10], [8], [9]. This refers to a case where a DG unit connected to a faulted feeder contributes to the fault current and thereby reduces the fault current seen by the feeder overcurrent relay. Depending on the type, the nominal rating and the location of the DG unit, as well as on the impedances between the DG unit, the fault location and the main source, the fault current seen by the feeder overcurrent protection relay may be reduced so that it does not operate when it should [8], [9]. Feeder earth fault protection is typically not affected by DG units because the zero sequence network has a discontinuity point at the MV/LV delta-wye step-up transformers, which are typically used for connecting DG units to distribution network [11], [12]. This, however, also means that earth faults occurring on the MV side of distribution networks cannot be detected from the LV side of the delta-wye transformer [10], [12].

DG units can also interfere with the functioning of fast automatic reclosing [10]. Fast automatic reclosing is based on removing temporary faults by de-energizing the faulted line for a short period, which is typically in the range of few hundreds of milliseconds to couple of seconds. If DG is connected to the line where automatic reclosing is performed, it may sustain the fault arc during the period when the line is meant to be de-energized and thereby prevent the successful operation of automatic reclosing. Such a situation may also lead to unsynchronized reclosing if the frequency in the isolated feeder drifts too much from the frequency of the main utility grid during the open time of the automatic reclosing. Unsynchronized reclosing may cause dangerous stresses to the DG units and may damage network components. For these reasons, there should always be a protection scheme that disconnects DG units quickly whenever DG units become isolated from the main utility grid. A situation where a DG unit becomes isolated from the main utility grid is referred to as

islanding or loss of mains (LOM). The protection scheme that is meant to avoid unintentional islanding is referred to as loss of mains protection or anti-islanding protection (AIP). Unintentional islanding may also be a safety hazard for utility field personnel, as it can energize lines that are meant to be de-energized. Moreover, customer devices may also be damaged due to poor power quality in the islanded network section. For these reasons, it is important that LOM protection should always rapidly detect islanding and disconnect the islanded DG units.

The unsynchronized reclosing problems caused by DG can be mitigated by using synchronism check relays. Synchronism-check protection monitors voltages on both sides of a circuit breaker and prevents reclosing if the frequencies, voltage magnitudes and phase angles are not aligned properly. Another option for avoiding the risk of unsynchronized reclosing is to follow the approach applied in France, where medium voltage overhead line feeders are typically equipped with voltage presence detectors [13]. However, the presence of DG units may hinder the reclosing function on such feeders by sustaining the voltage. Both of these approaches can successfully be used for avoiding unsynchronized reclosing, but this comes at the cost of degraded reliability of supply. This is because the majority of faults can be removed with the help of automatic reclosing [10]. It would therefore be very beneficial if LOM protection relays were able to disconnect DG units rapidly enough to enable the use of fast automatic reclosing.

1.2 Loss of mains protection

Unlike intentional islanding, which can be used to enhance the reliability of electricity supply, unintentional islanding is strictly prohibited because of the associated safety concerns. Therefore, all DG units have to be equipped with some type of anti-islanding protection scheme which detects islanding and trips the islanded DG unit. The LOM detection time requirement depends on the applied standard. According to the IEEE 1547 and UL 1741 standards, islanding should be detected and ceased within 2 seconds [14], [15]. According to the German standard VDE-AR-N 4105, DG units whose rating is up to 100 kVA and are connected to a low voltage network, must detect and cease to feed islanded circuits within 5 s [16]. However, considerably faster detection of islanding may be required if fast automatic reclosing is utilized on feeders having DG. In fact, in Japan, islanding has to be detected within 0.2 s [17]. However, unlike many other grid codes, the Japanese LOM protection test requirement does not mandate the use of a specific quality factor of the utilized parallel RLC test load [17]. The quality factor of the utilized parallel RLC test load has a significant impact on the performance of the LOM protection of DG units coupled via an inverter. This matter is discussed in more detail in chapter 2.5.

Most LOM protection schemes are based on detecting changes in chosen system quantities, such as voltage magnitude or frequency, which usually occur when a network section becomes islanded. These changes are mainly caused by the imbalance between production and consumption of real- and reactive power in the islanded circuit. There is, however, a risk that these imbalances are too small to make the monitored quantities drift outside of the predefined protection thresholds completely, or within the time specified in the regulations. In cases like this, LOM protection fails to detect islanding. This blind area in the active- and reactive power coordinate system is referred to as non-detection zone (NDZ).

Islanding can be detected with either local or remote methods. Remote methods are based on monitoring the status of the upstream circuit breakers that connect a network section with DG to the main grid. Whenever any of the monitored circuit breakers are opened, a disconnect signal is sent to all downstream DG units. These methods can provide rapid and reliable LOM protection provided that a suitable communication medium is utilized. However, the costs of implementing communication-based LOM protection schemes are typically rather high, which makes these methods unsuitable for small DG installations. Moreover, a LOM protection scheme based on local measurements is always required as a backup protection in case of failure in the communication link.

Local methods are further divided into passive and active LOM protection schemes. Passive LOM protection schemes are based on monitoring chosen system quantities, such as voltage magnitude, frequency, rate of change of frequency, etc. Passive methods are typically simple and applicable to all types of DG units. However, passive methods typically suffer from a relatively large NDZ. Active methods are based on detecting islanding based on the deliberate injection of small disturbances and monitoring the response of the system. With proper settings, some of the active LOM protection schemes are able to detect islanding even if the local power imbalance is negligible [18], [19]. The downside of these methods is that the injected disturbances may sometimes cause power quality problems. Another issue is that if these methods are implemented on a large scale, the injected perturbations may cancel each other out unless all the injections are synchronized. Moreover, if the injected perturbations are synchronized, the power quality problems are further amplified [20]. It is also important to bear in mind that most active LOM schemes are designed for inverter-coupled DG units. In fact, the presence of synchronous generators may degrade the performance of active LOM protection schemes [P2], [P7].

When the proportion of DG was still insignificant, distribution system operators (DSOs) preferred to use relatively sensitive LOM protection settings, as their main objective was to avoid unintentional islanding. Sensitive LOM protection settings help in avoiding the risks related to failed reclosings caused by DG. In addition, out-of-phase reclosings can cause dangerous stresses to DG units, which also favored sensitive LOM protection from the DG unit owner's point of view. However, using such sensitive LOM protection thresholds tends to cause nuisance tripping, e.g. during

voltage dips caused by remote faults. This did not use to be a major issue because the proportion of DG was insignificant from the perspective of power system stability. [21] However, as the proportion of DG already accounts for a significant percentage of the electric power generation capacity in some regions, TSOs have realized that too sensitive LOM protection settings can pose a risk to power system stability [22]. This is because faults in the transmission network can trigger huge amounts of adverse tripping of DG, as was, witnessed during the UCTE disturbance on the 4th of November 2006 [23].

In order to avoid such threats to system stability, TSOs have issued so-called fault ride through (FRT) requirements in their grid codes. These define how long generating units have to be able to stay connected and support the system stability during various kinds of disturbances. Consequently, DG units not only need to be able to ride through faults without losing their stability, but the LOM protection also has to be set to allow the FRT. In practice, this means that the undervoltage protection has to be in line with the low-voltage-ride-through (LVRT) requirements, which naturally degrades the performance of LOM protection. Some grid codes also require DG units to support the system voltages by feeding reactive current to the grid during the LVRT. This also has an effect on the performance of the LOM protection [P3].

1.3 The motivation and objectives of this thesis

The studies conducted have been motivated by the following key points:

- Unintentional islanding is a serious safety concern as it can endanger the lives of utility field personnel, cause damage to customer loads, and cause damage to both DG units and other network components due to out-of-phase reclosing.
- The LOM protection methods now widely in use have been reported to fail to detect islanding when the power imbalance between the islanded production and consumption is too small. Communication-based LOM protection schemes that are not susceptible to the NDZ problem do exist, but they tend to be too costly for small DG installations. Further development is thus needed.
- A Considerable amount of DG is now being connected, and consequently the risk of non-detected islanding is increasing all the time.
- Network utilities may not have comprehensive knowledge and tools for evaluating the possible risk of non-detected islanding in their networks.

- The requirements concerning the participation of DG in the ancillary services supporting power system stability have evolved. These requirements have impacts on the performance of LOM protection.
- DG technologies have evolved. In the past, the majority of generating units were directly-coupled induction or synchronous generators, whereas nowadays, the focus has shifted to converter coupled DG units. The converter can act as a suitable tool for implementing the desired perturbations utilized in active LOM protection methods, which enables new possibilities for LOM protection. On the other hand, the presence of different DG technologies in an islanded circuit can sometimes complicate the detection of islanding.

Thus, it is clear that unintentional islanding is a real safety risk and that there is a pressing need to further develop the existing LOM protection methods. The objectives of this thesis can be summarized as follows:

- Analyze the limitations of the most widely utilized LOM protection methods. That is, what kind of situations may lead to the failure of LOM protection.
- Analyze how low-voltage-ride-through and reactive current support functions affect the functioning of LOM protection.
- Help network utilities to understand the LOM risk better and, if possible, to develop analysis and design methods for evaluating the possibility of the risk of non-detected LOM.
- Develop new methods and schemes for establishing reliable and rapid LOM protection.

The developments in DG technologies have begun to shift the focus from directly-coupled generators to converter-coupled generating units. However, due to the long life cycle of generating units, the directly-coupled generators are still present. Irrespective of the types of DG units present in each part of the network, LOM protection should always detect the occurrence of islanding reliably and within the specified time. Studies, which analyze the performance of typical passive LOM protection in circuits, which are sustained either by a directly-coupled synchronous generator or a converter-coupled DG unit, can be found from the literature [24], [25]. However, the literature does not present cases where an islanded circuit contains both directly-coupled synchronous generators and converter-coupled DG. This thesis aims to fill this gap by studying how such a scenario differs from the cases where the islanded circuit is sustained only by one type of DG unit. Additionally, this thesis analyzes whether the possible differences have any consequences that protection engineers should take into account.

As DG has begun to replace conventional bulk power generation, it is evident that, in order to guarantee the stability of power systems, DG units need to provide the kind of ancillary services that have been provided the bulk power generating plants. LVRT requirements are a good example

of such ancillary services. It can be intuitively understood that the introduction of LVRT requirements complicates the functioning of LOM protection. However, at the time of writing this thesis, studies which analyze exactly how LVRT requirements affect LOM protection are completely lacking at least to the best knowledge of the author. Thus, this thesis aims to answer how significant an impact the introduction of LVRT requirements has on voltage and frequency monitoring-based LOM protection. Additionally, this thesis aims to analyze whether the reactive power support requirement has an impact on the functioning of conventional passive LOM protection.

Regarding the facilitation of LOM risk assessment for DSOs, the research question is to find out how DSOs can be aided in analyzing and understanding what kind of non-detected LOM risks exist in the network under their supervision. Additionally, it tries to see if there is a way to automate the non-detected LOM risk analysis, and whether it is possible to integrate such methods into the information systems utilized by DSOs. To the author's best knowledge, there are no such automated tools at present.

Many LOM protection methods have been proposed in the literature over the recent years. This thesis reviews LOM protection methods proposed in the literature, aims to identify their deficiencies and tries to determine whether some of these methods could be further developed, and if so, how this could be done.

1.4 Publications and evolution of the research work

This thesis includes eight publications. The research work began by analyzing how the typically applied minimum requirement for LOM protection actually fulfills the targets set for LOM protection [P1]. The research then continued by analyzing how having both directly-coupled synchronous generator based DG and converter-coupled DG in the islanded circuit complicates the detection of islanding [P2]. After this, the studies focused on analyzing how the effect of the grid supporting functions, namely low-voltage-ride-through and reactive current support, affect the performance of LOM protection [P3]. These studies led to a new idea, i.e. a network information system based LOM risk management tool. This tool was designed at the concept level and its principles are presented in [P4]. The research went on by developing a communication based protection automation concept for tackling DG related protection challenges [P5]. After this, the research focused on active LOM protection methods. The first active LOM protection method developed for this thesis is presented in [P6]. With the knowledge accumulated on active LOM protection methods, the research begun in [P2], which dealt with multiple types of DG in the same islanded circuit, was con-

tinued. However, this time the converter-coupled DG unit was equipped with an active LOM protection method, that is, Q-f droop based LOM protection. The results of this work are presented in [P7]. The research work on active LOM protection methods then finally resulted in the development of a considerably more sophisticated LOM protection scheme, which is presented in [P8]. Fig. 1.1 illustrates the focus of the publications.

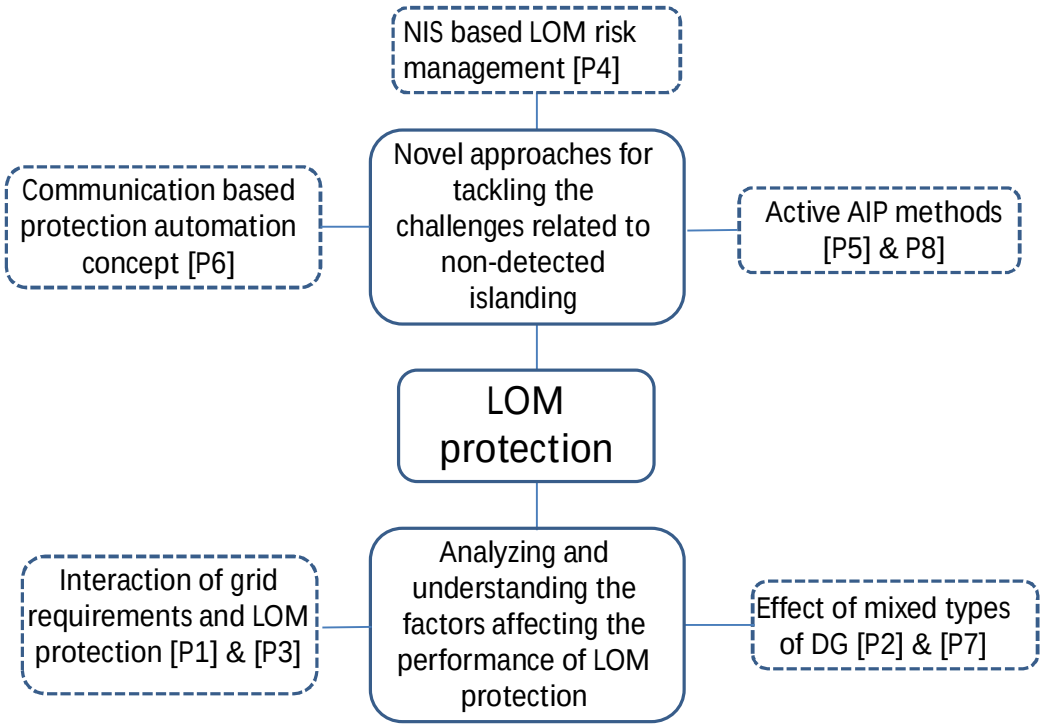

Fig. 1.1. *The inter-relations of the included publications*

- Publication [P1] studies how different kinds of LOM protection settings can be used to mitigate the problems caused by DG on fast automatic reclosing. The studies are based on real-time simulations in which a real commercial LOM relay was interfaced to a real-time simulator.
- Publication [P2] studied how the detection of islanding becomes more complicated when the islanded circuit contains both directly coupled synchronous generator based DG and DG coupled via power electronic converters. Analysis of the potential problems that such a scenario may cause to active LOM protection methods was also included in the publication. The studies presented in the publication are based on a large number of simulations performed using a laboratory set-up consisting of two different types of real-time simulators and a real LOM protection relay. The results were presented in the form of non-detection zone maps.

- Publication [P3] studied how low-voltage-ride-through and reactive current support requirements affect the performance of the most widely utilized passive LOM protection methods. The laboratory set-up used in [P2] was also used for the studies in publication [P3].
- Publication [P4] presented a novel network information system based tool for managing and evaluating the LOM risk at a concept level. This tool could help DSOs to evluate the probability of non-detected islanding in all parts of their networks, and guide them in choosing the most appropriate LOM protection schemes for each DG installation.
- Publication [P5] presented an active LOM protection method based on the combination of Q-f droop and reactive power variation.
- Publication [P6] presented a communication-based protection automation concept for tackling typical DG-related protection challenges. This concept can provide rapid LOM protection without any risk of non-detected islanding and it can be configured to be fully FRT compatible. The concept can also tackle typical DG-related protection challenges such as nuisance tripping and protection blinding, and it also has the potential to enhance the electricity distribution service to DG units by automatically changing the feeding path of the units at times when the original feeding path becomes faulted. Proof-of-concept tests comprising of real IEDs and a real-time simulator were successfully carried out.
- Publication [P7] continued the study started in [P2] but this time using an active LOM protection method, namely Q-f droop-based LOM protection, for the protection of the converter-coupled DG unit. Analysis on how the ratio of converter-coupled DG to directly-coupled synchronous generator-based DG affects the performance of LOM protection was also included.
- Publication [P8] presented an anti-islanding protection scheme for DG units connected via an inverter, which is based on reactive power versus frequency droop, rate of change of frequency (ROCOF) and frequency checking criterion. The method is based on driving the ROCOF to a predefined value during islanding by dedicated injection of reactive power. Using this method, islanding can be detected rapidly and reliably. Moreover, this can be accomplished with a smaller level of injected reactive power in comparison to conventional reactive power versus frequency droop-based LOM protection.

The author of this thesis is the corresponding author of all the eight above-listed original publications. The author has contributed to all the publications in the form of literature surveys, calculations, modeling, analysis, implementation of the laboratory set-ups and reporting.

All the publications have been written in collaboration with Prof. Sami Repo and Prof. Pertti Järventausta, who have contributed to the publications though guidance during the research work and by commenting on the publications prior to their publication. Prof. Sami Repo and Prof. Pertti Järventausta are also the supervisors of this thesis. Dr. Tech Kari Mäki contributed to [P1] by guiding the research work and by commenting on the publication. M.Sc. Anssi Mäkinen has contributed to publications [P2], [P3], [P5], [P7] and [P8] by designing the converter coupled DG models. Senior design engineer Kai Hiitelä from ABB contributed to [P6] by configuring the IEDs used in the laboratory set-up.

1.5 Outline and structure of the thesis

This thesis concentrates on the challenges posed to protection systems by the addition of DG, and in particular on LOM protection. The main emphasis of this thesis is on analyzing the factors affecting the performance of LOM protection and the shortcomings of commonly-utilized LOM protection methods. This thesis also proposes novel solutions for overcoming these challenges. As the focus of this thesis is not on modelling of DG units, verified realistic directly coupled synchronous generator and full converter coupled DG models were utilized in the studies.

The experiments for this thesis are primarily done using typical Nordic distribution network models, or in a standard type of test circuit used for analyzing LOM protection methods. A typical Nordic distribution network here refers to radially operated symmetrically loaded three phase MV overhead line or cable distribution feeders. The standard test circuit for analyzing LOM protection methods is a simplified model whose behavior resembles worst-case conditions for LOM protection. The principles of the standardized way of testing LOM protection methods are presented in chapter 2.5. To a limited extent, the studies of this thesis also considered power-system-level issues defined in existing grid codes, namely low-voltage-ride-through and reactive current support functions.

This thesis is organized as follows. Chapter 2 gives an introduction to the factors affecting the performance of LOM protection. The chapter gives an insight into issues such as how the power imbalance before the occurrence of islanding affects the performance of LOM protection, how the performance of LOM protection methods is typically tested, and how the type of the protected DG unit affects the performance of LOM protection. The chapter also briefly reviews the currently-utilized grid codes from the LOM protection point of view. Chapter 3 reviews the existing LOM protection methods. All three categories, that is, passive, active and communication-based LOM

protection methods, are included in the review. Chapter 4 summarizes the main points of the conducted studies and the developed methods. Finally, chapter 5 presents the final conclusions of the thesis and proposes future research topics related to the research work.

2 Factors affecting the performance of islanding detection

2.1 Introduction

The performance of LOM protection is dependent on many factors. For instance, the voltage magnitude and frequency in an islanded circuit are determined by the active and reactive power imbalance between the local production and consumption. The relations between voltage magnitude and frequency with the local imbalance between active and reactive power, on the other hand, depend on the type of the islanded DG unit(s) [24], [25]. The performance of LOM protection is also dependent on the control type of the local DG units. The way by which DG units are operated depends on the required grid-supporting features stipulated by the TSO, as well as possible active network management functionalities issued by the local DSO. Yet, to complicate the assessment of possible non-detected LOM risk further, the local demand and production typically vary throughout different times of the day and year. This chapter analyses how these factors affect the performance of LOM protection.

2.2 Power imbalance and islanding

Most LOM protection methods are based on detecting the changes in chosen system quantities, such as changes in voltage magnitude and frequency, which usually occur when a network section is islanded. These changes are mainly caused by the local imbalance between real- and reactive power production and consumption in the islanded network. During the normal grid-connected state, the local imbalance is compensated for by the import/export from/to the main utility grid. However, when a network section is islanded, the local power imbalances cause the voltage magnitude and/or frequency to drift from their original values, which can be used as an indication of islanding. There is, nevertheless, a risk that the local active and reactive power imbalances are so small that the transition to islanding does not cause any of the quantities measured by a LOM relay to drift out of the preset protection limits. In such cases, the LOM protection either completely fails to detect islanding, or fails to do so within an acceptable time. Such problematic power imbalances that lead to the failure of LOM protection are referred to as the non-detection zone (NDZ). Fig. 2.1 illustrates the approximate shape of the NDZ for traditional overvoltage- / undervoltage protection (OVP/UVP) and overfrequency- / underfrequency protection (OFP/UFP) for an island sustained by a synchronous generator (Graph a) on the left), and a converter-coupled DG unit (Graph b) on the right). As Fig. 2.1 illustrates, compared to the case where the island is sustained by a directly-coupled synchronous generator (case a in Fig. 2.1), in the case where the island is sustained by a converter-coupled DG unit (case b in Fig. 2.1) the boundaries of the NDZ that are determined by the functions

OFP, UVP, UFP and OVP are skewed by approximately 90 degrees. Voltage magnitude and frequency protection is probably the most utilized LOM detection method due to its simplicity, affordability and applicability to all types of DG units.

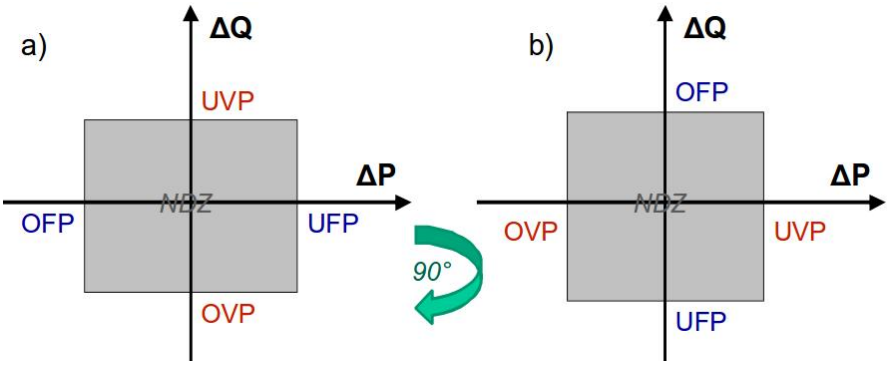

Fig. 2.1. *The non-detection zone concept [P2]*

The imbalance between the production of local DG and the consumption of local loads varies throughout the day in different network sections. This is because, typically, both the demand and the production vary throughout the day, and throughout the year. Because of this variation, the risk of unintended islanding also varies, as Fig. 2.2 illustrates. The local production of DG units is depicted as a straight red line in Fig. 2.2. However, in practice the local production also varies, especially if the local DG units are based on renewable energy sources such as wind or solar power. When evaluating the risk of non-detected islanding, it also has to be kept in mind that there are usually many potential sizes of islanding. That is, there are typically many switches whose opening may lead to the islanding of a DG unit, and consequently a DG unit may become islanded with various amounts of local loads. The black and yellow curves in Fig. 2.2, which represent the demands of two different sets of local loads, illustrate this issue. The areas that are marked with the text “Not okay” represent the periods during which LOM protection would fail to detect islanding [26].

It is noteworthy that delays in the operation of LOM protection may occur even with larger power imbalances. Such delays can also be very harmful because of the strict requirements for the operation times of LOM protection that are set by fast auto-reclosing. This stems from the fact that all DG units should be disconnected from the feeder in question within the open time of autoreclosing. This can be quite challenging if very short auto-reclosing open times (usually from 0.2s to 2s) are used. [21] It should also be borne in mind that it is not sensible to increase the autoreclosing open times too much because it degrades power quality. The size of the NDZ, as well as the operation times of the LOM protection, can be reduced by using stricter LOM protection settings, but this may increase the risk of nuisance tripping of the protected DG unit. Moreover, the LOM protection

settings typically have to be in line with the protection recommendations issued by the local DSO and with the grid code requirements issued by the TSO.

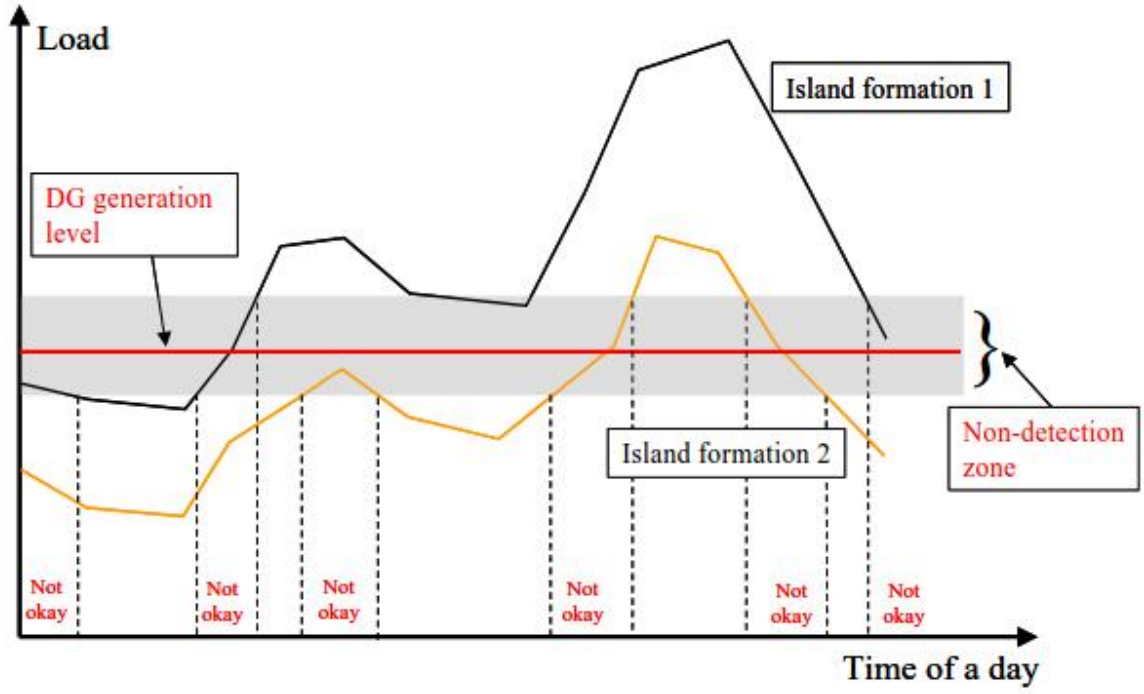

Fig. 2.2. *The probability of non-detected islanding varies all the time [26]*

2.3 Impact of different types of DG

The suitability of different LOM protection methods for DG units may be very different depending on the type of the DG unit which is to be protected. This stems from the fact that, the relationships between local active- and reactive power imbalances with voltage magnitude and frequency are dependent on the type of the protected DG unit [24], [25]. Moreover, active LOM protection methods, which are based on intentional injections of small perturbations into the network and monitoring the response of the system, can often easily be implemented for converter-coupled DG units, whereas, it is typically not possible without additional costs for directly-coupled induction or synchronous generators.

When an islanded circuit is sustained by a directly-coupled synchronous generator, it is mainly the active power imbalance which determines the frequency, while it is mainly the reactive power imbalance mainly which determines the voltage magnitude. However, these relations are profoundly different for an island sustained by a converter-coupled DG unit. In this case, the voltage magnitude

is determined by the active power imbalance, whereas, the reactive power imbalance mainly determines the frequency. [P2], [P7] These relationships are illustrated in Fig. 2.1. The reason for this can be better understood by examining the simple circuit in Fig. 2.3. If the DG unit in Fig. 2.3 is connected to the circuit via a converter, then during islanding the active and reactive power consumed by the load have to match with the active- and reactive power produced by the converter, as shown in (2.1) and (2.2) [27]-[29].

$$P_{\text{Load}} = \frac{V^2}{R} = P_{\text{Inv}} \tag{2.1}$$

where P_{Load} refers to the active power consumption of the load, V to the line-to-line voltage of the circuit, R to the resistance of the parallel connected RLC load and P_{INV} to the active power fed by the inverter.

$$Q_{\text{Load}} = V^2 \left(\frac{1}{2\pi f L} - 2\pi f C\right) = Q_{\text{Inv}} \tag{2.2}$$

where Q_{Load} and Q_{INV} refer to the reactive power consumption of the load and the reactive power fed by the inverter, f to the frequency of the studied circuit, and L and C are the inductance and capacitance of the load.

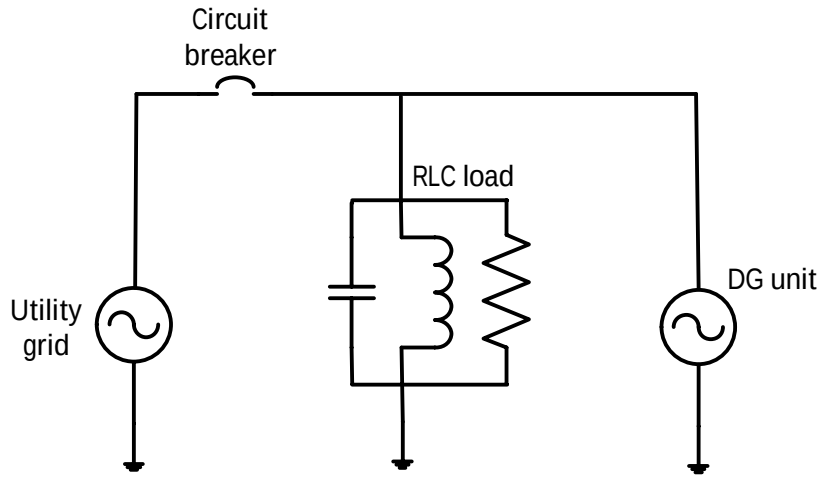

Fig. 2.3. *The basic structure of the circuit used for testing LOM protection methods*

As can seen from (2.1), the voltage in the circuit is determined by the active power imbalance. Correspondingly, assuming that the voltage magnitude is determined by the active power imbalance,

from (2.2) it can be concluded that the frequency will have to deviate to such a value that the reactive power consumed by the load is equal to the reactive power fed by the converter.

However, if the DG unit in Fig. 2.3 were a directly coupled synchronous generator, the relationship would be different. In this case, the frequency is tied to the speed of the synchronous generator. The factors affecting the speed of the generator can be analyzed with the help of the swing equation (2.3). Note that windage, friction and iron loss torque are ignored in the equation. In the equation, the term P_{m} refers to the mechanical power input to the generator, P_{e} is the electrical output power of the generator, G refers to the nominal power of the generator, f_{nom} is the nominal system frequency, H refers to the inertia constant and δ refers to the power angle (that is, the rotor angular displacement from the synchronously rotating reference). [30] The term $d^2\delta/dt^2$ thus represents the angular acceleration of the generator. Now, for instance, if the active power produced by the synchronous generator happens to be greater than the active power consumed by the load before the occurrence of islanding, the generator will accelerate after the occurrence of islanding. Correspondingly, the generator will decelerate if the active power consumed by the load is greater than the active power produced by the generator.

$$P_{\mathrm{m}} - P_{\mathrm{e}} = \frac{GH}{\pi f_{nom}} \frac{d^2\delta}{dt^2} \tag{2.3}$$

The voltage magnitude in the islanded circuit, on the other hand, is mostly determined by reactive power imbalance in the case of synchronous generator sustained power island [P2], [25].

When designing active LOM protection methods that are based on drifting frequency by injecting reactive power, it is important to understand the above explained relations between active- and reactive power imbalance with voltage magnitude and frequency. This is because active LOM protection methods designed for inverters may not function properly if the islanded circuit is sustained by both inverter coupled DG and synchronous generator based DG units. This has been analysed more in detail in [P7].

2.4 Grid code requirements and LOM protection

The control modes of the DG units also have an effect on the performance of LOM protection. For instance, the performance of voltage relays may become significantly degraded in a case where the islanded circuit is sustained by a directly-coupled synchronous generator that is set to control its terminal voltage in comparison to a case where the generator is set to unity power factor mode [25].

The control principles of inverter-coupled DG units also have a significant effect on the performance of LOM protection as was shown in [28]. The way by which DG units have to be operated is nowadays largely determined by grid code requirements issued by the regional TSO and by the possible active network management functionalities used by the local DSO. These aspects are analyzed below.

This chapter gives a brief overview of the power system supporting functions required in different grid codes. Special emphasis is given to the ENTSO-E grid code "Requirements for Grid Connection Applicable to all Generators (RfG)". ENTSO-E, which stands for the European Network of Transmission System Operators for Electricity, represents 42 TSOs from 35 European countries. ENTSO-E was established in 2009 with the aim of further liberalizing the electricity and gas market, and supporting the European energy and climate agenda. [31] The ENTSO-E grid code is given special emphasis in this report since Europe has been a pioneer in developing grid codes for wind power and solar PV, which constitute a significant proportion of DG capacity.

2.4.1 Overview of grid code requirements

The ENTSO-E grid code divides generating units into four different classes based on their maximum capacity as illustrated in table 2.1. Each of the sequential classes includes all the requirements of the previous classes plus additional requirements. If a new power generating module does not comply with the connection requirements set in the ENTSOe grid code, the [32] code states that the relevant system operator shall refuse the connection of this power generating module. Existing power generating modules are not subject to the rules set in [32], with the exception of class C and D power generating modules which have been signifcantly modernized, as defined in [32]. However, a local regulatory authority, or where applicable, a member state is free to decide to make an existing power generating module subject to all or chosen requirements specified in [32].

Table 2.1. *The division of DG units to four classes in ENTSOE-RfG [32]*

Synchronous area	Limit for maximum capacity threshold from which a generating unit is of type B	Limit for maximum capacity threshold from which a generating unit is of type C	Limit for maximum capacity threshold from which a generating unit is of type D
Continental Europe	1 MW	50 MW	75 MW
Great Britain	1 MW	50 MW	75 MW
Nordic	1.5 MW	10 MW	30 MW
Ireland and Northern Ireland	0.1 MW	5 MW	10 MW
Baltic	0.5 MW	10 MW	15 MW

The requirements concerning the minimum time periods for which power generating modules need to be capable of operating without being disconnected in different frequency ranges are identical for classes A to D in the ENTSO-E grid code. This can be seen from table 2.2, which describes these minimum time periods in different ENTSO-E areas.

Table 2.2. *Minimum time periods for which all power generating modules have to be capable of operating on different frequencies without disconnecting from the network [32]*

Synchronous area	Frequency range	Time period for operation
Continental Europe	47 Hz - 48.5 Hz	To be specified by each TSO, but not less than 30 minutes
	48.5 Hz - 49 Hz	To be specified by each TSO, but not less than the period for 47.5 Hz - 48.5 Hz
	49 Hz - 51 Hz	Unlimited
	51 Hz - 51.5 Hz	30 minutes
Nordic	47.5 Hz - 48.5 Hz	30 minutes
	48.5 Hz - 49 Hz	To be specified by each TSO, but not less than 30 minutes
	49 Hz - 51 Hz	Unlimited
	51 Hz - 51.5 Hz	30 minutes
Great Britain	47 Hz - 47.5 Hz	20 seconds
	47.5 Hz - 48.5 Hz	90 minutes
	48.5 Hz - 49 Hz	To be specified by each TSO, but not less than 90 minutes
	49 Hz - 51 Hz	Unlimited
	51 Hz - 51.5 Hz	90 minutes
	51.5 Hz - 52 Hz	15 minutes
Ireland and Northern Ireland	47.5 Hz - 48.5 Hz	90 minutes
	48.5 Hz - 49 Hz	To be specified by each TSO, but not less than 90 minutes
	49 Hz - 51 Hz	Unlimited
	51 Hz - 51.5 Hz	90 minutes
Baltic	47.5 Hz - 48.5 Hz	To be specified by each TSO, but not less than 30 minutes
	48.5 Hz - 49 Hz	To be specified by each TSO, but not less than the period for 47.5 Hz - 48.5 Hz
	49 Hz - 51 Hz	Unlimited
	51 Hz - 51.5 Hz	To be specified by each TSO, but not less than 30 minutes

The requirements concerning the minimum time periods for which power generating modules need to be capable of operating without being disconnected in different voltage ranges for longer periods of time are only clearly specified for class D power generating units in ENTSO-E grid code [32]. However, the ENTSO-E grid code does gives guidelines on how long generating units need to be capable of operating during short lasting voltage deviations. This matter is discussed in more in detail the next chapter. Basically, the requirements concerning the capability of generating units to operate at different voltages is to be determined by the responsible TSOs. Fig. 2.4 gives an example of how long generating units connected to the Finnish grid need to remain connected at different frequencies and voltages [34].

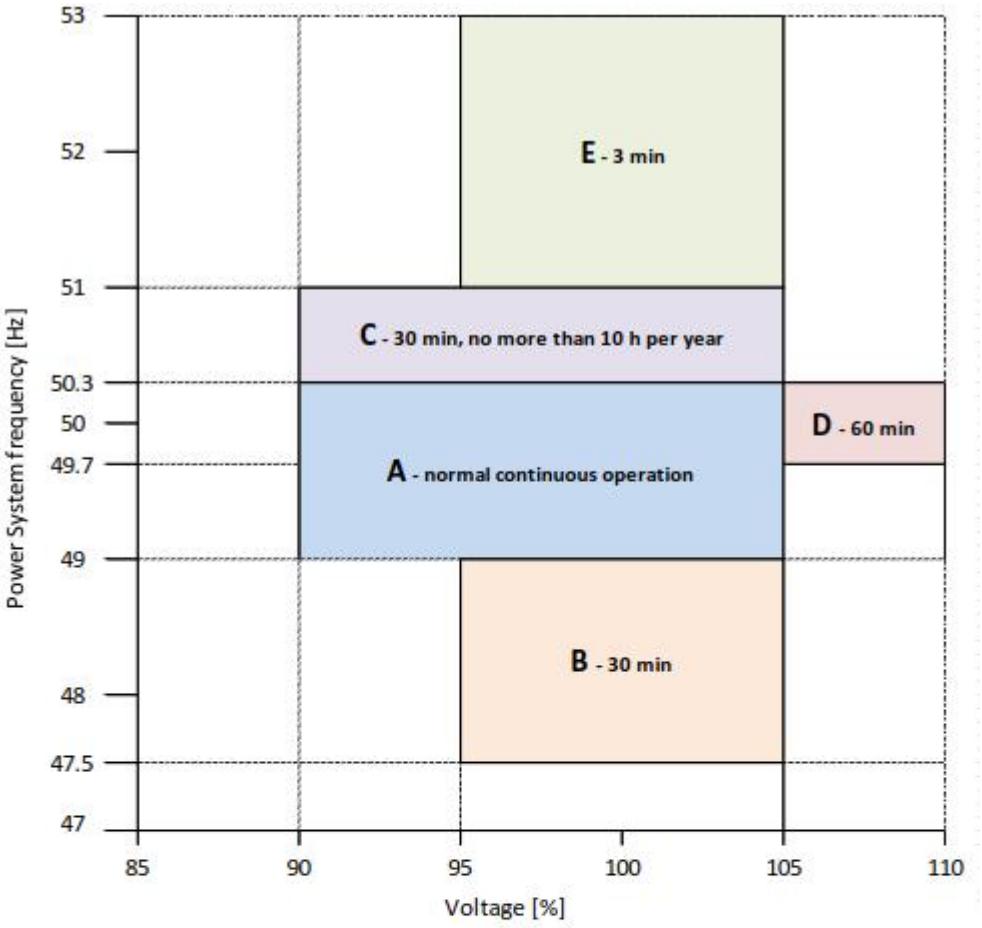

A:	Normal continuous operation	A decrease in the generation capacity of Active Power or Reactive Power as a result of the voltage and/or frequency of the Power System is not allowed
B:	30 min of continuous operation	A power decrease is allowed in such a way that the maximum permitted decrease at a level of 49 Hz is 0% and at a level of 47.5 Hz 15% (in the frequency range between these, the permitted decrease is determined linearly on the basis of reductions permitted at the borderline frequencies)
C:	30 min of continuous operation for a maximum total of 10 hours annually	A power decrease of 10% is permitted if it does not impose restrictions to continue operation at initial power output when frequency is restored to below 50.3 Hz
D:	60 min of continuous operation	The power is permitted to decrease a maximum of 10% of full power
E:	3 minutes of continuous operation	Rapid power decrease allowed

Outside the above-mentioned operating ranges, operation must continue within the limits allowed by technology, immediate disconnection not permitted

Fig. 2.4. *The requirements on how long generating units connected to the grid operated by the Finnish TSO Fingrid need to be capable of operating at different voltages and frequencies [34]*

The ENTSO-E grid code states that TSOs may also define a ROCOF withstand capability threshold under which DG units shall be capable of operating without being disconnected . [32]. If such is required, ROCOF based LOM protection naturally has to be set to enable this. The Finnish TSO, Fingrid, states that DG units, whose rated power is between 0.5 MW and 10 MW, shall be capable of staying connected to the network continously when the ROCOF is below 2 Hz/s, and for at least 1.25 s when the ROCOF is exactly 2 Hz/s. In the UK, the ROCOF recommendation is 1 Hz/s with a time delay of 500 ms for stations with a DG capacity equal to or above 5MW [33]. However, the ROCOF setting recommendation for synchronous generators commissioned before 1st of August 2016 is 0.5 Hz/s, with a time delay of 500 ms [33].

2.4.2 Fault ride through requirements

DG units were initially thought to have only a marginal effect on a large power system and TSOs thus had less stringent requirements for generating units connected to distribution networks [23]. This policy was also suited the DSOs since it enabled the use of sensitive LOM protection settings in voltage and frequency relays, and thus helped in preventing unwanted islanding and failed reclosings caused by DG. However, as the share of DG kept increasing, it was later realized that faults in the transmission system could lead to huge amount of tripping of DG units if too sensitive LOM protection settings were used. This was very apparent, for instance, during the UCTE disturbance on November 4th, 2006 [23]. In order to avoid these types of problems, TSOs began to issue more stringent connection requirements for DG units. For instance, voltage and frequency protection settings were required to be loosened in order to avoid tripping of DG units during fluctuations in voltage and frequency. TSOs also began to require low-voltage-ride-through (LVRT) capability from DG units, specifying the depth and duration of voltage dips that the generating units need to be capable of riding through without losing their stability. Some of the TSOs also began to require generating units to feed reactive current to the grid during voltage dips to support the system voltages. These LVRT and reactive current support requirements are typically referred to as the fault-ride-through (FRT) requirements.

The FRT requirements for DG units are also specified in the ENTSO-E grid code [32]. The ENTSO-E grid code states the different grid code requirements for DG units, which depend on the nominal capacity of the units. However, local TSOs can specify in more detail what kind of low-voltage-ride-through curve is required in their networks. ENTSO-E states that generating units must be capable of riding through voltage dips without losing their stability during symmetrical faults in which the phase-to-phase voltage stays above the LVRT curve. However, ENTSO-E does not give any specification for FRT requirements during asymmetrical faults, but only states that such specifications should be TSO-specific. Fig. 2.5 shows how the Finnish TSO, Fingrid, has implemented the LVRT requirement curve in its grid code. Fingrid requires generating units whose

nominal capacity is between 0.5MW and 100MW to comply with the LVRT requirement curve shown in Fig. 2.5. The vertical axis in Fig. 2.5 represents voltage on a per-unit scale, whereas the horizontal axis represents time in seconds."

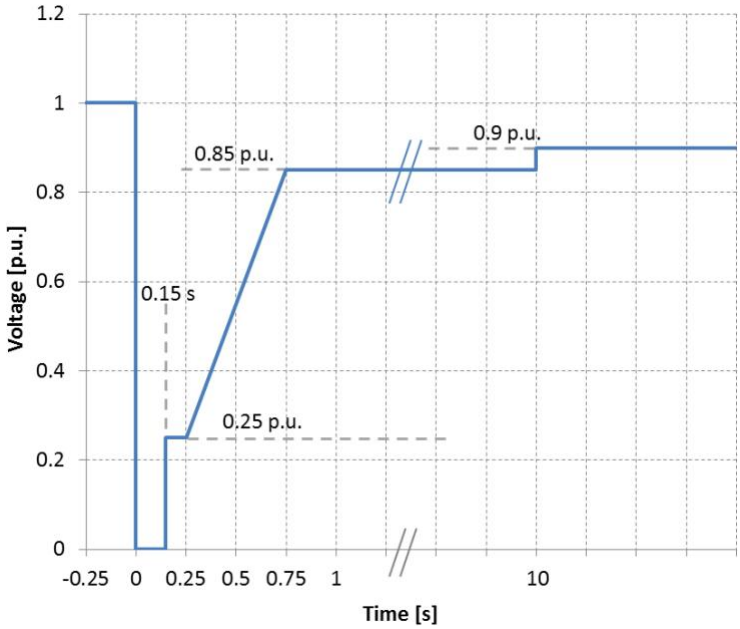

Fig. 2.5. *The LVRT requirement curve for generating units whose nominal capacity is between 0.5 MW and 100 MW in the Finnish transmission grid [34]*

Many grid codes also require DG units to support the system voltages during deep voltage dips by feeding reactive current during the LVRT. Mitigating the drop of voltages during deep voltage dips also helps in avoiding unwanted large-scale disconnection of DG units. Moreover, feeding reactive current during voltage dips also helps in improving the voltage recovery [35]. Contributing to fault currents also helps in ensuring the correct operation of protection relays. According to the ENTSO-E grid code, the relevant TSO shall have the right to require that power park modules in classes B to D have to be capable of supporting the grid by activating additional reactive power output during voltage dips. However, ENTSO-E does not specify the amount of required additional reactive current injection during voltage dips in detail, but simply states that the amount of injected reactive current should depend on the voltage. The responsible TSO should decide whether to give priority to active- or reactive power contribution from power park modules from which FRT is required [32].

Generating units connected to the medium and high voltage systems in Germany need to be able to ride through the faults and feed reactive current to support the stability of the system [36], [37]. However, during asymmetrical faults, the generating units are not allowed to feed reactive current

if it should lead the voltage at healthy phases to rise above 1.1 per unit. [36] Generating units connected to the German transmission system have to start supporting the system voltages by feeding additional reactive current when the voltage drops by more than 10 %, as illustrated in Fig. 2.6 [37]. If this happens, the generating unit has to inject at least 2 % of the rated current per percent of voltage drop, and also has to be capable of feeding the required amount of reactive power within 20 ms [37]. The steepness of the droop illustrated in Fig. 2.6 is expressed by the variable k, which should thus be equal to or higher than 2.0 p.u. However, wind power plants have to be designed so that the k factor is adjustable in the range 0 – 10 [38]. With a k factor value equal to 2.0 p.u., the generating unit has to feed reactive current equal to the rated current when voltage drops to 0.5 p.u. or more.

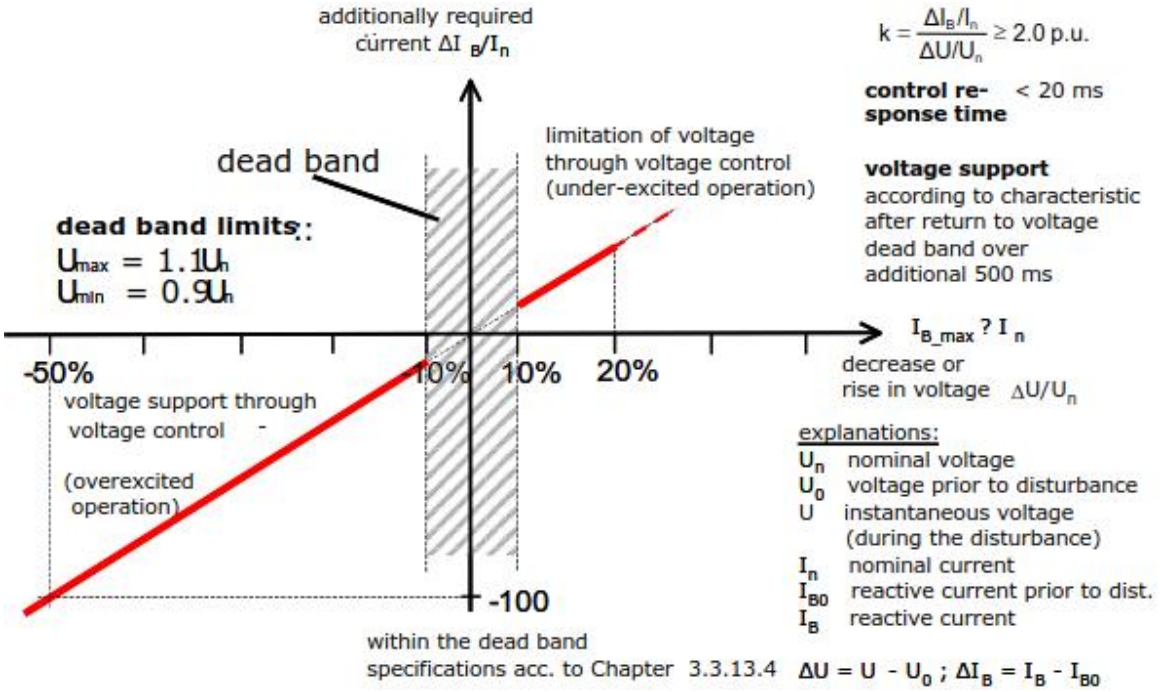

Fig. 2.6. *Reactive current support required during FRT from renewable based generating units [37]*

2.4.3 Frequency control

The purpose of the frequency control function is to contribute to the system stability by controlling the active power output of the plant as a function of system frequency. The ENTSO-E grid code states that DG units whose nominal power is 800W or more should comply with the P-f droop control, which is referred to as the limited frequency sensitive mode (LFSM-O mode) in [32]. In practice, this requirement means that the DG units need to contribute to the frequency stability of the power system by reducing their active power output proportionally to a dedicated active power versus frequency droop if the frequency should rise above a TSO-specific threshold. According to [32], this frequency threshold should lie between 50.2 Hz and 50.5 Hz and the droop setting is

between 2 % and 12 %. DG units have to be capable of activating the desired active power response with an initial delay that is as short as possible, but no longer than 2.0 s. When DG units are operated in the LSFM-O mode, the LFSM-O set point prevails over any other active power set-points. [32] The graph in Fig. 2.7 illustrates how the LFSM-O requirement is set in practice by the Danish TSO Energinet.dk. This requirement is meant for wind turbines and PV plants whose nominal power is above 11 kW. The standard value used by the Danish TSO for the threshold f_R depicted in Fig. 2.7 is 50.2 Hz. The frequency-response control has to start within 2 s of the detection of the change in frequency, and it should be completed within 15 s. [39], [40] ENTSO-E NC RfG has more stringent requirements for larger generating units (classes C and D) regarding frequency control. These units also need to be able to increase their production in the case of underfrequency.

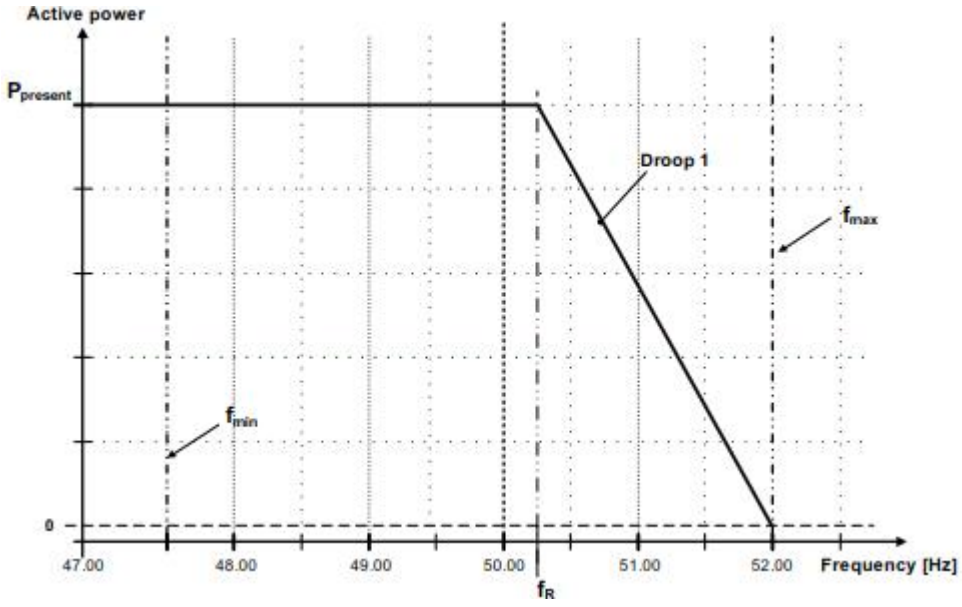

Fig. 2.7. *Frequency response requirement for wind power and PV plants larger than 11 kW [40]*

2.4.4 Voltage control

DG units can contribute to voltage control by controlling their reactive power output. The reactive power output can, for instance, be configured to be a function of the monitored voltage at the connection point, or it can be proportional to active power output. The voltage control potential of DG units can be further optimized by using a coordinated voltage control method, which optimizes the voltages of a whole distribution network by adjusting the voltage reference points of primary voltage and reactive power controllers, and utilizing all the available voltage control resources such as

the tap changers of transformers, capacitors, reactors, DG units and energy storages [4]. The Q-V droop for generating units connected to distribution networks is typically designed in such a way that there is a suitable deadband around the nominal voltage in order to minimize network losses.

As an example of an actual implementation of voltage control requirements, PV plants connected to the Danish grid must be equipped with reactive power and voltage control functions. Voltage control, reactive power control (*Q* control) and power factor mode are mutually exclusive, i.e., only one of these functions is activated at a time. The settings for these functions must be determined together by the local DSO and the TSO before commissioning. In the *Q* control mode, the reactive power is controlled independently of the active power output, whereas in the power factor control mode, the reactive power output is proportional to the active power output. When a PV plant is operated in the voltage control mode, the PV plant tries to maintain its PCC voltage at the set value by controlling its reactive power output according to the utilized voltage droop. [39]

2.4.5 Virtual inertia

Sudden fluctuations in power system frequency have traditionally been limited by the energy stored in the spinning masses of synchronous generators. However, the number of generating units that are decoupled from the grid frequency by means of power electronic devices, is increasing rapidly. This has raised concerns about the decreasing inertia in power systems. The introduction of virtual inertia (also known as synthetic inertia) to generating units that are decoupled from the grid frequency has been suggested as a remedy for this problem. Virtual inertia refers to a control scheme that makes a power electronic converter-coupled generating unit to emulate the synchronous generators' inertial response to frequency fluctuations. The ENTSO-E grid code states that the responsible TSO has the right to require virtual inertia from C and D class power park modules, and also has the right to specify the performance requirements and operating principle of the control system needed to provide synthetic inertia [32]. The Canadian TSO, Hydro Quebec, already requires virtual inertia from wind parks whose rated output is greater than 10 MW. The virtual inertia feature must be continuously in service, even though it is only used during major frequency deviations. The wind turbines must reduce frequency fluctuations to at least as much as a synchronous generator whose inertia constant equals to 3.5 s would do. [41]

Wind power plants are able to provide virtual inertia by extracting kinetic energy from the rotating masses of the wind turbine. However, this has a drawback, which is that the wind turbine's rotor will decelerate during the extraction of additional energy. Consequently, a portion of the power produced by the turbine is needed for re-accelerating the turbine's rotor back to its optimal speed, thus causing the wind power plant to feed a reduced amount of power to the grid for a certain period of time. This was witnessed in the synchronous area operated by Hydro Quebec in December 2015 when a transformer failure caused a loss of generation of more than 1600 MW thus causing the frequency to drop from the nominal 60 Hz to 59.1 Hz. The frequency would probably have dropped

by an additional 0.1 to 0.2 Hz if the virtual inertia function of the wind turbines hadn't provided an additional 126 MW to the grid. However, as the wind turbines decelerated as a consequence of the provision of virtual inertia, the frequency stayed at 59.4 Hz for several seconds before additional power reserves were able to raise the frequency back to the nominal 60 Hz. Under different conditions, this could have resulted in another frequency dip with severe consequences. Learning from this lesson, the German wind power manufacturer ENERCON has presented an upgraded version of virtual inertia that enables more smooth and tunable re-acceleration. [42]

2.4.6 Impact of grid code requirements on LOM protection

The paper [43] studied how the P-f and Q-V droop controls affect the performance of voltage magnitude and frequency-based LOM protection. The study was based on both steady state analysis and on verifying the obtained analytical results with the help of a lab-scale prototype in 31 selected power imbalance combinations. According to this study, using only one of these controls has no significant impact on the performance of LOM protection. However, if these controls are used simultaneously, the performance of LOM protection can be significantly degraded. The studies done by [13] drew similar conclusions. In fact, according to [13], the NDZ only increased by less than 1 % when only one of the P-f or Q-V droop controls was used. However, when both the P-f and Q-V droop controls were applied simultaneously, there was a significant increase in the size of the NDZ. Reference [13] also studied this effect with different quality factors of the parallel RLC load. The study showed that the NDZ increased particularly with lower values of quality factor, whereas, the effect was decreased when quality factor was increased. The quality factor values used in the study were from 2 to 10. The studies were based on steady state calculations and thus ignored dynamics of the islanded system, as well as the effect of possible active LOM protection methods. [13] Another study [44] performed a similar experiments which analyzed the effect of Q-V and P-f droop controls on the performance of LOM protection with the help of a transient simulation software (DIgSILENT Power Factory) in three different power imbalance conditions. In this study, [44] however, the researchers also studied how the addition of synthetic inertia affected LOM protection performance. As expected, the addition of synthetic inertia stabilized islanding and thus made the detection of the islanding more difficult.

2.5 Typical test procedure for testing LOM protection methods

A large number of different LOM protection methods have been proposed in the literature and by relay manufacturers. An unbiased test procedure is thus needed for assessing the different LOM

protection methods and for comparing their performances in a uniform manner. This chapter reviews the test procedures used for testing LOM protection methods.

Islanding test procedures for inverter-based DG units were initially carried out without any stabilizing components. This does not, however, reflect reality because real existing grids typically contain inductive and capacitive elements which store reactive power, and components that add inertia to an islanded circuit, such as induction machine loads. These types of components tend to stabilize frequency during islanding and thereby complicate the task of LOM protection. Due to this, the addition of rotating machine loads to the LOM protection test circuit was considered. However, in order to ensure reproducibility, all the test laboratories around the world would have had to use identical machine parameters, including inertia and friction. [45] Moreover, studies have shown that with proper parametrization, the effect of a single-phase induction motor can be simulated by a parallel RLC circuit [46]. Although that study concentrated on simulating the behavior of single phase induction machines using RLC circuits, the authors are of the opinion that three-phase induction machines can be simulated in the same way [46]. Using resonant circuits with constant quality factor instead of induction machines is useful since it also provides the benefit of scalability, which is to say that the circuit can be scaled to test any sizes of DG [45]. Thus, a resonant circuit tuned to grid frequency was chosen instead of the addition of induction generator. Fig. 2.8 illustrates the structure of the LOM protection test circuit.

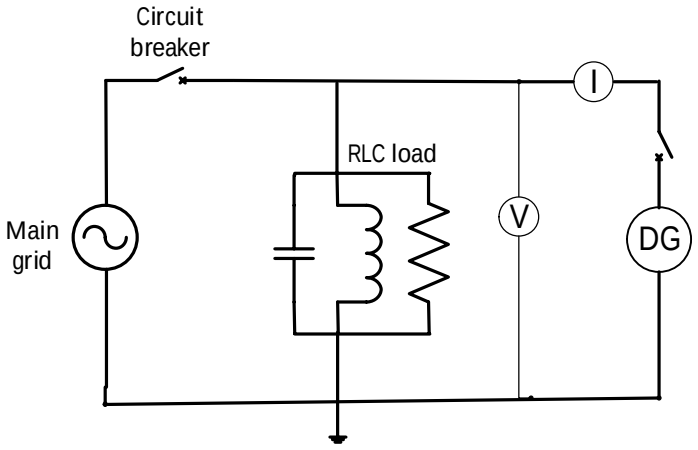

Fig. 2.8. *The structure of the circuit used for testing the performance of LOM protection methods*

The quality factor of a parallel RLC circuit is defined as the ratio of reactive power in the circuit to active power consumption. The quality factor of a parallel RLC load can be expressed as follows [15], [45]:

$$Q_f = R\sqrt{\frac{C}{L}} = 2\pi f_r RC = \frac{\sqrt{Q_L Q_C}}{P_{Load}} \quad (2.4)$$

where R, C and L refer to the resistance, capacitance and inductance of the parallel RLC load, f_r is the resonant frequency of the load and Q_L and Q_C refer to the inductive and capacitive reactive power consumed by the load. Loads with high quality factor value are especially problematic for LOM protection. A high value quality factor means that the circuit has large capacitances and small inductances and/or parallel resistances [20], [47].

The RLC load parameters for the tests are chosen so that the load consumes the desired amount of active- and reactive power while maintaining the desired quality factor value. After this, the circuit breaker in Fig. 2.8 is opened, thus isolating the remaining circuit from the main grid, and the time within which the LOM protection detects the islanding is captured. If the islanding detection time is within the allowed limits, the tested LOM protection method worked correctly at this specific operating point. The standards specify in more detail which operating points need to be tested. The tested LOM protection passes the test only if it correctly detects all the islanding scenarios within the allowed time.

There are several standards that define how LOM protection methods should be tested. However, the testing methods are all very similar. Some testing standards may, nevertheless, have different requirements concerning the quality factor of the parallel RLC load, as well as for the allowed LOM detection time. For instance, according to the standard [47], the quality factor of the parallel RLC load should be set to 1.0 and islanding should be detected and ceased within 2.0 s. The same requirements concerning LOM protection testing can be found from the standard [15], which is harmonized with the standards [14] and [47]. The standard [14] provides the specifications and requirements for testing LOM protection methods, whereas, the test procedures and evaluation are provided in [47].

2.6 Summary

There are many factors which affect the performance of LOM protection, such as the local active and reactive power imbalances in the islanded circuit, the characteristics of the loads, the DG unit types, the control modes of DG and the grid code requirements. The standard LOM protection test procedures take these factors into account. However, the thresholds of the tested LOM protection functions should be in line with the applied grid codes. Some of the grid supporting functionalities

required in the grid codes may require modifications in the control system of the DG unit used in the test. The effect of the grid supporting functionalities on the performance of LOM protection have been already studied in the literature, but further studies may be needed as the grid codes evolve.

3 Review of existing LOM protection methods

3.1 Introduction

LOM protection methods are typically divided into local and remote methods [20], [48]. The local methods can be further divided into passive and active LOM protection methods. Fig. 3.1 illustrates this division into three categories and gives a few examples of each category. In recent years, there have also been several publications proposing methods which are actually a combination of passive and active LOM protection methods. Such methods are sometimes referred to as hybrid LOM protection methods [48], [49]. This chapter presents a review of LOM protection methods. The first section presents passive LOM protection methods, whereas, the second section concentrates on active methods. The third section focuses on remote LOM protection methods.

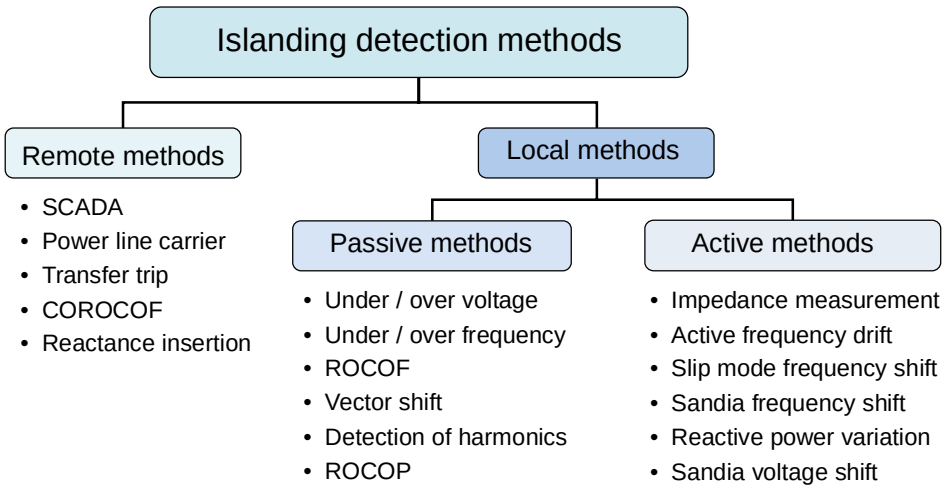

Fig. 3.1. *The categorization of islanding detection methods*

3.2 Passive LOM protection methods

Passive LOM protection methods are widely utilized due to their simplicity and low cost. These methods are based on monitoring chosen quantities which are typically based on local measurements. Most passive LOM protection methods are applicable to all types of DG units. The downside of passive LOM protection methods is that they are generally characterized by a large NDZ. This chapter gives a brief overview of these methods.

3.2.1 Voltage magnitude and frequency

Voltage magnitude and frequency relays protect from abnormal voltages and frequencies, but can also act as simple type of LOM protection. Voltage magnitude and frequency protection is required in practically all grid codes and standards. Voltage magnitude and frequency protection functions are often used in conjunction with more advanced LOM protection schemes, since voltage magnitude- and frequency-based LOM protection alone tends to be poor, especially if the grid code requires LVRT capability from the protected DG unit [P3].

Fig. 3.1 illustrates the thresholds specified for voltage magnitude and frequency in different standards and grid codes. The old German grid code VDE 0126-1-1 for LV connected DG units has been superseded by the new grid code VDE-AR-N 4105. As can be seen, the grid code VDE-AR-N 4105 has a considerably broader normal operation frequency range than the old grid code. The reasoning behind this is that when VDE 0126-1-1 was designed, the amount of DG connected to low voltage networks in Germany was relatively low and losing all the DG units connected to LV networks due to a rise in frequency was not a system-level concern. However, at the time of writing this thesis, solar PV capacity in Germany is already over 40 GW, of which a significant proportion is connected to LV networks [50], [51]. Consequently, the risk of losing huge amounts of DG generation if frequency had risen above 50.2 Hz was considered too great, so a broader normal operation frequency range was defined in the VDE-AR-N 4105 standard. Although it is rare for the frequency to rise above 50.2 Hz in a large power system, it is still considered possible and has indeed happened at least couple of time in Germany [51]. This retrofitting of new frequency protection thresholds for all LV-connected DG units in Germany was costly and time consuming [51]. Thus, when defining standards, it is very important (although also very challenging) to try to foresee the future requirements many years ahead.

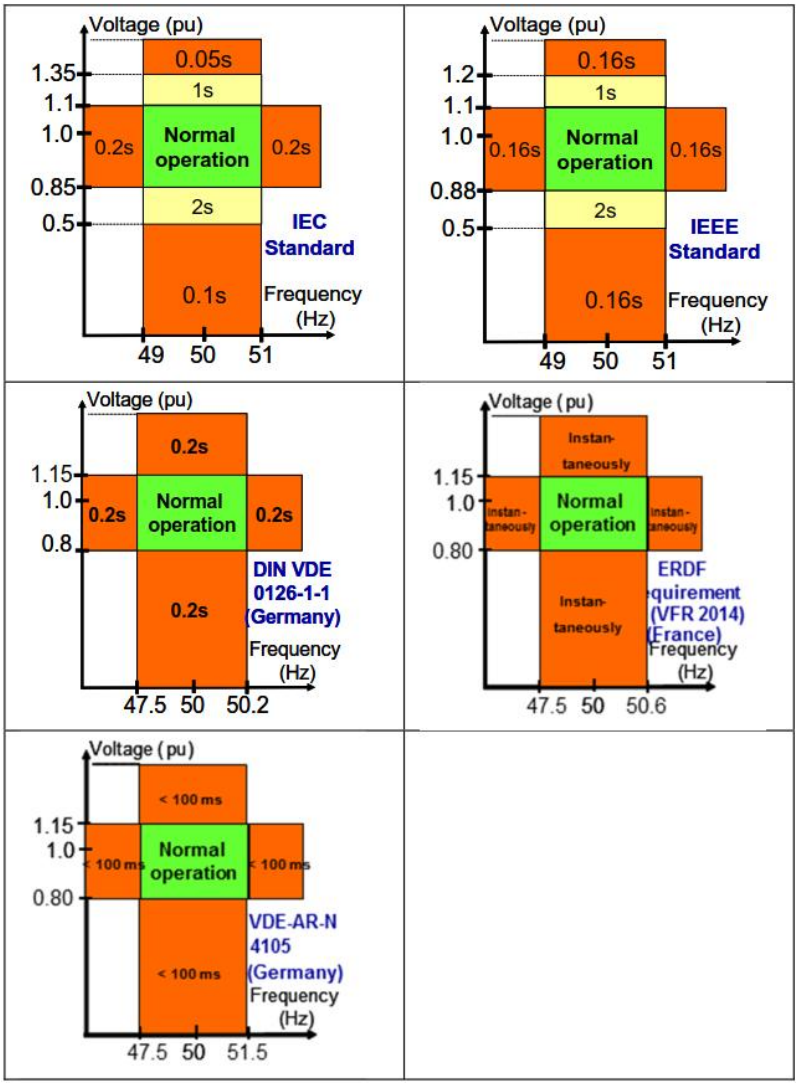

Fig. 3.1. *LOM protection thresholds on LV network by IEC, IEEE, Germany and France [52]*

3.2.2 Rate of change of frequency

When the power imbalance in the islanded circuit is not very large, it may take a relatively long time for the frequency to drift out of the utilized frequency protection limits. In cases like this, Rate of change of frequency (ROCOF)-based LOM protection can significantly speed up the detection of islanding. However, the protection thresholds for ROCOF have to be carefully planned in order to avoid unwanted tripping.

The operating principle of ROCOF relays is illustrated in Fig. 3.2. As the figure illustrates, the frequency is first estimated from the measured voltage waveform. The ROCOF, which is calculated

from the estimated frequency, is then filtered in order to eliminate high frequency transients. After the filtration process, the calculated ROCOF, which is indicated in Fig. 3.2 by the letter K, is then compared to the ROCOF setting value. If the calculated ROCOF exceeds the tripping threshold, while the measured terminal voltage is above a chosen minimum voltage threshold, a trip command is initiated. [53]

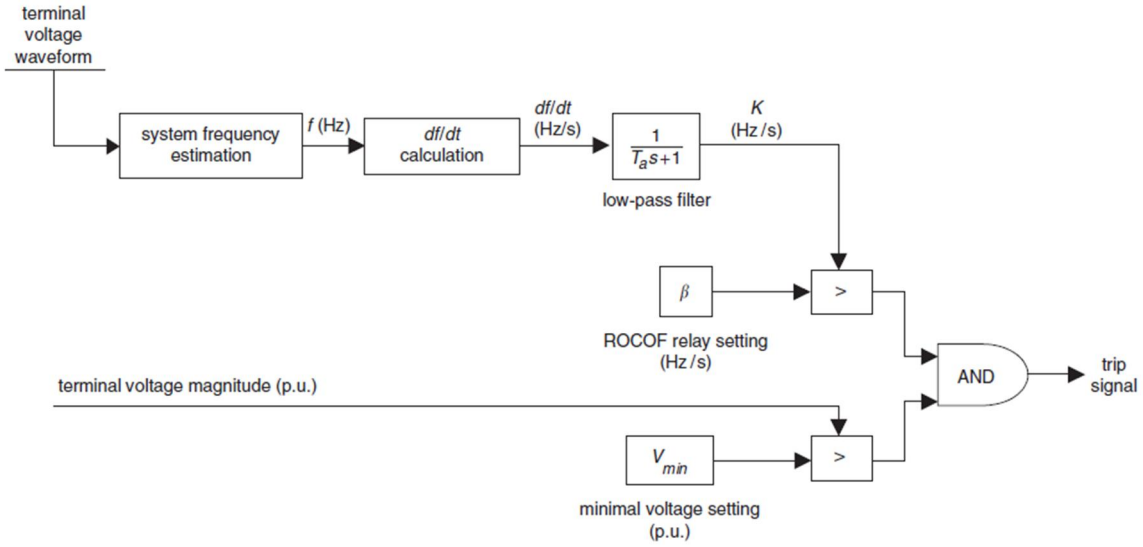

Fig. 3.2. *The principle of ROCOF based LOM protection [53]*

There are problems with the security of a ROCOF relay. This is because nuisance tripping of ROCOF relays may occur due to loss of bulk generation in the high voltage grid, or due to faults or switching in the local network, especially if a narrow measuring window or if very sensitive tripping threshold is used. The minimum number of measuring periods is normally two, which is equal to 40ms at a 50 Hz system. [3]

ROCOF-based LOM protection has a couple of advantages over conventional frequency protection. Firstly, it can detect rapid changes in frequency before the governors have time to respond, and secondly, ROCOF provides potentially considerably faster detection times when the power imbalance in the islanded circuit is relatively small [54]. However, ROCOF-based LOM protection alone is not able to detect islanding when the power imbalance in the islanded circuit is very small [P3].

3.2.3 Vector shift

Vector shift relays constantly monitor the duration of each voltage cycle and trip if the duration of the monitored cycle has changed by more than the tripping threshold in comparison to the previously measured cycle. Vector shift relays were initially designed for the LOM protection of directly-coupled synchronous generators. Thus, their operating principle can better be explained by analyzing a simple network model fed in parallel by a synchronous generator-based DG unit and the main

power grid as shown in Fig. 3.3. During normal operation, the terminal voltage of a synchronous generator lags behind the electromotive force of the generator by the rotor displacement angle δ due to the current fed by the generator, as shown on the left hand side of Fig. 3.4. If the connection from the network partially fed by the generator to the main power grid is suddenly lost, the current fed by the generator either increases or decreases depending on the power imbalance between the local production and consumption. Consequently, the generator either accelerates or decelerates which causes a shift to the rotor displacement angle δ as shown on the right hand side of Fig. 3.4. [3], [55]

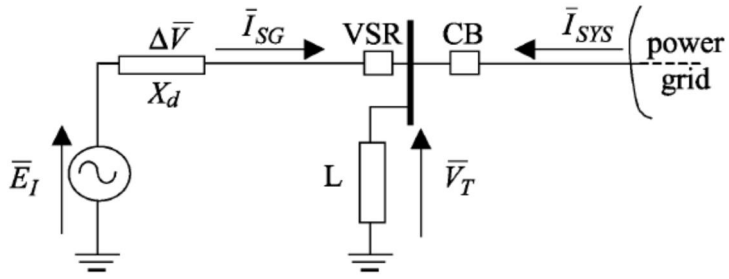

Fig. 3.3. *A simple network model with a synchronous generator based DG unit [*55*]*

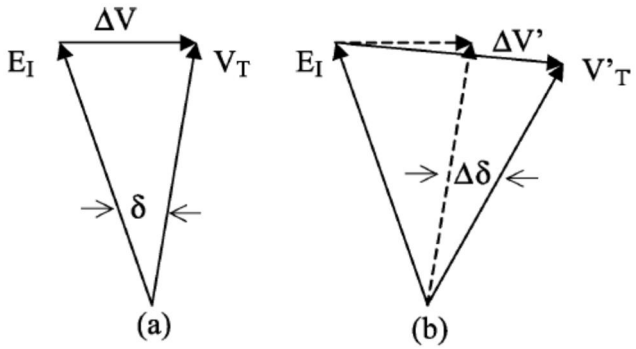

Fig. 3.4. *The voltage vectors of the generator during normal (a) and island mode (b) [55]*

Fig. 3.5 illustrates the same phenomenon in a time domain. The moment at which the generator becomes islanded is marked with the letter A in the figure. Commercial vector shift relays measure the length of each cycle and compare the measured value to the reference. A trip signal is issued if the difference between the measured and the reference cycle length is larger than the predefined threshold. [55]

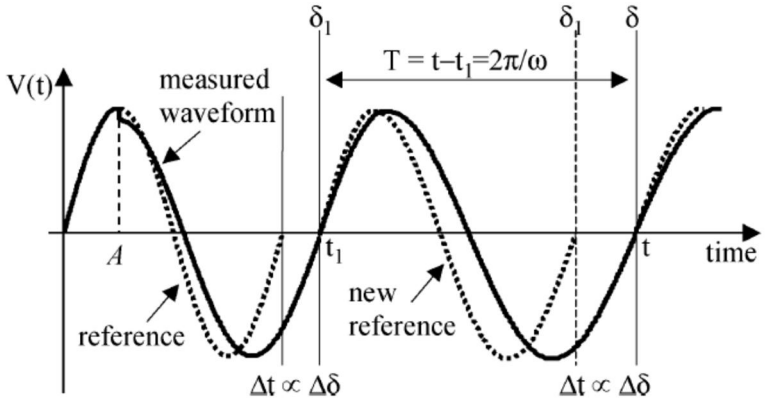

Fig. 3.5. *The voltage vectors of the generator during normal (a) and island mode (b) [55]*

The downside of vector shift relays is the difficulty of choosing appropriate settings. This stems from the fact that the starting of certain loads like motors causes phase shifts that can initiate nuisance tripping [20]. Vector shift relays can also be blinded if the local load closely matches the production. Vector shift relays are still widely used. However, some countries like Denmark and Germany have forbidden the use of vector shift relays due to the risk of nuisance tripping [56].

3.2.4 Other passive methods

A large number of passive LOM protection methods in addition to those presented above have been proposed in the literature. This subsection gives a brief introduction to these methods.

The rate of change of power (ROCOP) method, as its name implies, monitors the output power of the protected DG unit and aims to detect islanding based on sudden changes in the output power. The idea behind this is that the output power of the DG unit often changes during the transition to islanding. This method has been shown to have fair performance in the presence of unbalanced loads [57], but its effectiveness is reduced in the presence of balanced loads [58]. Moreover, the use of this method is problematic for DG units whose output power varies significantly, such as wind or solar power based DG units [58].

Rate of change of voltage (ROCOV) is not a widely utilized LOM protection method. However, it has been proposed to be used together with other LOM protection methods; for instance ROCOV and changes in power factors were proposed by [59]. The use of ROCOV could, nevertheless be problematic if the protected DG unit needs to have LVRT capability.

Rate of change frequency over power (df/dP) is considerably larger for systems with small generating capacity in comparison with large power systems. This can be used for islanding detection [60]. The df/dP method is more sensitive [60] and less prone to nuisance tripping [58] than plain ROCOF. However, this method is not immune to the NDZ problem.

Neutral voltage displacement is primarily meant for earth fault protection purposes, but according to [61], it can be added to a LOM relay to aid LOM protection. However, the method only operates as a consequence of earth faults and does not help in detecting islanding caused by other incidents. The practical use potential for this method for LOM protection purposes is further limited as neutral voltage displacement caused by MV side earth faults cannot be detected from the LV side of a delta-wye type transformer. Moreover, the operation times of neutral voltage displacement function at DG sites has to be coordinated with the feeder protection, so that the DG unit is not tripped due to earth faults at adjacent feeders. The required coordination time for this makes this method rather slow [54].

Harmonics detection based LOM protection, which is mainly applicable for converter-coupled DG units, is based on monitoring the total harmonic distortion (THD) of the connection point voltage. The main idea behind the method is that the output currents of the converters contain a certain amount of harmonics. When the utility grid is present, the harmonic currents fed by the converter do not distort the voltages at the connection point of the DG unit significantly, as the utility grid presents a low impedance path for the harmonic currents. However, when the protected DG unit becomes islanded, the harmonic currents flow to the local islanded loads whose impedance is typically significantly larger than the impedance of the utility grid, and thus cause distortion in the connection point voltage. The THD of the voltage may also increase due to the non-linear voltage response of certain loads and islanded step-up transformers used for connecting DG units. When the predefined tripping threshold of the THD of the voltage is exceeded, the method gives a trip command. It is, however, challenging to choose a threshold that does not lead to tripping during normal operating conditions and yet ensures that islanding can be detected. This method may fail to detect islanding, especially when the islanded load has a high quality factor, that is, the load exhibits a certain amount of low pass characteristics that attenuate high frequencies. Another challenging issue for this method is that the voltage THD may be higher than expected in normal grid-connected operation due to the high amount of power electronics in the local loads and the high amount of converter-coupled DG. [20]

Voltage unbalance monitoring can also be used to facilitate islanding detection. The idea behind this is that the voltage unbalance often varies after losing the connection to the main grid, even if the local demand would not change significantly because of changes in network configuration. [62] This method can only be used in multiple-phase systems and it is mostly effective in networks which contain significant amounts of customers connected to a single phase [54]. Moreover, this method alone cannot guarantee reliable LOM detection and it is, therefore, usually supplemented with some other methods, such as harmonic detection and voltage magnitude monitoring [62].

The authors in [63] proposed an islanding detection method based on the spectral analysis of the voltage waveform at the point of common coupling. The measured voltage period at the PCC is filtered and used for setting the command period of the inverter. This should have very little influence on the power quality provided that the grid frequency is constant. When islanding occurs, any tiny perturbation in voltage tends to cause a transient due to the filter, and there will thus be a distinct low frequency signature in the proportional power spectral density variable. However, this method may be prone to nuisance tripping caused by certain disturbances, and the inventors of this method are, therefore, planning to combine this method with an active method in order to avoid nuisance tripping problems. [63]

Many LOM protection methods based on wavelet transform have been proposed in the recent years. The wavelet transform is a mathematical function that can be used for obtaining a time-frequency representation of a signal. The transform is especially advantageous for representing the time-frequency representation of a non-stationary signal (i.e. a signal that consist of time-varying spectral components) for applications where time and frequency localization are needed. Islanding detection is one such application and a large number of LOM protection methods utilizing the wavelet transform have been proposed in the literature in recent years, such as [64]-[68]. Choosing a suitable arbitrarily chosen threshold that guarantees satisfactory protection sensitivity and security may be challenging for wavelet transform-based LOM protection [66].

The basic idea of computational intelligence based LOM protection methods is to mimic human intelligence [69]. These LOM protection methods can be based, for instance, on techniques such as decision tree classifiers [70], artificial neural networks [71] and fuzzy logic controls [72] techniques. Computational intelligence based methods can also be based on harnessing active LOM protection methods as proposed in [73]. Categorization of computational intelligence based methods to passive or active thus depends on whether they utilize passive or active methods for the detection of islanding.

3.3 Active LOM protection methods

Active LOM protection methods are based on injecting small perturbations into the grid and monitoring the response of the system. When the grid is present, the injected perturbations are not able to cause significant changes due to the presence of the stabilizing main power grid. However, if the connection to the main power grid is lost, the injected perturbations are designed to alter the chosen quantities significantly enough for the detection of islanding.

3.3.1 Slip mode frequency shift

The idea of slip mode frequency shift (SMS) is to apply positive feedback on the phase of the connection point voltage in order to destabilize the inverter of a DG unit when the unit becomes islanded. When DG units are operated at unity power factor, the phase angle between the output current of the inverter and the connection point voltage is controlled to zero. In this LOM detection method, however, the angle between voltage and output current is set to be a function of the deviation of the frequency of the last cycle from the nominal operating frequency as shown in equation 3.1. [74], [20]

$$\theta = \theta_m \cdot sin\left[\frac{\pi \cdot (f - f_r)}{2(f_m - f_r)}\right] \tag{3.1}$$

where f_m is the frequency at which the maximum phase shift θ_m occurs, f_r is the nominal frequency and f represents the frequency of the previous cycle. [74] The principle of the method is further illustrated in fig. 3.6. As the figure illustrates, the phase response curve of the inverter is made steeper than the load phase curve in the vicinity of the nominal frequency (60 Hz in the figure) which makes the line frequency an unstable operating point for the inverter. During grid-connected mode the utility voltage provides a stable reference for the inverter, but during island mode there is no such stabilizing reference. As a result, the positive feedback will start to destabilize the frequency during island mode unless the frequency is exactly at the intersection point of the two curves in Fig. 3.6 (60 Hz in this case). The frequency of the power island will then gradually drift to either of the two intersections points (A or C in Fig. 3.6). The phase response curve of the inverter should be designed so that the intersection points A and C are outside the UFP / OFP limits which makes it easy for the frequency protection to detect islanding. [20]

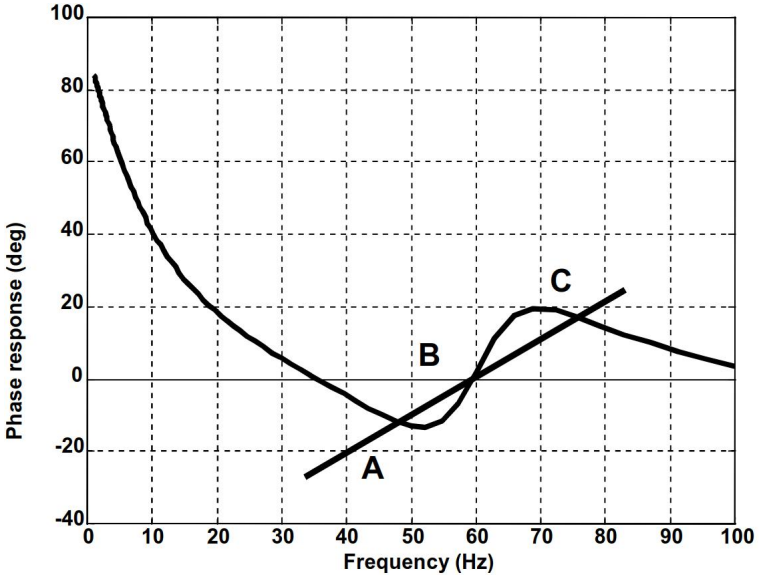

Fig. 3.6. *The operating principle of slip mode frequency shift method [20]*

Slip mode frequency shift is implemented by modifying the input filter of the phase-locked loop which is relatively simple. This method is fairly attractive because the NDZ of this method is relatively small and also because the power quality problems caused by this method are rather small in comparison to many other active methods. However, system level stability and transient response problems may occur when this method is used widely or if high positive gains are utilized in the positive feedback. [20] Moreover, a non-detected islanding may occur if the load line is steeper than the SMS line in the unstable region, i.e. between the intersection points A and C in Fig. 3.6 [75].

The authors of [76] proposed an improved version of the SMS method, namely automatic phase shift (APS), which introduces an additional phase shift. This additional phase shift is aimed at breaking the possible stable operation points that could lead to non-detected islanding when the basic SMS method is used. However, according to [77], the operation time of the APS method can sometimes be long or the method may completely fail to detect islanding because the additional phase shift is only added at each possible stable operating point. With the aim of overcoming this deficiency, [77] proposed another method based on the principles of the SMS method, that is adaptive logic phase shift.

3.3.2 Active frequency drift

The idea in active frequency drift (AFD) method is to manipulate the current waveform injected by the inverter so that there is a continual tendency for the frequency to go up or down. This is achieved by controlling the period of the output current of the protected DG unit so that is has an offset to the measured voltage waveform. During the grid-connected state, this maneuver is not able to

change the frequency of the grid. However, if the protected DG unit is islanded, the frequency has a tendency to drift up if the period of the reference signal of the inverter current is shorter than the period of the voltage. Accordingly, the frequency has a tendency to drift down if the period of the current reference signal is longer than the period of the measured voltage. [78] This manipulation has only a minor effect on the utility frequency during grid-connected conditions since the inverter output current is reset for each cycle of the utility network voltage. However, when the protected DG unit becomes islanded, the frequency is determined by the output current and the local load impedance. [74] The basic idea of the AFD method can be seen from Fig. 3.7. T_{Vutil} is the period of the main grid voltage, whereas, T_{Ipv} is the period of the sinusoidal part of the current injected by the inverter. The current injected by the inverter is equal to zero for a short period, which is marked with t_{z} in the figure. The ratio of t_{z} to half of T_{Vutil} is called the chopping factor. [20] The chopping fraction can be expressed as in equation 3.2.

$$cf = \frac{2 \cdot t_{\mathrm{z}}}{T_{\mathrm{Vutil}}} \tag{3.2}$$

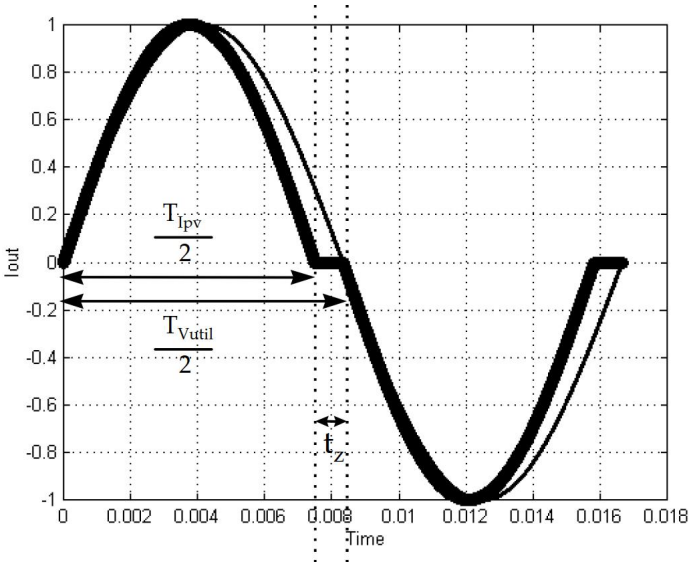

Fig. 3.7. *The operating principle of active frequency drift method [20]*

When this kind of current is fed to a resistive load in an islanded circuit, the voltage follows the current and reaches the zero crossing point earlier than normal. This, further on, causes a phase error between the connection point voltage and the injected current. In order to correct this phase error, the inverter then increases the frequency of the injected current. The voltage response of the resistive load will again be such that the zero crossing point is reached earlier than expected, which

again causes the inverter to increase the frequency of its current output. This goes on until the frequency has drifted outside the OFP / UFP limits, which can then be detected by the frequency protection. [20]

This method is simple to implement in DG units connected via a micro-controlled inverter. However, there would have to be an agreement concerning the direction of the frequency manipulation between manufacturers in order for this method to be utilized in cases where several DG units are to be protected by this method. This method is probably of little practical value because its NDZ is fairly large in comparison to the NDZs of other active methods. [20]

3.3.3 Sandia frequency shift

Sandia frequency shift, which is also known as active frequency drift with positive feedback, can be seen as an improved variant of active frequency drift. As discussed, active frequency drift suffers from a fairly large NDZ. In order to alleviate this problem, [27] proposed that the chopping fraction in the AFD method should be made a function of the frequency as shown in equation 3.3.

$$cf = cf_0 + K(f_{\mathrm{CCP}} - f_{\mathrm{Grid}}) \tag{3.3}$$

where cf_0 represents the chopping fraction when there is no frequency error, K is the chosen gain, f_{CCP} is the frequency at the connection point of the DG unit and f_{Grid} is the main grid frequency. When the DG unit in question becomes islanded and there is a small positive deviation in the measured frequency f_{CCP}, the error term ($f_{\mathrm{CCP}} - f_{\mathrm{Grid}}$), and consequently the chopping fraction, increase, and as a result, the inverter increases its output frequency. This will go on until the measured frequency reaches the OFP limit. Accordingly, a negative initial deviation in measured frequency will gradually make the frequency reach the UFP limit (in this case chopping fraction becomes negative which means that the period of the inverter current is longer than the period of the connection point voltage). [20]

3.3.4 Other active LOM protection methods

Reactive power export error detection is based on adjusting the protected DG unit to feed a certain amount of reactive power to the grid. The idea behind this is to select a level of reactive power production that can only be maintained during the grid-connected state. Thus, when the protected DG unit becomes islanded, the reactive power output of the DG changes significantly, which can be used as an indication of islanding. [49], [58] This method has high sensitivity, but due to its slow operation time, it is mainly suitable for back-up protection purposes [79].

The fault level monitoring method is based on the fact that power islands have a lower short circuit capacity than large systems [61]. The fault level can be determined with an arrangement, where a

shunt inductor connected via a thyristor switch is triggered near the voltage zero, and the current flowing through the shunt inductor is then monitored. This method provides rapid operation times but has the disadvantage of introducing a small glitch at the voltage zero crossover point. [79]

The idea behind the impedance monitoring method [20] is to vary the amplitude of the output current, and thus also the output power of the DG unit converter. During islanding, this output current variation will cause a change in the connection point voltage, which can be used for islanding detection. In practice, this method monitors the change of impedance, that is dV/di. Hence the name, impedance monitoring.

The Sandia voltage shift method applies positive feedback on the voltage magnitude. The method is based on making the output power of the protected DG unit a function of voltage magnitude. Whenever the connection point voltage of the protected DG unit decreases, this LOM protection method orders the DG unit to reduce its output power. If the DG unit is islanded, the reduction in output power will result in a further decrease in voltage magnitude. Consequently, the Sandia voltage shift method will order the protected DG unit to further decrease its output power. This cycle continues until voltage magnitude has dropped below the utilized undervoltage protection limit. [20] This is fairly effective, especially if used in conjunction with a suitable frequency drifting-based LOM protection method, but it also has some shortcomings, particularly, that reducing the output power results in lost revenue for the owner of the DG unit. Because of this, this method is not among the most attractive LOM protection methods.

Reactive power variation (RPV)-based LOM protection methods are favorable in the sense that they do not cause current distortion, unlike many other active LOM protection schemes [80]. Modifying the reactive power output of the DG is also economically more reasonable than modification of the active power output. References [81]-[83] are examples of RPV-based methods. If the injection of periodical reactive power pulses is undesirable, another similar type of approach is to use a dedicated reactive power versus frequency (Q-f) droop, which aims to destabilize islanded circuits [29]. The DG unit itself is typically the source of the desired reactive power variations but it is also possible to use an external reactive power compensator for this purpose [84]. However, in this case the method is referred to as the reactive power compensation method [84].

3.4 Remote LOM protection methods

With proper design, configuration and settings, remote methods can provide rapid LOM protection without the risk of non-detected islanding. However, due to the risk of malfunction in the communication scheme, a local LOM protection should always be used as a back-up protection. The ENTSO-E grid code also states that LOM protection should not solely rely on the network operators' switchgear position signals. It is also good to bear in mind that remote LOM protection methods are only as reliable as the utilized communication medium.

3.4.1 Transfer trip scheme

Transfer trip, which is also known as the disconnect signal scheme, is based on detecting islanding by monitoring the status of chosen upstream circuit breakers and sending a trip signal to the relevant downstream circuit breakers whenever an opening of an upstream circuit breaker should cause islanding. The utilized communication medium can be based on many different kinds of solutions such as pilot wires, public telecommunication wires, radio channels etc. [54]. Fig. 3.8 illustrates the operating principle of a transfer trip scheme. Whenever the opening of an upstream circuit breaker causes a network section containing DG to become islanded, a disconnect signal is sent to the relevant IEDs at the DG sites.

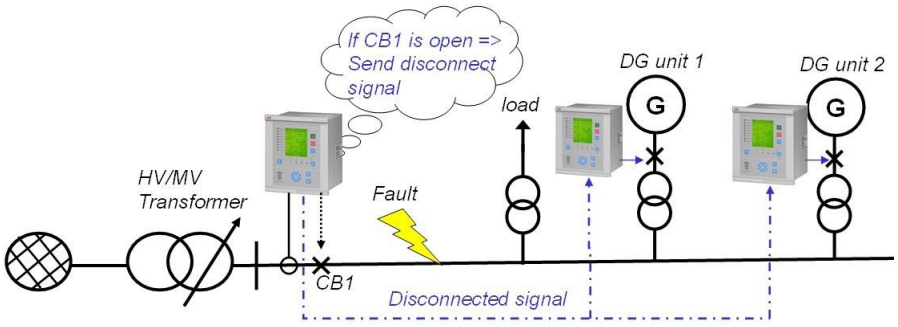

Fig. 3.8. *The operating principle of transfer trip method*

With an appropriate communication medium and operating logic, this method is one of the most effective LOM protection methods. That is, this scheme is completely immune to the NDZ problem and can meet the LOM protection requirements set by fast automatic reclosing, provided that suitable communication medium is utilized. The downside of this method is that the high requirements set for the communication medium tend to make this LOM protection method too expensive for small DG installations [54]. Moreover, a local LOM protection method is always needed for back-up protection purposes. The disadvantage of the high investment cost could probably be alleviated to some extent by utilizing the applied communication scheme additionally for other purposes. Such

an idea is presented in [85], which uses the optical links between consecutive differential- or distance protection IEDs for LOM protection purposes as well. Extending the parallel use of the utilized communication medium from solely protection-related tasks to control and measurement-related signaling would probably further reduce the cost of the transfer trip scheme.

3.4.2 Power line carrier based LOM protection

Power line carrier (PLC)-based LOM protection is based on continuously sending a subharmonic signal to the protected network from a central location using the power line carrier. Whenever an upstream circuit breaker is opened, all the local PLC receivers at the DG unit sites downstream from this circuit breaker stop receiving the centrally injected PLC signal. The local IEDs at the DG sites then interpret this as a sign of islanding and issue trip signals to disconnect the DG units in question. The PLC signal generator is typically placed at the substation, whereas the signal detectors are installed on the local LOM IEDs at the DG unit sites. [86], [87]. Special attention should paid when choosing the frequency of the PLC signal [88]. A low signal frequency is superior to high signal frequencies [87]. This is because low frequency signals propagate through distribution transformers, which means that the signal can also be received on low voltage networks [87]. Thus, using suitable low frequency PLC signals, this method can also be used for the LOM protection of small-scale DG units connected to the low voltage network. However, it is important to ensure that the chosen PLC is frequency is not too close to the system's resonant frequency [88].

3.4.3 SCADA/DMS based LOM protection

This method is based on extending the SCADA to cater for all the DG units. Whenever the opening of a switch should lead to islanding of a network section, the SCADA system can determine which DG units need to be disconnected. This method is advantageous in the sense that it does not have to be configured to a certain network section, i.e. the method can be used for any network and can be extended to cover larger network areas [89]. However, the downside of this method is the associated high cost of establishing the required communication infrastructure. As with other communication based LOM protection methods, the operation time of SCADA-based LOM protection is highly dependent on the utilized communication medium.

3.4.4 Other communication-based methods

The phasor measurement unit (PMU)-based LOM protection method is based on placing one phasor measurement unit to measure the voltage and phase at the substation, and another at the DG site. The measurements at the substation are time-stamped and sent to the relay at the DG site, which then compares the two measurements and assesses whether the DG unit is connected to the main

grid or not. Small delays do not cause any harm since the time-stamping enables accurate comparison of the two measurements. [90] However, the functioning of this method is completely dependent on the functioning of the communication channel. This problem can be alleviated by using a phase-locked loop or "a digital synchronous generator" in the relay so that there would be a reference grid frequency for a while, even after the sudden loss of communication. [91]

The comparison of rate of change of frequency (COROCOF)-based LOM protection method is based on comparing two ROCOF measurements taken from different locations. One measurement point is at the substation and the other one at the DG unit connection point. If the ROCOF at the substation changes significantly, a block signal is sent from the COROCOF IED located at the substation to the DG relay. The COROCOF relay at the DG site thus trips only if it detects a sufficiently high change in frequency and it does not receive a block signal from the substation. This significantly reduces the risk of nuisance tripping as any system-wide frequency transients that exceed the ROCOF tripping threshold cause the COROCOF IED at the substation to issue a block signal to the COROCOF IED located at the DG site. [61], [91], [98]

Islanding detection can also be facilitated by applying the reactance insertion method. The idea behind this method is that a large reactance is connected to the potential island side of the circuit breaker that connects the potential power island to the grid. The reactance, which is typically a capacitor bank, is switched on after a suitable delay time once the circuit breaker connecting the potential island circuit to the main grid opens. The delay is needed for ensuring that the connected reactance cannot stabilize the islanded circuit. That is, the delay has to be long enough to give the utilized LOM protection time to operate before switching the reactance on. If the existing power imbalance before the reactance is switched on is so small that the utilized LOM protection does not detect the islanding, then the power imbalance will change sufficiently after the insertion of the reactance. Although the reactance insertion method clearly facilitates islanding detection, it suffers from a couple of significant drawbacks. Firstly, there may be several consecutive switches, whose opening may lead to islanding, and a suitable reactance would have to be placed next to all these switches. Secondly, islanding detection using this approach is rather slow due to the required delay time between the opening of a relevant switch and insertion of the reactance. [92]

The authors in [93] and [94] suggest that the internet could be used as a medium for taking care of the necessary communication between network nodes for establishing efficient LOM protection. The transfer trip scheme and the broadcasting of a reference utility frequency or phase angle were evaluated as suitable applications in [93]. An internet-based communication channel could naturally be used for various other active network management purposes, such as active voltage control or frequency reserve purposes. However, the reliability of the communication channel has to be very high and the cyber security issues related to the use of internet need to be taken into account. [94] It is advisable to use additional passive LOM detection as a back-up protection since failures may

sometimes occur in the communication system. However, the passive back up LOM protection can be set to have loose settings at all times when the communication channel is working, and stricter settings only whenever the local relays at DG unit sites detect a failure in the communication channel. [94] proposes that the communication channel self-check could be performed every 5 s.

3.5 Summary

Passive methods are affordable and do not degrade power quality unlike the active LOM protection methods. Furthermore, passive methods are applicable to all types DG units. Because of these benefits, many passive methods such as voltage magnitude and frequency, ROCOF and vector shift-based LOM protection methods are still widely used. However, the downside of these methods is that they fail to detect islanding when the power imbalance is not sufficiently large.

Active LOM protection methods are typically characterized with better performance than the passive LOM protection schemes. Some active methods are even able to detect balanced islanding, as long as they are configured properly. This, however, comes at the cost of degraded power quality. One problematic issue related to the use of active methods is that the functioning of these methods may be impaired if the injected disturbances between the DG unit installations protected by these methods are not synchronized with each other, or if different kinds of active LOM protection methods are used in the same network area. In such cases, there is a danger that the injected disturbances may cancel each other's effect and thus degrade the performance of these methods. On the other hand, synchronizing the injection of disturbances raises concerns about degraded power quality.

When properly designed, communication-based LOM protection methods are typically technically superior to local LOM protection methods. This is because communication-based LOM protection methods do not rely on local measurements, and they are thus immune to the NDZ problem. In addition, these methods can be configured to be fully compatible with the various requirements set in the grid codes. However, these methods tend to require costly investments in the required communication mediums. The utilized communication scheme has to be highly reliable because communication-based LOM protection schemes are completely dependent on the reliable functioning of the communication. Because of the dependency on the communication scheme, grid codes typically require that a local LOM protection is additionally used as a back-up protection system. It is thus important to plan the local back-up protection settings so that they are also in line with the grid code requirements. Communication-based LOM protection schemes are a good choice for large DG installations where the cost of establishing the required communication infrastructure is not too large in comparison to the cost of the DG installation. From the cost point of view, it is also helpful

if the utilized communication medium can also be used for other purposes than only for LOM protection. The PLC-based LOM protection may also be a relatively cost effective choice for the protection of a large group of DG units serviced by the same substation. This is because the highest cost related to this type of LOM protection scheme is borne by the PLC signal generator situated at the substation. The cost of the PLC signal generator may be reasonable if it can be split between a high number of DG installations.

4 Studies performed and methods developed

This chapter briefly reviews the highlights of the eight publications on which this thesis is based. The utilized simulation tools and the principles of the laboratory set-up are presented in the first section. The second section focuses on analyzing how islanding detection differs between when the islanded circuit is sustained only by converter-coupled DG and when it is sustained by synchronous generators. The extent to which the presence of synchronous generators complicates the performance of active LOM protection is also analyzed in this section, which also includes a brief analysis of the effects that the FRT requirements have on LOM protection. Section 4.3 presents the main principles of the proposed NIS-based LOM risk management concept, section 4.4 discusses the active LOM protection schemes which were developed and 4.5 presents the communication-based protection automation concept. The chapter concludes with 4.6, the discussion section.

4.1 The tools and methods used for the simulations

The simulation studies in this thesis were all performed using the electromagnetic transient simulation software RSCAD and PSCAD. RSCAD is a dedicated software used for interfacing to the RTDS® (real time digital simulator). RTDS provides accurate electromagnetic transient simulation for power system studies. An RTDS cubicle consists of a number of processor cards, input and output cards, protocol converter cards and a power supply unit. RTDS was used for the simulation studies in publications [P1], [P2], [P3] and [P6]. Using a real-time simulator like RTDS, it is possible to perform hardware-in-the-loop simulations and thus connect real physical devices, such as protection relays, so that they can function as part of the simulation. This is accomplished by taking selected measurements from the model run by the RTDS as outputs from the simulator. In the studies for this thesis, the measurement signals were amplified to a realistic scale for the protection relays with the help of combined voltage and current amplifiers. Based on the measurements fed by the amplifier, the protection relay then made its possible control decisions and sent the digital control commands back to the RTDS via copper wires. Real protection relays were used in the protection impact studies in publications [P1], [P2], [P3] and [P6]. Some of the studies used a combination of two real-time simulators, namely RTDS and dSPACE. The dSPACE is a well-proven tool for modelling power electronics and control systems. In such cases, a detailed model of a full converter-connected wind turbine was run by the dSPACE simulator, whereas the network model was implemented on the RTDS simulator side. The principles and benefits of connecting these two types of real-time simulators are described in more detail in [95], [96]. In addition to the real time simulators,

the PSCAD software, (used for the simulation studies of [P5], [P7] and [P8]) is a well-known electromagnetic transient simulation program for PC platforms.

The principles of the laboratory set-up, which consisted of two real-time simulators and a protection relay, is illustrated in Fig. 4.1. The network model, modelled with RSCAD, is run in real time by the RTDS simulator shown in the bottom left corner. The dSPACE simulator, which is above the RTDS simulator in the diagram, is simulating the behavior of the modelled wind turbine. The required signal exchange between the two real-time simulators is established via analogue D/A and A/D converters mounted in the simulators. Voltage measurements from the connection point of the DG unit are fed from the RTDS to an omicron CMS156 amplifier, which amplified the voltage measurements to a suitable scale for the LOM relay. Based on the measurements, the LOM relay then issued trip signals back to the RTDS in the form of digital signals via copper wires whenever the protection thresholds were exceeded for the set delay time. These trip signals were then configured to control the state of the circuit breaker connecting the DG unit to the network.

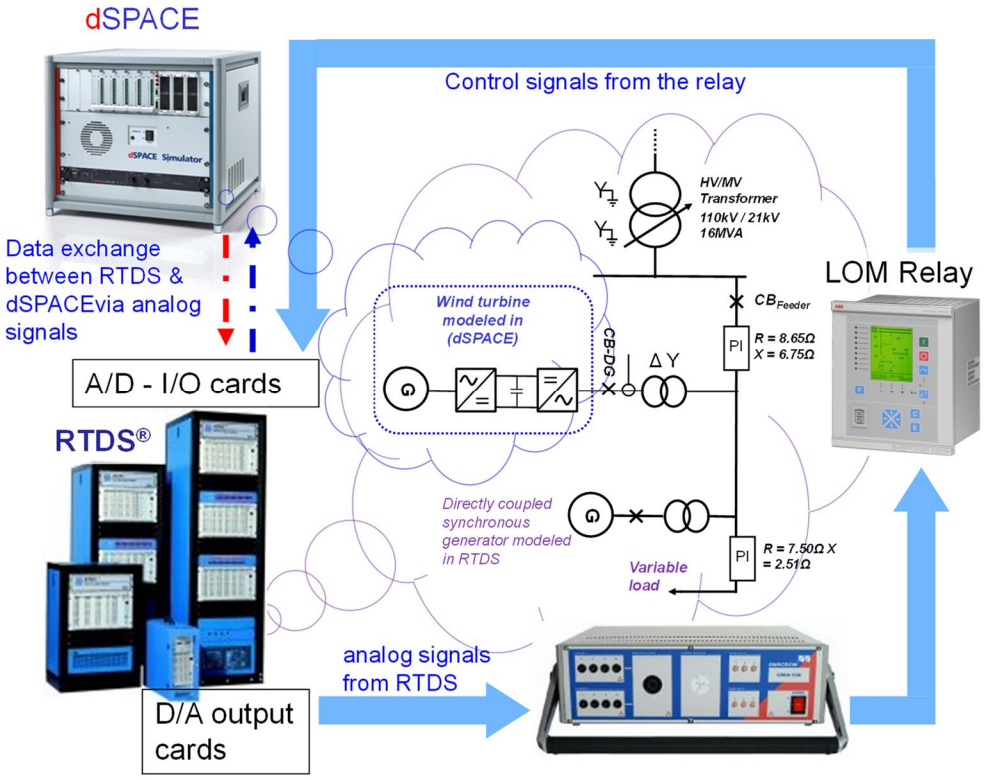

Fig. 4.1. *The real-time simulation laboratory setup [P2]*

4.2 Protection impact studies

4.2.1 Fast automatic reclosing and LOM protection

Failed automatic reclosing and unsynchronized reclosings are one of the main problems with unintentional islanding. The studies started by analyzing how some of the most widely-utilized passive LOM protection schemes can cope with the requirements set by fast automatic reclosings, and how different variables affect their success [P1]. A real LOM protection relay equipped with voltage magnitude, frequency and ROCOF-based LOM protection was used in the study, as was a feeder protection relay equipped with two-stage definite time overcurrent protection and automatic reclosing functions. The analyzed variables were the autoreclosing open time, the LOM protection settings, the active- and reactive power imbalances and the fault types and locations. The simulation model used in the study consisted of a 21 kV medium voltage feeder fed by a 110 kV source via a 110/21 kV transformer and a 1.6 MW-rated directly-coupled synchronous generator. This was connected to the end of the feeder via a step-up transformer. The studies showed that the success rate of fast ARs was very bad when only voltage magnitude and frequency functions were enabled in the LOM relay. The success rate improved significantly when the ROCOF function to the LOM relay. Furthermore, extending the AR open time from 300 ms to 500 ms also improved the success rate of ARs quite remarkably. Another fact the studies showed that the success rate of ARs could also be enhanced with stricter LOM protection settings. However, this measure is not usually possible with the LOM protection settings typically stipulated in the grid codes. Indeed, many grid codes now require the DG units to have LVRT capability as well, which means that less sensitive undervoltage protection settings have to be applied.

4.2.2 The effects of different types of DG unit on LOM protection

Unintentional islanding may not only damage customer equipment (due to poor power quality) but it also poses a potential threat for utility line workers. Thus, it is also important to analyze how islanding can be detected when it is caused simply by a switching action rather than a fault. This is because faults usually result in large fluctuations in the voltage magnitude and cause frequency transients that make the detection of islanding relatively easy. However, when islanding occurs simply due to the opening of a connecting switch, the transition to islanding can be very smooth depending on the local power imbalance in the islanded circuit. This kind of situation can be much more challenging for LOM protection. The studies thus continued by analyzing scenarios in which the islanding was caused simply by a switching action. The emphasis in this study was on analyzing the relations between local active- and reactive power imbalances with voltage magnitude and frequency for an island sustained by different types of DG units. The NDZs of voltage magnitude and

frequency-based LOM protection were mapped based on a great number of simulations in four different scenarios. In the first scenario, the island was sustained only by a synchronous generator, while in the second scenario, it was sustained only by a full converter-connected wind turbine. The simulated NDZ maps showed that the relations between active- and reactive power with voltage magnitude and frequency depend on the type of the DG unit which is sustaining the island. When the island is sustained by a directly-coupled synchronous generator, it is mainly the active power imbalance that determines the frequency in the islanded circuit, while the reactive power imbalance mainly determines the voltage. However, it is the other way round when the islanded circuit is sustained by a converter-coupled DG unit, as shown in Fig. 4.2.

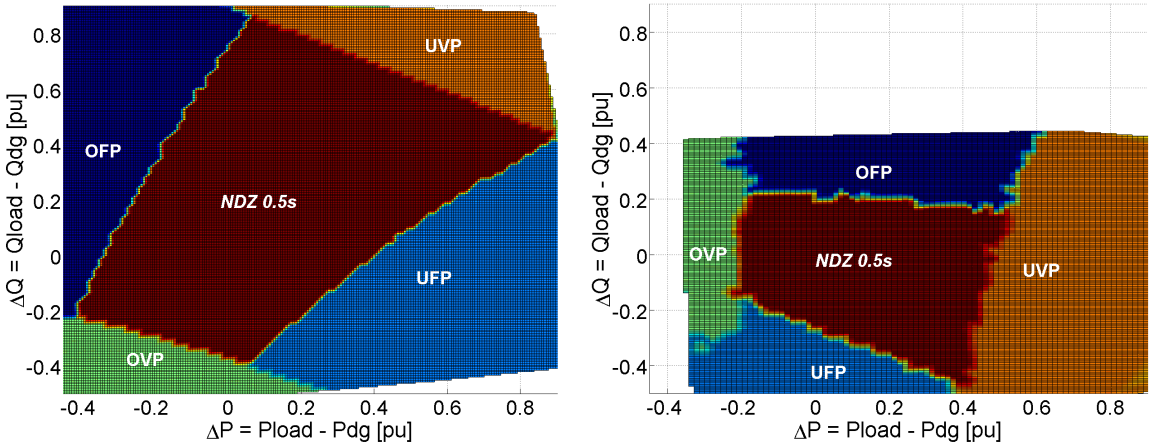

Fig. 4.2. *NDZ of voltage and frequency-based LOM protection when the island is sustained by a directly coupled synchronous generator (left) or a converter coupled DG unit (right) [P2]*

In the third scenario, these two different types of DG units were connected in parallel, and the NDZ of voltage magnitude and frequency-based LOM protection was mapped in the same way, based on a great number of simulations. Although the size of the NDZ changed slightly, the relationships between the active- and reactive power with voltage magnitude and frequency remained close to what they had been when the islanded circuit was only sustained by a synchronous generator. This can be seen by comparing Figs. 4.2 and 4.3. In other words, the synchronous generator dominated the relationships between active- and reactive power with voltage magnitude and frequency.

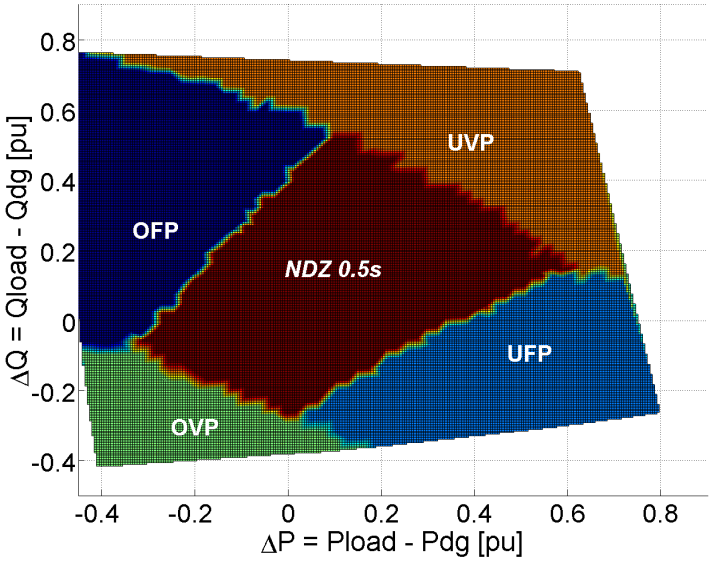

Fig. 4.3. *NDZ of voltage and frequency-based LOM protection when the island was sustained by a directly-coupled synchronous generator and a converter-coupled DG unit [P2]*

The fact that the synchronous generator dominated the relationships between active- and reactive power with voltage magnitude and frequency over the converter-coupled DG unit may have implications for certain active LOM protection schemes. For instance, frequency drifting-based active LOM protection schemes are based on the assumption that the frequency of an islanded circuit can be manipulated by varying the reactive power output of the islanded DG unit. As the NDZ map in Fig. 4.3 illustrates, this assumption may not be valid when the islanded circuit contains both directly-coupled synchronous generator based DG and converter-coupled DG.

The potential threat to the functioning of active LOM protection methods caused by the presence of directly-coupled synchronous generators was analyzed in more depth in [P7]. In this study, the converter-coupled DG unit was equipped with an active LOM protection method, namely Q-f droop-based LOM protection. With suitable Q-f droop settings, this method was able to detect islanding within the required two seconds, even if the power imbalance was set to be non-existent as it is shown on the left in Fig. 4.4. However, when the converter-coupled DG unit was in parallel with a directly-coupled synchronous generator-based DG unit and the power imbalance was set as non-existent, islanding could no longer be detected within 2 s. This is shown on the right in Fig. 4.4. However, the studies indicated that despite the fact that the reactive power injection controlled by the Q-f droop now mainly affected voltage magnitude instead of frequency, the change in voltage changed the consumption of the islanded load, which then altered the active power imbalance as well. This sequence eventually led the frequency to drift out of the utilized frequency protection

limits, as illustrated on the right in Fig. 4.4. However, the detection of islanding took almost 4 s, which is not satisfactory.

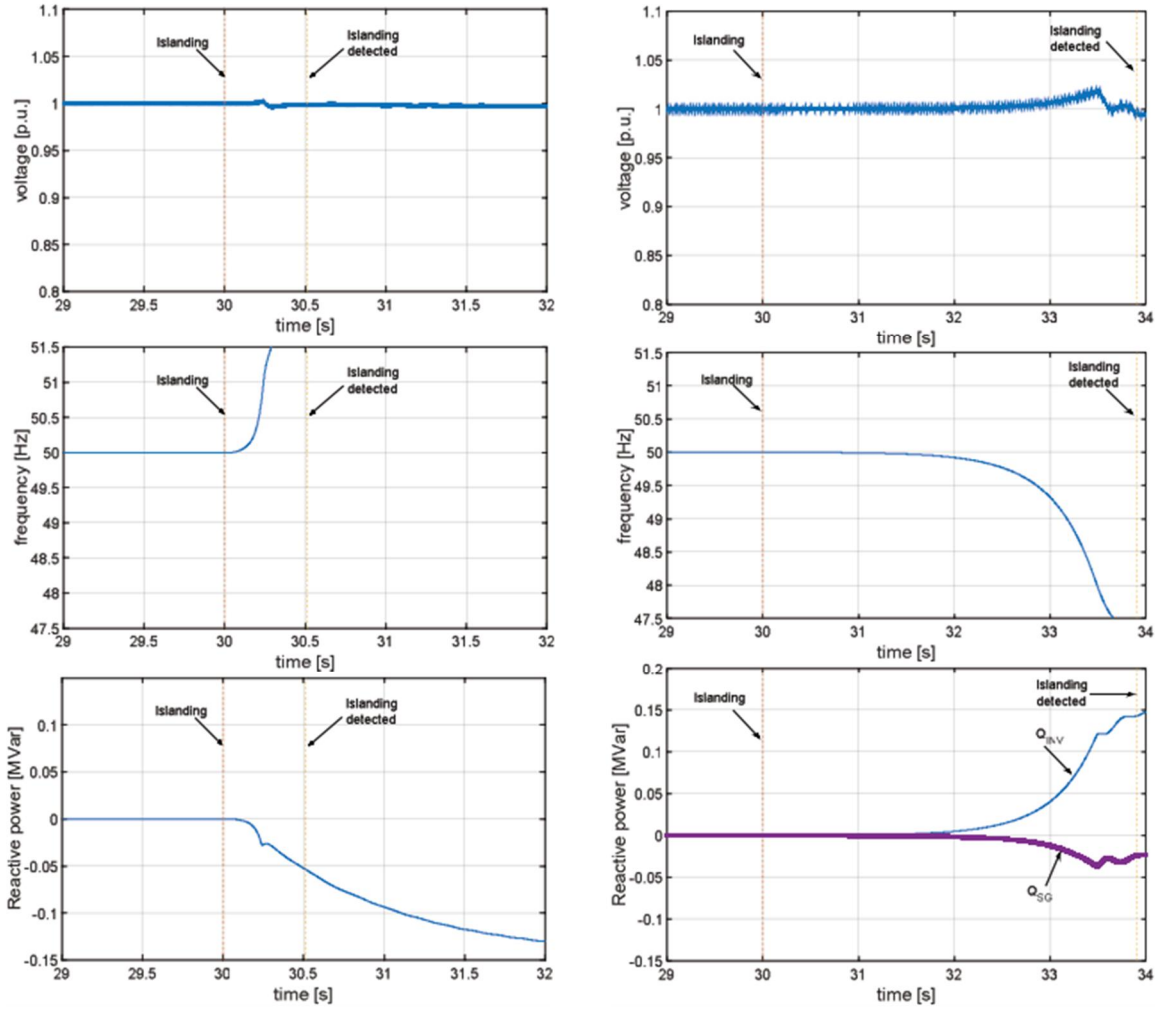

Fig. 4.4. *Islanding is successfully detected when the island is sustained only by a converter-coupled DG unit that is equipped with Q-f droop-based LOM protection (on the left), whereas, islanding is not detected within 2 s when the island is sustained by a directly-coupled synchronous generator and a converter-coupled DG unit [P7]*

Fig. 4.5 gives a broader view of how the performance of Q-f droop-based LOM protection is affected by the presence of a synchronous generator [P7]. The vertical axis represents the islanding detection time, whereas the horizontal axis represents the setting used in the Q-f-droop based LOM protection. The larger the value of the multiplier constant k, the more strongly the reactive power output of the inverter is commanded to react to deviations in frequency. In all the simulated scenarios, the frequency protection delay was set to be 200 ms. Starting from the curves on the left-hand side of Fig. 4.5, the yellow curve represents the case where the island is sustained only by one

inverter-coupled DG unit equipped with Q-f droop-based LOM protection. This curve indicates that islanding detection time can be reduced to approximately 500 ms by using a k multiplier constant value 2.0 in the Q-f droop. The green curve in Fig. 4.5 represents a case where two identical inverter-coupled DG units are connected in parallel, and both of them are equipped with the Q-f droop-based LOM protection. When comparing the yellow and the green curves, one can observe that there is hardly any difference between them. This implies that Q-f droop-based LOM protection is not notably affected when the island is sustained by multiple parallel-connected inverter-coupled DG units that are equipped with Q-f droop. However, the islanding detection time increases significantly if the two inverter-coupled DG units are operating in parallel, but only one of them is equipped with the Q-f droop-based LOM protection. This is understandable, since in order to have the same effect on frequency, the amount of reactive power injected by the inverter-coupled DG unit equipped with Q-f droop-based LOM protection should be doubled when the active power generation in the islanded circuit is doubled [P7]. However, when the inverter-coupled DG unit which is not equipped with Q-f droop is replaced by a directly-coupled synchronous generator with the same nominal power, the performance of LOM protection deteriorates yet more significantly. This case is represented by the dashed red line in Fig. 4.5. This shows that islanding cannot be detected within 2 s, even if the k multiplier constant is increased to as large as 4.0. Fig. 4.5 also presents a case where two inverter-coupled DG units (both equipped Q-f droop based LOM protection) are operating in parallel with one directly-coupled synchronous generator (the purple curve). In this case, the ratio between the inverter-coupled DG to directly-coupled synchronous generator-based DG was two to one. The dashed light blue line represents a similar case, the difference being that the ratio between the inverter-coupled DG and the synchronous generator-based DG is now three to one. The curves show that the performance of the LOM protection gets closer to the original performance indicated by the yellow and green curves as the ratio between the inverter-coupled DG and the directly-coupled synchronous generator-based DG increases.

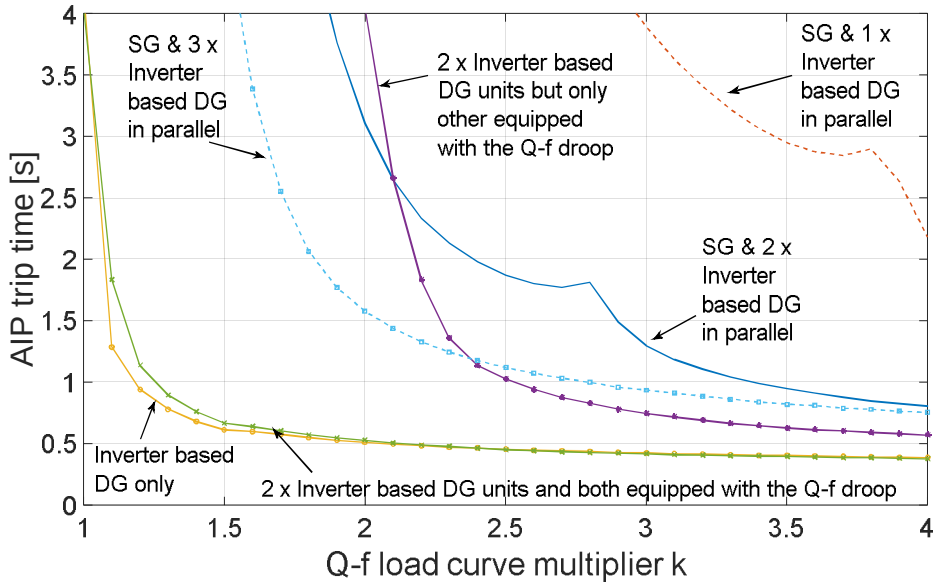

Fig. 4.5. *The effect of the Q-f droop multiplier constant k on islanding detection time [P7]*

The curves in Fig. 4.5 were produced using a synchronous generator whose inertia constant was 0.7 s. Fig. 4.6 illustrates how the inertia constant of the synchronous generator affects the performance of Q-f droop-based LOM protection when two inverter-coupled DG units are both equipped with Q-f droop based LOM protection and are connected in parallel with a synchronous generator. By analyzing both Fig. 4.5 and Fig. 4.6 together, one can have a rough indication of how much the Q-f droop-based LOM protection is degraded by the presence of the synchronous generator.

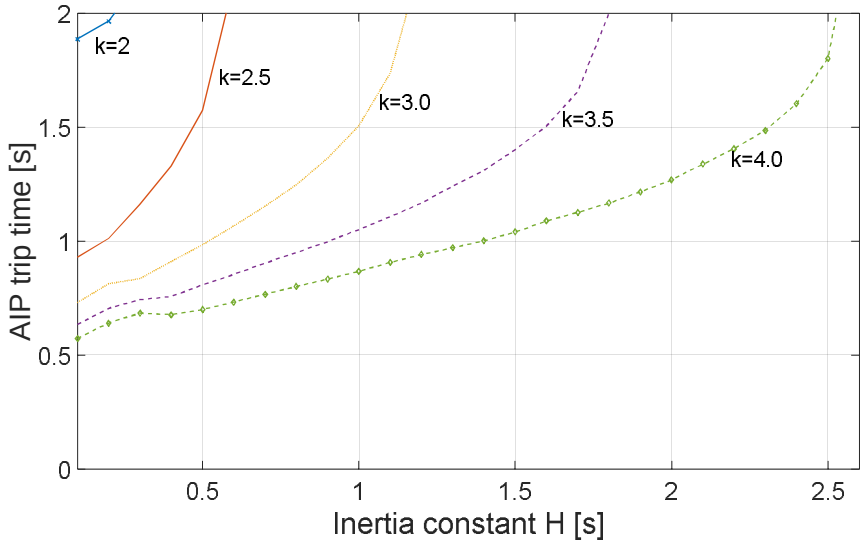

Fig. 4.6. *The effect of inertia constant H on islanding detection performance [P7]*

4.2.3 The effects of FRT requirements on LOM protection

As the use of DG has grown strongly in recent years, many TSOs now require DG units to have FRT capability. In order to fulfill the FRT requirements, DG units not only need to be able to ride through deep voltage dips, but the LOM protection also has to be set to allow this. Many grid codes also require DG units to support the system voltages during LVRT by feeding reactive current into the grid as a function of the voltage. The effect of FRT requirements on LOM protection was analyzed in [P3]. The studies were based on a similar real-time simulation laboratory set-up as was used in [P2]. The studies revealed that the LVRT requirement significantly degrades the performance of LOM protection. This degradation is illustrated with the help of the two NDZ maps in Fig. 4.7. The left-hand side of Fig. 4.7 represents a case where the voltage magnitude and frequency monitoring-based LOM protection was not FRT compliant, whereas the NDZ on the right represents a case where the LOM protection was set to be in line with the LVRT requirements of the Finnish TSO, Fingrid. A comparison of the two NDZs shows that although the NDZ area where it took more than 1.5 s is approximately the same, there is a long extended NDZ area on the right where it took more than 0.7 s to detect islanding. The effect of the reactive current support feature on LOM protection can be seen from Fig. 4.8. As the figure illustrates, the NDZ now twisted significantly. Thus, large reactive power imbalances could still lead to problems in islanding detection.

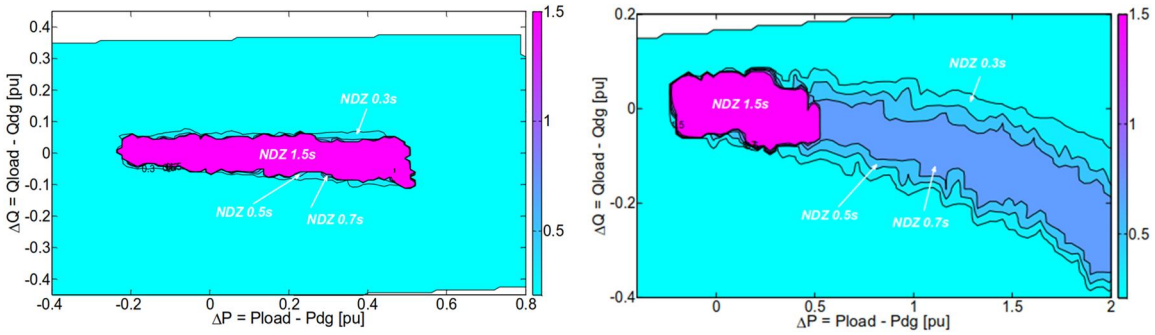

Fig. 4.7. *The effect of LVRT requirements on voltage and frequency based LOM protection [P3]*

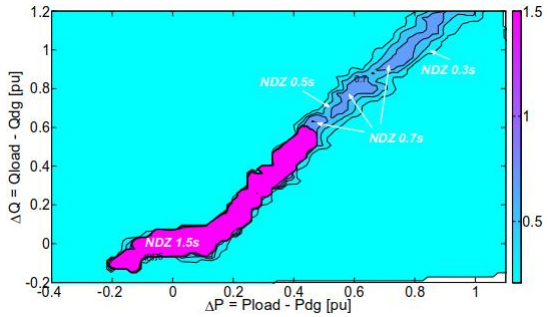

Fig. 4.8. *The effect of LVRT and reactive current support on LOM protection [P3]*

4.3 Network information system-based LOM risk management

It is challenging for the DSOs to evaluate what kind of non-detected LOM risks exist in their networks, and to choose appropriate LOM protection schemes for each DG installation. The knowledge gained in studies [P1] - [P3] gave rise to the idea of an automated LOM risk management tool for DSOs. The tool, which is designed at the concept level, evaluates what kind of power imbalances between local production and consumption might exist in different parts of the analyzed network simply by utilizing the existing calculation tools embedded in modern network information systems. By comparing the possible power imbalances to the predetermined NDZs of the optional LOM protection methods, this LOM risk management tool evaluates which of the optional LOM protection methods are most suitable for each DG unit installation [P4]. Figures 4.9 and 4.10 illustrate how the LOM risk assessment method evaluates the power imbalances, assesses the existing non-detected islanding risk and proposes suitable LOM protection schemes for each DG installation.

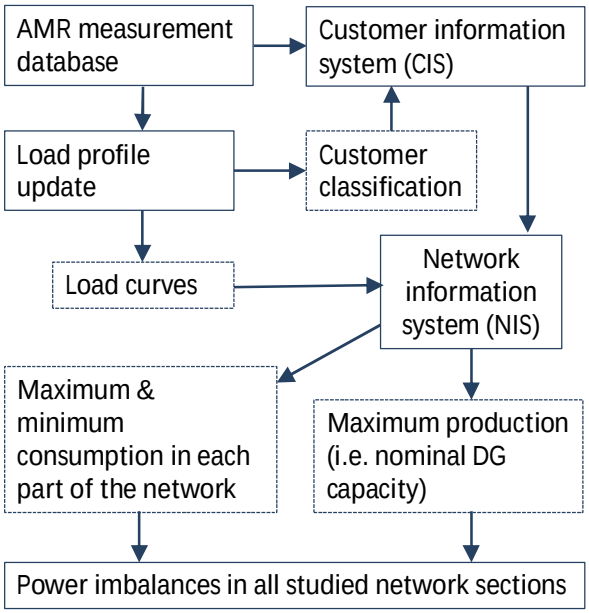

Fig. 4.9. *The principle for estimating power imbalances [P4]*

As Fig. 4.9 shows, the estimates of consumption in the studied network sections is based on utilizing the customer data stored in the customer information system. The modeling of the loads is done with the help of customer-class specific hourly load curves, which are typically divided into between 20 and 50 customer classes. The load curves of each customer, which contain mean and standard deviation values of consumption for every hour throughout the year, is scaled based on the customer's annual energy consumption. However, the accuracy of this estimate can be further improved by utilizing the hourly consumption data provided by the automatic meter reading (AMR) system, as proposed in [97]. Once the estimate of minimum consumption is obtained, the possible

power imbalances in the studied network sections can then be evaluated by comparing the estimated minimum consumption to the maximum production. The risk of non-detected islanding can then be evaluated by comparing the possible power imbalances with the predefined NDZ estimates of the optional LOM protection schemes, as illustrated in Fig. 4.10. The procedure could also take certain predefined preferences into account when evaluating the most suitable LOM protection method for the user, as Fig. 4.10 illustrates. This LOM risk management method could help utility protection engineers significantly in the process of choosing most suitable LOM protection schemes for each DG installation, in raising awareness of possible non-detected LOM risks. [P4]

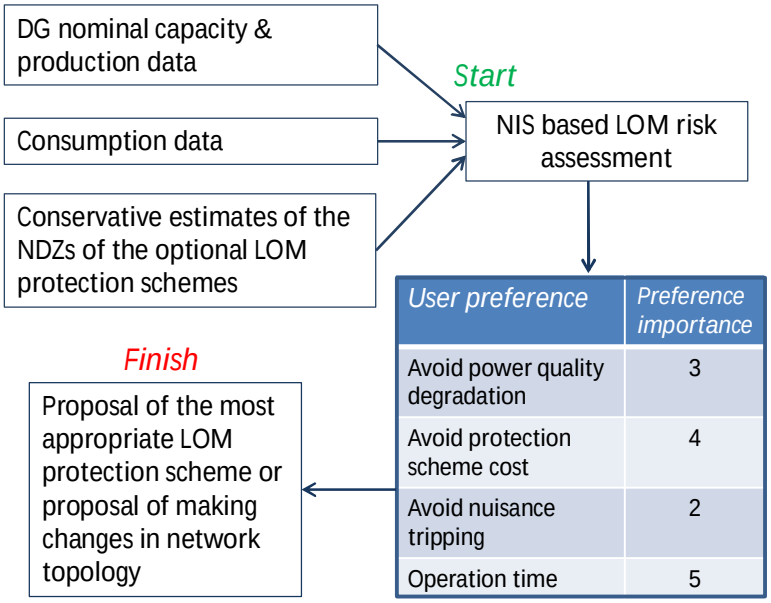

Fig. 4.10. *The NIS based LOM risk assessment procedure [P4]*

4.4 The developed local methods

Two active LOM protection methods were developed during this research work. The first is based on the constant injection of small reactive power pulses and a specific reactive power versus frequency droop [P5]. This method can detect balanced islanding, but it has few drawbacks arising from the constant injection of reactive power pulses and the relatively large reactive power injection required to ensure reliable detection of islanding. A considerably more advanced LOM protection method was subsequently developed, which is based on a combination of a dedicated Q-f droop, a ROCOF function and a frequency checking criterion [P8]. With this method, islanding is detected by forcing the rate of change of frequency to a desired value with the help of a dedicated reactive

power versus frequency droop and by using a specific frequency-checking criterion. This method is able to provide sensitive, secure and rapid LOM protection. Moreover, this achieved with only a modest injection of reactive power. The method is especially advantageous if the utilized grid codes or standards specify broad frequency protection thresholds, which is typical in Europe. This is because the islanding can already be detected well before the moment when the frequency drifts outside the utilized frequency protection thresholds. The operating principle of this method is illustrated in the flowchart in Fig. 4.11.

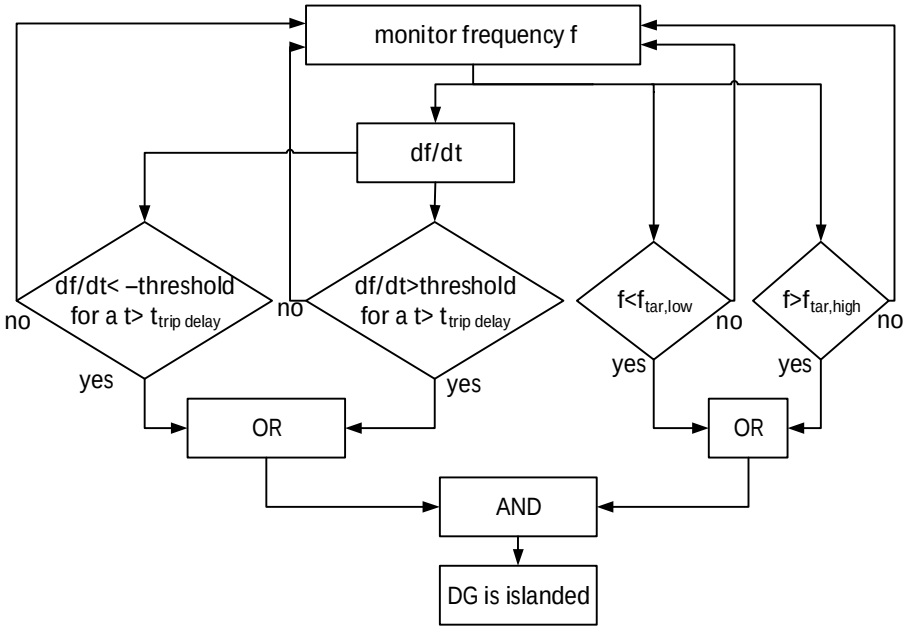

Fig. 4.11. *The operating principle of the LOM protection method presented in [P8]*

As illustrated in Fig. 4.11, this method constantly monitors the frequency and the ROCOF. If the monitored frequency should deviate from the nominal frequency, the *Q-f* droop orders the protected inverter-coupled DG unit to feed or absorb reactive power in inverse proportion to the detected frequency deviation. However, the reactive power reference given by the droop is rate-limited before being fed to the control system of the inverter, which means that the ROCOF only reaches the desired value but does not significantly exceed it. This maneuver reduces the injection of reactive power, especially during short-lasting frequency transients. Whenever the protected DG unit is connected to the main power system, the injected or absorbed reactive power is not able to change the frequency of the power system. However, should the protected DG unit become islanded, the injection or absorption of reactive power causes the monitored ROCOF to a target value, which is larger or lower than the utilized ROCOF tripping thresholds by a suitable margin. However, a trip command is issued only if the ROCOF stays above or below the utilized ROCOF tripping thresholds for a period of time that is longer than the utilized tripping delay while the frequency additionally reaches a certain value ($f_{\mathrm{tar,low}}$ or $f_{\mathrm{tar,high}}$). This additional frequency-checking criterion is aimed at

reducing the risk of unwanted tripping. [P8] Fig. 4.12 illustrates how the LOM protection method proposed in [P8] improves islanding detection in a case where the local active- and reactive power imbalances are set to be negligible. In a case like this, islanding cannot be detected only by using voltage magnitude, frequency and ROCOF-based LOM protection, as is illustrated on the left-hand side of Fig. 4.12. However, when the active LOM protection method proposed in [P8] is utilized, islanding is detected in 433 ms, as is illustrated on the right-hand side of Fig. 4.12. The DG unit used in this study was a 0.5MW-rated full converter-coupled wind turbine.

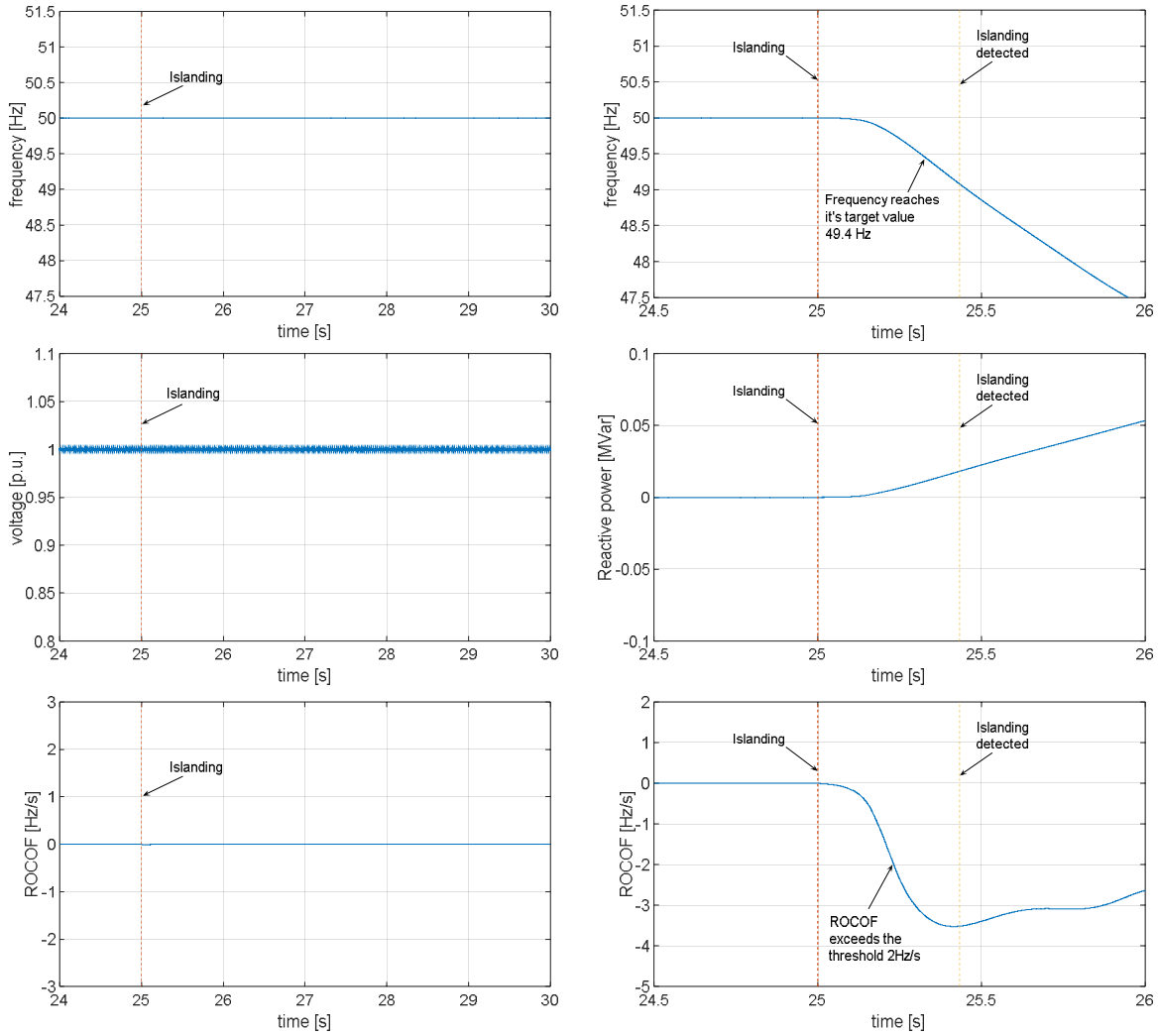

Fig. 4.12. *Monitored frequency, voltage and ROCOF when no active LOM protection is applied (on the left) and when the active LOM protection presented in [P8] is applied (on the right) [P8]*

Fig. 4.13 illustrates the tripping time map of the LOM protection method proposed in [P8] in an active power imbalance versus reactive power imbalance coordinate system. As can be seen from

the figure, islanding was detected in less than 550 ms in all the simulated power imbalance scenarios. Moreover, the reactive power imbalance combinations that lead to an islanding detection time higher than 300 ms are extremely small. That is, the reactive power consumption in the islanded circuit has to be extremely close to the reactive power production in the islanded circuit in order for the proposed LOM protection method to need more than 300 ms to detect the islanding.

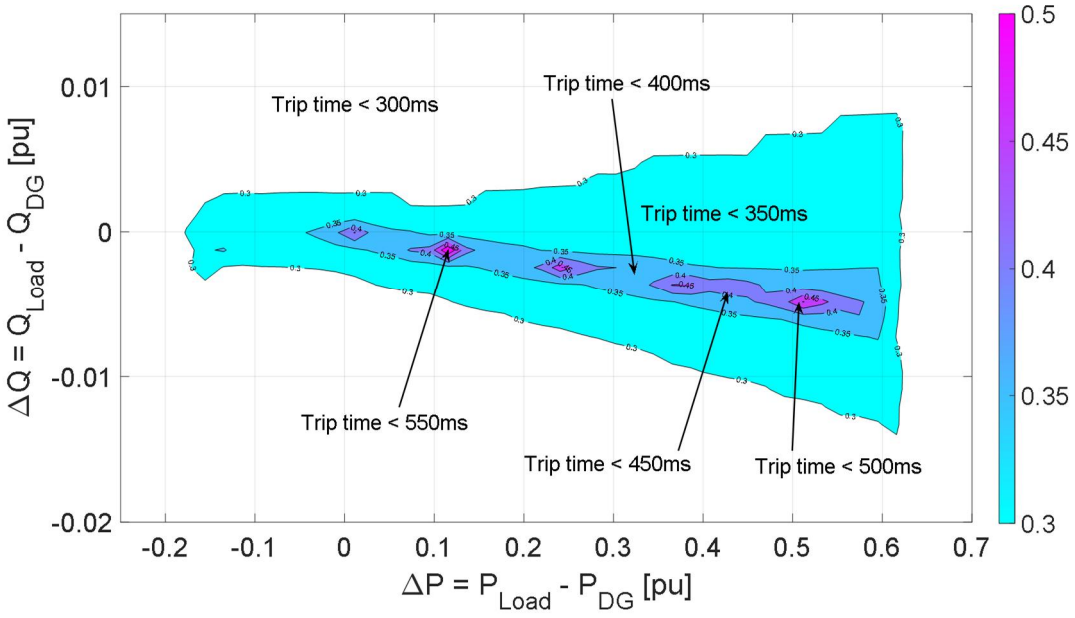

Fig. 4.13. *Tripping time map in an active power imbalance versus reactive power imbalance coordinate system [P8]*

The method proposed in [P8] is designed not to interfere with the frequency or voltage control of power systems during normal operating conditions. This design principle is valid when the frequency is close to its nominal value. However, if the frequency happens to deviate significantly from the nominal value for some reason other than islanding, the injection of reactive power may have an effect on the power system. If the frequency drops, for instance, due to a sudden disconnection of a large generating plant, DG units equipped with Q-f droop will start to inject reactive power to the grid. This has the tendency to raise the local voltages, and consequently, the consumption of voltage-dependent loads. An increased active power demand, in turn, has a tendency to further drive the frequency down. On the other hand, if the frequency is above the nominal, the DG units equipped with Q-f droop absorb reactive power. This has a tendency to lower the voltages, and thus also the consumption of the loads. Therefore, the use of Q-f droop on large scale would have an undesirable impact on frequency control. At the distribution network level, this effect could either be positive or negative, depending on the prevailing voltages in the distribution network.

Because of these issues, it is advisable to analyze the effects of using active LOM protection methods on a very large scale.

The commissioning tests for active LOM protection schemes are somewhat more complex than the commissioning tests for passive LOM protection schemes. This is because of the positive feedback feature used in many active LOM protection methods. Thus, simply using an amplifier with predefined test signals is not suitable for this purpose. Instead, a real-time simulator or real islanding test should be used to verify the functioning of the utilized protection scheme. One option for performing the commissioning tests for active LOM protection schemes is simply to verify the functioning of the utilized protection functions and the utilized positive feedback controls separately. If such an approach were used, the commissioning engineers would have to rely on the factory tests to evaluate the actual performance of the active LOM protection scheme.

4.5 The communication-based protection automation concept

A communication-based protection automation concept was also developed as a part of the work for this thesis. This protection automation concept, which is largely based on the ideas presented in [85], is based on utilizing local measurements and intelligence together with inter-IED communication for better and more rapid decision-making. This concept can be used to tackle typical DG-related protection problems, such as protection blinding, the nuisance tripping of feeders and DG units, and of course, non-detected islanding. In addition, this concept is also designed to enhance the reliability of the distribution service for DG units in networks that are operated in an open ring configuration. This idea is based on arranging an alternative feeding route to a DG unit when its original feeding route is faulted. [P6] The horizontal inter-IED communication was established using the generic object-oriented substation event (GOOSE) defined in the IEC-61850 standard, whereas the optical link between sequential IEDs was used for vertical level communication. The vertical communication could also be established using GOOSE if a suitable communication link is available.

The automatic feeding route change feature was demonstrated with the help of a laboratory set-up consisting of five real IEDs and RTDS [P6]. The test arrangement is illustrated in Fig. 4.14. When a fault occurs at feeder A, the differential protection IEDs marked as “IED A1” and “IED A2” first isolate the fault by commanding the circuit breakers “CB_A1” and “CB_A2” to open. After this, “IED A2” then immediately sends a trip command to the “LOM IED” to disconnect the islanded DG unit. After the disconnection of the DG unit, “IED A2” commands the normally open disconnector “D_B” to close, and after a designated delay, to send a close CB permit to the “LOM IED”.

However, the DG unit circuit breaker “CB-DG” is only closed once the synchronism check function has ensured that the voltage magnitude-, frequency- and phase differences between the DG unit side and the network side of the switch “CB-DG” are within the tolerated limits. If this sequence of switching is successful, the feeding path of the DG unit is changed from feeder A to feeder B and the DG unit can continue supplying power. Such a successful sequence, which was simulated using RTDS and the test set-up shown in Fig. 4.14, is illustrated in Fig 4.15. The uppermost graph in Fig. 4.15 illustrates the medium voltage side currents fed by the DG unit, whereas, the graph below this presents the statuses of the switches. The three lower graphs in Fig. 4.15, reading from the top to bottom, show the voltage magnitudes on both sides of the DG unit circuit breaker, the voltage frequency on the DG unit side of the circuit breaker, and the angle difference of the voltages on the two sides of the circuit breaker. The statuses of the switches show that the protection system is able to disconnect the DG unit very rapidly once it becomes islanded.

The success of the automatic change in the feeding path depends on many factors, such as the DG unit type, the inertia constant of the generator and its nominal power, the mechanical input power at the time of switching and the grid parameters. This is because the DG unit is not able to feed electrical power to the grid during the switching sequence, whereas the primary energy source of the DG unit will most likely continue feeding the same input power to the DG unit. Consequently, in the case of a directly coupled generator, the input power provided by the prime mover accelerates the generator because the electrical counter-torque of the generator falls to close to zero during the switching sequence. If the generator accelerates excessively, it is not possible to reconnect it back to the grid. This was observed in the studies of [P6], where the switching sequence was only successful when the mechanical input torque of the studied 1.6 MW-rated synchronous generator was less than 0.37 pu. Nevertheless, this automatic feeding path change is likely to be easier for converter-coupled DG units. This stems from the fact that the synchronization rules applied in the synchronism check function are not as strict for converter-coupled DG units as they are for directly-coupled synchronous generators. Moreover, the speed of a generator behind a converter is decoupled from the grid frequency, which may enable reconnection to the grid even if the generator should accelerate significantly. However, certain countermeasures may be needed to avoid overspeed problems and excessive voltage rise in the DC link of the converter. [P6]

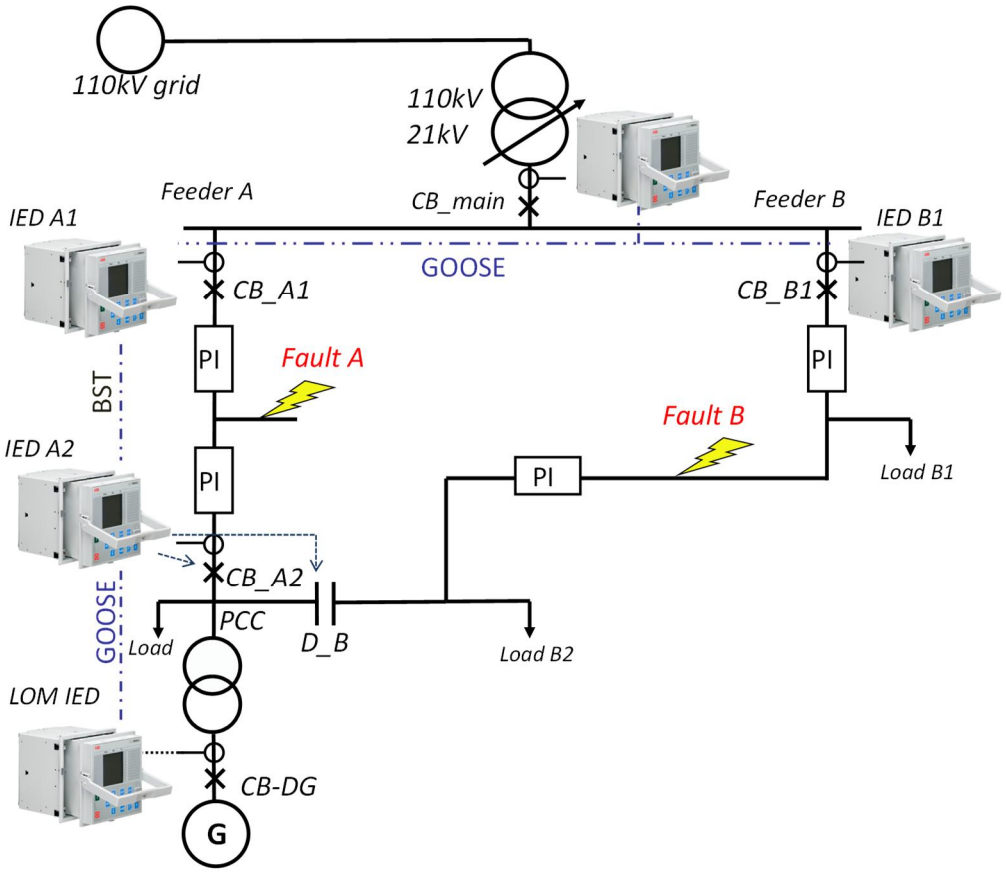

Fig. 4.14. *The network model used for demonstrating the proposed concept [P6]*

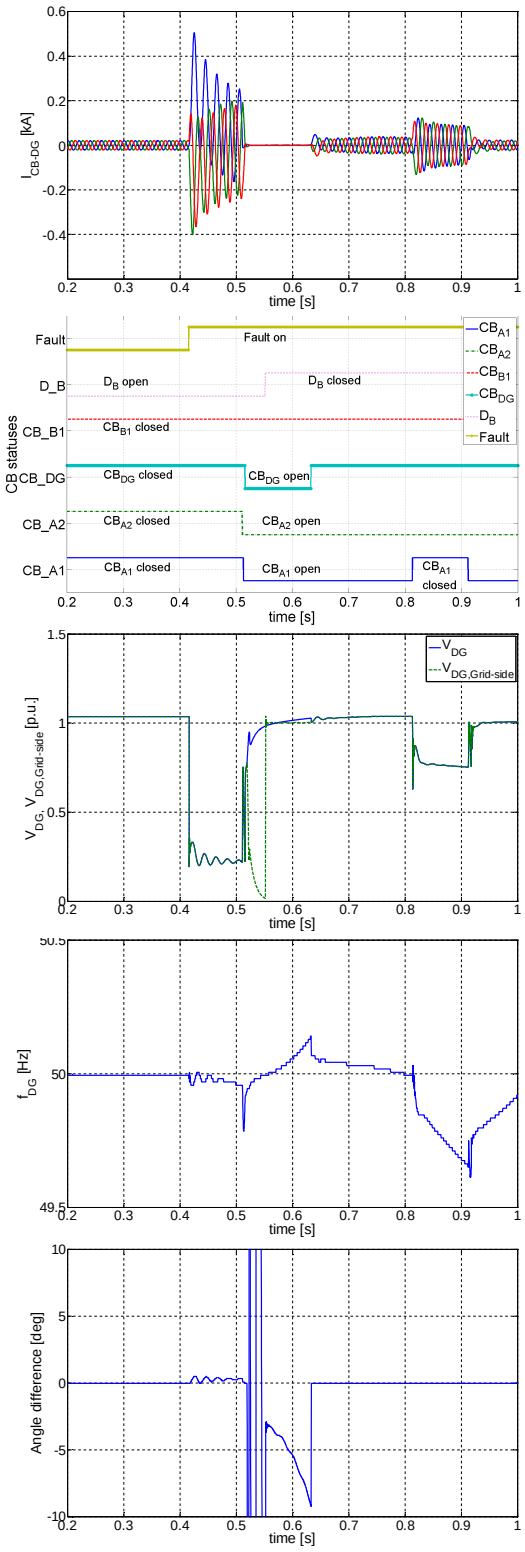

Fig. 4.15. *The network model used for demonstrating the proposed concept [P6]*

4.6 A general philosophy of utilizing the developed methods

The methods developed in this thesis serve slightly different purposes. On the one hand, DSOs could use the NIS-based LOM risk management tool for evaluating what kind of power imbalances may exist in different parts of their networks. If this evaluation indicates that the load is always significantly larger than the maximum generation capacity of the local DG units, then there is no risk of non-detected islanding so passive LOM protection methods should be sufficient. Nevertheless, it is advisable to evaluate if more DG is likely to be connected to the network area in the coming years. On the other hand, if the evaluation indicates that the local power imbalances may sometimes be rather small, more advanced LOM protection is required. Should this be the case, it is advisable to check the ratio between the converter-coupled DG capacity and the directly-coupled synchronous generator-based DG capacity. If the converter-coupled DG capacity is several times larger than the directly-coupled synchronous generator-based DG capacity, then high-performance active LOM protection, such as the method proposed in [P8] is a sensible choice. This provides reliable and rapid LOM protection for a relatively low cost. However, if the power imbalances in the analyzed network sections can sometimes be small, and the ratio between converter-coupled DG units and directly-coupled synchronous generator-based DG is not large, then communication based methods would be called for, such as the one presented in [P6]. The communication-based LOM protection in [P6] is very rapid and completely immune to the NDZ problem, which thus ensures that the DG units protected by this method are rapidly disconnected whenever they become islanded, irrespective of the prevailing power imbalance. The communication-based LOM protection can be used for the protection of all the DG units in the problematic network area, or alternatively, solely for the LOM protection of the synchronous generator-based DG unit(s). This kind of LOM protection planning approach is illustrated in Fig. 4.16.

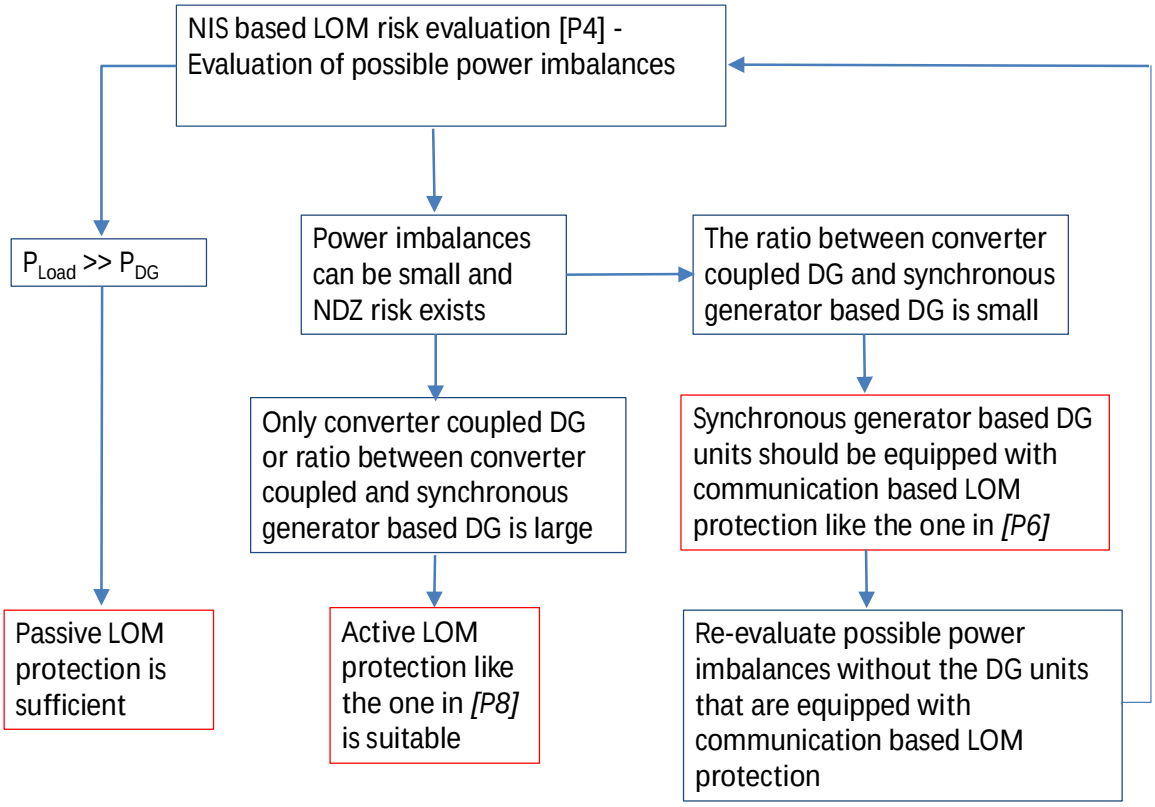

Fig. 4.16. *The philosophy of applying the developed methods*

If the communication-based LOM protection is only applied for the synchronous generator-based DG unit(s), then the possible power imbalance evaluation should be re-run, but this time without the DG unit(s) that are equipped with communication-based LOM protection. This is because the DG unit(s) equipped with communication-based LOM protection are disconnected rapidly, irrespective of the existing power imbalances, thus only leaving the DG units protected with local LOM protection schemes in the islanded circuit. Therefore, the DSO should evaluate whether the production of the remaining DG units can match the consumption of the local loads, and then decide whether passive LOM protection is sufficient, or whether active LOM protection is needed to ensure reliable LOM protection for the remaining DG units.

The use of active LOM protection methods is somewhat problematic, so DSOs should have a clear strategy for their use. This stems from the fact that the performance of active LOM protection is degraded if only some of the DG units in the islanded circuit are equipped with active LOM protection, while the rest are equipped with passive LOM protection methods [P7]. Problems may arise if a DSO first decides to require only passive LOM protection for DG unit installations because the DG capacity in the network area is still low, but then later has to stipulate the use of active LOM protection to accommodate additional DG installations. Furthermore, if different types of active

LOM protection methods are used in the same network area, it is also advisable to ensure that the different types of active LOM protection schemes do not interfere with each other's operation.

DSOs should have clear and transparent rules for sharing the costs incurred by establishing reliable LOM protection. The sharing of costs is obvious if a single DG unit is connected to a distribution network and equipped with a suitable LOM protection scheme. However, it is less straightforward if a number of DG units with insignificant capacity in comparison to local demand, are initially equipped with simple, passive LOM protection schemes, and then later, as more DG units are added to the network, this LOM protection can no longer be relied upon. If this happens, and the new DG units need to be equipped with more expensive, communication-based LOM protection, then it is vital that clear and transparent rules for allocating the costs of implementing the required communication medium should already be in place. For example, allocating all the additional costs to the most recent DG unit owners would be considered by them unfair, and could lead to a good deal of customer dissatisfaction. One solution for this problem would be to require the use of suitable active or communication-based LOM protection methods for all DG installations. The costs incurred by the implementation of the possibly needed communication infrastructure could first be allocated to the pioneer DG unit installations, but then later redistributed as more DG unit installations are added to the network, i.e. the pioneer DG unit owners could receive a refund as more DG units utilizing the same communication infrastructure are connected.

5 Conclusions and suggestions for future research

5.1 Summary

Unintentional islanding is strictly prohibited because of the safety hazards. Therefore, all DG units need to be equipped with LOM protection, which should reliably and rapidly disconnect the protected DG unit whenever it is unintentionally separated from the main utility grid, i.e., islanded. However, most of the LOM protection methods currently in use fail to detect islanding in a timely manner when the power imbalance between the production and consumption in the islanded circuit is small. The set of power imbalance combinations that lead to non-detected islanding is referred to as the non-detection zone (NDZ). The size of the NDZ depends on many factors, such as the LOM protection method, the type- and control mode of the protected DG unit, and the protection settings. The size of the NDZ could be reduced by applying stricter LOM protection settings, but this is not usually possible as the LOM protection settings are typically predefined in the utilized standards or grid codes. The reason why very sensitive LOM protection settings are not allowed is that if too sensitive LOM protection settings are used, events such as voltage dips caused by faults at the transmission grid level may lead to massive unwanted disconnection of DG units. As DG capacity continues to increase, so does likelihood of the occurrence of problematic power imbalances for LOM protection, which consequently increases the risk of non-detected islanding. Thus, there is a clear need to develop better solutions for reducing this risk.

A wide variety of LOM protection methods have been proposed in the literature. These methods can be divided into three categories: passive-, active- and communication-based methods. Passive methods are based solely on monitoring chosen system quantities such as voltage magnitude and frequency. These methods are affordable and can be used for all types of DG units. However, they typically suffer from large NDZs. Active LOM protection methods are based on deliberately injecting small disturbances (often referred to as perturbations) into the grid, and monitoring the response of the system. When a DG unit protected by an active LOM protection is connected to the main utility grid, these disturbances typically only have a marginal effect on the system quantities due to the stabilizing effect of the large power grid. However, should a DG unit protected by an active LOM protection method become islanded, the perturbations alter the monitored system quantities considerably more because the stabilizing influence of the main utility grid is removed, and this can be used as an indication of islanding. Active LOM protection methods are typically designed for DG units coupled via converter, because the converter can function as a suitable tool for implementing the desired perturbations. Some active LOM protection schemes are even able to detect balanced islanding. Despite all the above, active LOM protection methods have their own drawbacks. For instance, they may degrade the power quality, or have other unfavorable effects on the

utility grid. Moreover, active LOM protection schemes may not work so well when an islanded circuit is sustained by multiple DG units. This stems from the fact that the injected perturbations may cancel each other out unless they are synchronized. Here though, the problem is that synchronizing the injection of the desired perturbations may have unfavorable effects on the utility grid. Communication-based LOM protection methods are usually better than passive and active methods in the sense that they are completely immune to the NDZ problem, and with a suitable communication medium in place, they are extremely rapid. The drawback here is the cost, which is often too high for small DG installations. It is also worth remembering that communication-based LOM protection methods are only as reliable as the communication scheme they use, so it is mandatory to use local passive or active LOM protection methods for back-up protection purposes.

This thesis has focused on analyzing the problems related to the detection of islanding and has developed solutions to many of these problems. The factors affecting the performance of LOM protection have been thoroughly analyzed, in addition to which, the effects of fault-ride through requirements specified in grid codes on LOM protection have been studied. The research has shown that passive LOM protection methods such as voltage magnitude, frequency and ROCOF protection fail to detect islanding even if the local power imbalances are relatively large.

This thesis has also analyzed how active- and reactive power imbalances affect voltage magnitude and frequency when the islanded circuit contains both converter- and directly-coupled synchronous generator-based DG units. When an islanded circuit is only sustained by directly-coupled synchronous generator-based DG, it is the active power imbalance which mainly determines the frequency, whereas the reactive power imbalance mainly determines the voltages. Conversely, in an islanded circuit sustained only by converter-coupled DG, it is mainly the reactive power imbalance which determines the frequency and the active power imbalance, which mainly determines the voltages. If the islanded circuit contains both converter-coupled DG and directly-coupled synchronous generator-based DG, the relationships between the active- and reactive power and the voltage magnitude and frequency resemble that of an islanded circuit which is sustained only by directly-coupled synchronous generator-based DG. Consequently, many of the active LOM protection schemes may not function as intended when the islanded circuit contains both directly-coupled synchronous generator-based and converter-coupled DG [P2], [P7]. The degree to which the presence of directly-coupled synchronous generator-based DG complicates the detection of islanding depends on factors such as the inertia constants of the synchronous generators and the ratio between the converter-coupled DG units and directly-coupled synchronous generators [P7].

The research for this thesis has developed a number of new solutions for establishing reliable and rapid LOM protection. The first of these is a NIS-based LOM risk management tool, which has been designed at the concept level. This procedure, which is based on the existing functionalities

embedded in modern NISs, can be used for evaluating the existing LOM risk in the studied network sections, and will assist DSOs in choosing the most appropriate LOM protection methods for the DG units in their networks. In addition to this tool, two active LOM protection methods and a communication-based protection automation concept have been developed. The first of the active LOM protection methods was based on a combination of reactive power variation and a dedicated Q-f droop. The knowledge gained during the development of this method later resulted in a significantly more sophisticated active LOM protection method, which is based on forcing the ROCOF index of an islanded circuit to a predefined value by applying a dedicated Q-f droop [P8]. This method can detect the islanding of a circuit sustained by converter-coupled DG reliably and rapidly. The communication-based protection automation concept is not only able to provide reliable and rapid LOM protection, but also improves the reliability of the distribution service to DG units by automatically providing them with an alternative feeding path if the original feeding path is faulted [P6]. This method is based on inter-IED communication and predefined switching logic.

The proposed methods are suitable for different purposes. The NIS-based LOM risk assessment is firstly useful in evaluating the adequacy of utilized or planned LOM protection methods. If the LOM risk assessment indicates that the power imbalances are always very large, then passive methods can be used due to their low cost and the fact that they do not degrade power quality. However, if the LOM risk assessment reveals that passive LOM protection is not sufficiently reliable, then active or communication based LOM protection schemes are recommended. If the ratio between the converter-coupled DG and the directly-coupled synchronous generators in the network sections is great enough, there are advanced active LOM protection methods available which can provide reliable and rapid LOM protection, such as the one proposed in [P8] However, if there are significant amount of directly coupled DG units in the studied network sections, then communication-based LOM protection, such as the scheme described in [P6], should be used to ensure reliable LOM protection.

5.2 Contribution of the thesis

The main contributions of this thesis can be summarized as follows.

- The limitations of voltage magnitude, frequency based LOM protection methods have been analyzed thoroughly. The differences between the functioning of these protection functions in islands sustained by either converter-coupled DG units or directly-coupled synchronous generators have been studied. The potential risks of frequency drifting-based active LOM protection methods in scenarios where the island is sustained by both directly-coupled synchronous generators and converter-coupled DG units have been identified.

- The effects FRT requirements on the LOM protection of a full converter-coupled DG unit have been illustrated. The studies showed that both LVRT- and reactive current support requirements significantly degrade the performance of LOM protection.

- A LOM risk assessment procedure has been developed for facilitating DSOs in managing the non-detected LOM risk and in choosing suitable LOM protection methods for each DG installation. The procedure evaluates what kind of power imbalances are possible in the analyzed network sections. By comparing these power imbalances to predetermined NDZs of optional LOM protection methods, the procedure can inform which of the optional LOM protection methods are sufficient for each DG unit installation.

- Two active LOM protection methods and a communication-based protection automation concept have been developed. The first of the developed active methods is based on constant injection of reactive power pulses and a dedicated Q-f droop. The second developed active LOM protection method is based on forcing the monitored ROCOF index to a desired value using a dedicated Q-f droop. The communication based protection automation concept is aimed at tackling typical DG related protection problems but also for automatically changing the feeding path of the protected DG unit in case if the original feeding route becomes faulted.

5.3 Future work

As the proportion of DG in the total generating capacity of the grid increases, it is evident that DG units will have to contribute more to the provision of system supporting services. The grid codes are thus in constant evolution. This poses a challenge to the developers of LOM protection methods, as the protection methods need to be compliant with the applied grid code. The active methods developed in this thesis may already need certain modifications in order to be fully compliant with the most recent developments in grid codes. In particular, there is a need for more studies concerning the potential interaction between local voltage control and active methods. Nevertheless, the communication-based protection automation concept [P6] is already fully grid code-compliant since it does not need to interfere with the controls of the protected DG unit(s).

The LOM risk assessment method should be a considerable help to DSOs in managing the existing LOM risk and in choosing the most suitable LOM protection schemes for their networks. It should thus be further refined to an actual implementation. The task of determining the NDZs for the optional LOM protection methods would be most likely be reasonable task because DSOs typically

have a rather limited selection of possible LOM protection schemes. However, the actual implementation to an existing NIS would require close co-operation with NIS developers and LOM protection specialists. Research institutions with suitable simulation tools and knowledge would probably be needed for determining the NDZs of alternative LOM protection schemes.

References

[1] General Secretariat of the Council. "European council (23 and 24 October 2014) - conclusions", EUCO 169/14, 24th of October, 2014. Available online: http://data.consilium.europa.eu/doc/document/ST-169-2014-INIT/en/pdf

[2] European Commission 2030 Energy strategy. Available online: http://ec.europa.eu/energy/en/topics/energy-strategy-and-energy-union/2030-energy-strategy

[3] N. Jenkins, R. Allan, P. Crossley, D. Kirschen and G. Strbac, *Embedded Generation*. London, UK: The Institution of Electrical Engineers, 2000, 273 p.

[4] A. Kulmala, "Active voltage control in distribution networks including distributed energy resources" Ph. D. dissertation, Dept. of Electrical Engineering, Tampere University of Technology, Tampere, Finland, 2014

[5] K. Mäki, "Novel methods for assessing the protection impacts of distributed generation in distribution network planning" Ph. D. dissertation, Dept. of Electrical Engineering, Tampere University of Technology, Tampere, Finland, 2007

[6] P. M. Andersson, *Power System Protection*, McGraw-Hill: IEEE Press, New York, USA, 1999, 1305p.

[7] E. Lakervi and E. J. Holmes, *Electricity distribution network design*, The institution of electrical engineers, 2nd ed. London, U.K., 1995, 325p.

[8] K. Mäki, S. Repo and P. Järventausta, "Blinding of feeder protection caused by distributed generation in distribution network", *in Proc. 5th WSEAS International Conference on Power Systems and Electromagnetic Compatibility*, Corfu, Greece, August 2005

[9] K. Kauhaniemi and L. Kumpulainen, "Impact of distributed generation on the protection of distribution networks", *in Proc. Eight IEE International Conference on Developments in Power System Protection*, Amsterdam, Netherlands, April 2004

[10] L. K. Kumpulainen and K. T. Kauhaniemi, ”Analysis of the impact of distributed generation on automatic reclosing” *in Proc. IEEE PES Power Syst. Conf. Expo*, New York, USA, Oct. 2004

[11] K. Mäki, S. Repo and P. Järventausta, “Impacts of distributed generation on earth fault protection in systems with isolated neutral”, *in Proc. 19th Int. Conf. on Electricity Distribution*, Vienna, Austria, May 2007

[12] L. K. Kumpulainen and K. T. Kauhaniemi, ”Aspects of the effects of distributed generation in single-line-to-earth faults”, *in Proc. International Conference on Future of Power Systems,* Amsterdam, Netherlands, November 2005

[13] J. Bruschi, F. Cadoux, B. Raison, Y. Besanger and S. Grenard, “Impact of new European grid codes requirements on anti-islanding protection: a case study”, *in Proc. 23rd International Conference on Electricity Distribution (CIRED)*, Lyon, France, June 2015

[14] IEEE standard for interconnecting distributed resources with electric power systems, IEEE Std 1547-2003, 2003

[15] Inverters, Converters, and Controllers for Use in Independent Power Systems, Underwriter Laboratories Inc. Standard UL1741, 2001

[16] *Power generation systems connnected to the low-voltage distribution network*, VDE Standard VDE-AR-N 4105:2011-08, 2011

[17] A. Ellis, Y. Miyamoto, S. Gonzalez, M. Ropp, D. Schutz and T. Sato, ”Comparative analysis of anti-islanding requirements and test procedures in the United States and Japan”, ”, *in Proc. 39th IEEE Photovoltaic Specialist Conf.*, Tampa, USA, June. 2013

[18] P. Mahat, Z. Chen and B. Bak-Jensen, “Review of islanding operation of distribution system with distributed generation,” *in Proc. Power and Energy Society General Meeting*, Detroit, USA, July 2011

[19] R. Teodorescu, M. Liserre and P. Rodriquez, *Grid converters for photovoltaic and wind power systems,* John Wiley-IEEE, Chichester, U.K., 2011, 398p.

[20] W. Bower and M. Ropp. “Evaluation of Islanding Detection Methods for Photovoltaic Utility-Interactive Power Systems, International Energy Agency”, Report IEA PVPS T5-09: 2002, March 2002

[21] P. Lund, O. Mogstad, V. Neimane, A. Pleym and O. Samuelsson, “Connection of distributed generation – effect on the power system”, SINTEF Energy Research, Trondheim, Norway, Tech. Rep. TR A5785 , March 2003

[22] O. Samuelsson and N. Stråth, “Islanding detection and connection requirements”, ”, *in Proc. Power Engineering Society General Meeting,* Tampa, USA, June 2007

[23] Union for the co-ordination of transmission of electricity (UCTE). Final report - System Distrurbance on 4 November 2006, [Online]. https://www.entsoe.eu/fileadmin/user_upload/_library/publications/ce/otherreports/Final-Report-20070130.pdf

[24] Z. Ye, A. Kolwalkar, Y. Zhang, P. Du and R. Walling. “Evaluation of anti-islanding schemes based on nondetection zone concept”, *IEEE Trans. Power Electronics*, vol. 19, pp. 1171-1176, Sept. 2004

[25] J. C. M. Vieira, W. F. Freitas, W. Xu and A. Morelato. “An Investigation on the Nondetection Zones of Synchronous Distributed Generation Anti-Islanding Protection”, *IEEE Trans. Power Delivery*, vol. 23, pp. 593-600, April 2008

[26] W. Xu, K, Mauch and S. Martel, An assessment of distributed generation islanding detection methods and issues for canada, CETC-Varennes 2004-074 (TR) 411-INVERT, July 2004

[27] M. Ropp, M. Begovic and A. Rohatgi, “Analysis and performance assessment of the active frequency drift method of islanding detection”, *IEEE Trans. Energy Conversion*, Vol. 14, pp. 810-816, Sept. 1999

[28] H. H. Zeineldin, E. F. El-Saadany and M. M. A. Salama. “Impact of DG Interface Controls on Islanding Detection and Nondetection Zones”, *IEEE Trans. Power Delivery*, vol. 21, pp. 1515-1523, July 2006

[29] H. H. Zeineldin, “A Q-f droop curve for facilitating islanding detection of inverter-based distributed generation,” *IEEE Trans. Power Electron*., vol. 24, pp. 665–673, Mar. 2009

[30] D. P. Kothari and I. J. Nagrath, *Modern Power System Analysis*. 3rd edition. New Delhi, India: Tata McGraw-Hill Publishing Company Limited, 2003

[31] ENTSO-E website (2016), https://www.entsoe.eu/about-entso-e/Pages/default.aspx

[32] ENTSOE RfG, (2016, April). Establishing a network code on requirements for grid connection of generators, Commission Regulation (EU) 2016/631. Official Journal of the European Union, [Online] http://eur-lex.europa.eu/legal-content/EN/TXT/PDF/?uri=CELEX:32016R0631&from=EN

[33] Energy networks assocation, Engineering recommendation G59, issue 3, amendment 1, August 2014

[34] Fingrid Plc. (2013, Sept.). Specifications for the Operational Performance of Power Generating Facilities, [Online]. http://www.fingrid.fi/en/customers/Customer%20attachments/Connection/2013/Specifications%20for%20the%20Operational%20Performance%20of%20Power%20Generating%20Facilities%20VJV2013.pdf

[35] G. Lammert, T. Hess, M. Schmidt, P. Schegner and M. Braun, "Dynamic grid support in low voltage grids – fault ride through and reactive power/voltage support during grid disturbances", *in Proc. Power Systems Computation Conference (PSCC)*, Wroclaw, Poland, August 2014

[36] BDEW Technical guideline, Generating plants connected to medium-voltage network, June 2008

[37] Verband der Netbetreiber (VDN) Transmission code 2017. Network and system rules of the German transmission system operators

[38] Verordnung zu Systemdiestleistungen durch Windenergieanlagen, Bundesgesetzblatt jahrgang 2009 Teil I Nr. 39

[39] Technical regulation 3.2.2 for PV power plants with a power output above 11 kW, Energienet.DK, Doc. 14/17997-39, 2015

[40] Technical regulation 3.2.5 for wind power plants above 11 kW, Energienet.DK, Doc. 13/96336-43, 2016

[41] Hydro Quebec. Transmission provider technical requirements for the connection of power plants to the Hydro-Quebec transmission system

[42] P. Fairley. “Can synthetic inertia from wind power stabilize grids?” IEEE Spectrum, 7th of November, 2016. Available online: http://spectrum.ieee.org/energywise/energy/renewables/can-synthetic-inertia-stabilize-power-grids?utm_source=Tech+Alert&utm_campaign=TechAlert_11-10-16&bt_alias=eyJ1c2VySWQiOiAiOGExOTFmMjMtYjZiOC00NTliLWE2NTctN2UxN2Q3YTQzMDEyIn0%3D&utm_medium=Email

[43] S. Lissandron, R. Sgarbossa, L. D. Santa, P. Mattavelli, R. Turri and A. Cerretti, “Impact of Non-Simultaneous P/f and Q/V Grid Code Requirements on PV Inverters on Unintentional Islanding Operation in Distribution Network”, *in Proc. 6th IEEE International Symposium on Power Electronics for Distributed Generation Systems (PEDG)*, Aachen, Germany, August 2015

[44] F. Bignucolo, A. Savio, R. Sgarbossa, R. Turri and A. Cerretti, “Combined effects of distributed generation grid code requirements on the transient behaviour of islanded systems”, *in Proc. CIRED Workshop*, Helsinki, Finland, June 2016

[45] A. Woyte, R. Belmans and J. Nijs, “Testing the Islanding Protection Function of Photovoltaic Inverters” *in Proc. Power and Energy Society General Meeting*, Toronto, Canada, July 2003

[46] M. Ropp, R. Bonn, S. Gonzalez and C. Whitaker. “Investigation of the Impact of Single-phase Induction Machines in Islanded Loads – Summary of Results”, Sandia National Laboratories Report SAND2002-1320, May 2002

[47] IEEE Standard Conformance Test Procedures for Equipment Interconnecting Distributed Resources with Electric Power Systems, IEEE 1547.1 – 2005, 2005

[48] P. Deshbhratar, R. Somalwar and S. G. Kadwane, “Comparative analysis of islanding detection methods for multiple DG based system”, *in Proc. Int. Conf. on Electrical, Electronics, and Optimization Techniques (ICEEOT)*, Chennai, India, March 2016

[49] P. Mahat, Z. Chen and B. Bak-Jensen, “Review of islanding detection methods for distributed generation,” *in Proc. 3rd Int. Conf. on Electric Utility Deregulation and Restructuring and Power Technologies*, Nanjing, China, April 2008.

[50] B. Burger. (2017, Jan.). Power generation in Germany – assessment of 2016. Frauenhofer Institute for Solar Energy Systems. [Online]. Available: http://www.modernpowersystems.com/features/featuredealing-with-the-50.2-hz-problem/

[51] M. Döring. (2013, Jan.). Dealing with the 50.2 Hz problem. Modern Power Systems. [Online]. Available: http://www.modernpowersystems.com/features/featuredealing-with-the-50.2-hz-problem/

[52] T. Quac-Tuan, ”New methods of islanding detection for photovoltaic inverters”, *in Proc. IEEE PES Innovative Smart Grid Technologies Conference Europe*, Ljubljana, Slovenia, Feb. 2017

[53] J. Vieira, W. Freitas, Z. Huang, W. Xu and A. Morelato, “Formulas for predicting the dynamic performance of ROCOF relays for embedded generation applications,” *IEE Proc. Generation, Transmission and Distribution*, vol. 153, pp. 399-406, July 2006

[54] R. Brüdlinger, C. Mayr, A. Causebrook, J. Dahmani, D. Nestle, R. Belhomme, C. Duvauchelle and D. Lefebvre, “State of the art solutions and new concepts for islanding protection”, Österreichisches Forschung und Prüfzentrum Arsenal GbmH, Vienna, Austria, DISPOWER project Deliverable 2.2, Feb. 2006

[55] W. Freitas, W. Xu, C. M. Affonso and Z. Huang, “Comparative analysis between ROCOF and vector surge relays for distributed generation applications,” *IEEE Trans. Power Delivery*, vol. 20, pp. 1315-1324, April 2005

[56] H. Laaksonen, “Need for New Islanding Detection Schemes and Prioritization with Generator Grid Code Requirements”, *International Review of Electrical Engineering (I.R.E.E.)*, Vol. 11, N. 2, March 2016

[57] M. A. Redfern, O. Usta, G. Fielding, “Protection against loss of utility grid supply for a dispersed storage and generating unit”, *IEEE Trans. Power Delivery*, vol. 8, pp. 948-954, July 1993

[58] J. Yin, L. Chang, C. P. Didduch., “Recent developments in islanding detection for distributed power generation”, *Large Engineering Systems Conference On Power Engineering*, Halifax, Canada, July 2004

[59] S. K. Salman, D. J. King and G. Weller, "New loss of mains detection algorithm for embedded generation using rate of change of voltage and changes in power factors", *in Proc. 7th IEE Int. Conf. on Developments in Power System Protection*, Amsterdam, Netherlands, April 2001

[60] F. S. Pai and S. J. Huang, "A detection algorithm for islanding-prevention of dispersed consumer-owned storage and generating units", *IEEE Trans. Energy Conversion*, vol. 16, pp. 346-351, Dec. 2001

[61] S. P. Chowdhury, S. Chowdhury and P. A. Crossley, "Islanding protection of active distribution networks with renewable distributed generators: A comprehensive survey", *Electric Power Systems Research*, Volume 79, pp. 984-992, June 2009

[62] S. I. Jang and K. H. Kim, "An islanding detection mthod for distributed generations using voltage unbalance and total harmonic distortion of current", *IEEE Trans. Power Delivery*, vol. 19, pp. 745-752, April 2004

[63] J. Yin, C. P. Diduch and L. Chang, "Islanding detection using proportional power spectral density", *IEEE Trans. Power Delivery*, vol. 23, pp. 776-784, April 2008

[64] A. Pigazo, M. Liserre, R. Mastromauro, V. Moreno and A. Dell'Aquila, "Wavelet-based islanding detection in grid-connected PV systems", *IEEE Trans. Industrial Electronics*, vol. 56, pp. 4445-4455, July 2008

[65] M. Hanif, U. D. Dwivedi, M. Basu and K. Gaughan, "Wavelet based islanding detection of DC-AC inverter interfaced DG systems", *in Proc. 45th Int. Universities Power Engineering Conference*, Cardiff, UK, Sept. 2010.

[66] S. Alshareef, S. Talwar and W. G. Morsi, "A new approach based on wavelet design and machine learning for islanding detection of distributed generation", *IEEE Trans. Smart Grid*, Vol. 5, pp. 1575-1583, July 2014

[67] H. T. Do, X. Zhang, N. V. Nguyen, S. S. Li and T. T. Chu, "Passive-islanding detection method using the wavelet packet transform in grid-connected photovoltaic systems", *IEEE Trans. Power Elecronics*, vol. 31, pp. 6955-6967, Oct. 2016

[68] H. Laaksonen, “Novel wavelet transform based islanding detection algorithms”, International Review of Electrical Engineering (IREE), vol. 8, pp. 1796-1805, December 2013

[69] J. A. Laghari, H. Mokhlis, M. Karimi, A. H. A. Bakar and H. Mohamad, ”Computational intelligence based techniques for islanding detection of distributed generation in distribution network: a review”, *Energy Conversion and Management*, vol. 88, pp. 139-152, December 2014

[70] K. El-Arroudi and G. Joos, “Data mining approach to threshold settings of islanding relays in distributed generation”, *IEEE Trans. Power Delivery,* vol. 22, pp. 1112-1119, July 2007

[71] M. S. Elnozahy, E. F. El-Saadany and M. M. A. Salama, “A robust wavelet-ANN based technique for islanding detection”, *in Proc. IEEE Power and Energy Society General Meeting*, Detroit, USA, July 2011

[72] S. R. Samantaray, K. El-Arroudi, G. Joos and I. Kamwa, “A fuzzy rule-based approach for islanding detection in distributed generation”, *IEEE Trans. Power Delivery*, vol. 25, pp. 1427-1433, May 2010

[73] R. Ghazi and N. Lotfi, “A new hybrid intelligent based approach to islanding detection in distributed generation”, *in Proc. 45th International Universities Power Engineering Conference*, Cardiff, UK, September 2010

[74] G. A. Smith, P. A. Onions, D. G. Infield, “Predicting islanding operation of grid connected PV inverters”, *IEE Proc. Electric Power Applications,* vol 147, pp. 1-6, January 2000

[75] M. E. Ropp, M. Begovic, A. Rohatgi, G. A. Kern, R. H. Bonn and S. Gonzalez, “Determining the relative effectiveness of islanding detection methods using phase criteria and nondetection zones”, *IEEE Trans. Energy Conversion,* Vol. 15, pp. 290-296, Sept. 2000

[76] G. K. Hung, C. C. Chang and C. L. Chen, “Automatic phase-shift method for islanding detection of grid connected photovoltaic inverters”, *IEEE Trans. Energy Conversion,* vol. 18, pp. 169-173, Feb. 2003

[77] J. Yin, L. Chang and C. Diduch, “A new adaptive logic phase-shift algorithm for anti-islanding protections in inverter-based DG systems”, *in Proc. 36th IEEE Power Electronics Specialist Conference,* Recife, Brazil, June 2005

[78] G. A. Kern, “SunSine300, utility interactive AC module anti-islanding test results”, *in Proc. 26th IEEE Photovoltaic Specialists Conf.*, Anaheim, USA, Oct. 1997

[79] P. O’Kane and B. Fox, “Loss of mains detection for embedded generation by system impedance monitoring” , *in Proc. 6th Int. Conf. on Developments in Power System Protection*, Nottingham, UK, March 1997

[80] Y. Jin, Q. Song and W. Liu, “Anti-islanding Protection for Distributed Generation Systems Based on Reactive Power Drift”, *in Proc. 35th IEEE Industrial Electronics conf.*, Porto, Portugal, Nov. 2009

[81] J. Zhang, D. Xu, G. Shen, Y. Zhu, N. He and J. Ma, “An improved islanding detection method for a grid-connected inverter with intermittent bilateral reactive power variation”, *IEEE Trans. Power Electron.*, vol. 28, pp. 268-278, January 2013

[82] Y. Zhu, D. Xu, N. He, J. Ma, J. Zhang, Y. Zhang, G. Shen and C. Hu, "A novel RPV (Reactive-Power-Variation) Antiislanding method based on adapted reactive power perturbation," *IEEE Trans. Power Electron*., vol. 28, pp. 4998-5012, Nov. 2013

[83] X. Chen and Y. Li, ”A Nondestructive Islanding Detection Method Based on Adaptive and Periodic Disturbance on Reactive Power Output of Inverter-Based Distributed Generation”, *Journal of Applied Mathematics*, vol. 2014, pp. 1-11, July 2014

[84] T. Funabashi, K. Koyanagi and R. Yokoyama, “A review of islanding detection methods for distributed resources”, *in Proc. IEEE Power Tech Conference*, Bologna, Italy, June 2003

[85] O. Rintamäki and K. Kauhaniemi, ”Applying modern communication technology to loss-of-mains protection,” *in Proc. 20th Int. Conf. on Electricity Distribution*, Prague, Czech Republich, June 2009.

[86] O. Abarrategui, I. Zamora and D. M. Larruskain, "Comparative analysis of islanding detection methods in networks with DG", *in Proc. 19th Int. Conf. on Electricity Distribution*, Vienna, May 2007.

[87] L. Kumpulainen, I. Ristolainen and K. Kauhaniemi, "Loss-of-mains protection – still an issue with distributed generation," *in Proc. 19th Int. Conf. on Electricity Distribution*, Vienna, Austria, May 2007

[88] S. Voima, P. Välisuo and K. Kauhaniemi, "Power line carrier based loss of mains protection in medium voltage distribution networks", *in Proc. 13th Int. Conference on Developments in Power System Protection*, Edinburgh, UK, March 2016

[89] F. Coffele, P. Moore, C. Booth, A, Dysko, G. Burt, T. Spearing and P. Dolan, "Centralized loss of mains protection using IEC-61850", *in Proc. 10th IET Int. Conf. on Developments in Power System Protection*, Manchester, UK, April 2010

[90] A. Ishibashi, M. Imai, K. Omata, S. Sato, T. Takagi, Y. Nakachi and S. Ogawa, "New type of islanding detection system for distributed generation based on voltage angle difference between utility network and distributed generation site", *in Proc. Eighth IEE Interternationl Conference on Developments on Power System Protection*, Amsterdam, Netherlands, April 2004

[91] N. Stråth, "Islanding detection in power systems", Licenciate thesis, Dept. of Industrial Electrical Engineering and Automation, Lund University, Lund, Sweden, 2005

[92] M. Ropp, M. Begovic and A. Rohatgi, "Prevention of islanding in grid-connected photovoltaic systems", *Progress in Photovoltaics,* Vol. 7, pp. 39-59, 1999

[93] D. Laverty, D. J. Morrow and T. Littler, "Internet based loss-of-mains detection for distributed generation", *in Proc. 42nd Int. Universities Power Engineering Conf.,* Brighton, UK, Sept. 2007

[94] M. Delfanti, M. Merlo, G. Monfredini, V. Olivieri, M. Pozzi and A. Silvestri, "Hosting dispersed generation on Italian MV networks: towards smart grids", *in Proc. 14th Int. Conf. on Harmonics and Quality of Power*, Bergamo, Italy, Sept. 2010

[95] K. Mäki, A. Kulmala, S. Repo and P. Järventausta, ”Studies on grid impacts of distributed generation in a combined real-time simulation environment”, *in Proc. International Conference on Power Systems Transients,* Lyon, France, June 2007

[96] A. Mäkinen, H. Tuusa, “Wind Turbine and Grid Interaction Studies Using Integrated Real-Time Simulation Environment”, *in Proc. Nordic Workshop on Power and Industrial Electronics*, Espoo, Finland, June 2008.

[97] A. Mutanen, M. Ruska, S. Repo and P. Järventausta, ”Customer classification and load profiling method for distribution systems”, *IEEE Trans. Power Delivery,* vol. 26, pp. 1755-1763, May 2011

[98] C. G. Bright, “COROCOF: comparison of rate of change of frequency protection. A solution to the detection of loss of mains”, *in Proc. Seventh International IEE Conference on Developments in Power System Protection*, Amsterdam, Netherlands, April 2001

Publication 1

O. Raipala, S. Repo, K. Mäki and P. Järventausta, "Studying the effects of distributed generation on autoreclosing", *in Proc. 9th Nordic Electricity Distribution and Asset Management Conference*, Aalborg, Denmark, September 2010

STUDYING THE EFFECTS OF DISTRIBUTED GENERATION ON AUTORECLOSING WITH A REAL TIME DIGITAL SIMULATOR AND REAL PROTECTION RELAYS

Ontrei Raipala, Sami Repo, Kari Mäki and Pertti Järventausta
Tampere University of Technology, Finland
Ontrei.raipala@tut.fi

ABSTRACT

The functioning of fast autoreclosing (AR) on feeders including distributed generation (DG) is often mentioned as one of the main concerns related to DG. AR has a significant importance for the reliability of electricity supply since the majority of faults on overhead distribution lines are cleared with the help of AR. The situation is, however, becoming more difficult as DG is connected along distribution lines. This stems from the fact that DG can sustain the voltages during the open time of the circuit breaker performing the AR thus causing the AR to fail. It is, therefore, crucial that all DG units on the tripped feeder are disconnected before the reclosing attempt. The disconnection is meant to be taken care by the loss of mains (LOM) protection which all major DG unit installations need to be equipped with.

This paper first examines the AR problems caused by DG based on literature survey and then studies how different kinds of protection settings influence the successfulness of AR based on simulations. The simulations were carried out using a real time digital simulator (RTDS®) which enables the connection of real protection relays to be a part of the simulation. The results indicated that the successfulness of AR is strongly dependent on the chosen protection settings and from the prevailing imbalance between production and consumption.

INTRODUCTION

The amount of small scale generation units connected distribution networks (distributed generation, DG) seems to be growing rapidly worldwide. DG can have many beneficial effects on the usage of distribution networks (e.g. reduction of losses, voltage support, improved reliability) [1] but, on the other hand, DG also raises new challenges related to network protection, operation (e.g. voltage rise problem, rising fault levels) and planning (e.g. dimensioning of network components). These challenges need to be overcome in order to allow a high penetration level of DG.

One of the main challenges with DG is related to loss of mains (LOM) protection which is meant for preventing unintentional islanding. Islanding refers to a situation where a network section, that includes DG and customer loads, becomes isolated from the main grid thus leaving the DG feeding the local loads alone. A network section can become isolated from the main grid, for instance, as a result of a fault on a line which causes the overcurrent (OC) relay of the feeder in question to trip. Unintended islanding is not tolerated because it raises safety risks for the utility personnel, it can cause auto-reclosing (AR) failures, DG units as well as other network components may be damaged as a result of an out-of-phase reclosing and due to the risk of customer devices being damaged as a result of poor power quality in the island zone. [2]

Unintentional islanding is a challenging issue since the most utilized LOM protection methods fail to detect islanding under certain conditions. Moreover, even a reasonably short delay in the operation of LOM relay can render AR unsuccessful. Intentional islanding, on the other hand, can have a tremendously positive effect on the reliability of the supply, but it is out of the scope of this paper.

THE EFFECT OF DG ON AUTORECLOSING

AR is meant for removing temporary faults automatically without causing an extended interruption in the supply of electricity. This is achieved by opening a circuit breaker (CB) connecting the faulted feeder to the supplying grid for a short period of time and then reclosing the CB. During the open time (usually from 0.2s to a couple of seconds) of this CB, there is no source feeding the fault arc which leads to the extinguishment of the arc. Typically, in case if the first reclosing sequence should fail, one or two more reclosings sequences are made before the CB is ordered into permanent open position for the repair time. [3] AR has a great significance for the reliability of electricity supply since, e.g., in Finland about 90% of faults on overhead lines are temporary in nature [4] and thus also clearable by AR. The situation, however, becomes a bit more complicated in the presence of DG since the fault arc is usually extinguished only after all DG units on the feeder are disconnected. This is because the DG units that remain connected to the feeder during the autoreclosing open time can sustain the voltages and thus also the fault arc on the feeder in question. A certain period during which the voltage is equal to zero is also necessary after the extinguishment of the fault arc so that the ionized gas created by the fault arc has time to disperse [5]. The time required for the de-ionization of the fault is dependent on many factors like the fault type, fault duration (arcing time), magnitude of the fault current, wind conditions, circuit voltage, etc [6].

It is also important to pay special attention to the reclosing of the feeder CB in order to avoid dangerous stresses to the DG unit (caused by out of phase reclosing). This kind of coordination between the feeder protection and LOM relays is, however, quite challenging, especially in case if fast reclosing is applied [7]. Synchro check and dead line voltage relays could, therefore, be a reasonable option for backing up LOM protection. Out of phase reclosings can be avoided this way, but this back up protection, on the other hand, can naturally stop the reclosing attempt and thereby lead to a permanent interruption of supply. [8] Because of the challenging nature of this coordination, it may sometimes be necessary to use longer CB open times or more sensitive LOM protection settings to ensure correct protection sequence, or sometimes even give up on the use of fast AR. Very sensitive LOM protection settings have the disadvantage that they may cause nuisance tripping of the DG unit during disturbances. [9] Prolonged AR open time are also disadvantageous because they degrade supply quality and, moreover, the prolonged open time still does not guarantee correct operation of LOM protection in all cases [10]. A failed and a successful reclosing sequence are illustrated in figure 1. The left figure illustrates a failed reclosing sequence, whereas, the right figure shows a successful one. In the left figure, a DG unit connected to the feeder, where the autoreclosure is applied, maintains the voltage during the CB open time thus causing the reclosing action to fail. In the right figure, on the other hand, the LOM protection disconnects the DG unit in time and the network is thus de-energized resulting in a successful reclosing.

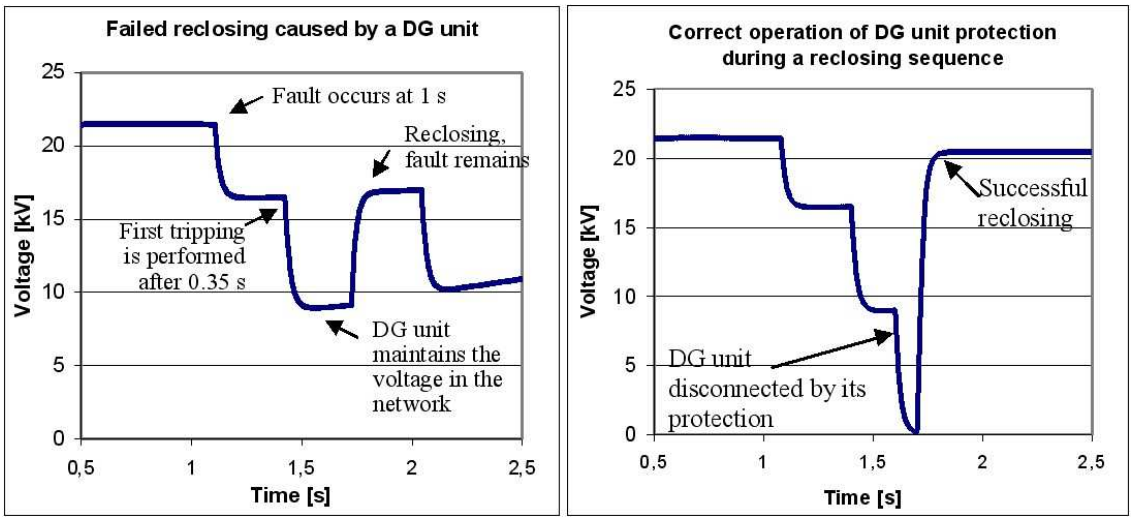

Figure 1. Reclosing problems caused by DG [9]

The authors in [11] suggest that the use of single pole reclosing could significantly enhance the integration of DG. When single pole reclosing is used, only the faulted phase is tripped and reclosed during one phase faults. Naturally the faulted phase needs to be tripped off from two ends so that the fault arc is neither fed by the substation nor by any DG units. Single pole reclosing has the advantage that DG units on the reclosed line do not necessarily need to be disconnected during one phase faults since it is still possible to continue feeding trough the two non-faulted phases. Another advantage is that the interruption disturbances to LV customers are slightly reduced [12]. Reference [11] also states that the continuity of supply is improved when single pole reclosing is applied since in certain countries many customers are connected only to phase. However, for the utilization of single pole reclosing it is necessary to install single pole circuit breakers and detection methods for determining the faulty phase [12]. Single pole reclosing, as itself, does not solve the DG related AR problems in radial distribution networks that do not have any reclosers along the feeders due to the fact that the faulted phase needs to be tripped from two ends.

CATEGORIZATION OF THE LOM DETECTION METHODS

LOM detection methods can be divided into three categories. These are communication based methods, local passive methods and local active methods. Figure 2, which is based on [13] and [14], illustrates this division into the three categories and gives some examples of each category. Reference [14], however, suggests that there is actually a third subgroup in local methods and names it as hybrid techniques. Overvoltage- (OV), undervoltage- (UV), overfrequency- (OF) and underfrequency- (UF) protection, which are categorized in the figure as passive LOM detection methods, can also be considered as basic generator protection functions but they also perform the task of LOM protection.

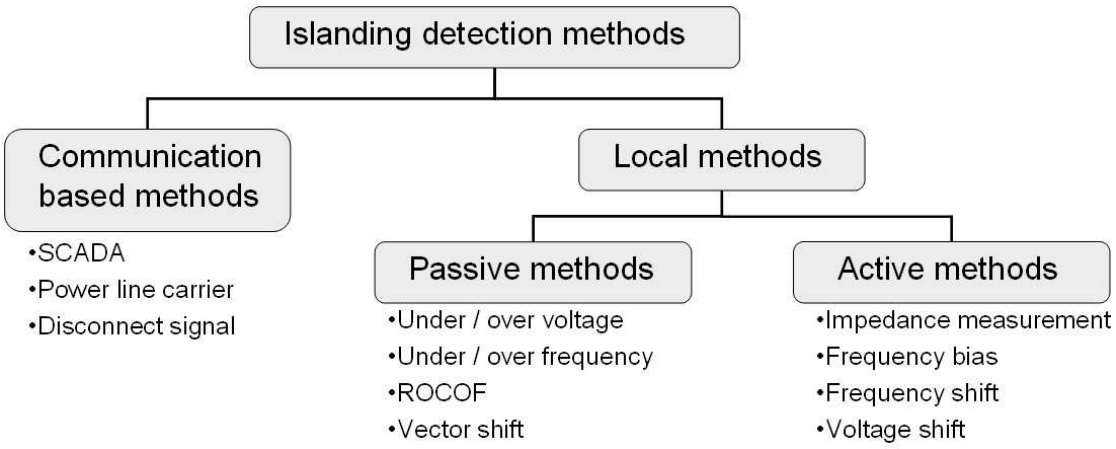

Figure 2. The categorization of LOM detection methods

Passive methods are based on locally measuring some system quantities like voltage and frequency. The idea in passive methods is that some changes in the measured quantities usually take place during the transition to islanding mode. These changes are mainly caused by the imbalance between real- and reactive power production and consumption in the islanded network. There is, nevertheless, a risk that this imbalance is so small that transition to a power island does not cause any of the quantities measured by a LOM relay to drift out of the preset limits. In cases like, the LOM protection fails to detect islanding. This blind area of LOM protection in the surroundings of the production- consumption equilibrium is called the non-detection-zone (NDZ). [9] All passive LOM detection methods have a NDZ of some kind. The size of the NDZ can, of course, be reduced to some extent by applying stricter LOM protection settings but this, on the other hand, tends to cause unwanted tripping of DG units which, in some cases, can even threaten the stability of whole power system [7]. Moreover, it has to be kept in mind that the NDZ can never be removed completely when using passive LOM detection methods because the NDZ is found from the same frequency and voltage ranges where power system normally operates. Despite the NDZ problem, however, passive LOM detection methods are the most utilized ones due to their low cost and applicability to all DG units.

Active LOM protection schemes are based on forcing the protected DG unit to try to make small changes in some of the system quantities like current waveforms and then detecting the response of the system. The idea behind this is that the DG unit is only capable of manipulating the system quantities when the connection to the main grid has been lost. [13] Active LOM protection schemes are typically applied in inverter connected DG units because the inverter works as a suitable tool for implementing these small changes. [9] Active LOM protection schemes do not suffer from the NDZ problem but they usually provide slower detection because changing the system quantities takes time. The deterioration of power quality due to the manipulation of the power system quantities is another disadvantage of the active methods. [15]

In the hybrid detection methods the idea is to combine the advantages of passive and active methods. A passive and an active method are combined in such a way that the active method is only used when the passive method suspects that the DG unit in question has become islanded. This brings the advantage that perturbations to the network are only inflicted when the passive detection method in question has first suspected islanding. Hybrid methods have small NDZ but they, on the other hand, provide slow detection times since two detection methods are used in sequence. [14]

Communication based methods are not based on detecting any changes in system quantities and they are, therefore, immune to the NDZ problem. In these methods, whenever a circuit breaker is opened, the idea is to somehow signal all the DG units downstream that the connection to the main grid has been lost. Reference [13] divides communication based methods in three categories which are the disconnect signal-, power line carrier- and the SCADA based method. In the disconnect signal scheme the idea is such that a disconnect signal is send to all relays downstream from the opened circuit breaker. A very promising example of this kind of method which also enables some additional user definable data to be transferred between relays is presented by the authors [16]. Power line carrier method is based on an idea where a subharmonic signal is continuously send to the network from a central location with the help of power line carrier. Whenever a circuit breaker is opened, all the DG units downstream from this breaker stop receiving the signal and they can thus be tripped off the network. Reference [13] suggests that this method could be the best choice because it provides very reliable LOM protection with reasonable implementation costs. The idea in the SCADA method is to extend SCADA to cater all the DG units and thereby, whenever a power island is unintentionally created, to remotely disconnect all the DG units in the power island. Communication based methods in general seem to be superior to the other LOM detection methods from the technical point of view but they, on the other hand, require higher investments. It is, however, noteworthy that communication based LOM protection methods are, of course, only as reliable as the utilized communication medium.

THE SIMULATION ENVIRONMENT

The simulation studies of this paper were performed with the help of real-time-digital-simulator (RTDS®). RTDS performs network calculations and communications between external devices in real time which enables the interaction studies between real physical devices and modeled power systems. One RTDS module consists of a rack which contains a number of various kinds of processor cards, communication cards and channels and a power supply unit. The graphical user interface to RTDS modules is provided by a dedicated software suite called RS-CAD. This CAD-program is installed to a PC workstation which is connected to the RTDS rack through an Ethernet cable. Power systems are first modeled in the draft mode of RS-CAD, whereas, the simulation is controlled in the runtime mode either manually or by a predefined script. [17] The simulation environment used in the simulation cases of this paper is presented in figure 3.

The voltage and current measurement signals from the RTDS had to be amplified to a realistic scale for the relays. For this purpose, the monitored signals from the D/A output cards of the RTDS module were first connected to a combined current and voltage amplifier (Omicron CMS156) which amplified the signals to a proper scale for the relays as figure 3 illustrates. Based on these amplified measurement signals, the relays (an OC relay and a LOM relay) made their control decisions concerning state of the circuit breakers that were modeled in the RS-CAD network model. The digital control signals from the relays were connected to the DOPTO (digital optical isolation system) card mounted in the RTDS rack via copper wires.

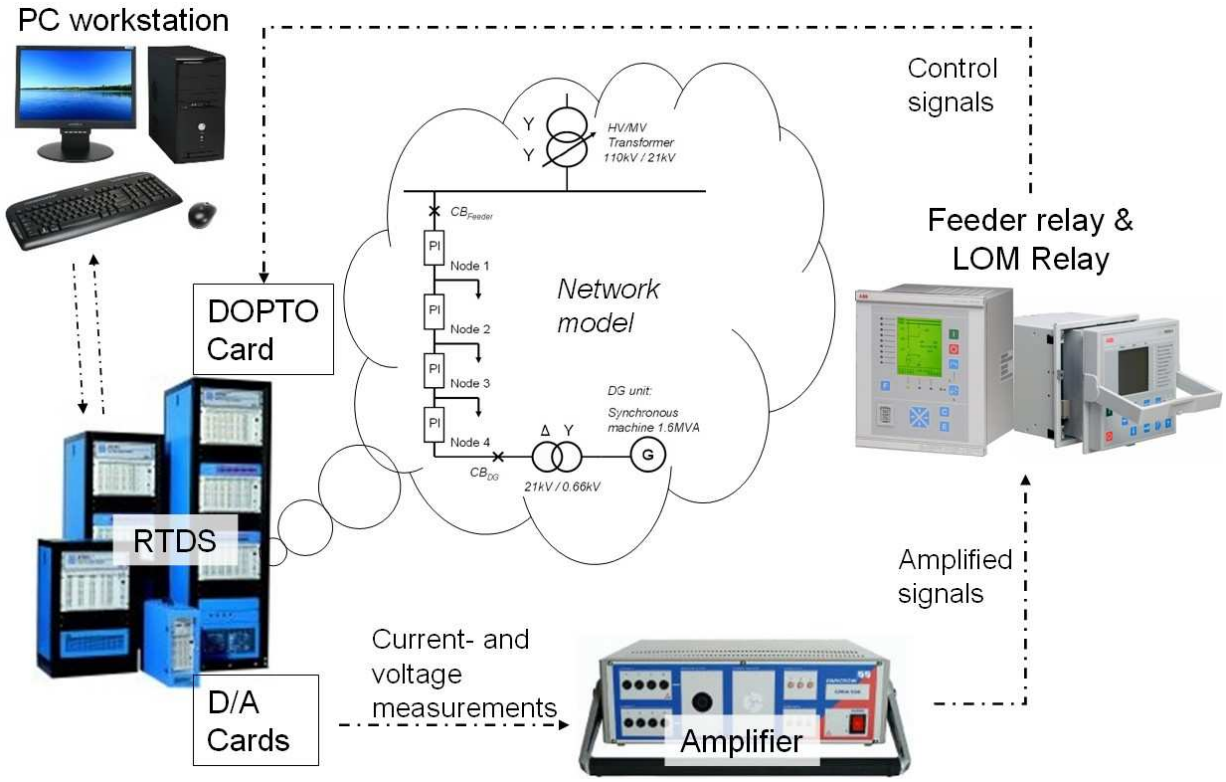

Figure 3. The utilized real time simulation environment

The OC relay used in these simulation studies was an original OC relay, whereas, the LOM relay was a multifunctional relay which was configured to function as a LOM relay. The protection functions that were configured to this LOM relay were under voltage- (UVP), over voltage- (OVP), under frequency- (UFP), over frequency- (OFP) and rate of change of frequency (ROCOF) protection.

THE SIMULATION MODELS

The idea in these simulation cases was to test how well autoreclosing (AR) works on a feeder that includes a DG unit and additionally to find out what variables have the most significant effect on the functioning of AR. The network model that was used in the simulations is a strongly simplified solidly grounded overhead line MV network which includes one feeder. This network model and the relays that where set to control the two circuit breakers (CBs) in the model are shown in figure 4. A 1.6MVA rated synchronous generator was connected to the end of this feeder and a LOM relay was set to control the CB connecting this DG unit to the feeder. Respectively an overcurrent relay was set to control the feeder CB as shown in figure 4. The settings for both of the utilized relays are also visible in figure 4. The synchronous generator, which represents a hydro power plant, is quite challenging from the LOM protection point of view due to its good voltage control capabilities and because it was capable of catering the maximum demand on the feeder. The loads on the feeder were modeled as star connected constant current loads.

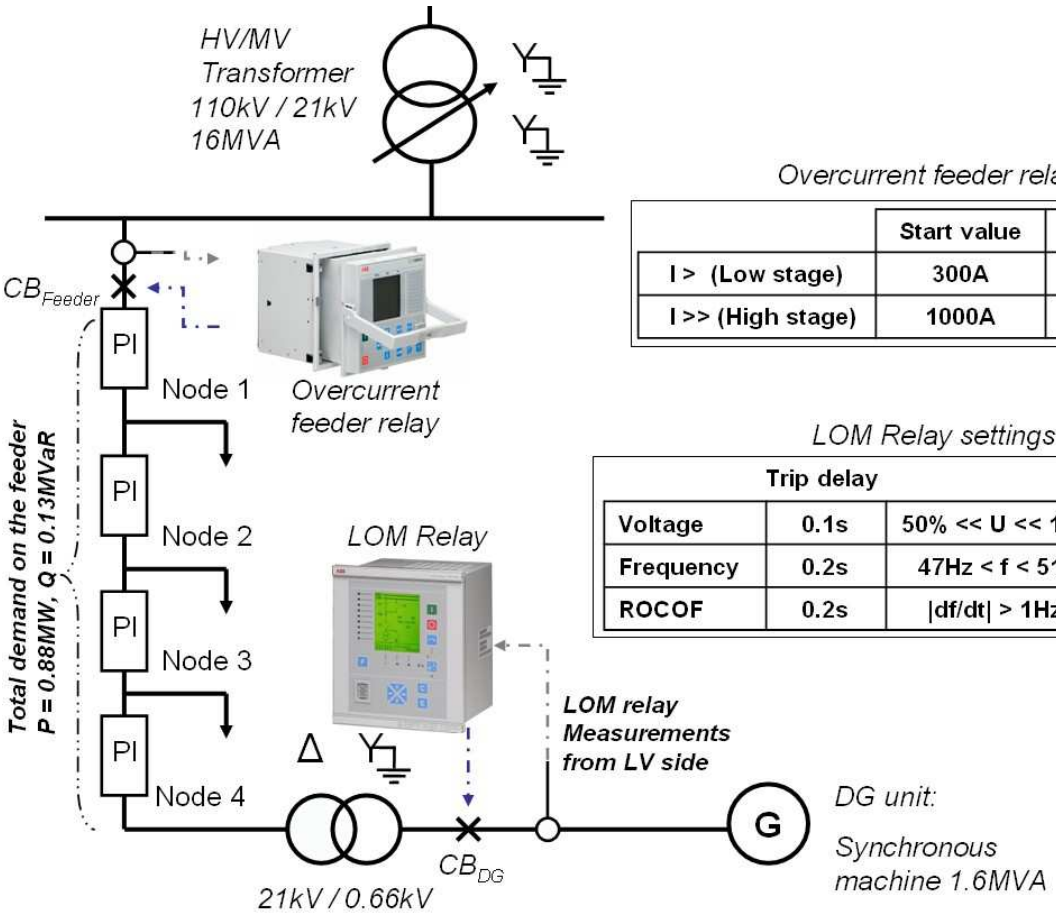

Overcurrent feeder relay settings

	Start value	delay
I > (Low stage)	300A	220ms
I >> (High stage)	1000A	80ms

LOM Relay settings

	Trip delay		Trip delay
Voltage	0.1s	50% << U << 110%	0.05s
Frequency	0.2s	47Hz < f < 51Hz	0.2s
ROCOF	0.2s	|df/dt| > 1Hz/s	0.2s

Figure 4. The utilized network model and the relays controlling the CBs

THE SIMULATION RESULTS AND ANALYSIS

The successfulness of AR is dependent on many factors such as on the dead time setting of the AR sequence (from the feeder relay), on the LOM protection settings (from the LOM relay) and on the duration of the fault that launches the AR sequence. The two first mentioned can be influenced by changing the relay settings, whereas, the fault arc is mostly dependent on the prevailing voltage which, in turn, after the opening of the feeder CB, is only maintained by the DG unit.

The aim of these simulation studies was to examine what mostly affects the successfulness of AR. For this purpose, the studies were divided into seven cases and in each case different values were given for the examined variables. The basic idea of the chosen cases can be seen from table 1. In each case, the demand on the feeder (0.88MW and 0.13MVar) was left untouched, whereas the mechanical torque setting of the DG unit was altered from 0.2pu to 1.0pu by 0.1pu steps. This torque range was gone through first with unity power factor and then with 0.95_{ind} power factor. For each DG unit production setting, two types of faults (a one-phase and a three-phase fault) were inflicted into nodes 1 – 4 of the examined feeder. The "successful AR sequence %" values in table 1 are, thus, mostly only comparable to each other and their purpose is just to give an indication of the effect of the various changes in protection settings.

Table 1. The basic ideas of the seven studied cases

	LOM protection operate delay	AR open time	ROCOF limit	U<< threshold	>f> limits [Hz]	Successful AR sequences %
case 1	Figure 4 settings	300ms	not used	50% x Un	47 < f > 51	50.00
case 2	Figure 4 settings	300ms	**1Hz/s**	50% x Un	47 < f > 51	77.08
case 3	Figure 4 settings	**500ms**	1Hz/s	50% x Un	47 < f > 51	90.97
case 4	Figure 4 settings	500ms	1Hz/s	**85% x Un**	47 < f > 51	95.83
case 5	Figure 4 settings	500ms	1Hz/s	85% x Un	**49.5 < f > 50.5**	95.83
case 6	Figure 4 settings	500ms	**0.5Hz/s**	85% x Un	47 < f > 51	97.92
case 7	**Minimum**	500ms	0.5Hz/s	85% x Un	47 < f > 51	100.00

It was assumed in these studies that the AR is successful if the dead time on the feeder, i.e. the time during which the voltage on the feeder is zero, is longer than 100ms. The duration of the fault was chosen to be such that the fault lasted till the reclosing but not long enough to cause a second AR sequence. This is the way the situation actually looks like from the LOM relay point of view, i.e., the fault arc does not disappear before the LOM relay operates. The simulations can be better understood by examining figure 5, which shows various graphs related to one of the simulations in case 3.

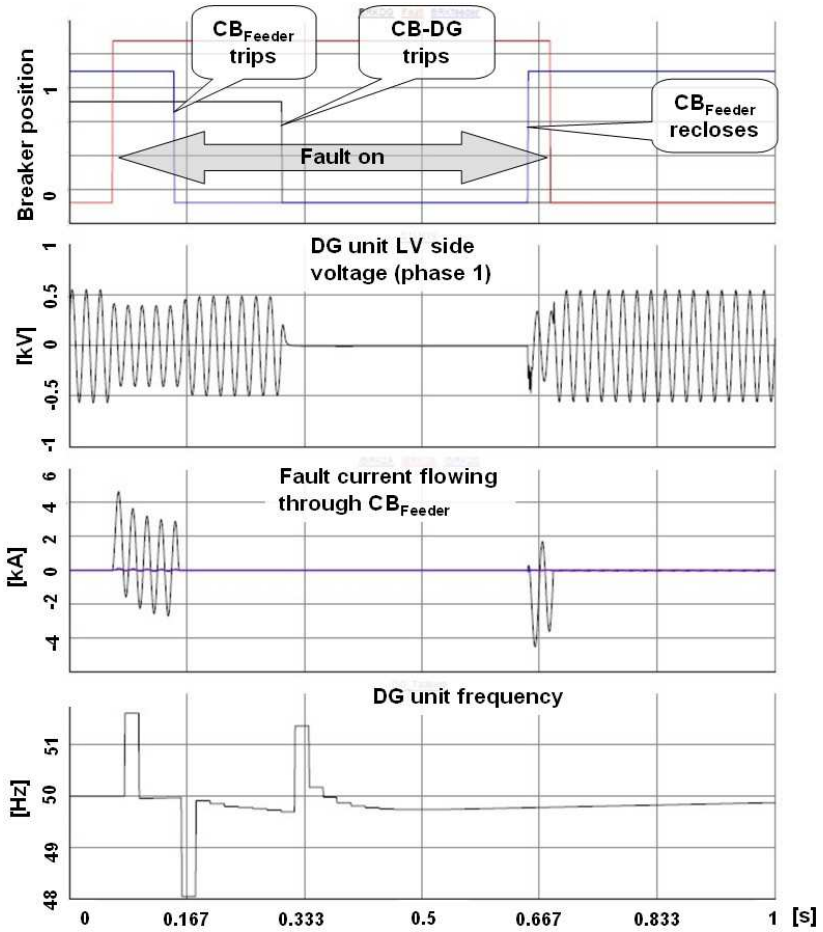

Figure 5. Various graphs from simulation case 3, where a 1phase fault occurs at node 1 (DG unit settings were Pf = 1.0, Tm=0.7)

The topmost graph in figure 5 represents the states of the relays and also the duration of the fault. As it can be seen from the figure, the duration of the fault is set so that the fault lasts till the reclosing but ends very short after it as already previously explained. It can also be seen from the figure that in this particular simulation case there was clearly enough time during which the voltage equals to zero for the extinguishment of the fault arc. The second topmost graph represents the LV side voltage (phase 1) of the DG transformer (see figure 4). As the graph shows, the DG unit is able to maintain the connection point voltage of the faulted phase still after the feeder relay has operated and the voltage drops to zero only after the operation of the DG unit circuit breaker. The next graph below shows the fault current flowing through the feeder circuit breaker which naturally drops to zero at the moment when the feeder circuit breaker trips. The undermost graph represents the frequency of the DG unit.

The protection settings that were used in the seven simulation cases are taken from a bunch of different recommendations so that the studies would be realistic. The LOM protection settings used in case 1 are equal to those that the Finnish electricity association SENER [18] recommends for DG units connected to distribution networks. The time (300ms) which was chosen as the AR open time is also a commonly utilized value in Finland. It was found in the simulations that the AR successfulness percentage was quite poor when these protection settings were used. In order to improve the situation, the ROCOF function was included in the LOM relay in the next case. As it can be seen from table 1, the situation improved significantly although still roughly one fifth of the ARs were unsuccessful. The next improvement attempt was to prolong the AR open time setting of the feeder relay in case 3. This improvement made the AR successfulness rate rise from 77.08% to 90.97%. Figure 6 represents the distribution of AR problems in relation to active power imbalance in case 3. The horizontal axis represents the active power flowing from the substation toward the feeder just before the fault. It can be seen from the figure that the AR problems are found from a narrow range of active power imbalance axis which is obviously the NDZ of the LOM protection.

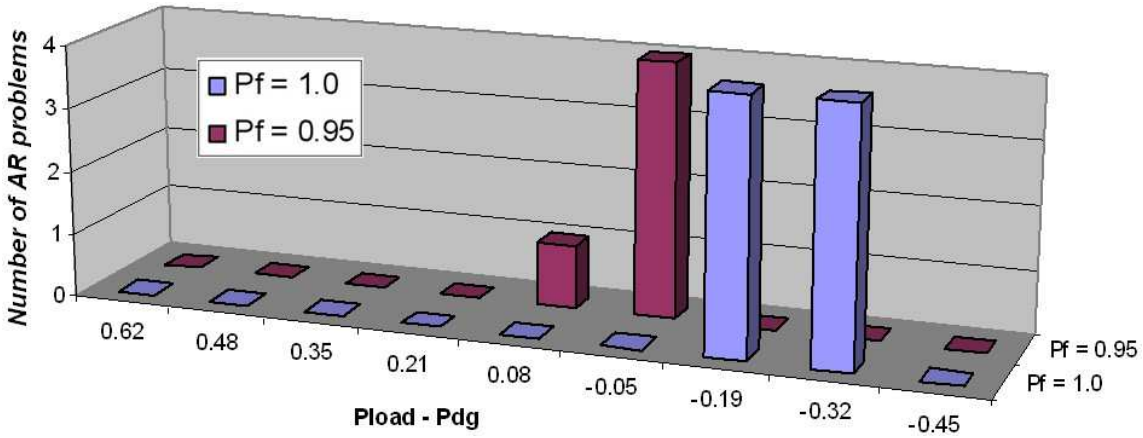

Figure 6. The distribution of AR problems in relation to active power imbalance on the feeder

Since about 9% of the ARs still failed in case 3, the voltage limit of the LOM relay was set to a stricter value in case 4. With this measure, a successfulness rate of 95.83% was reached. In case 5, the idea was to improve the situation by applying stricter frequency limits. This, however, did not bring any further improvement in this particular case as table 1 shows. Case 6 examined the effect of having a stricter ROCOF treshold. By changing the ROCOF setting from 1Hz/s to 0.5Hz/s a successfulness rate of 97.92% was reached. Finally, a successfulness rate of 100% was

achieved in case 7 by applying shorter operate delays. The delay for ROCOF was set to 0.12s (minimum setting in this relay type), whereas, for frequency protection the delay was set to 0.1s. Although the settings used in case 7 managed to raise the successfulness rate to 100%, it must be noted that such strict settings would quite likely also cause nuisance tripping of the DG unit.

Table 2 presents how large share of the successful AR sequences were detected by UV and ROCOF in each case. As it can be seen from the table, all of the successful AR sequences were cleared by these two functions. OV and frequency protection were either slower than UV and ROCOF, or they were not tripped at all in any of the examined situations. OV and frequency protection, however, might have an important role in clearing other kinds of disturbance situations. The share of UV protection was fairly high in all of the studied cases. One reason for this was the fact that UV protection cleared all three phase faults successfully. A large share of the ARs would, however, still have failed if ROCOF was not utilized (e.g. some 15% in case 7).

Table 2. The detection shares of OV and ROCOF protection functions and the share of failed ARs

	UV protection share %	ROCOF protection share %	Failed AR Sequences %
case 1	50.00	0.00	50.00
case 2	50.00	27.08	22.92
case 3	50.00	40.97	9.03
case 4	84.72	11.11	4.17
case 5	84.72	11.11	4.17
case 6	84.72	13.19	2.08
case 7	85.42	14.58	0.00
Total	69.94	16.87	13.19

CONCLUSIONS

The simulations indicated that a high successfulness rate of AR can be reached with relatively simple LOM protection provided that strict LOM relay settings are used. Strict LOM relay settings, however, have the disadvantage that they make the protected DG unit prone to nuisance tripping which is unwanted both from the DNO- and the owner of the DG unit point of view. Nuisance tripping of DG can also be risky for the system stability in certain areas where DG penetration is high. The simulation results also indicated that UV protection has a very significant role in ensuring a high successfulness level of ARs. The utilization of strict UV thresholds may, however, not be allowed in the future if DG units are needed to contribute to system stability – that is, if the fault ride trough (FRT) requirements are diffusing to MV level as well. The utilization of strict UV limits is clearly conflicting with the FRT requirements which demand that generation units are able to ride trough deep voltage dips without losing their stability.

Another option for improving the successfulness of ARs is prolongation of AR open times. This option is unfortunately also unwanted since this measure has a degrading effect on power quality. The problems with AR and unintentional islanding could, of course, be tackled by equipping all DG units with a LOM protection technology that is not prone to the NDZ problem. Communication based LOM protection methods are one of such solutions but they generally require some additional capital compared to passive and active detection methods. There is thus clearly a strong need to develop new LOM detection methods for DG units that are both reliable and cost effective.

REFERENCES

[1] Barker, P. P., De Mello, R. W. "Determining the Impact of Distributed Generation on Power Systems: Part 1 – Radial Distribution Systems", Power Engineering Society Summer Meeting, 2000. IEEE. July 2000. Vol. 3, pp. 1645-1656

[2] Brüdlinger, R., Bletterie, B., Unintentional islanding in distribution grids with a high penetration of inverter-based DG: Probability for islanding and protection methods, Power Tech, Russia, June 2005

[3] E.Lakervi & E.J.Holmes, Electricity distribution network design, London, UK, IEE Power series 21, 325 p, 1995

[4] Sähköenergialiitto ry & Energia-alan Keskusliitto ry, Keskeytystilasto 2003, Helsinki 2004, 21p. (Finnish)

[5] IEEE Power Engineering Society, IEEE Guide for Automatic Reclosing of Line Circuit Breakers for AC Distribution and Transmission Lines, IEEE Std. C37.104™-2002

[6] Kim, I-D., Cho, H-S., Park, J-K., "A variable dead time circuit breaker auto-reclosing scheme using artificial neural networks", Electrical Power and Energy Systems 21 (1999) 269-277, June 1998

[7] Pleym, A., et. al., Connection of distributed generation – effect on the power system, Norway, March 2003, Report of CODGUNet work package 5, 115p.

[8] Kumpulainen, L., Kauhaniemi, K., "Analysis of the impact of distributed generation on automatic reclosing", Power Systems Conference & Exposition, October 2004, New York

[9] Mäki, K., Novel Methods for Assessing the Impacts of Distributed Generation in Distribution Network Planning, Doctoral dissertation, 2007

[10] Kumpulainen, L., Kauhaniemi, K., Verho, P., Vähämäki, O., "New Requirements on System Protection caused by Distributed Generation", 18th International Conference on Electricity Distribution, 2005, Turin

[11] Figueroa, M., A., Orduña, E., "Application of Single Pole Auto-Reclosing in Medium Voltage Distribution Networks for improving Integration of Distributed Generation", Transmission & Distribution Conference and Exposition: Latin America, 2006, August 2006

[12] Repo, S., Mäki, K., Järventausta, P., Electricity Distribution and Distributed Generation, DENSY project final report, Tampere, 2008, 59 p.

[13] Samuelsson, O., Stråhl, N., "Islanding detection and connection requirements", Power Engineering Society General Meeting, June 2007

[14] Mahat, P., Chen, Z., Bak-Jensen, B.," Review of Islanding Detection Methods for Distributed Generation", DRPT 2008, April 2008, Nanjing, China

[15] Abarrategui, O., Zamora, I., Larruskain, D. M., Comparative analysis of islanding detection methods in networks with DG, 19th International Conference on Electricity Distribution, 2007, Vienna

[16] Rintamäki, O., Kauhaniemi, K. "Applying modern communication technology to loss-of-mains protection", CIRED 2009, Prague

[17] RTDS Technologies, RTDS Manual Set

[18] Finnish Electricity Association SENER, "Pienvoimaloiden liittäminen jakeluverkkoon", SENER publishing series, Helsinki, Finland 2001 (Finnish)

Publication 2

O. Raipala, A. S. Mäkinen, S. Repo and P. Järventausta, "The effect of different control modes and mixed types of DG on the non-detection zones of islanding detection", *in Proc. International Conference on Electricity Distribution (CIRED) Workshop 2012*, Lisbon, Portugal, May 2012

THE EFFECT OF DIFFERENT CONTROL MODES AND MIXED TYPES OF DG ON THE NON-DETECTION ZONES OF ISLANDING DETECTION

Ontrei Raipala
Tampere University of Technology, Finland
Ontrei.raipala@tut.fi

Anssi Mäkinen
TUT, Finland
anssi.makinen@tut.fi

Sami Repo
TUT, Finland
sami.repo@tut.fi

Pertti Järventausta
TUT, Finland
pertti.jarventausta@tut.fi

ABSTRACT

Loss of mains protection (LOM) is among the most challenging issues related to the integration of distributed generation (DG). This paper presents simulation studies on the effect of multiple DG units on LOM protection. The results reveal an operational risk related to the active LOM detection methods. The effect of voltage droop control of the DG on the form of the NDZ is also studied.

INTRODUCTION

The growth of distributed generation capacity brings upon many potential benefits but also raises new challenges. Among these challenges, unintentional islanding is considered to be among the most difficult issues. Islanding refers to situation where a network section including both customer loads and DG becomes isolated from the main grid. Unintentional islanding is forbidden because it raises safety hazards for utility personnel and may cause damage to DG units as well as to network components. All DG units thus need to be equipped with a loss of mains (LOM) protection scheme which ensures that unintentional islanding does not occur. Moreover, it is also important for the utilization of intentional islanding that the transition to islanding is rapidly detected so that the DG units in the islanded circuit can switch their control modes in order to sustain the frequency and voltages in the island.

A large number of various LOM detection methods have been presented in the literature [1-4]. Many of these are methods are claimed to show high performance. It is thus important that the performance of these methods can be assessed in an objective way. The determination of the non-detection zone (NDZs) of LOM detection algorithms is a suitable approach for this. NDZs can be represented in a load parameter space [1, 2] or in a power mismatch (ΔP, ΔQ) space [5, 6]. Power mismatch space is suitable for the assessment of passive LOM detection methods, whereas, for the assessment of active LOM detection schemes, it is advisable to utilize load parameter space [2]. The authors [5] presented studies in which the NDZ of voltage magnitude and frequency based LOM protection for a circuit which included a converter coupled DG unit. Similar studies with the exception that the protected DG unit was a directly coupled synchronous generator were presented by the authors [6]. However, there seems to be no studies concerning the NDZ in a case where the islanded circuit contains both directly as well as converter coupled DG units in the literature. This paper aims to fill this gap.

LOSS OF MAINS PROTECTION

Most of the LOM protection methods are based on detecting the changes in some system quantities such as voltage and frequency. These changes, which usually take place when islanding occurs, are mainly caused by the imbalance between the production and consumption of real- and reactive power in the island. There is, however, a risk that this imbalance is so small that the transition to island mode does not cause any of the quantities measured by a LOM relay to drift out of the preset limits. In cases like this, LOM protection fails to detect islanding. This blind area of LOM protection in the surroundings of the production-consumption equilibrium is called the NDZ. [5, 6] The grey area in Fig. 1 illustrates the conceptual shape of the NDZ for traditional overvoltage- (OVP) / undervoltage (UVP) and overfrequency- (OFP) / underfrequency based LOM protection (UFP) in power mismatch space. As the left side of the figure illustrates, reactive power imbalance (ΔQ) is mainly related to UVP/ OVP limits and active power imbalance (ΔP) mainly to UFP/ OFP limits, when the islanded network is maintained by a directly coupled synchronous generator [6]. However, the boundaries formed by the protection functions in the NDZ twist approximately 90 degrees in relation to the active- and reactive power axes when the protected DG unit is constant power controlled converter coupled generating unit as the right side of fig 1 illustrates. [5].

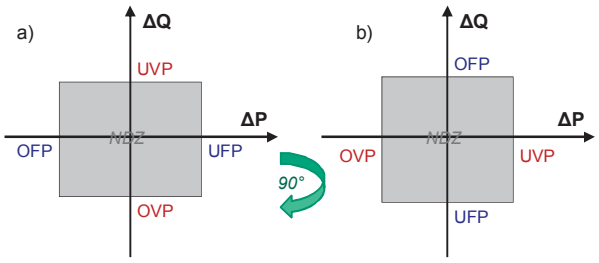

Fig. 1. Non-detection zone for voltage and frequency based LOM protection when the protected DG unit is a) directly coupled synchronous generator b) constant power controlled converter coupled generating unit

Categorization of LOM detection methods

LOM detection methods can be divided into four groups. These are communication based methods, local passive-, local active-, and hybrid methods. A short introduction to these methods is given in the following.

Passive methods are based on locally measuring certain system quantities, such as voltage and frequency. The idea behind these methods is that changes in the measured quantities usually occur during the transition to islanding.

Passive methods are the most utilized ones due to their low cost and applicability to all DG units. However, most of these methods have a fairly large NDZ. [3,4]
Active LOM protection schemes are based on constantly injecting small perturbations into the network and measuring the response of the system. The idea behind this is that the system quantities can only be manipulated when islanding occurs. [4] Some active detection schemes can even detect balanced islanding, but they tend to provide slower detection because changing the system quantities takes time [3].
Hybrid methods attempt to combine the advantages of passive and active methods. This is done by activating the chosen active method only when the chosen passive method suspects islanding. This approach reduces the power quality problems caused by the active method remarkably since the active method is, most of the time, not activated. However, the utilization of two sequential methods usually results to longer detection time [3].
The idea in the communication based LOM protection schemes is to signal all the downstream DG units whenever the opening of an upstream switch causes the connection to the main grid to be lost. These schemes are immune to the NDZ problem because they are not based on local measurements. Communication based methods are superior to the other LOM detection methods from the technical point of view but they are also generally more costly and vulnerable to communication failures. [4]

SIMULATION ENVIRONMENT

The studies were performed using a unique real time simulation environment consisting of two types of real time simulators, namely the dSPACE and the RTDS®. The dSPACE is a well proven tool for modelling control systems and power electronics, whereas, the RTDS provides very accurate real time electromagnetic transient simulation for power systems. This environment, which is depicted in Fig. 2, also enables the connection of real external devices to be connected to function as a part of the simulation. More information on the simulation environment can be found from [7].

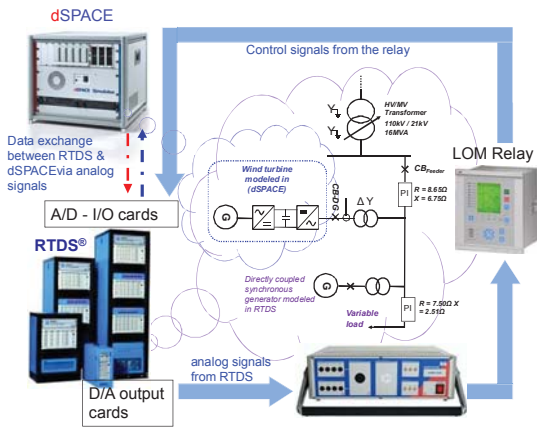

Fig. 2. The utilized simulation environment

The RTDS, which consists of a number of processor cards, and I/O cards, was used for running the power system modelled with the help of a dedicated program called RSCAD. A real LOM relay was set to control the DG unit circuit breaker in the power system model. The voltage signals from the connection point of the DG were first given as analog output signals to a Omicron CMS156 amplifier, which amplified the signals to proper scale for the use of the LOM relay. The LOM relay then sent its control decisions concerning the DG unit circuit breaker back to the RTDS as digital signals via copper wires. The utilized LOM protection settings, which are shown in table I, were not taken from any specific standard but they are very close to many European national recommendations [8].

Table I. The utilized LOM relay protection setings

Protection function	Threshold	delay
Voltage	0.8 x Un & 1.15 x Un	0.2 s
Frequency	49 Hz & 51 Hz	0.2 s

A full power converter connected wind turbine (FCWT) was modelled with the help of Matlab that was equipped with Simulink and Real Time Workshop. This model was then compiled for the use of the dSPACE simulator. The connection between the two real time simulators was established via analog signals as shown in Fig. 2.

SIMULATION MODELS

A simple distribution network model, which is shown in Fig. 3, was modelled with the help of RSCAD for performing these studies. The model consists of voltage source representing the main grid, a 110kV/21kV rated HV/MV transformer, one medium voltage distribution feeder which is represented by two π-line representations and a variable load at the tail part of the distribution feeder. Additionally, a directly coupled 1.6MVA rated hydro power driven synchronous generator (SG) was connected to the mid-section of the feeder via a 0.66kV/21kV step up transformer. All the above described components were simulated by the RTDS, whereas, the in-detail modelled FCWT was simulated by the dSPACE as shown in Fig. 3. This 500kVA rated DG unit is presented in detail in [7].
The reactive power control of the SG model was realized using a cascade control, where a control loop determined the set point of the automatic voltage regulator with the aim of maintaining the reactive power output at a target value. Certain simplifications, namely the omission of the turbine controller modeling and the assumption of constant torque were made in the models. These measures are justified since hydro power plants have relatively high inertial mass which makes them respond to changes slowly, whereas, LOM protection studies are dealing with short timeframes only. The omission of turbine controller is justified because DG units are typically not attending to frequency control.

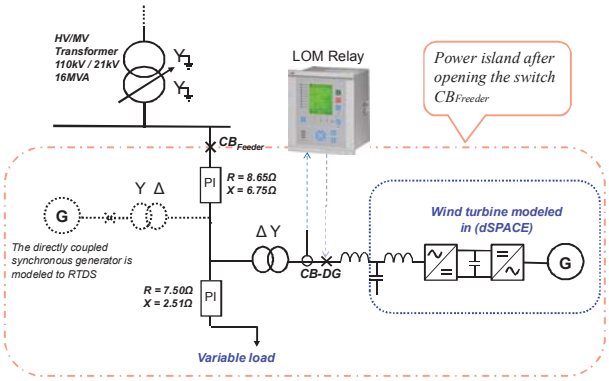

Fig. 3. The utilized simulation model

The power imbalance on the feeder was varied in small steps by varying the demand of the controllable constant impedance type load connected to the tail part of the feeder. For each combination of power imbalance, the CB_{Feeder} switch was opened after the output power of the DG unit had stabilized. The resulting power island was then maintained only by the DG until the LOM relay operated. In each case, the active and reactive power imbalance, the operation time of the LOM relay as well as certain other parameters were captured. The NDZs for the studied cases, which will be presented in the following chapter, were determined based on this stored data.

SIMULATION RESULTS

The effect of DG type on the NDZ

The purpose of the first simulation study was to verify the phenomenon presented in Fig 1. The results of this study can be seen from Figs. 4, which represents the NDZ of UVP/OVP and UFP/OFP based LOM protection in a case where the only DG unit was the directly coupled SG unit, and 5, which represents the NDZ of the same protection functions when the protected DG unit was the FCWT which was operated in constant reactive current mode [7]. The green colour in Figs. 4 - 7 represents the power imbalance area (in terms of ΔP and ΔQ) where the OVP function tripped within 0.5s, whereas the light blue area similarly represents the respective area for UFP function, dark blue colour for OFP function and orange colour for UVP function. The red area in the middle of these four areas represents the set of power imbalance combinations where none of the four functions detected the islanding within 0.5s. The axes in the figures are in per unit (pu) values, where the utilized base value in each case is the total generation on the feeder before the islanding. The base values were thus 1.35 MVA in Fig. 4, 0.48 MVA in figures 5 and 7, and 1.83 MVA in Fig. 6.

By comparing Figs. 4 and 5, it can be seen that the NDZ as well as the four trip regions in Fig. 5 have twisted approximately 90 degrees in the clockwise direction in comparison to the ones in Fig. 4. This result is in line with the earlier studies in [5 and 6].

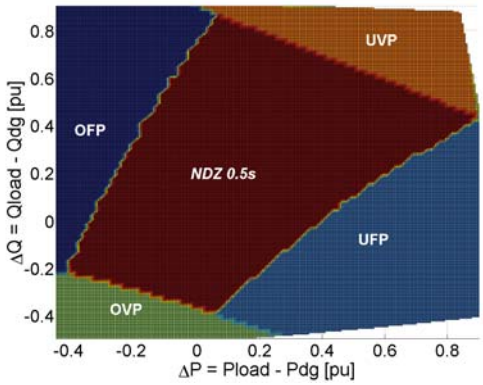

Fig. 4. The NDZ when the protected unit was the SG

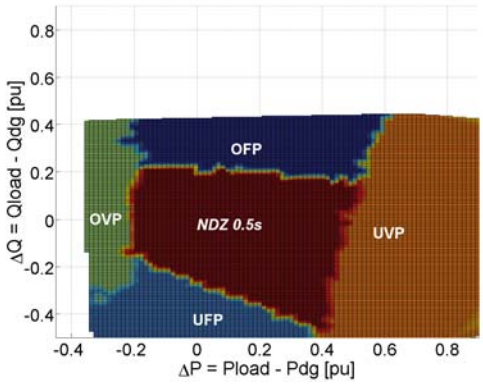

Fig. 5. The NDZ when the protected DG unit was the FCWT

The effect of mixed type of DG on the NDZ

In the following study, the FCWT and 1.6MW rated directly coupled SG were connected in parallel as presented in Fig. 3. The NDZ resulting from this study is shown in Fig. 6. By comparing Figs. 4 and 6, it can be seen the two NDZs have a similar type of shape and interestingly, the trip regions of the four protection functions in Fig. 6 are located very similarly as in Fig. 4. This means that the directly coupled SG seems to have dominated the relations between active- and reactive power imbalance with frequency and voltages.

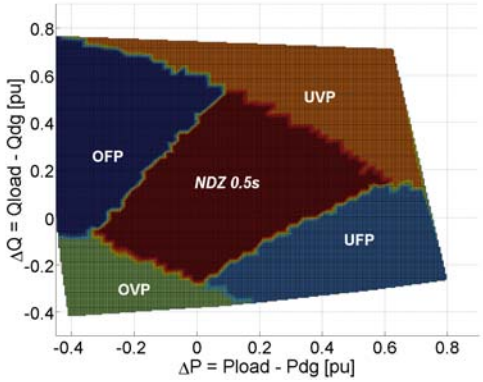

Fig. 6. The NDZ when both of the DG units were connected

This phenomenon can have implications on the functioning of certain active LOM detection schemes, since most of

them assume that reactive power imbalance mainly determines frequency and active power mainly determines the voltages in an islanded network. Reactive power fluctuation method, for instance, is based on making small changes in its reactive output power based on the frequency response of the system it measures. However, reactive power doesn't necessarily affect frequency when the islanded circuit contains both converter connected DG and directly coupled SG as shown in Fig. 6. This scenario may thus lead to the malfunctioning of certain active methods.
It is noteworthy that the nominal power of the directly coupled SG was larger compared to the one of the FCWT. However, this kind of scenario is realistic since many of the converter connected DG units, such as photovoltaic and micro turbines, are small sized in comparison with directly coupled SGs.

The effect of voltage droop control of DG on the NDZ
In the following study, a voltage droop with a 5 percent deadband was added to the grid side converter control system. The droop was adjusted so that the FCWT gave maximum available reactive power output at 50 percent voltage deviation. The SG unit was disconnected and the simulations were repeated. Fig. 7, which represents the resulting NDZ, shows that the NDZ bends from both ends due to the droop, whereas, the deadband of the droop prevents the bending from the middle part of the NDZ. It is also interesting that the UVP trip region has enlarged to cover some of the power imbalance points which previously belonged to the UFP trip region. The bending of the NDZ in the right most side of Fig. 7 shows that the NDZ region can include surprising ΔP & ΔQ combinations depending on the utilized control mode of the protected DG unit.

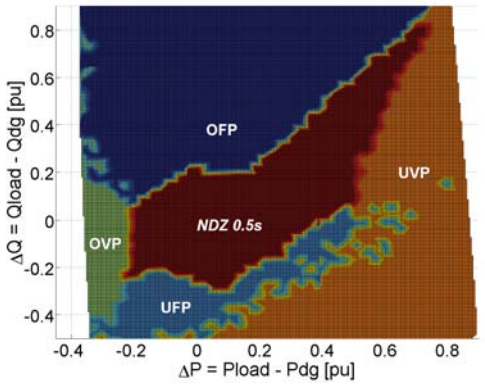

Fig. 7. The NDZ when the protected unit was the FCWT which was operated in voltage droop mode (5% deadband)

DISCUSSION

The simulations indicate that the assumption between ΔP & voltages as well as ΔQ & frequency during islanding, which many active LOM detection schemes assume, is not always valid. It is problematic that even though this assumption may be valid at the time of installing a converter connected unit, it can later be invalidated once a synchronous generator is installed nearby.
It is noteworthy that albeit certain active LOM detection schemes may be considerably degraded in the presence of SGs, they may still function after the LOM protection of the SG unit has operated. This, however, causes an additional delay to the operation of the active scheme.

CONCLUSIONS

This paper studied the effect of mixed type of DG on the NDZs of LOM protection. A directly coupled and a converter coupled DG unit were connected in parallel in order to study the combined effect on the NDZ. The simulations revealed a potential operational risk for certain active LOM detection methods. This risk should be taken into account in the design of these protection schemes. The simulations also revealed that the addition of voltage droop on grid side converter control system of the DG unit can extend the NDZ area to cover surprising power imbalance combinations.

REFERENCES

[1] W. Bower and M. Ropp, 2000, "Determining the Relative Effectiveness of Islanding Detection Methods Using Phase Criteria and Nondetection Zones", *IEEE Trans. on Energy Conversion,* Vol. 15, No. 3

[2] L. A. C. Lopes and H. Sun, 2006, "Performance Assessment of Active Frequency Drifting Islanding Detection Methods", *IEEE Trans. on Energy Conversion*, Vol. 21, No. 1

[3] Mahat, P., Z. Chen and B. Bak-Jensen, 2008, "Review of Islanding Detection Methods for Distributed Generation", *Proc. of DRPT 2008*

[4] Samuelsson, O. and Stråth, N., 2007, "Islanding detection and connection requirements", *Proc. of Power Engineering Society General Meetings*

[5] Z. Ye, A. Kolwalkar, Y. Zhang, P. Du and R. Walling, 2004, "Evaluation of Anti-Islanding Schmes Based on Nondetection Zone Concept", *IEEE Trans. on Power Electronics*, Vol. 19, No. 5

[6] J. C. M. Vieira, W. Freitas, W. Xu and A. Morelato, 2008, "An Investigation on the Nondetection Zones of Synchronous Distributed Generation Anti-Islanding Protection", *IEEE Trans. on Power Delivery*, Vol. 23, No. 2,

[7] A. Mäkinen, 2008, "Wind Turbine and Grid Interaction Studies Using Integrated Real-Time Simulation Environment", *Proc. of Nordic Workshop on Power and Industrial Electronics*

[8] V. Van Thong and R. Belmans, 2010, "Maximum penetration level of distributed generation with safety criteria", *Euro. Trans. Electr. Power,* Vol. 20, No. 3.

Publication 3

O. Raipala, A. S. Mäkinen, S. Repo and P. Järventausta, "Interaction of fault ride through requirements and loss of mains protection", *in Proc. International Conference on Renewable Energies and Power Quality (ICREPQ'13)*, Bilbao, Spain, March 2013

International Conference on Renewable Energies and Power Quality (ICREPQ'13)
Bilbao (Spain), 20th to 22th March, 2013
Renewable Energy and Power Quality Journal (RE&PQJ)
ISSN 2172-038 X, No.11, March 2013

Interaction of fault ride through requirements and loss of mains protection

O. Raipala[1], A. S. Mäkinen[1] S. Repo[1] and P. Järventausta[1]

Department of Electrical Energy Engineering
Tampere University of Technology
Korkeakoulunkatu 3, FI-33720 Tampere (Finland)
Phone: +358 3 311 511, e-mail: **Ontrei.raipala@tut.fi**

Abstract. The strongly growing DG capacity is raising concerns related to unintentional islanding. Unintentional islanding is prohibited due to the associated safety risks, and it is therefore mandatory to equip all DG units with some kind of loss of mains (LOM) protection. However, large amounts of unnecessary tripping of DG units cannot be tolerated anymore as the share of DG has already reached a significant share of the total installed power generation in certain regions. Certain grid codes thus require DG units to be able to ride through remote faults and support the power system. It is generally known that grid codes and LOM protection objectives are of somewhat controversial. However, it appears that no papers have studied the relation of LOM protection performance and fault ride through requirements thoroughly with simulations. This paper aims to fill this gap by providing extensive simulations which show how exactly the grid code requirements affect the performance of LOM protection. The studies are performed in a unique simulation environment consisting of two different types of real time simulators and a real LOM relay.

Key words

Loss of mains protection, anti-islanding protection, FRT requirements, Non-detection zone, real time simulation

1. Introduction

The rapidly increasing amount of DG has raised concerns related to unintentional islanding. Unintentional islanding is prohibited due to the associated safety risks which are:

1) Unsynchronized reclosing which may damage network components and DG units
2) Failed reclosing of a distribution feeder due to DG back feeding
3) Customer devices may be damaged due to poor power quality in the islanded circuit
4) Lines that are thought to be de-energized can be energized by DG. This is a safety risk for utility field personnel.

All DG units thus need to be equipped with some type of loss of mains (LOM) protection which ensures that unintentional islanding does not occur. The operation speed requirement for LOM protection may vary from case to case. For instance, the utilization of fast reclosing, i.e. aforementioned reasons number 1 and 2, require rapid islanding detection times from LOM protection (typically from 0.2s to a couple of seconds). These requirements can be avoided by not using reclosing. However, this is highly undesirable from supply reliability point of view since the majority of faults are temporary in nature and can thus be cleared with the help of reclosing. For instance, in Finland about 90% of faults on overhead lines are temporary in nature and thus also clearable by automatic reclosing [1]. A reasonable option is to extend the open time of the circuit breaker during fast reclosing to provide enough time for LOM protection to operate.

Very sensitive LOM protection settings, however, also have disadvantages. This stems from the fact that faults in transmission network can launch huge amounts of adverse tripping of DG units which was, for instance, seen during the UCTE disturbance in the 4th of November 2006 [2]. Because of this risk, system operators have issued grid codes that define how long generating units have to be able to stay connected and support the system stability during various kinds of disturbances. These fault ride through (FRT) requirements were originally meant only for large wind parks connected to high voltage (HV) grids. However, the rapid growth of DG has led these requirements to diffuse to medium voltage (MV) and low voltage (LV) levels as well.

It is generally known that the objectives of LOM protection are of somewhat controversial with the objectives of FRT requirements. However, it appears that no papers have studied the relation of LOM protection performance and FRT requirements thoroughly with simulations. This paper aims to fill this gap by providing extensive simulations which show how exactly the grid code requirements affect the performance of LOM protection. The studies are performed in a unique simulation environment consisting of two different types of real time simulators and a real LOM relay.

2. Non-detection zone of LOM protection

The non-detection zone (NDZ) is a suitable approach for assessing the performance of different LOM protection

algorithms. NDZs can be represented in a load parameter space [3], [4] or in a power mismatch (ΔP, ΔQ) space [5], [6]. Power mismatch space is suitable for the assessment of passive LOM detection methods, whereas, for the assessment of active LOM detection schemes, it is advisable to utilize load parameter space [3]. More information concerning the NDZ concept can be found from references [3] and [4].

The behaviour of voltage magnitude and frequency in an islanded circuit are largely dependent not only on the characteristics of the DG unit(s) in the island, but also on the characteristics of the islanded load(s). The loads used in islanding detection tests are usually modelled as parallel RLC circuits with a quality factor (Q_f) ranging from 1.0 to 2.5. A quality factor value of 2.5 is typically utilized in North American standards even though it is higher than what would be expected for a typical parallel RLC load [7]. However, there have been plans to reduce the Q_f of islanding test load from 2.5 to 1.0 [7]. The quality factor, which defines the relative energy storage and dissipation of an RLC circuit, is defined in IEEE-929-2000 standard for a parallel RLC circuit in equation 1 [3], [7], [8].

$$Q_f = R\sqrt{\frac{L}{C}} \tag{1}$$

3. Simulation environment

The simulation studies presented here were conducted using a unique real time environment consisting of two types of real time simulators. The dSPACE is a well proven tool for modelling control systems and power electronics, whereas, the RTDS provides very accurate real time electromagnetic transient simulation for power systems. This environment, which is depicted in Fig. 1, also enables the connection of real external devices to be connected to function as a part of the simulation. More information on the environment can be found from [9].

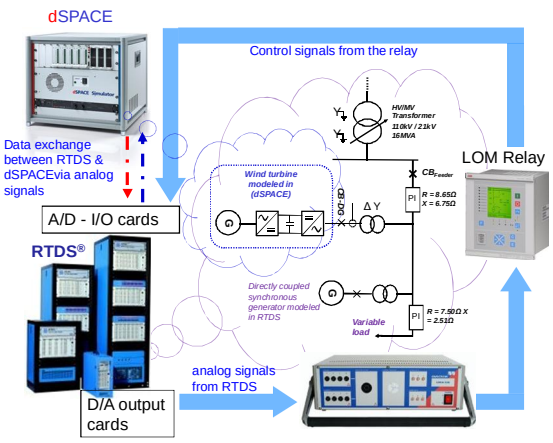

Fig. 1. The simulation environment

The RTDS, which consists of a number of processor cards and I/O cards, was used for running the power system modelled with the help of a RSCAD. A real LOM relay was set to control the DG unit circuit breaker in the power system model. The voltage signals from the connection point of the DG were first given as analogue output signals to a Omicron CMS156 amplifier, which amplified the signals to proper scale for the LOM relay. The LOM relay then sent its control decisions concerning the DG unit circuit breaker back to the RTDS as digital signals.

A. Typical LOM relay settings

The utilized LOM protection functions in the studies of this paper were undervoltage-, overvoltage, underfrequency and overfrequency protection. The LOM protection settings that were utilized for simulating the NDZs in Figs. 4 - 6, which are shown in table I, were not taken from any specific standard but they are very close to many European national recommendations [10].

Table I. – LOM protection settings

Protection function	Threshold	delay
Voltage	0.8 x Un & 1.15 x Un	0.2 s
Frequency	49 Hz & 51 Hz	0.2 s

B. FRT compliant LOM relay settings

Low voltage ride through (LVRT) requirement is mostly related to loosening the undervoltage protection (UVP) threshold of LOM protection. However, certain other methods, as for instance rate of change of voltage, which are based on detecting islanding with the help of change in voltage, may also need to be loosened to allow the LVRT. The blue line in Fig. 2 illustrates the shape of LVRT curve for generating units in the range of 0.5MW to 100 MW required by the Finnish transmission system operator Fingrid. Generating units need to be able to ride through faults in which the voltage does not drop below the blue curve in the figure, which represents the HV connection point voltage in per unit scale. The red line in Fig. 2 represents the two step approximation of the FRT curve which was utilized in the LOM relay.

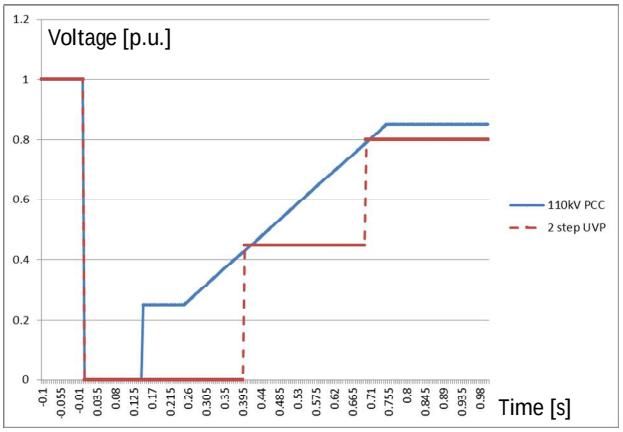

Fig. 2. The FRT requirement curve of Fingrid (blue line) and the utilized FRT compatible LOM protection UVP settings (red line)

The UVP settings had to be very simplified as shown in the figure because of the limited amount of configurable steps in the utilized protection relay. Relay manufacturers should take the FRT requirements into account in the UVP function blocks and design a user friendly way for making the UVP settings compatible with utility grid

codes. The FRT compatible UVP settings are also shown in table II. However, modern grid codes require generating units not only to be able to ride through faults but also to be able to support the voltages by feeding reactive power during grid faults [11], [12]. This issue will be taken into account in the simulation studies presented in chapter 5.

Table II. – The FRT compatible LOM protection settings

Protection function	Threshold	delay
Undervoltage low stage	0.8 x Un	0.7 s
Undervoltage high stage	0.45 x Un	0.4 s

It is noteworthy that the FRT compatibility is also related to communication based LOM protection methods since remote methods are typically equipped with a local LOM protection method for back up purposes. Thus, without coordination, the local back up protection may cause unwanted tripping during voltage dips. On the other hand, applying such back up protection settings that will enable the FRT will naturally degrade the performance of back up protection. One option to avoid this problem is to use continuous supervision of the communication channel instead of back up protection and immediately disconnect the protected DG unit whenever a malfunction in the communication channel is detected. However, as this kind of approach also causes unwanted tripping of DG, it would be more reasonable to only switch to the use of local back up protection once a malfunction in the communication channel is detected. This would ensure reliable and FRT compatible LOM protection.

4. Simulation models

A simple distribution network model, which is shown in Fig. 3, was modelled with the help of RSCAD for performing these studies. The model consists of voltage source representing the main grid, a 110kV/21kV rated HV/MV transformer, one MV distribution feeder which is represented by two π-line representations and a variable load at the tail part of the feeder. All the above described components were simulated by the RTDS, whereas, the modelled full converter connected wind turbine unit was simulated by the dSPACE as shown in Fig. 3. The modelling of this 500kVA rated DG unit is based on [13]. The synchronization to the grid voltage is carried out using synchronous reference frame phase locked loop (SRF-PLL) [14]. However, in one of the simulated cases another synchronization method was used in order to examine the significance of utilized synchronization method from LOM protection point of view. In this examined method, synchronization is implemented exploiting a PLL together with zero crossing detection of the phase a-supply voltage [15]. This method responds to changes fairly slowly since the zero crossing instants can only be detected once per half cycle of the utility voltage [15].

The power imbalance on the feeder was varied in small steps by varying the demand of the parallel RLC load connected to the tail part of the feeder. For each combination of power imbalance, the CB_{Feeder} switch was opened after the output power of the DG unit had stabilized. The resulting power island was then maintained only by the DG until the LOM relay operated. In each case, the active and reactive power imbalance, the operation time of the LOM relay as well as certain other parameters were captured. The NDZs for the studied cases, which will be presented in the following chapter, were determined based on this stored data.

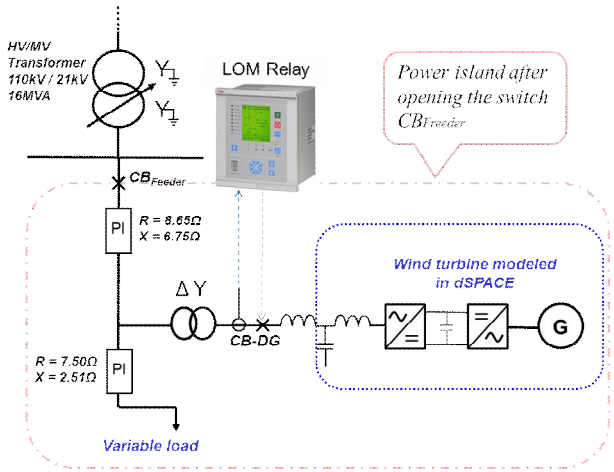

Fig. 3. The utilized simulation model

5. Simulation studies

This chapter, which presents the simulated NDZs, is divided into four subchapters. The first subchapter illustrates the effect of utilized synchronization method and the quality factor of the load on the performance of LOM protection. The second subchapter studies how exactly the performance of LOM protection is degraded when UVP function is set to allow the LVRT. The third subchapter demonstrates how reactive power support of DG affects the performance of LOM protection. Finally, the fourth subchapter examines how the addition of ROCOF function can enhance the situation. The quality factor was kept at 1.0 in all the simulation studies presented here except for the NDZ presented in Fig 6.

A. NDZ of a typical LOM protection

The LOM relay was configured according to the settings shown in table I in the studies of this subchapter. In the first simulated NDZ, the utilized synchronization method of the grid side converter (GSC) was a simple zero crossing based PLL (see [15] for more details). Fig. 4 shows the resulting NDZ. The quality factor of the load was kept at 1.0 in the simulations.

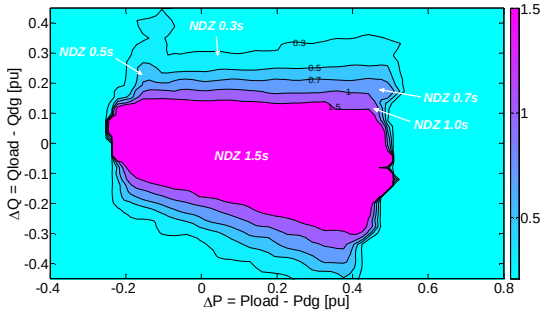

Fig. 4. The NDZ of LOM protection when the utilized synchronization method of the GSC was a PLL based on zero crossings. Q_f was 1.0.

The pink coloured area marked with the sign “NDZ 1.5s” in Figs. 4 - 9 represents the set of power imbalance combinations where LOM protection failed to isolate the DG unit within 1.5s from the beginning of the islanding. The other layers marked with the signs “NDZ 1.0s”, “NDZ 0.7s”, “NDZ 0.5s” and “NDZ 0.3s” respectively refer to relay operation times 1.0s, 0.7s, 0.5s and 0.3s. This means that the smaller the size of NDZ is, the better the performance of LOM protection is. This multi-layer NDZ format is more suitable for showing the effect of the FRT compatible LOM protection settings compared to the basic NDZ format as it will be seen from the later results.

In all the rest of the following simulations, the utilized synchronization method of the GSC was the SRF-PLL [14]. The resulting NDZ, which is shown in Fig. 5, is considerably smaller than the one in Fig 4. The comparison between Figs. 4 and 5 thus clearly illustrates that the importance of the utilized synchronization method of the grid side converter should not be underestimated.

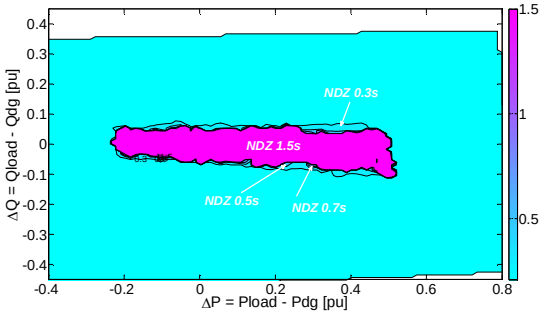

Fig. 5. The NDZ of LOM protection when the utilized synchronization method of the GSC was the SRF-PLL.

The quality factor of the parallel RLC load was now changed from 1.0 to 0.1 and the previous simulations were repeated. Fig. 6 shows the resulting NDZ. By comparing Figs. 5 and 6 it can be clearly seen that the size of the NDZ reduces significantly in the ΔQ range as the quality factor of the parallel RLC load is reduced to 0.1.

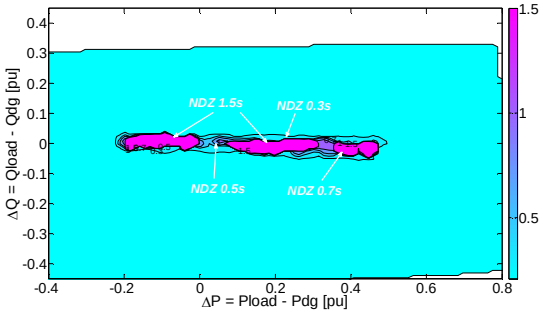

Fig. 6. The effect of reducing Q_f to 0.1.

B. NDZ of FRT compliant LOM protection

In the following case, the UVP function of the LOM relay was set to allow the LVRT by utilizing the settings presented in table II. Fig. 7 represents the resulting NDZ. It can be seen from the figure that the NDZ now extends considerably further in the positive ΔP axis direction than what it did with the original settings (Fig. 5). It can be seen from Fig. 7 that the size of the NDZ area where it took more than 1.5s to detect islanding is approximately same as in Fig. 5. However, a long extended NDZ area where it took more than 0.7s is now added to the original NDZ. It is noteworthy that UVP function trip region was not reached in the simulated NDZ, that is, the NDZ would extend even further towards the positive ΔP axis direction than what Fig. 7 shows. Note that the scaling in Fig. 7 is very different from the scaling in earlier figures. The quality factor was kept at 1.0.

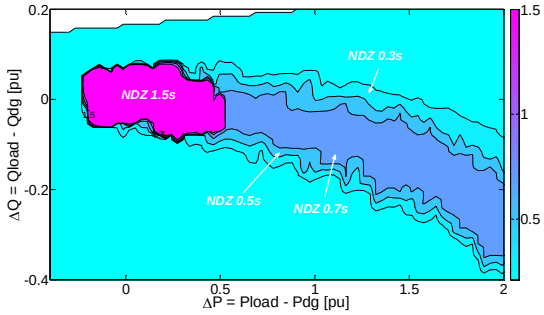

Fig. 7. NDZ of a FRT compatible LOM protection. Q_f was 1.0.

A clear bending can be seen in Fig. 7. This is caused by a sequence of events. Firstly, let us analyze the power imbalances during islanding with the help of equations 2 and 3. The relation between active power imbalance and voltage can be expressed with equation 2, whereas, the relation between reactive power imbalance and the frequency can be expressed by equation 3:

$$\Delta P = P_{Load} - P_{DG} = \frac{U^2}{R} - P_{DG} \quad (2)$$

$$\Delta Q = Q_{Load} - Q_{DG} = \frac{U^2}{X} - Q_{DG} = \frac{U^2}{2\pi fL - \frac{1}{2\pi fC}} - Q_{DG} \quad (3)$$

where U refers to the voltage at the load node, X is the reactance of the load and f refers to the frequency in the studied circuit. The losses are included in P_{Load} and Q_{Load}. Note that when an islanded circuit is sustained only by a converter connected DG unit, reactive power imbalance mainly determines the frequency and active power imbalance mainly determines the voltages in the island [4], [6]. Let us now consider a situation where a large initial active power deficiency is present in the circuit (i.e. a large ΔP) at the time when islanding occurs. It can be seen from equation 2 that due to the large ΔP the voltage is forced to decrease in order to bring a new balance between production and consumption in the islanded circuit because R and P_{DG} are fixed.

In this study, the GSC of the DG unit is controlled to operate with unity power factor during nominal operation mode. In order to achieve this goal, the reactive power generated by the LCL-filter capacitor of the GSC should be compensated. The compensation is done in the GSC control system by selecting a proper constant reactive current reference [9]. Thus, the GSC feeds a fixed constant inductive current component which compensates the reactive power produced by the filter capacitor at nominal voltage. However, when the voltage drops due to the large initial ΔP value, the reactive power produced by the filter capacitor reduces proportionally to the square of the voltage, whereas, the compensation power drawn by the DG unit (Q_{DG}) is only directly proportional to voltage.

Hence, the DG unit consumes reactive power with large ΔP values due to the reduced voltage. NDZ can only occur if there is a balance between produced and consumed reactive power. Hence, during significantly decreased voltage caused by large ΔP, the NDZ can exist only if the network load generates the reactive power (ΔQ<0) which is consumed by the DG. As a consequence, the NDZ bends to the negative side of ΔQ**.**

C. The effect of reactive power support of DG units

As already mentioned, modern grid codes usually also require generating units to be capable of supporting the power system during voltage dips by feeding reactive power into the grid. In the following case, a voltage droop with a 5 percent deadband was added to the GSC control system. The droop was adjusted so that the DG unit gave maximum available reactive power output at 0.5 per unit voltage. Fig. 8 shows the resulting NDZ. As the figure illustrates, the NDZ area now covered surprisingly large reactive power imbalances. This result shows that the performance of LOM protection is dangerously degraded when DG units are required to both be able to ride through faults and to provide voltage support by feeding reactive power.

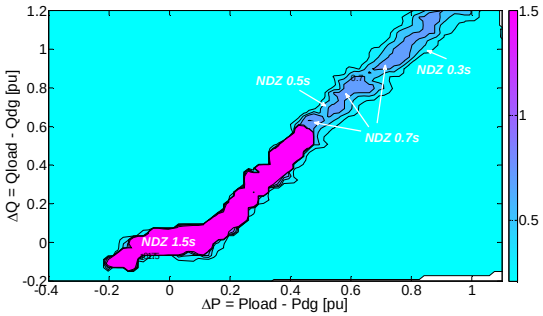

Fig. 8. The NDZ when a voltage droop control (5% deadband) was added to the GSC control system. Q_f was 1.0.

The reason for the bending of the NDZ in Fig. 8 is caused by the addition of the voltage droop. This can be understood by analysing the positive ΔP half of the graph. The greater the value of ΔP in this half of the figure, the greater is the decrease in the voltage at the DG- and at the load node. When the voltage drops below 95 percent of its nominal value at the DG connection point, the GSC begins to feed reactive power into the grid. Hence, an inductive load large enough has to be present in the islanded circuit in order for a NDZ to exist. The larger the initial ΔP value, the greater is the reactive power production of the DG unit during islanding, and the larger is the required value of the inductive load for the NDZ to exist. This causes the NDZ to bend as shown in Fig. 8.

Similar reasoning can be used for understanding the bending in the negative ΔP half of the Fig. 8. The smaller the ΔP value is, the more the voltage at the DG node increases. Thus, due to the voltage droop control, the DG unit begins to consume reactive power. Hence, a capacitive load that produces the reactive power consumed by the DG unit has to be present in order for the NDZ to exist. Consequently, the smaller the ΔP value, the larger is the required value of the capacitive load for the NDZ to exist. This causes the NDZ to bend in the negative ΔP half.

D. The effect adding ROCOF function

The rate of change of frequency (ROCOF) is one of the most utilized LOM protection methods. In the following case, the ROCOF function was added to the relay and its threshold was set to 1Hz/s with a 0.2s operate delay time. Fig 9 shows the resulting NDZ. The comparison between Figs. 8 and 9 shows that the addition of ROCOF reduces the size of the NDZ considerably from its ΔQ boundaries. However, the ROCOF is not able to reduce the size of the NDZ in the ΔP direction as expected.

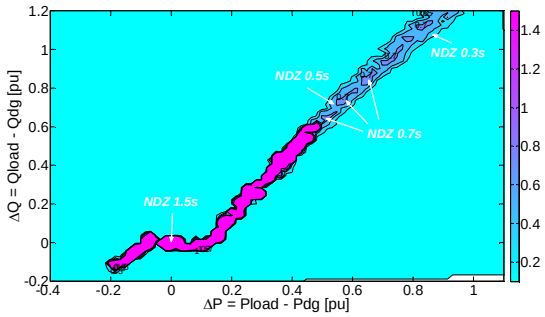

Fig. 9. The NDZ when the GSC was operated in voltage droop mode and the ROCOF function was set to 1Hz/s. Q_f was 1.0.

6. Discussion

Certain observations can be made from the simulated NDZs. Firstly, when analysing the effect of changing the normal UVP settings to FRT compatible settings, that is, comparing figures 5 and 7, one can see that the performance of LOM protection degrades significantly when changing to LVRT compatible UVP settings. This degrading is seen from the NDZ area which extends further than 2 in per unit scale. However, it is not as easily seen whether the addition of voltage droop control makes the situation more difficult to LOM protection. This can be assessed by evaluating which power imbalance combinations in the NDZ area are actually probable. Loads are normally on the inductive side rather than capacitive side, i.e., loads consume some, although typically small amount of reactive power. On the other hand, DG units in MV and LV networks are at present usually operated at unity power factor, i.e., they neither consume nor produce reactive power. This means that in most cases there is a small deficiency of reactive power in islanded circuits prior to the islanding event. Thus, such power imbalance combinations where $\Delta Q = Q_{load} - Q_{DG} > 0$ are much more probable than those where $\Delta Q < 0$ as illustrated in Fig. 10.

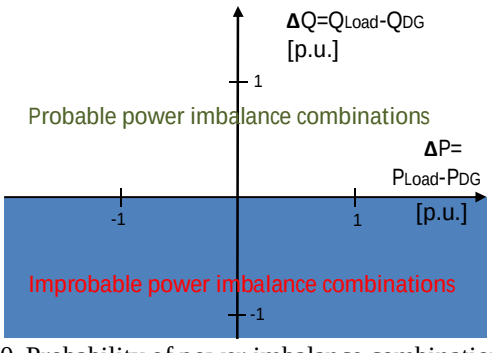

Fig 10. Probability of power imbalance combinations

It is nevertheless possible that the power imbalance could be on the capacitive side if for instance some poorly dimensioned compensation equipment is installed in the islanded circuit. However, this is not common as network operators usually have additional fees for significant reactive power production and consumption in medium voltage network level for discouraging such behaviour.

When examining Fig. 7 with the help of the idea presented in Fig. 10, it can be observed that a large portion of the NDZ area is situated in the improbable ΔQ range. This is illustrated in Fig. 11, which shows the improbable ΔQ range in the NDZ which was already presented in Fig. 7. Now, by evaluating which part of the NDZ in Fig. 8 is situated in the improbable ΔQ range, which is illustrated in Fig. 12, one can clearly observe that the situation becomes considerably more challenging to LOM protection when the voltage droop control is included.

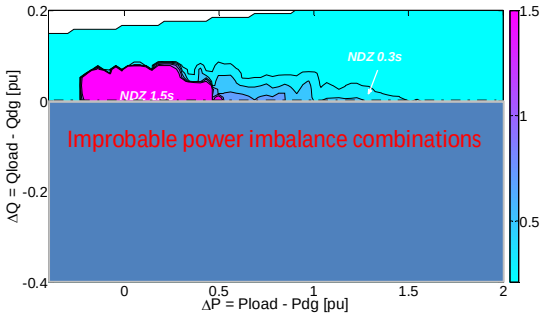

Fig. 11. The improbable power imbalance values in Fig. 7

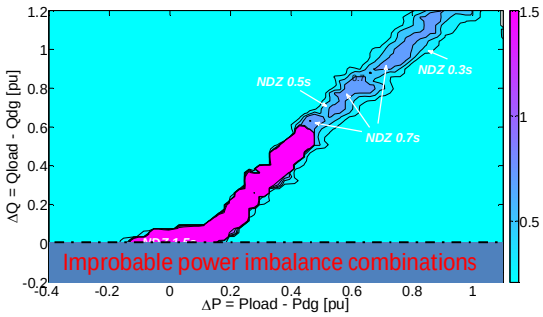

Fig. 12. The improbable power imbalance values in Fig. 8

However, in the future DG units may be utilized for controlling local voltages by consuming or producing reactive power. Voltage rise is probably a more common problem in the connection points of DG units than voltage drop. Thus, DG units would more likely be used for consuming reactive power and thus for preventing excessive voltage rise. This supports the idea presented in Fig. 10. However, DG units could in some cases also be used for producing reactive power and thus for preventing excessive voltage drop. This would lower the improbable power imbalance combinations boundary in Fig. 10.

7. Conclusion

This paper studied the effect of FRT requirements on LOM protection. The studies were based on a large number of simulations conducted in a unique real time simulation environment including a real LOM relay. It was observed that when LOM protection is set to allow DG units to ride through faults, the performance of UVP function is significantly degraded. In fact, in these studies, the NDZ region extended to further than 2 per unit in real power imbalance. Another observation was that the reactive power support which is required in many modern grid codes has a significant effect on the performance of LOM protection. Problematic situations for LOM protection may exist with surprisingly large reactive power imbalance points when the studied DG unit is set to support the system during voltage dips by feeding reactive power. It was also observed that the utilized synchronization method of the GSC may have a significant effect on the performance of LOM protection.

References

[1] Sähköenergialiitto ry & Energia-alan Keskusliitto ry, Keskeytystilasto 2003, Helsinki (2004), 21p.

[2] UCTE, System Disturbance on 4 November 2006, Final Report

[3] L. A. C. Lopes and H. Sun, "Performance Assessment of Active Frequency Drifting Islanding Detection Methods", IEEE Trans. on Energy Conversion, Vol. 21, No. 1, pp. 171 - 180, 2006

[4] M. Ropp et al., "Determining the Relative Effectiveness of Islanding Detection Methods Using Phase Criteria and Nondetection Zones", IEEE Trans. on Energy Conversion, Vol. 15, No. 3, pp. 290 - 296, 2000

[5] J. C. M. Vieira, W. Freitas, W. Xu and A. Morelato, "An Investigation on the Nondetection Zones of Synchronous Distributed Generation Anti-Islanding Protection", IEEE Trans. on Power Delivery, Vol. 23, No. 2, 2008

[6] Z. Ye, A. Kolwalkar, Y. Zhang, P. Du and R. Walling, "Evaluation of Anti-Islanding Schemes Based on Nondetection Zone Concept", IEEE Trans. on Power Electronics, Vol. 19, No. 5, 2004

[7] W. Xu, K. Mauch and S. Martel, an Assessment of Distributed Generation Islanding Detection Methods and Issues for Canada, CETC-Varennes 2004-074 (TR) 411-INVERT, Canada (2004), 53p.

[8] IEEE Std. 929-2000, IEEE Recommended Practice for Utility Interface of Photovoltaic (PV) Systems, Sponsored by IEEE Standards Coordinating Committee 21 on Photovoltaics, New York (2000), 26 p.

[9] A. Mäkinen and H. Tuusa, "Wind Turbine and Grid Interaction Studies Using Integrated Real-Time Simulation Environment", in Proc. NORPIE2008

[10] V. Van Thong and R. Belmans, "Maximum penetration level of distributed generation with safety criteria", European Trans. on Electric Power, Vol. 20, No. 3, pp. 367-381, 2010

[11] E. ON Netz GmbH, Requirements for Offshore Grid Connections in the E.ON Netz network, E. ON Netz GmbH, Bayreuth (2008)

[12] VDN, TransmissionCode 2007 Netz- und Systemregeln der Deutschen Übertragungsnetzbetreiber. Germany (2007), 90p.

[13] A. S. Mäkinen, H. Tuusa, "Impact of strength of fault current path on the operation of decoupled double synchronous reference frame – phase locked loop", to be published in ICREPQ'13 in March 2013

[14] R. Teodorescu, M. Liserre and P. Rodríguez, Grid Converters for Photovoltaic and Wind Power Systems, John Wiley & Sons, Ltd., UK (2011), 398p.

[15] M. Routimo, Developing a Voltage-Source Shunt Active Power Filter for Improving Power Quality, Doctoral thesis, Tampere University of Technology, Tampere (2008), 86p.

Publication 4

O. Raipala, S. Repo and P. Järventausta, "Network information system based loss of mains risk management", *in Proc. 22nd International Conference on Electricity Distribution (CIRED)*, Stockholm, Sweden, June 2013

Available at: https:\\doi.org\10.1049/cp.2013.0742

NETWORK INFORMATION SYSTEM BASED LOSS OF MAINS RISK MANAGEMENT

Ontrei RAIPALA
Tampere University of Technology – Finland
Ontrei.raipala@tut.fi

Sami REPO
TUT
sami.repo@tut.fi

Pertti JÄRVENTAUSTA
TUT
pertti.jarventausta@tut.fi

ABSTRACT

A large variety of different loss of mains (LOM) protection schemes is nowadays available. Network utilities are facing a difficult task when trying to decide which of the available schemes is the most appropriate choice for each DG installation. This paper presents a novel network information system based concept for aiding in this task and in managing the LOM risk.

INTRODUCTION

The amount of DG is growing strongly. This brings potential benefits, but a number of challenges related to the integration of DG are also present. Unintentional islanding is one of the most troublesome of these challenges. This is due to the associated safety problems such as failed reclosings, damage caused by out of phase reclosings, safety hazard for utility field personnel and risk of customer loads being damaged due to poor power quality. Because of these concerns, it is mandatory to equip all DG units with some kind of loss of mains (LOM) scheme which disconnects the protected DG whenever it becomes islanded.

There are a large number of different LOM protection methods. Generally the methods can be divided into four categories which are passive, active, hybrid and communication based methods. Passive methods are affordable, simple and applicable to all types of DG units but commonly suffer from relatively large non-detection zone (NDZ). Many active methods have a very small sized NDZ, but these methods generally have a degrading effect on power quality. Hybrid methods create less power quality problems compared to active methods but their operation times also tend to be slower as several methods are used in sequence. Communication based methods can usually eliminate the unintentional islanding problem completely, but the high cost of implementing these methods makes it unreasonable to utilize these kinds of methods for the protection of small DG installations. Moreover, a local LOM detection scheme is always needed for backup protection in case if the communication medium fails.

All four classes of LOM protection methods thus have their pros and cons, and consequently potential utilization cases. For instance, for converter connected DG units it is often favorable to utilize active or hybrid LOM detection schemes, whereas, for directly coupled DG units they are rarely an option. Sometimes the network utility may also forbid the use of active methods due to power quality issues. Because of the large variety of LOM protection schemes, there should be a simple way by which one can assess which method is the best choice for each DG installation. This paper proposes a network information system based LOM risk assessment procedure as a solution to this need.

THE RISK OF NON-DETECTED ISLANDING

The performance of most LOM detection schemes is highly dependent on the power imbalance in the islanded circuit. Large imbalances between production and consumption lead to large deviations in voltage magnitude and frequency in a circuit separated from the main grid. Such a situation is easy to detect for LOM protection. However, LOM protection may become completely non-operational in situations where the power imbalance before the transition to islanding is of minor scale. The set of active- and reactive power imbalance combinations where LOM protection fails to detect islanding rapidly enough is referred to as the NDZ.

The imbalance between the production of a local DG unit and the consumption of local loads varies throughout the day and throughout the year. Consequently, the risk of unintended islanding also varies most of the time. The size of the NDZ depends on the utilized LOM protection scheme. It can be reduced by applying stricter LOM protection settings but this is usually restricted by the fault ride through requirements and protection security issues. There is, however, yet another factor that affects the risk of non-detected islanding. This is the fact that a DG unit can become isolated from the main grid with various amounts of local loads [1].

LOM RISK ASSESSMENT

The risk of non-detected islanding can be evaluated by comparing the load and the local DG generation on the studied network section. Obviously there is no non-detected LOM risk if the minimum local demand is clearly larger than the local DG generation capacity. However, certain theoretically possible combinations may never occur in practice. For instance, in the north maximum demand occurs during winter season when electric heating is needed, whereas, the production of photovoltaic is lower during winter period than during summer season.

Estimation of imbalances

Network information system (NIS) has become an essential planning tool for almost every distribution network operator.

In Nordic thinking, a typical NIS includes network component data and plenty of calculation functionalities combined to a graphical interface. NIS's usually show the geographical image of the network area on the background in order to help the user to visualize the work better. NIS can be used for many purposes such as network documentation, asset management, network configuration planning, investment planning and construction planning.

Modern NIS provides an excellent platform for the LOM risk assessment. Data from medium and low voltage networks and DG units are already embedded in modern NIS. Data needed to model customers is taken from customer information system. Loads are typically modeled with the help of customer class specific hourly load curves. Maximum and minimum consumption values for all network sections could be calculated with the help of these load curves and nominal data of the studied DG units. This concept is illustrated in Fig. 1.

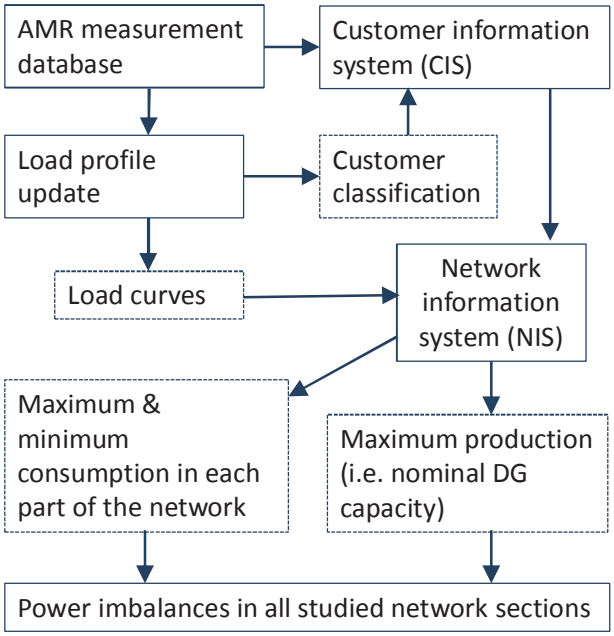

Fig. 1. Estimation of imbalances

The load curves, which are typically divided from 20 to 50 customer classes, contain mean and standard deviation values (normal distribution is nearly always assumed) for electrical energy consumption for every hour of the year. The load curve of each customer is scaled based on the customer's annual energy consumption. If the load is assumed to be normally distributed, the value of load in a calculation which is carried out with a certain confidence level is quantified using the cumulative probability density function of normal distribution. Typical confidence levels used for maximum capacity calculations are 99% and 95% and 1 and 5% for minimum consumption. The possible inaccuracies in the load curves or customer classification could be corrected by utilizing hourly consumption data provided by Automatic meter reading (AMR) system as proposed in [2]. Special customer can be modelled with individual customer specific load curves using real AMR data [2].

All in all, with this approach NIS could be harnessed to calculate the active- and reactive power imbalances for every hour of the year based on statistical load curves and nominal DG capacity. The analysis of imbalances can be realized for all network sections which can theoretically become islanded, i.e. which can be divided by switches.

NDZ risk probability assessment

Evaluating the non-detected LOM risk based on the imbalance between consumption and DG nominal capacity leads to conservative results. The actual probability of the non-detected LOM risk could be determined by extending the load curve based NIS calculation with production curves and then analysing the results of combined load and production curve calculations. Due to the stochastic nature of DG units, production curves are based on long-term statistics of wind speed, water flow, solar radiation or temperature etc. Reference [3] has proposed a method for creating production curves based on very simple initial data of production units and a calculation method for analysing distribution networks for planning purposes. If multiple production curves are utilized in the evaluation, the user would be given a probability of the actual non-detected LOM risk in the form of power imbalance probability distribution.

Determination of the NDZs

NDZ risk margins of optional LOM protection schemes would have to be added to a database. Conservative NDZ estimates should be utilized since the NDZ region not only depends on the protection scheme and protection settings, but also on the DG unit type, utilized control mode of the DG units and characteristics of the loads. For instance, synchronous generators are considerably more challenging from LOM detection point of view than induction generators. Moreover, a converter coupled DG unit behaves very differently than a directly coupled generating unit. [4] – [6]

The estimation of the NDZ regions is a laborious task but it is, nonetheless, doable. This task could be done within a reasonable time frame by using a real time simulator as presented in [4]. The difficult task in such estimation is choosing an appropriate simulation model. A simulation model for testing the performance of LOM protection of a photovoltaic converter is defined in standards [7] and [8]. Although this model is not originally meant for studying the performance of LOM protection in the presence of directly coupled generators, it could also be utilized for this purpose. The parallel RLC load utilized in the model is appropriate for obtaining a conservative NDZ estimate of a LOM protection of a directly coupled synchronous generator as the load equals to a constant impedance load from the synchronous generator point of view. According to [5], constant impedance type load

is appropriate for obtaining a conservative NDZ estimate. A suitable quality factor value for the parallel RLC load could be 2.5. This leads to very conservative NDZ estimates since a quality factor value 2.5 is considerably higher than what would be expected from a real load [1].

The modeling of the DG unit(s) is naturally an essential issue for obtaining realistic NDZ estimates. The simulation model should probably include a converter coupled DG and a directly coupled synchronous generator in parallel since the relationship between active- and reactive power with voltage magnitude and frequency is different for directly connected and converter connected DG units [4]. The exciter of the synchronous generator should be set to control the terminal voltage [5]. Another aspect which requires consideration is the inertia constant of synchronous generators. The larger the inertia constant of the machine, the more stable the machine is and thus consequently, the more challenging the situation is to LOM protection. What comes to the control of converter coupled DG units, constant power controlled DG units lead to the largest NDZ [6].

One challenge in the NDZ estimation of different schemes is that the utilized LOM protection settings often vary to some extent from utility to utility. This could be overcome by having NDZs with several protection settings in the database. Another option would be to have the NDZs defined with one relatively loose protection settings. However, this could lead to excessively conservative results in certain cases. Another disadvantage is that it would not be straightforward to add new optional LOM detection schemes since their NDZs need to be defined by simulation studies.

THE LOM RISK ASSESSMENT PROCEDURE

Fig. 2 illustrates the principle of the proposed NIS based LOM risk assessment procedure. At first, the nominal DG capacity, consumption data and conservative NDZ estimates of the optional LOM protection schemes are fed to the procedure. The procedure then examines with the help of NIS if there are any parts of the network where a NDZ risk exists. First, a simple comparison between the nominal power ratings of studied DG units and the annual minimum load on the studied network area is realized. From local LOM protection point of view, the situation is only acceptable in case if minimum demand is sufficiently larger than maximum DG generation capacity. A certain margin which takes into account the expected DG capacity- and load growth in the following years is highly advisable. This comparison then gives the minimum possible active and reactive power imbalances. These imbalances are then compared to the NDZ regions of the optional LOM protection schemes. It is evident that if the minimum annual power imbalance is very large, then the performance requirements for LOM protection are low. In such case, it would be unwise to invest in costly communication based LOM detection schemes. Moreover, active LOM protection schemes could be set to inject less/lower perturbations if simple passive schemes were sufficient for reliable islanding detection.

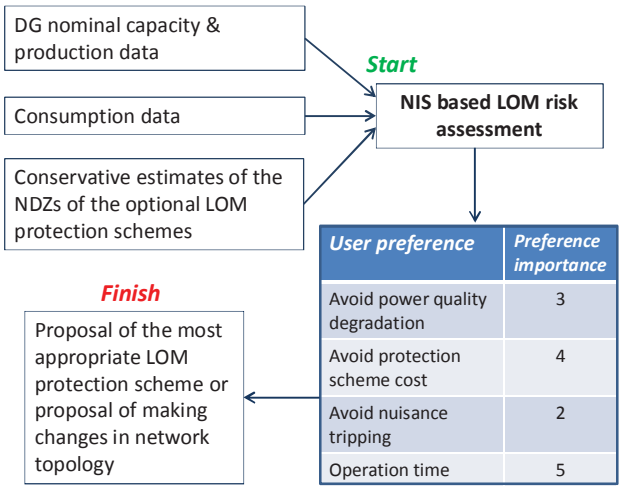

Fig. 2. The NIS based LOM risk assessment procedure

The procedure could also take into account certain user definable preferences as for instance operation time or avoidance of power quality problems. These preference factors would naturally be predefined so that the user was to simply give an importance value to each feature. Finally, the procedure would list few of the most appropriate LOM detection schemes. Optionally, the procedure could also be configured to propose changes in network topology. The idea behind this is that it may sometimes be possible to eliminate the non-detected LOM risk simply by opening and closing certain switches and thereby altering the possible power imbalances in the studied circuit.

As already discussed, certain theoretically possible combinations of production and consumption may never occur in practice. This can be taken into account by performing more detailed hourly analysis of power imbalance based on probability distributions for the potential NDZ risk areas. These network areas can be found out by the simple comparison, i.e., by comparing annual minimum load with the nominal capacity of DG. However, from protection planning point of view it may be more troublesome and risky to take into account the stochastic behaviour of production side since production curves are not accurate in the same way as load curves are and power imbalance probability should therefore be considered as a qualitative supportive guidance for decision making of LOM protection [3].

APPLICATION IN NETWORK OPERATION

The LOM risk assessment could also be extended to aid in network operation. This extension should be integrated to distribution management (DMS) system rather than NIS since the purpose of this extension is to aid in the continuous network operation rather than long term planning. However,

the idea of this "real time" application is very similar to that of NIS based procedure. Moreover, network modelling and calculation applications in DMS are mostly based on the same modules as in NIS.

This DMS application is started by using the NIS based LOM risk assessment procedure for assessing appropriate risk margins for demand in each of the studied network sections. This is done by assessing how much larger the demand in each of the studied network section should be in comparison to the nominal capacity of the local DG. Naturally the different performance characteristics of each LOM protection scheme has to be taken into account in this phase. The real time application could then assess the NDZ risk based on the hourly consumption estimates which were scaled based on AMR measurement data and the calculated risk margin. Whenever the imbalance between demand and DG nominal data is large enough, no risk exists. However, if the imbalance was smaller than the calculated margin, the procedure could suggest disabling reclosing functionality of feeder protection relay in the problematic parts of the networks and warn the field crews about the LOM risk. The procedure could also suggest changes in network topology. In a rare and very dire long lasting LOM risk situation, the DG in the problematic network section could be ordered not to operate at their full output power.

DISCUSSION

Running the proposed NIS based procedure for the whole network with large amount of possible switching configurations would require a fairly large amount of computation. However, this is not a major problem since it would be sufficient to run the procedure for the whole network only on an annual basis. Naturally the procedure should additionally be run always when new DG is installed but only for analysing the network sections that are affected by the addition of the new DG units. Another potential use case for the procedure would be to assess the LOM risk whenever network topology changes are planned.

The proposed procedure is applicable only to medium voltage (MV) networks and very large low voltage networks. This is because it is not reliable to assume a certain minimum demand from a small number of customers. The procedure should thus always check that the network section under study contains enough customers for making such an assumption. The main benefits of this procedure are thus in MV-level reclosing coordination planning and in assessing the LOM risk caused by changes made in network topology.

CONCLUSIONS

This paper presented a novel NIS based concept for managing LOM risk. The concept takes advantage of existing calculation features embedded in modern NISs. However, certain additional data is required for the functioning of the proposed procedure. For instance, the NDZs of the optional LOM protection schemes need to be mapped to a database so that the procedure can evaluate the suitability of different schemes for each case. The procedure could help network utilities greatly in choosing appropriate LOM protection schemes for each case and avoid unnecessary investments in communication based LOM protection methods in cases where a local LOM protection scheme is sufficient. The LOM risk assessment could also be extended aid in network operation.

REFERENCES

[1] W. Xu, K. Mauch and S. Martel, 2004, *an Assessment of Distributed Generation Islanding Detection Methods and Issues for Canada*, CETC-Varennes 2004-074 (TR) 411-INVERT, Canada

[2] A. Mutanen, M. Ruska, S. Repo and P. Järventausta, 2011, "Customer Classification and Load Profiling Method for Distribution Systems", *IEEE Trans. on Power Delivery,* Vol. 26, 1755-1763

[3] S. Repo, H. Laaksonen and P. Järventausta, 2005, "Statistical Models of Distributed Generation for Distribution Network Planning", *Proceedings CIRED Conference and Exhibition 2005*

[4] O. Raipala, A. Mäkinen, S. Repo and P. Järventausta, 2012, "The Effect of Different Control Modes and Mixed Types of DG on the Non-Detection Zones of Islanding Detection", *Proceedings CIRED Workshop 2012*, paper 237

[5] J. C. M. Vieira, W. Freitas, W. Xu and A. Morelato, 2008, "An Investigation on the Nondetction Zones of Synchronous Distributed Generation Anti-Islanding Protection", *IEEE Trans. on Power Delivery*, Vol. 23, 593-600

[6] Z. Ye, A. Kolwalkar, Y. Zhang, P. Du and R. Walling, 2004, "Evaluation of Anti-Islanding Schemes based on Nondetection Zone Concept", *IEEE Trans. on Power Electronics*, Vol. 19, 1171-1176

[7] 929WG – Photovoltaic Working Group, 2000, *IEEE Recommended Practice for Utility Interface of Photovoltaic (PV) Systems,* IEEE Std. 929-2000

[8] Underwriters Laboratories Inc., 2001, *Inverters, Converters, and Controllers for Use in Independent Power Systems,* UL Std. 1741

Publication 5

O. Raipala, A. S. Mäkinen, S. Repo and P. Järventausta, ”A novel anti-islanding method based on the combination of a Q-f droop and RPV”, *in Proc. 5th IEEE PES Innovative Smart Grid Technologies Conference Europe (ISGT)*, Istanbul, Turkey, October 2014

Available at: https:\\doi.org\10.1109/ISGTEurope.2014.7028849

Errata

i. In the discussion chapter, it is erroneously said that DG units equipped with the proposed method would consume reactive power in case of a drop in the power system frequency. The proposed method would actually feed reactive power during a drop in frequency, which would have a tendency to raise the voltages. A rise in voltages would increase the consumption of voltage dependent loads. This would have a tendency to lower the frequency. Similarly, in the same discussion chapter, it is erroneously said that the proposed method would react to a rise in frequency by ordering the DG unit to feed reactive power. The proposed method would actually react to a rise in frequency by ordering the DG unit to absorb reactive power. This would have a tendency to lower the voltages, and consequently, to decrease the consumption of voltage dependent loads. Thus, the method would have a degrading effect on power system frequency stability.

A Novel Anti-islanding Protection Method Based on the Combination of a Q-f Droop and RPV

Ontrei Raipala, Anssi Mäkinen, Sami Repo, Pertti Järventausta
Department of Electrical Engineering
Tampere University of Technology
Tampere, Finland

***Abstract*—All distributed generating units need to be equipped with an anti-islanding (AI) protection scheme in order to avoid unintentional islanding. Unfortunately most AI methods fail to detect islanding when the islanded load matches with the production in the island. Another concerning issue is that certain active AI protection schemes may cause power quality problems. This paper proposes an AI protection method which is based on the combination of a specially designed reactive power versus frequency (Q-f) droop, and a constantly injected reactive power variation (RPV) pulse. The method is designed so that the injection of reactive power is of minor scale during normal operating conditions. Yet, the method shows high performance during islanding. Simulations were performed with the help of PSCAD/EMTDC in order to analyze the performance of the method. The results indicate that the method is able to detect islanding within 2 seconds even in a perfectly balanced island.**

***Index Terms*—Distributed generation (DG), islanding detection**

I. INTRODUCTION

The rapidly increasing amount of distributed generation (DG) units is raising concerns related the functioning of distribution network protection. Especially challenges related to anti-islanding (AI) protection have been studied widely in the recent years. AI protection is meant for ensuring that no generating units are left feeding customer loads in islanded circuits. The avoidance of unintentional islanding is important due to the associated safety hazards for utility personnel but also because DG units and network components may be damaged as a consequence of unsynchronized reclosing of the islanded circuit. In addition, customer loads in the islanded circuit may be damaged due to poor power quality. Due to these potential risks, the IEEE 1547 standard states that islanding should be detected and ceased within 2 s at maximum [1]. However, faster detection may be required if fast automatic reclosing is utilized on the feeder where the DG unit(s) are connected.

AI protection methods can be divided into passive, active and communication based methods. Passive methods are based on locally measuring certain system quantities, such as voltage and frequency. The idea behind these methods is that some changes in the measured quantities usually occur during the transition to islanding. Passive methods are popular due to their low cost and applicability to all DG units. The downside of these methods is that most of these methods fail to detect islanding in case if the production in the islanded circuit closely matches with the load in the same islanded circuit. The problematic active- and reactive power imbalance combinations which lead to non-detected islanding are referred to as the non-detection zone (NDZ). Active AI methods, which are based on drifting voltage magnitude or frequency out of the predefined thresholds by deliberate injection of perturbations, are usually characterized by a smaller NDZ in comparison with the passive methods. However, the better islanding detection performance of active methods comes at the cost of degraded power quality. Communication based methods are immune to the NDZ problem but they are usually applied only to DG units of larger nominal power due to their high implementation cost.

The high performance of active AI methods have received considerable attention due to the fact that many of them are capable of detecting islanding even when there is no power mismatch between production and consumption in the islanded circuit. Especially frequency drift based AI methods have been highlighted. [2], [3] Reactive power variation (RPV) is one of the effective ways for drifting frequency out of the underfrequency (UF) or overfrequency (OF) limits. Reference [4] presented an AI method based on constant bilateral injection of RPV pulses. The injected RPV pulse varies between two values, i.e., ±2.5% of the active power. However, this method still has a NDZ according to [5]. Reference [6] presented an intermittent bilateral RPV method in which there is also a zero period in the RPV pulse in addition to the maximum and minimum values ±5% of the active power. This method is designed to be capable of detecting islanding within 2.0s. Reference [7] proposed an AI protection method, which is based on equipping the DG interface with an appropriate reactive power versus frequency droop. The droop is designed so that the DG unit loses its stability once islanding occurs. Reference [5] presented an RPV method which monitors frequency and injects RPV pulses whose magnitude is varied according to the detected frequency error. The method is able to eliminate the NDZ and also reduce the amount of injected reactive power in comparison with traditional bilateral RPV method. The

direction of the injected RPV pulse is determined by the monitored frequency. This paper presents a novel RPV method which combines a specially designed reactive power versus frequency droop and a constant injection of RPV pulses. The droop is designed so that no reactive power is fed during normal frequency variation range, whereas, a strong response is given if frequency should deviate outside of the normal variation range. The continuously fed RPV pulse ensures that the method does not have a NDZ.

The paper is organized as follows. Chapter II provides a brief overview of an islanded circuit and the principle behind RPV based AI. The proposed AI method can be found from chapter III. The simulation models are presented in chapter IV and the results obtained using the models are given in chapter V. Finally, a discussion part is found from chapter VI and conclusions are given in chapter VII.

II. ISLANDED CIRCUIT

Most AI protection methods are based on detecting the changes in system quantities such as voltage and frequency. These changes, which usually take place when islanding occurs, are mainly caused by the imbalance between the production and consumption of real- and reactive power in the island. The relations between active- and reactive power with voltage and frequency can better be understood by examining a case where an inverter is feeding a parallel load connected to the circuit as shown in Fig. 1. During islanding, the active- and reactive power consumed by the load have to match with the production of the inverter as expressed in (1) and (2), where V refers to line to line voltage of the circuit and the subscripts INV and Load refer to inverter and load. Thus, from (1) it can be seen that voltage is proportional to active power. Consequently, assuming that voltage is determined by P_{INV} and R, a clear relation between reactive power and frequency can be seen from (2). Frequency f will deviate to such a value that the reactive power consumed by the load matches with the production of the islanded DG in the island. This can be expressed as in (2).

$$P_{\text{INV}} = \frac{V^2}{R} = P_{\text{Load}} \tag{1}$$

$$Q_{\text{Load}} = V^2 \left[\frac{1}{2\pi f L - \frac{1}{2\pi f C}} \right] = Q_{\text{Inv}} \tag{2}$$

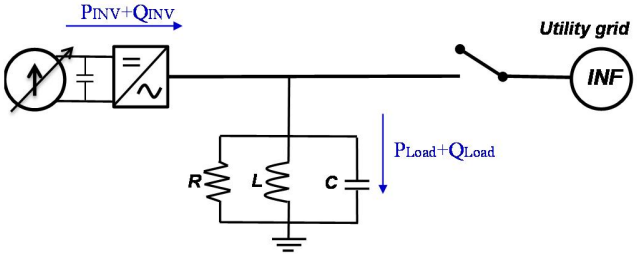

Figure. 1. A simple circuit for islanding detection analysis.

It can be seen from (2) that frequency is inversely proportional to the reactive power produced by the inverter. For instance, if Q_{INV} increases to a positive direction, frequency will have to decrease in order for the two sides in (2) to be equal. If the islanded DG unit is operating in unity power factor mode and thus producing zero reactive power, the frequency will deviate to such a value that the reactive power of the load is also zero. This is the resonance frequency of the load (3). If the resonance frequency is within the allowed frequency protection limits, then the island cannot be detected by frequency relays.

$$f_r = \frac{1}{2\pi\sqrt{LC}} \tag{3}$$

This simple analysis of an islanded circuit shows that by varying the reactive power produced by the inverter, one can also cause the frequency to drift. This is the principle of RPV based AI methods.

III. THE PROPOSED AI PROTECTION METHOD

In the studies of this paper, a reactive power variation (RPV) based AI protection method was chosen. This method is set to feed/absorb reactive power in relation to the deviation of measured frequency from the nominal frequency as shown in Fig. 2. The control of the inverter, and thus also the proposed RPV method, is established using the d-q synchronous reference frame. This enables independent control of active and reactive power [2]. The vertical axis in Fig. 2 presents the q component of the inverter current, whereas, the horizontal axis represents frequency. The droop in Fig. 2 is configured so that the Iq component is equal to zero when the frequency deviation is within ±0.1Hz, i.e. in its normal variation range. However, if frequency drifts outside of this deadband, the Iq component of the inverter current is determined according to the droop shown in Fig. 2.

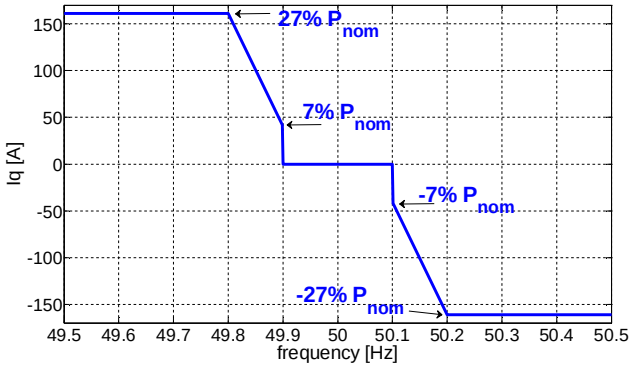

Figure. 2. The utilized anti-islanding inverse droop

At a frequency deviation equal or greater than ±0.2Hz, the Iq component reaches its highest/lowest value ±161.19A which corresponds to ±27% of the active current component, i.e. 0.975 power factor in the studied 500kVA rated DG unit used in the studies of this paper. The efficiency of the droop could have been improved slightly by replacing the ±7% of P_{nom} steps directly with the ±27% of P_{nom} steps. However, the utilized shape of the droop was preferred since frequency may sometimes deviate more than 0.1Hz from its nominal value. In fact, reference [8] indicates that the quality of

frequency has degraded in Nordic power system during recent years and the number of events outside normal frequency range is already significant. Should the frequency deviate outside of the normal variation range, the utilized droop gives a smoother response from both distribution network and transmission system operator point of views.

The droop based RPV described above could result to non-detected islanding if the consumption of the islanded loads would closely match with the power produced by the islanded DG. In order to avoid this problem, an additional constant variation of reactive current whose shape is illustrated in Fig. 3, is used together with the above described droop. The magnitude of the injected RPV pulse is at a value which corresponds to 3% of the nominal active power (i.e. 17.91A) for a period of 100ms. After this, the RPV pulse is equal to zero for a period of 100ms. The direction of the RPV pulse is decided by the measured frequency. A frequency higher than the nominal leads to a negative RPV pulse, whereas a frequency lower than the nominal leads to a positive pulse. During normal grid connected operation, this pulse will not cause any significant changes in voltage magnitude or frequency. However, should islanding occur, the injected RPV pulse will cause the frequency to drift out of the deadband of the utilized droop in Fig. 2. After this, the injected reactive current is increased or decreased according to the droop in Fig. 2. The magnitude of the injected reactive power ordered by the proposed AI method is set to be proportional to the active power production of the DG unit.

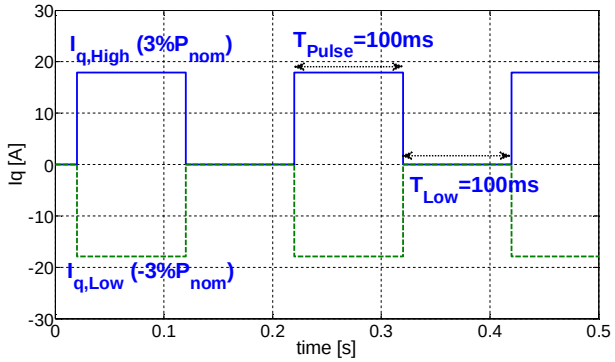

Figure 3.The utilized constant RPV pulse

The voltage magnitude protection limits used in the studies of this paper were 0.85pu and 1.1pu for undervoltage (UV) and overvoltage (OV). Respectively, the limits were 48Hz for UF and 51Hz for OF. The operation delays were 200ms for both voltage magnitude and frequency protection. These settings are used by Finnish distribution network operators. The proposed method is able drift the frequency out of the utilized UF/OF limits and thus cause the frequency protection to trip within 2 s even if there would be a perfect match between the consumption of the islanded load and the DG unit as mandated by the IEEE 1547 standard [1] .

It is noteworthy that the utilized frequency protection thresholds have a large impact on the islanding detection performance. This should be taken into account when comparing AI protection methods. For instance, the frequency thresholds used in [5] were considerably tighter (49.5Hz for UF and 50.5Hz for OF). Had the frequency limits in [5] been the same as in this study, i.e. 48Hz and 51Hz, the required reactive power injection of the discussed method for driving frequency from nominal to 48Hz would have been 20% of active power instead of the 5% of active power discussed in the paper. This shows that the required RPV pulse for driving frequency from nominal to the UFP/OFP limits is lower in the proposed method in comparison with the one presented in [5]. Due to this, the injected reactive power during normal operating conditions at nominal frequency is lower in the proposed method in comparison with the one presented in [5]. Moreover, frequency stays close to nominal most of the time during normal grid connected conditions. Consequently, the method proposed in [5] would be feeding its peak RPV injection most of the time.

IV. Simulation Models

A simple islanding test circuit was modeled with the help of PSCAD software for these studies. The model, which is depicted in Fig. 4, consists of a 110kV source which is feeding the studied islanded circuit via a HV/MV transformer and a circuit breaker (CB_{Feeder}). An RLC load was connected to the studied circuit as shown in Fig. 4. The R, L and C values of these parallel connected RLC loads were chosen so that the quality factor (Q_f) of the loads was 2.5 at each chosen level of active and reactive power consumption as suggested in [9]. Quality factor of a parallel RLC load can be represented as two pi times the ratio of the maximum stored energy to the energy dissipated per cycle at a given frequency [9]. In mathematical terms, Q_f can be presented as in (4). The R, L and C values of the load were calculated from (5) – (7) thus taking the quality factor of the load (4) into account.

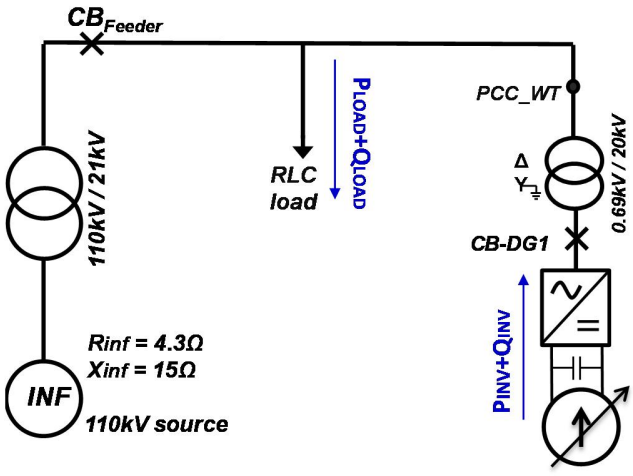

Figure 4.The utilized simulation model

$$Q_f = \frac{R}{\omega_0 L} = \omega_0 C = R\sqrt{\frac{C}{L}} \quad (4)$$

$$R = \frac{V^2}{P_{\text{Load}}} \tag{5}$$

$$C = \frac{V^2 Q_f^2 + \sqrt{V^4 Q_{Load}^4 + 4 Q_{Load}^2 Q_f^2 R^2}}{2 Q_{Load} \omega R^2} \tag{6}$$

$$L = \frac{C R^2}{Q_f^2} \tag{7}$$

The utilized DG unit was a 500kVA rated full converter connected wind turbine (FCWT) which is presented in [10]. This DG unit was connected to the circuit via a step up transformer as shown in Fig. 4. The control system, LCL filter and network side converter parameters of this model are the same as in [10] with the exception that the phase locked loop model from the PSCAD library is used as a synchronization method. The reference of the reactive current was set so that the reactive power measured from the point of common coupling (PCC_WT in Fig. 4) was 0kVar during nominal operation (500kW). The FCWT was equipped with a RPV based AI protection that was presented in chapter III.

V. Simulation Results

This chapter presents the simulation results of the AI studies which were obtained using the PSCAD/EMTDC. Islanding was set to occur at time 10.0s in all the presented simulation cases for ensuring that everything had stabilized before islanding took place. The first case presents a situation where the studied DG unit becomes islanded while there is a perfect power balance in the islanded circuit. After this, another simulation case is done for examining how the phase and direction of the injected RPV pulse at the time of islanding can affect the performance of the method.

A. Islanding during perfect power balance

In the first case, the performance of the studied RPV method was examined in an islanding scenario where the load was set to match the production of the DG unit. The resonance frequency of the load was set to 50.0Hz and the quality factor of the load was 2.5. Thus, the power exchange with the main grid was of negligible order before the islanding event. In this islanding scenario, both voltage magnitude and frequency stayed very close to their nominal values during the islanding when the RPV was not enabled and the islanding could not have been detected by passive voltage magnitude and frequency based islanding detection. However, by enabling the RPV, the frequency rose above 51Hz in approximately 195ms and the relay tripped in 395ms. The q-component of the inverter current and the active- and reactive power values are shown in Fig. 5. One can clearly observe the inverse relation between the frequency and the injected reactive power by looking at the second and third graphs from the top. It can also be seen from Fig. 5 that the Iq value is approximately -13A already during normal state when the RPV pulse is at its zero phase. The Iq is controlled to this value in order to compensate the effect of the LCL filter capacitor. At the time 10.1s the Iq reaches its negative peak value -173.1A (=-161.2A-11.9A) to which it is limited.

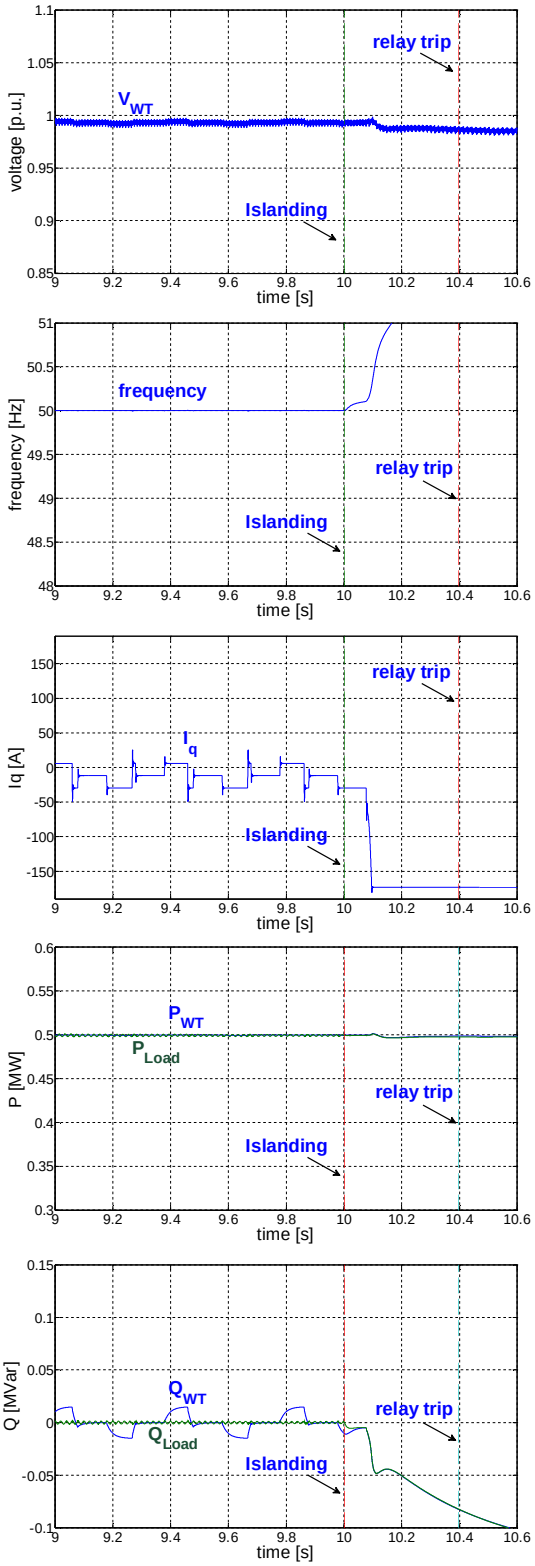

Figure 5. Monitored voltage magnitude, frequency, q-component of the inverter current and active- and reactive power values. The initial phase angle of the injected RPV pulse is set to 40°.

Note that the frequency before islanding moment was set to 50.00Hz and, therefore, the injected RPV pulse is not unilateral. In real network conditions the frequency is most of the time slightly different from nominal which would result to a unilateral RPV injection as described in chapter III. This AI protection was not found to have a NDZ when the detection time requirement was 2.0s.

B. *The phase and direction of the RPV pulse at the moment of islanding*

The performance of the proposed AI method can be of somewhat affected by the phase of the injected RPV pulse at the moment of islanding. The most difficult situation for the method is a case where the zero time of the RPV pulse starts at the beginning of islanding and the following high period of the RPV causes the frequency to drift towards UF. It obviously requires more effort to drift the frequency from 50Hz to the utilized UF limit 48Hz instead of the OF limit 51Hz.

The initial phase of the RPV pulse was adjusted so that the above mentioned worst case scenario occurs. This case is shown in Fig. 6. It can be seen that this time it took 0.85s for the relay to trip. The reason for the large difference between the AI protection operation time between the cases presented in Figs. 5 and 6 is that in the case presented in Fig. 5 it was the OF protection that tripped, whereas, in the case presented in Fig. 6 UF protection tripped. Additionally, the RPV pulse was in an unfavorable phase in relation to the moment of islanding as it can be seen from the graph presenting the q component of the inverter current and from the graph presenting the reactive power output of the DG unit.

VI. DISCUSSION

The proposed method is designed to perturb the system operation as little as possible during normal operating conditions, i.e. when frequency is within its normal variation range. However, the proposed method reacts with a considerably larger response when frequency drifts out of its normal operating range. Let us consider a case such that the frequency of the examined power system drops by 0.5Hz due to multiple failures or disconnections of large power plants. In such case, all the DG units equipped with the proposed method would begin to consume reactive power. However, instead of having an effect on the system frequency, the consumption of reactive power would cause the voltage to drop in the distribution networks containing DG equipped with the proposed AI method. This is because the frequency of a large power system is determined by the speed of synchronous generators. The reduced voltage would cause the consumption of voltage dependent loads to decrease in the distribution networks containing these DG units. In large scale, this would benefit the system with a frequency considerably lower than the nominal. However, if the frequency was not to return back to nominal in a short time, the on-load tap-changers of the HV/MV transformers would react to the reduced voltage by tapping up and thus causing the reactive power transferred through the transmission lines to increase. This eventually, would have a negative impact on the voltage stability of the system.

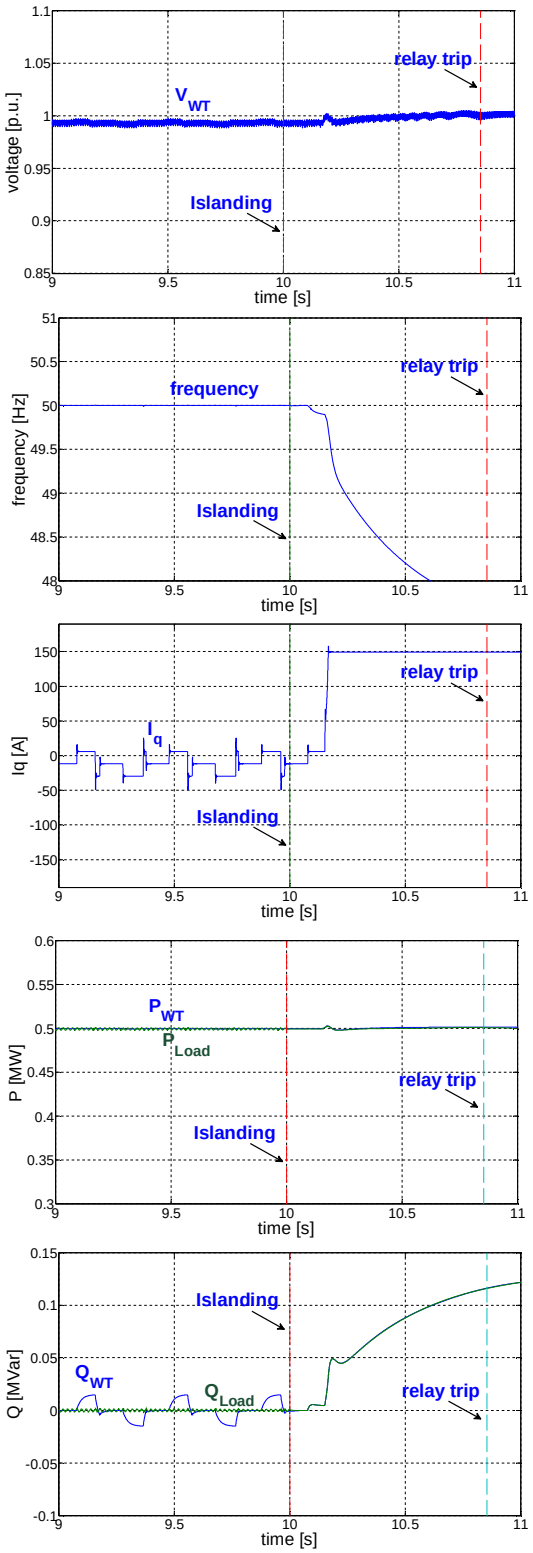

Figure 6. Monitored voltage magnitude, frequency, q-component of the inverter current and active- and reactive power values. The initial phase angle of the injected RPV pulse is set to 220°.

On the other hand, if the system frequency should rise, for instance due to a sudden disconnection of a major load, the proposed AI method was to react by ordering the DG unit to feed reactive power. This would increase the local voltages, and thereby also increase the consumption of local loads. This would have a stabilizing effect on the system in an overfrequency situation.

It is noteworthy that this method was tuned to function with the frequency and voltage protection limits utilized by the Finnish distribution network operators. If this method was used in a country with very different voltage magnitude and frequency requirements, especially the droop should be modified to fit the local requirements better. If the utilized voltage and frequency protection limits were stricter than the ones used in this study, the maximum value of the droop could be reduced. The RPV pulse would not require major modification unless the desired deadband was desired to be different.

VII. CONCLUSIONS

This paper presented a novel anti-islanding protection method which is based on the combination of reactive power droop and constant injection of RPV pulses. The droop is controlling the injection of reactive power based on the detected frequency error. The shape of the droop is designed so that the operation of the protected DG unit is not affected during normal operating conditions. This is established by designing a suitable deadband to the droop. However, in order to eliminate the NDZ, a constantly injected reactive power pulse with a magnitude corresponding to 3% of the active power is used together with the droop. The required injection of reactive power is smaller than in most of the RPV based anti-islanding methods proposed earlier. Yet, the proposed method is able to fulfill the 2.0s detection time requirement mandated by international standards even in perfectly balanced islanding. Further studies are, nevertheless, needed to verify the functioning of the proposed method in multi inverter case.

REFERENCES

[1] IEEE Standard for Interconnecting Distributed Resources with Electric Power Systems, IEEE Standard 1547, 2003

[2] R. Theodorescu, M. Liserre and P. Rodriquez, *Grid Converters for Photovoltaic and Wind Power Systems*, West Sussex, UK; Wiley

[3] P. Mahat, Z. Chen and B. Bak-Jensen, "Review of Islanding Detection Methods for Distributed Generation" in *Proc.DRPT 2008*, pp. 2743-2748.

[4] J. B. Jeong, H. J. Kim, K. S. Ahn and C. H. Kang, "A Novel Method for Anti-Islanding using Reactive Power", in *Proc. INTELEC '05*, pp. 101-106

[5] Y. Zhu, D. Xu, N. He, J. Ma, J. Zhang, Y. Zhang, G. Shen and C. Hu, "A Novel RPV (Reactive-Power-Variation) Antiislanding Method Based on Adapted Reactive Power Perturbation", *IEEE Trans. Power Electronics*, vol. 28, pp. 4998-5012, November 2013

[6] J. Zhang, D. Xu, G. Shen, Y. Zhu, N. He and J. Ma, "An Improved Islanding Detection Method for a Grid-Connected Inverter With Intermittent Bilateral Reactive Power Variation" *IEEE Trans. Power Electronics*, vol. 28, pp. 268-278, January 2013

[7] H. H. Zeineldin, "A Q-f Droop Curve for Facilitating Islanding Detection of Inverter-Based Distributed Generation", *IEEE Trans. Power Electronics*, vol. 24, pp. 665 – 673, March 2009

[8] Z. W. Li, O. Samuelsson and R. Garcia-Valle "Frequency Deviations and Generation Scheduling in the Nordic System", in *Proc. 2011 IEEE Trondheim PowerTech*

[9] IEEE Recommended Practice for Utility Interface of Photovoltaic (PV) Systems, IEEE Standard 929-2000, 2000

[10] A. S. Mäkinen and H. Tuusa, "Impact of strength of fault current path on the operation of decoupled double synchronous reference frame – phase locked loop", in *Proc. 2013 Int. Conf. on Renewable Energy and Power Quality.*

Publication 6

O. Raipala, S. Repo and P. Järventausta, "A communication based protection system for solving DG related protection challenges", *in Proc. 23rd International Conference on Electricity Distribution (CIRED)*, Lyon, France, June 2015

A COMMUNICATION BASED PROTECTION SYSTEM FOR SOLVING DG RELATED PROTECTION CHALLENGES

Ontrei RAIPALA
Tampere University of Technology - Finland
Ontrei.raipala@tut.fi

Sami REPO
TUT - Finland
sami.repo@tut.fi

Pertti JÄRVENTAUSTA
TUT - Finland
pertti.jarventausta@tut.fi

ABSTRACT

This paper presents a communication based protection automation system which is designed for solving DG related protection problems. The system is able to tackle problems related protection blinding, nuisance tripping of feeders and generators and problems related to unintentional islanding. Moreover, the system can be configured to allow low voltage ride-through without compromising loss of mains protection. However, the system also has the potential of enhancing the reliability of electricity distribution service to DG units by automatically switching an alternative feeding path if the original feeding route is faulted.

INTRODUCTION

The amount of distributed generation (DG) connected to distribution network level is growing strongly. DG has many potential benefits on the usage of distribution systems such as reducing distribution losses, improving voltage profiles, levelling demand peaks and increasing reliability of distribution service to consumers. However, DG also raises a number of new challenges. The main challenges related to distribution system protection raised by the addition of DG are protection blinding, nuisance tripping of intelligent electric devices (IEDs), failed reclosing and unintentional islanding [1].

Establishing a reliable loss of mains (LOM) protection is particularly challenging if fast automatic reclosing (AR) utilized. AR is meant for removing temporary faults automatically without causing an extended interruption in the supply of electricity. This is achieved by opening a circuit breaker (CB) connecting the faulted feeder to the supplying grid for a short period of time and then reclosing the CB. AR has a great significance for the reliability of electricity supply since, e.g., in Finland the majority of faults on overhead lines are temporary in nature (e.g. due to lighting strikes or storms) and thus also clearable by AR. LOM protection has to be able to detect islanding and disconnect islanded DG units rapidly enough for the fault arc to extinguish during fast automatic reclosing. For instance, in Finland the circuit breaker open time used in fast automatic reclosing is typically 300 ms, which in practice means that DG units should be disconnected approximately within 200 ms in order to ensure a dead time of 100 ms for the ionized gasses created by the fault arc to disperse. Moreover, LOM protection has to be able to detect islanding even though the load in the islanded part of network would match the power produced by the islanded DG units. Certain active LOM protection methods are able to meet these requirements but this comes at the cost of degraded power quality because active methods are based on detecting islanding by deliberately injecting perturbations to the network. However, these methods may not function properly if the islanded network contains both inverter coupled and directly coupled synchronous generators [2]. Moreover, even though there would be only inverter based DG units in the islanded circuit, the active LOM protection methods have to be synchronized with each other in order to ensure reliable LOM protection. However, this usually means that the power quality problems caused by the active LOM protection method become even more severe.

Despite the high number of publications dealing with these problems, protection concepts being capable of taking all the protection problems related to DG into account are scarce. This paper presents a protection concept for distribution networks which aims to solve all the DG related protection challenges. The studied system is largely based on the ideas presented in [3]. However, the studied protection automation system was also designed to increase the reliability of distribution service to DG units. This kind of service may be attractive to the owners of large DG units that are connected to remote locations, since even short outages may be harmful to them. The idea behind the proposed protection automation configuration is that distribution networks are often built meshed but operated in radial mode. In many cases a customer may have two or more line routes through which the supply is provided. This potential can be harnessed with a proper intelligence.

THE PROTECTION AUTOMATION SYSTEM

The idea of the proposed protection system is explained with the help of Fig. 1. In this example figure, there are two medium voltage feeders fed by the transmission grid via a HV/MV transformer. The first feeder, i.e. feeder A, is protected by two line differential protection IEDs. There is also a DG unit connected to the tail part of the feeder which is protected by a LOM IED. The other feeder is protected by an overcurrent protection IED. All the IEDs which are situated near to each other are communicating with each other using the generic object

oriented substation event (GOOSE) defined in the IEC 61850 standard. The protection communication link between the differential protection IEDs A1 and A2 is established using an optical wire and digital signals. The bandwidth of the optical link is high enough to enable the sending of user definable information in addition to the differential protection related communication. This sending of additional binary signals between the differential IEDs is referred to as the binary signal transfer (BST) [3]. GOOSE messages can also be used for establishing the vertical communication instead of BST if line differential protection is not used in the network. However, suitable communication channel such as optical cable or 4G/LTE wireless communication link is needed in such case.

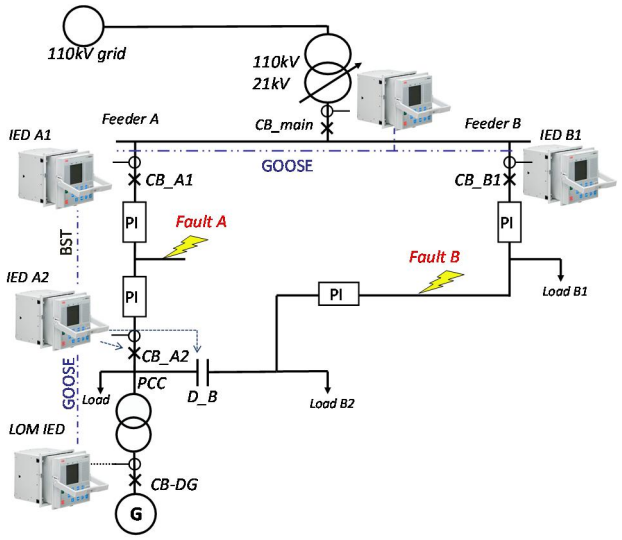

Figure 1. The examined network model

The proposed protection concept is able to tackle DG related protection problems. Nuisance tripping problems can be reliably avoided by sending blocking signals between IEDs. For instance, if a fault occurred on feeder B at such a distance that IED B1 tripped on its low stage, i.e. time delayed overcurrent stage, it could still cause a voltage dip at the DG terminals deep enough to cause an unwanted tripping of the DG unit. This can be avoided if IED B1 sends a block command to the LOM IED once IED B1 detects a fault on the feeder which it is protecting. Protection blinding problems caused by fault current contribution from DG can, on the other hand, be tackled by the use of differential protection. If desired, the system can also be made fully fault ride through (FRT) compatible by setting the LOM IED undervoltage protection (UVP) function to allow the low voltage ride-through (LVRT). Moreover, this does not compromise LOM protection because the transfer trip issued by IEDs A1 and A2 will always rapidly and reliably trip the DG unit whenever the DG unit becomes islanded, irrespective of the power imbalance in the islanded circuit. The communication delays in the system are of minor scale. Sending a block signal from IED B1 first via GOOSE to IED A1, then via BST to IED A2 and finally from IED A2 to LOM IED would take less than 30 ms according to [3]. If there should be any abnormalities in the communication, the LOM IED automatically switches stricter settings for providing better LOM protection.

The system is also designed to be able to enhance the reliability of distribution service to DG units in networks which are operated in an open ring configuration. The idea behind this is that IEDs can be made to control the disconnector separating the two feeders. This can be explained again with the example shown in Fig. 1. When a fault occurs at fault location A, the differential protection isolates this fault by opening circuit breakers CB_{A1} and CB_{A2}. IED A2 then immediately sends a trip command to the LOM IED since unintentional islanding is prohibited. After this, IED A2 sends a close command to the normally open disconnector D_B, and after a chosen delay, a close permit to the LOM IED. However, the actual closing time of the DG unit circuit breaker is decided by the synchronism check function.

The switching sequence has to be accomplished in a short period of time since the generator accelerates when it is unable to feed power to the grid while the mechanical power given by the prime mover remains constant. If the generator accelerates excessively, the reconnection back to the network is not possible. The proposed switching sequence is more likely to be successful if the generator is connected to the network via frequency converter. This is firstly because the synchronization rules are not as strict for inverter connected DG units as for directly connected synchronous generators. Secondly, the speed of the generator behind the frequency converter is decoupled from the frequency of the main grid and reconnection to the grid may still be possible even if the generator would have accelerated considerably. In fact, it is advisable to let the generator accelerate instead of feeding all the available power from the generator to the DC-link in order to limit the DC link voltage during LVRT [4]. However, countermeasures may be needed to avoid overspeed problems. The DC-link voltage rise can also be mitigated by activating a breaking chopper in the DC link [4].

LABORATORY SETUP

The studies were done with the help of the RTDS (real time digital simulator). RTDS was chosen for these studies because it performs the electromagnetic transient simulations needed for simulating the functioning of a power system in real time, and enables the connection of real external devices to function as a part of the simulation. Two ABB RED615 differential protection IEDs, one REF615 overcurrent protection IED and one REF615 which was configured to function as a LOM IED were connected to the RTDS. The voltage and current

measurements from the IED locations shown in Fig. 1 were amplified to a realistic scale for the IEDs with the help of three Omicron CMS156 amplifiers. The IEDs then sent their protection and control commands back to the RTDS via digital signals for controlling the circuit breakers and the diconnector D_B as illustrated in Fig. 1.

The protection settings used in the IEDs are shown in Table I. For more information concerning the differential protection parameters, refer to [5]. In addition to these, a simple synchronism check function was implemented with the help of the components available in RSCAD component library. This synchronism check function, which is activated by a digital signal sent from IED_A2 (see Fig. 1), checks that the voltage magnitude- and frequency are within the allowed limits (ΔV and Δf). The function also checks that the phase difference (Δ angle) between the voltages on both sides of the DG unit circuit breaker is within the allowed range. The settings for this function are also displayed in table I.

Table I. The utilized protection settings

Line differential prot.		**Synchronism check settings**		
function	threshold	function	threshold	
High op. val.	4000 %In	Δ V	0.08 xUn	
Low op. val.	200 %In	Δ f	0.5 Hz	
End sect. 1	100 %In	Δ angle	10 deg	
Slope sect. 2	50%			
End sect. 2	500 %In			
Slope sect. 3	150%			
Operate delay	45 ms			
I_nominal	100 A			
Overcurrent prot. (B1)		**Loss of mains protection**		
function	threshold	function	threshold	delay
I> Start value	250 A	UVP	0.8 p.u.	200 ms
I> delay	220 ms	OVP	1.15 p.u.	200 ms
I>> Start value	1000 A	OFP	51 Hz	200 ms
I>> delay	80 ms	UFP	48 Hz	200 ms

SIMULATION MODELS

The network model which is shown in Fig. 1 was used for these simulations. The parameters of the PI line models and the loads are shown in table II. The DG unit used in the studies was a 1600kVA rated hydro power driven synchronous generator connected via a 0.66kV/21kV step-up transformer. The inertia constant of the machine was 2s. The reactive power control of the generator was realized using a cascade control, where a control loop determined the set point of the automatic voltage regulator with the aim of maintaining the reactive power output at a target value. Certain simplifications, namely the omission of the turbine controller modelling and the assumption of constant torque were made in the studies. These measures are justified since hydro power plants have relatively high inertial mass which makes them respond to changes slowly, whereas protection studies are dealing with short timeframes only. Moreover, the omission of turbine controller is justified because DG units are typically not attending to frequency control.

Table II. The parameters of the utilized network model

From	**To**	**R+ [Ω]**	**X+ [Ω]**
Substation	Fault point A	6.00	5.56
Fault point A	Feeder A end	2.64	1.19
Substation	Fault point B	8.13	6.23
Fault point B	Feeder B end	5.42	4.15
110kV voltage source impedance		39.60	88.20
Loads		**P [kW]**	**Q [kVAr]**
Load at feeder A		833.65	274.01
Load B1		220.50	72.50
Load B2		220.50	72.50

SIMULATION RESULTS

This chapter presents a selection of the simulation results that were done using the presented laboratory setup and simulation models. The first case presents how the proposed system can be used to avoid unwanted tripping of DG. An unwanted tripping of the DG unit may take place if the connection point voltage of the DG unit drops below the utilized UVP limit due to a fault on the adjacent feeder. A case, where a three phase fault was inflicted on fault point B (see Fig. 1) was simulated and the results from this case are shown in Fig. 2. The top most graph represents currents flowing through CB_{B1} and the graph below this respectively represents the MV side currents fed by the DG unit. The statuses of all the circuit breakers marked in Fig. 1 are displayed at the third graph. This graph also shows when the fault pulse is inflicted. It can be seen from the top most graph, that the rms value of the current flowing through CB_{B1} is below the high stage overcurrent protection setting (I>>) and IED B1 thus trips with its low stage overcurrent protection (I>) approximately 220 ms from the starting of the fault (see table I). Note that the mechanical opening time of the circuit breaker causes an additional delay of 50 ms. The current flowing through CB_{B1} thus drops to zero approximately after 270 ms from the beginning of the fault. The synchronous generator based DG unit begins to swing slightly at the time when CB_{B1} opens as it can be seen from the currents fed by the DG unit. However, the DG unit stabilizes after a while.

The lower most graph represents the connection point voltage of the DG unit. It can be seen from this graph that the voltage drops below the utilized UVP threshold 0.8p.u. This would cause the LOM IED to trip unwantedly. However, the unwanted tripping of the DG unit is avoided because as IED B1 detects the fault on its

feeder, it sends a block command via IEDs A1 and A2 to the LOM IED. Unwanted tripping of the DG unit could, in certain circumstances, also be caused by the tripping of rate of change of frequency protection due to adjacent feeder faults [1]. However, such unwanted tripping of DG can be similarly blocked as the UVP function.

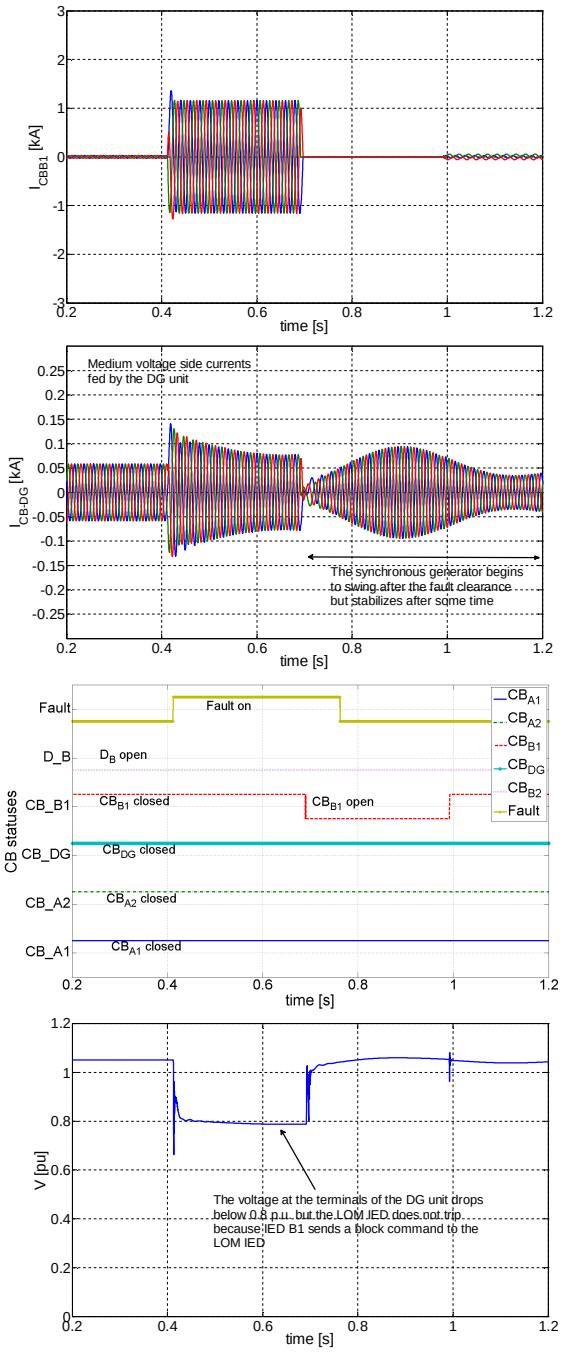

Figure 2. The unwanted tripping of the DG unit is avoided due to the block command sent by IED_{B1}

The following case presents a case where a three phase permanent fault occurs at fault point A. This causes the differential protection IEDs A1 and A2 to trip and open their circuit breakers in approximately 95ms (45ms IED operate delay + 50 ms circuit breaker mechanical opening delay). The graphs related to this case are shown in Fig. 3. IED A2 then sends a trip command to the LOM IED. In this laboratory setup the LOM IED trips approximately 4ms after IEDs A1 and A2 (the optical cable between the IEDs A1 and A2 is fairly short). This simulation shows that the examined protection system can tackle the unintentional islanding problem very rapidly and reliably.

Starting from the top, the graphs in Fig. 3 represent the MV side current fed by the DG unit, circuit breaker statuses, voltage magnitudes from both sides of the CB_{DG}, voltage frequency from the DG side of the circuit breaker and the phase difference between the voltages on both sides of CB_{DG}. It can be seen from the graphs that CB_{DG} is closed again when voltage magnitude-, frequency and the phase difference are within the tolerated limits. The delay between the closing of disconnector D_B and closing of CB_{DG} is caused by the synchronism check function and the mechanical closing delay of circuit breaker CB_{DG} (closing delay for the switches is assumed to be 60 ms). Note that voltage at the grid side of the circuit breaker drops to zero when both the DG unit circuit breaker as well as disconnector D_B are open. During this time the angle difference naturally fluctuates strongly because the voltage at the grid side of CB_{DG} is zero. A negative angle difference in Fig. 3 signifies that angle of the generator voltage is leading the voltage of the grid.

CB_{A1} tries to clear the fault by performing automatic reclosing as it can be seen from the "CB statuses" graph. Note that CB_{A2} is kept open during the automatic reclosing sequence so that the tail part of the feeder can be safely switched to feeder B already before the automatic reclosing. There is a voltage dip at the DG terminals when CB_{B1} recloses to the faulted line. However, there is no risk of nuisance tripping of the DG unit since the differential IEDs operate much faster in comparison to the UVP function of the LOM IED. If there should be a fault outside of the area protected by the differential protection IEDs on feeder A, for instance, in the DG unit transformer, the overcurrent function which is used as back up protection in IED A1 trips feeder A and sends a transfer trip command to the LOM IED.

In this simulation, the mechanical torque of the generator was set to 0.36p.u. If the value of the mechanical torque is increased from this, the angle difference drifts away from the tolerated limits. This is because the generator accelerates when it is unable to feed the power given by the prime mover. In this case, the electrical output power of the DG unit falls to zero once the DG unit is disconnected and thus the generator will accelerate. The successfulness of the feeding path change depends on many factors such as the inertia constant of the machine, nominal power of the generator and network structure.

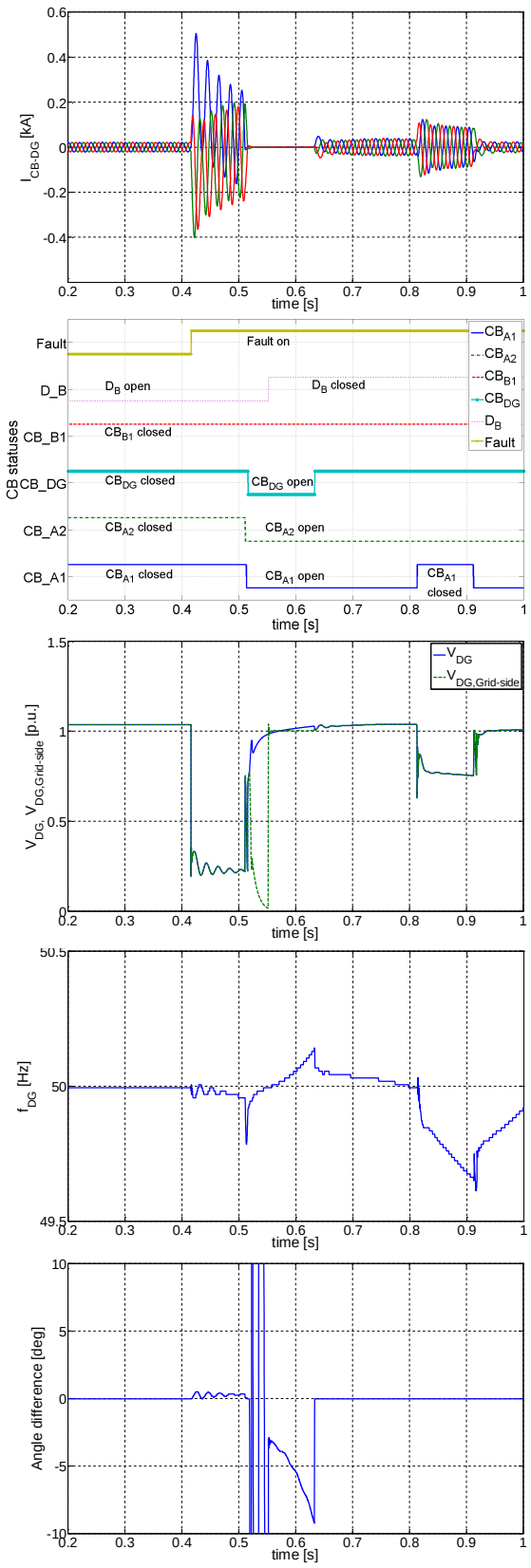

Figure 3. Feeding path of the DG unit changed

CONCLUSIONS

This paper presented a protection automation concept based on inter-IED communication. The horizontal communication between IEDs is established using the GOOSE messages defined in the IEC-61850 standard, whereas, the vertical communication is done by using the optical link between differential protection IEDs. The vertical communication can also be established using GOOSE messages but suitable communication link such as an optical cable or 4G/LTE communication link is needed in this case. The proposed concept is able to tackle typical DG related protection challenges such as protection blinding, nuisance tripping of feeders and DG units as well as non-detected islanding. Moreover, the rapid operation of the LOM protection provided by the concept ensures that fast automatic reclosing can be used on feeders that contain DG. The proposed concept can also be configured to allow DG units to be FRT compatible without compromising the performance of LOM protection. The system can also automatically switch the feeding path of DG units in open ring network configurations in case if the original feeding path becomes faulted. A simulation case demonstrating this feature is presented in this paper. This simulation case was done using a directly coupled synchronous generator based DG unit which is the most difficult type of DG from the feeding path change option point of view.

REFERENCES

[1] K. Mäki, A. Kulmala, S. Repo and P. Järventausta, 2007, ”Studies on grid impacts of distributed generation in a combined real-time simulation environment”, *Proceedings CIRED conference*

[2] O. Raipala, A. Mäkinen, S. Repo and P. Järventausta, 2012, ”The effect of different control modes and mixed types of DG on the non-detection zones of islanding detection”, *Proceedings of CIRED workshop*

[3] O. Rintamäki and K. Kauhaniemi, 2009, “Applying modern communication technology to loss-of-mains protection”, *Proceedings CIRED conference*

[4] A. Mäkinen, O. Raipala, K. Mäki, S. Repo and H. Tuusa, 2009, ”Fault ride through studies of full power converter wind turbine in a real time simulation environment”, *Proceedings Nordic wind power conference*

[5] O. Rintamäki and J. Ylinen, 2008, “Communicating line differential protection for urban distribution networks”, *Proceedings CICED conference*

Publication 7

O. Raipala, A. S. Mäkinen, S. Repo and P. Järventausta, ”Performance analysis of Q-f droop anti-islanding protection in the presence of mixed types of DG”, *in Proc. 2015 IEEE Innovative Smart Grid Technologies Conference (ISGT) Asia*, Bangkok, Thailand, November 2015

Available at: https:\\doi.org\10.1109/ISGT-Asia.2015.7387060

Performance Analysis of Q-f droop Anti-Islanding Protection in the Presence of Mixed Types of DG

Ontrei Raipala, Sami Repo, Pertti Järventausta
Tampere University of Technology
Department of Electrical Engineering
Tampere, Finland

***Abstract*—This paper analyses the performance of a Q-f droop based anti-islanding protection (AIP) scheme when the islanded circuit contains both inverter based DG and directly connected synchronous generator (SG) based DG. It is found that the performance of the AIP method is significantly degraded when SG is present in the island. This is because frequency cannot be directly manipulated by injecting reactive power when SG is present. However, feeding reactive power still indirectly affects frequency and the Q-f droop based AIP scheme thus still facilitates islanding detection. The simulation results aim to bring awareness to which extent the presence of SG degrades the performance of the Q-f droop based AIP.**

***Index Terms*—Distributed power generation, islanding, power system protection.**

I. INTRODUCTION

The electric power systems are facing significant changes due to the rapid growth of distributed generation (DG). The addition of DG to distribution systems brings many potential benefits to the utilization of power systems but it also raises challenges. Unintentional islanding is one of the DG related concerns. Islanding refers to a situation where a network area including customer loads and DG is separated from the main grid. Unintentional islanding is prohibited due to the associated safety concerns, and all DG units thus need to be equipped with an anti-islanding protection (AIP) scheme which ensures that unintentional islanding is always detected and ceased. According to the IEEE 1547 standard, islanding should be detected and ceased within 2 s at maximum [1]. However, faster detection may be required if fast automatic reclosing (AR) is utilized on DG feeders.

AIP methods can be divided into passive, active and communication based methods. Passive methods are based on simply monitoring chosen system quantities such as voltage magnitude, frequency, rate of change of frequency etc. However, these methods fail to detect islanding within a timely manner if the islanded load closely matches with the production in the islanded circuit. Communication based AIP schemes can overcome this challenge as their operation time almost completely depends on the utilized communication channel. However, despite of their high performance, communication based AIP schemes are often too costly to implement for small DG installations. Many active methods, which are based on destabilizing islanded circuits by deliberate injection of small perturbations, can also be configured to detect islanding even in a perfectly balanced islanded circuit [2], [3]. Active methods are typically applied to inverter based DG units although some active methods have also been developed for directly coupled synchronous generator (SG) based DG [4], [5]. The behavior of an islanded circuit sustained by only inverters is significantly different in comparison with the behavior of an islanded circuit sustained by SG only. That is, the time constants related to SG sustained circuits are greater than inverter sustained circuits and the relation between active- and reactive power with voltage magnitude and frequency are different [6]. This fact may cause the active methods designed for inverter based DG units to fail to detect islanding in case if the islanded circuit contains both SG and inverter based DG. This paper aims to analyze the challenges related to establishing reliable AIP for such mixed DG circuits. A simulation model in which an inverter based DG is equipped with the reactive power versus frequency (Q-f droop) AIP is constructed using PSCAD/EMTDC. A SG model is placed in parallel with the inverter based DG unit for analyzing how the performance of the AIP is affected. The simulation studies aim to bring awareness to which extent the presence of SG degrades the performance of active AIP implemented to inverters.

This paper is organized as follows. Chapter two focuses on presenting the relations between active- and reactive power with voltage magnitude and frequency during islanding. The reactive power versus frequency (Q-f) droop based AIP is also presented in the chapter along with a brief overlook on solutions for overcoming the non-detected islanding challenge in the mixed DG case. Chapter III presents the utilized simulation models which are modelled using the PSCAD/EMTDC and the simulation results can be found from chapter IV. Finally, conclusions are drawn in chapter V.

II. BASIC ANALYSIS OF ISLANDED CIRCUITS

A. The influence of active- and reactive power imbalance

Passive AIP methods are based on detecting the changes in system quantities such as voltage and frequency. These changes, which usually take place when islanding occurs, are

mainly caused by the imbalance between the production and consumption of real- and reactive power in the island. There is, however, a risk that this imbalance is so small that the transition to island mode does not cause any of the quantities measured by an AIP relay to drift out of the preset limits. In cases like this, AIP fails to detect islanding. This blind area of AIP in the surroundings of the production- consumption equilibrium is called the Non-detection zone (NDZ).

The relations between active- and reactive power with voltage and frequency can be understood by examining a case where an inverter is feeding a parallel load as shown in Fig. 1. During islanding, the active- and reactive power consumed by the load have to match with the production of the inverter as expressed in (1) and (2), where V refers to line to line voltage of the circuit and the subscripts INV and load refer to inverter and load. Thus, from (1) it can be seen that voltage is proportional to active power. Consequently, assuming that voltage is determined by P_{INV} and R, a clear relation between reactive power and frequency can be seen from (2). Frequency f will deviate to such value that the reactive power consumed by the load matches with the production of the islanded DG in the island. This can be expressed as in (2).

$$P_{INV} = \frac{V^2}{R} = P_{Load} \tag{1}$$

$$Q_{Load} = V^2\left(\frac{1}{2\pi fL} - 2\pi fC\right) = Q_{INV} \tag{2}$$

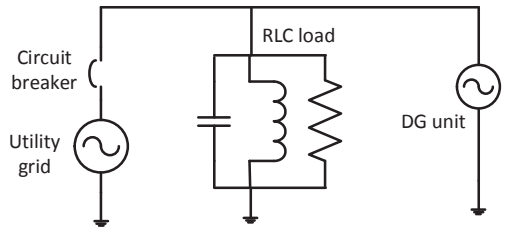

Figure 1. A simple circuit for islanding detection analysis

However, if the inverter based DG unit is replaced by a directly coupled SG, the frequency is determined by the speed of the generator. The factors determining the speed of the generator can be analyzed with the help of the swing equation (3). It is noteworthy that -windage, friction and iron-loss torque are ignored in (3):

$$P_m - P_e = \frac{GH}{\pi f_{nom}}\frac{d^2\delta}{dt^2} \tag{3}$$

where P_{m} is the mechanical power input to the generator, P_{e} is the electrical power output of the generator, G refers to the nominal power of the generator, f_{nom} is the nominal system frequency, H refers to inertia constant and δ is the power angle (i.e., rotor angular displacement from synchronously rotating reference) [7]. The term $d^2\delta/dt^2$ thus represents the angular acceleration of the generator. If there is more active power load in the island in comparison with the active power produced by the generator before the islanding, the generator will decelerate. Respectively, the generator will accelerate if the active power demand in the islanded circuit is less than the power produced by the generator before the islanding. Islanding detection related studies are dealing with short time frames only and consequently, the mechanical power input P_{m} can be assumed to be constant.

B. The Q-f droop based AIP

In the studies of this paper, a reactive power versus frequency droop (Q-f droop) based AIP method was chosen. This method, which was originally presented by [2], is set to feed/absorb reactive power proportionally to the measured frequency. The mathematical equation describing the functioning of this method can be formulated by first rewriting (2) as follows [3], [8].

$$Q_{Load} = P_{Load}Q_f\left(\frac{f_r}{f} - \frac{f}{f_r}\right) \tag{4}$$

where the resonance frequency of the load f_r and quality factor Q_f can be expressed as:

$$f_r = \frac{1}{2\pi\sqrt{LC}} \tag{5}$$

$$Q_f = R\sqrt{\frac{C}{L}} = 2\pi f_r RC \tag{6}$$

Now, the idea behind this method is to control the reactive power reference Q_{ref} of the protected DG unit by a Q_{ref}-f droop curve which is steeper than the Q_{Load} versus frequency characteristic curve of the load [2]. This can be achieved by multiplying (4) by a constant k which should be larger than 1 for ensuring that the frequency cannot stabilize inside the utilized under- and overfrequency protection (UFP/OFP) thresholds. However, one should avoid using a larger value of k than what is needed for establishing sensitive and rapid AIP in order to avoid excessive feeding/absorption of reactive power. The reactive power reference is proportional to the active power reference P_{ref}. For more information concerning the Q-f droop based AIP method, refer to [2] and [8].

$$Q_{ref} = kP_{ref}Q_f\left(\frac{f_r}{f} - \frac{f}{f_r}\right) \tag{7}$$

The UFP/OFP thresholds were chosen to be 47.5Hz and 51.5Hz in the studies of this paper. This is in line with the settings utilized in continental Europe [9]. The tripping delay

was chosen to be 200ms.The parameter k in (7) was set to 2.0 and f_r was set to 50.0Hz. The quality factor parameter Q_f was chosen to be equal to 1.0 because the IEEE 1547 standard assumes this value to represent the realistic worst case scenario. Note that the actual value of the Q_f is unknown in real systems and the Q_f setting in (7) should thus be set according to the assumed worst case scenario in order to ensure proper functioning of the AIP in all circumstances.

C. *Solutions for overcoming the mixed DG AIP challenge*

SG based DG units make the detection of islanding more difficult not only because of the averaging effect but also because of the fundamentally different characteristics in comparison to converter coupled DG units. The averaging effect refers to a case in which the performance of an active AIP method degrades when the islanded circuit contains multiple DG units but only part of the islanded DG units are equipped by the active AIP scheme. When SG is present, frequency is tied to the speed of the synchronous generator and cannot thus change as rapidly as in a case where the islanded circuit is only sustained by inverter coupled DG. Moreover, frequency is closely linked to the active power imbalance in the islanded circuit while reactive power imbalance mainly affects voltage magnitude when the islanded circuit is sustained by SG. This is profoundly different in comparison to a case where the island is sustained by inverters. In an inverter sustained island, voltage magnitude is mainly determined by the active power imbalance in the islanded circuit while the reactive power imbalance mainly determines the frequency. Due to these reasons, there is a high risk that active AIP schemes do not function properly when the islanded circuit contains both SG and inverter based DG.

The most reliable solution for establishing reliable AIP for circuits containing mixed types of DG is to equip the synchronous generator with a communication based AIP such as transfer trip. When islanding occurs and the communication based AIP first disconnects the SG, many kinds of active AIP are available for converters that can reliably detect islanding. However, if the DG units are located close to each other, it is worthwhile to consider of equipping all the DG units with the same communication based AIP.

Another type of approach is to first evaluate if there even exists a risk that the islanded load can match the islanded production closely. Such an evaluation can, for instance be done with a concept proposed in [10]. Traditional passive methods will suffice in case if the power imbalance is always significant. The size of the NDZ of passive methods can also be reduced by utilizing stricter passive AIP thresholds for SG based DG units as proposed in [5]. This does not pose a major security risk for the stability of the whole interconnected power system since SG based DG units are rather rare in comparison to converter based DG units.

One option is to equip the SG based DG units with an active AIP as discussed in [4]. Especially the reactive power positive feedback AIP scheme can be effective for SG provided that the excitation system can execute the desired reactive power references rapidly enough. However, there is a risk of conflict if the SG in the islanded circuit is equipped with such an AIP scheme which aims to destabilize voltage magnitude by injecting/absorbing reactive power while the converters are equipped with an RPV scheme which aims to destabilize frequency by injecting or absorbing reactive power. In such a case, these methods may cancel each other's efforts to destabilize voltage magnitude or frequency.

III. THE UTILIZED AIP METHOD AND SIMULATION MODELS

This chapter presents the simulation models used for studies of this paper. A simulation model consisting of a 110kV source, an HV/MV transformer, an RLC load and two types of DG units, was used for the studies of this paper. The first DG unit was a converter coupled 500kVA rated wind turbine which is shown in Fig. 2. This model is presented more in detail in [11]. A 500kVA rated directly coupled SG was connected in parallel with the converter based DG unit. The reactive power control of the SG was realized using a cascade control, where a control loop determined the set point of the automatic voltage regulator with the aim of maintaining the reactive power output at a target value. Certain simplifications, namely the omission of the turbine controller modeling and the assumption of constant torque were made in the simulations. The parameters of the of the simulation model are shown in table I along with the control system parameters of the inverter.

The control system of the inverter is depicted in Fig. 3. The vector control of the grid side converter was established in a reference frame synchronized to the connection point voltage of the inverter by using a phase locked loop component from the PSCAD master library. The output of the dc-link voltage controller is the d-component of the inverter converter current. The aim of the dc-link voltage controller is to maintain constant dc-link voltage and thereby ensure that the generated active power is fed into the network. The reference value for the reactive power is given according to (7). The q-component of the current was limited to 194.5 A which corresponds to 0.95 power factor at rated power, whereas, the d-component of the current was limited to 900 A. The parameters of the utilized simulation model and control system are shown in table I. Note that the symbols in table I refer to Fig. 2 and Fig. 3.

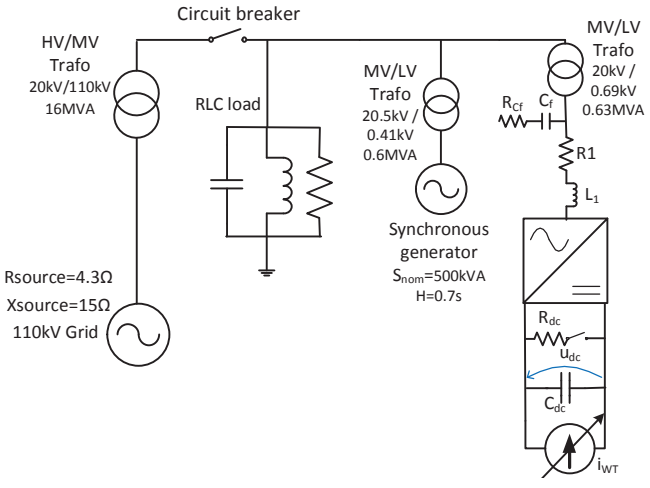

Figure 2. The simulation model

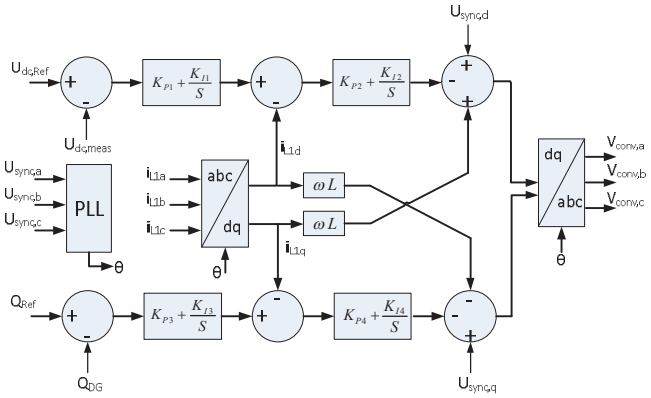

Figure 3. The control system of the inverter

The purpose of these simulation studies was to analyze the performance of the Q-f droop based AIP. The modelling of the mechanical parts of the wind turbine was thus not taken into account because the mechanical time constants are considerably larger than time constants related to the discussed AIP. The mechanical parts, the generator and generator side converter were thus modelled as a current source i_{WT} in the DC-link of the frequency converter whose value can be obtained as follows:

$$i_{WT} = \frac{P_{gen}}{u_{dc}} \qquad (8)$$

TABLE I. THE PARAMETERS OF THE SIMULATION MODEL

DG inverter controller parameters			
$K_{p1} = 4.0$	$K_{p2} = 0.6$	$K_{p3} = 0.01$	$K_{p4} = 0.6$
$K_{I1} = 0.025$s	$K_{I2} = 0.003$s	$K_{I3} = 6.0$s	$K_{I4} = 0.003$s
110 kV Grid parameters			
$f_{nom} = 50$Hz	grid resistance = 4.3Ω		grid reactance = 15Ω
HV / MV transformer (110 kV / 21 kV)			
$S_n = 16$MVA	copper losses = 0.0052pu		$X_{leakage} = 0.103$pu
Transformer of the inverter based DG (21 kV / 0.69 kV)			
$S_n = 0.63$MVA	copper losses = 0.0026pu		$X_{leakage} = 0.038$pu
Filter parameters			
L_1=300 μH	$R_1 = 2.4$mΩ	$C_f = 0.2$mF	$R_{cf} = 0.25$Ω
Parameters of the inverter based DG unit			
$S_{nom} = 0.5$MVA	$C_{dc} = 22$mF	$R_{dc} = 2$Ω	$U_{dc,nom} = 1100$V
SG based DG unit			
Sn=500kVA	H=0.7s	Excitation type: IEEE AC5A	
Transformer of the SG based DG unit			
Sn=0.6MVA	copper losses=0.0072pu		$X_{leakage} = 0.06$pu

The resistance R, inductance L and capacitance C of the parallel connected RLC load were chosen so that the quality factor of the load was 1.0 throughout the studies of this paper. This is in line with the IEEE 1547 standard [1].

IV. SIMULATION RESULTS

This chapter presents the simulation studies which were done by using PSCAD/EMTDC. First a baseline case is shown where the inverter based DG unit is sustaining the islanded circuit alone. It is shown that islanding can easily be detected by using the Q-f droop based AIP method in this case. After this, the SG based DG unit is connected in parallel with inverter based DG unit and several cases analyzing this mixed DG scenario are simulated.

A. Inverter sustained power island

A baseline case, where the power imbalance between the production of the inverter and the consumption of the load was set to be minor (less than 0.0001pu) was first simulated. In a case like this, islanding cannot be detected by passive monitoring of voltage magnitude and frequency. However, the Q-f droop based active AIP was enabled in this case and the parameter k in (7) was set to 2.0. The simulation results of this case are shown in Fig. 4.

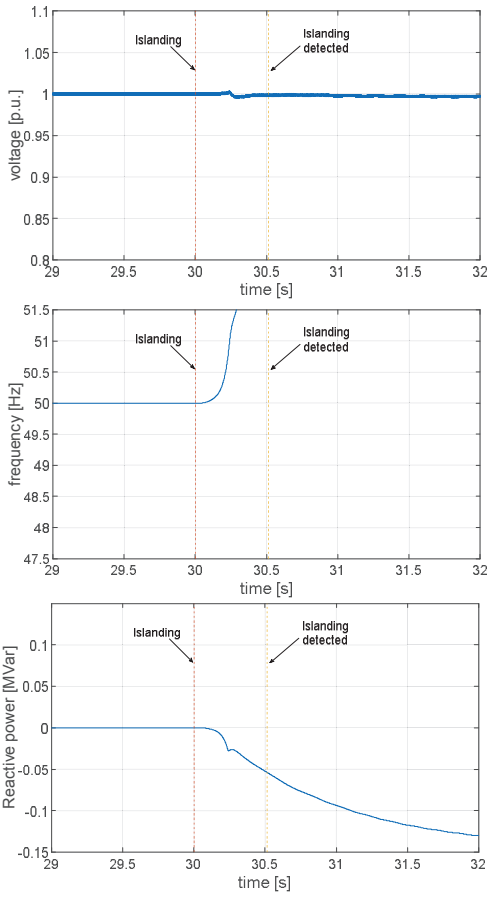

Figure 4. Voltage magnitude, frequency and the reactive power fed by the inverter when the island is sustained only by the inverter based DG unit. The Q-f droop is enabled for facilitating islanding detection.

As islanding occurs at time 30.0s, the Q_{ref}-f droop orders the inverter to consume reactive power according to (7). This causes the frequency to rise which again causes the inverter to absorb even more reactive power. This trend continues until frequency drifts out of the utilized OFP threshold 51.5Hz. The AIP trips 200ms after the frequency has drifted above 51.5Hz due to the chosen tripping delay.

B. Power island sutained by mixed types of DG

Now both the SG and inverter based DG units were connected in parallel and the previous simulation was again repeated. The load was set to match the combined production of the two DG units. Both DG units were set to operate at their nominal power. The SG was operating at unity power factor, whereas, the reactive power reference of the inverter based DG was determined by (7). However, islanding could not be detected within 10 seconds under these circumstances when the value of the parameter k was equal to 2.0. Thus, the value of the parameter k was increased to 3.0. The simulation results of this case are shown in Fig. 5.

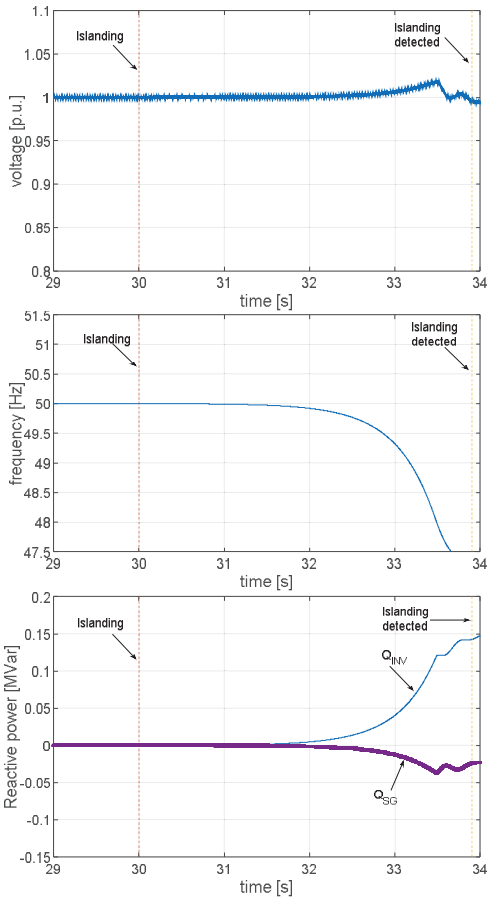

Figure 5. Voltage, frequency and the reactive power fed by the DG units when the inverter based DG unit is connected in parallel with the SG.

It can be seen from the graphs that the SG stabilized the frequency to such an extent that the AIP method was not able to drift the frequency out of the utilized UFP/OFP limits within 2.0s. However, the frequency did eventually drift below 47.5Hz in approximately 3.9s. The reason for this is that despite that the reactive power injected by the inverter mainly affected the voltage magnitude due to the presence of the SG, the change in voltage changed the consumption of the RLC load, and thereby also the active power imbalance. This can be seen by rewriting (3) with the help of (1) to represent a case where the islanded circuit contains both SG and inverter based DG as in (9). The change in voltage leads to a change in the active power consumed by the load, which again causes the angular acceleration term in (9) to change. This naturally changes the voltage frequency of the islanded circuit.

$$P_m - \left(\frac{V^2}{R} - P_{INV} \right) = \frac{GH}{\pi f_{nom}} \frac{d^2\delta}{dt^2} \tag{9}$$

Fig. 6 illustrates how the k parameter in (7) affects the performance of the AIP in six different scenarios. The orange colored curve presents AIP time versus parameter k value when the island was sustained only by the inverter based DG unit, whereas, the green curve represents a case where there were two inverter based DG units operating in parallel which were both equipped with the Q-f droop. One can observe that there was hardly any difference between these two cases. The purple colored curve represents a scenario where there were two inverter based DG units but only one of them was equipped with the Q-f droop. As it can be seen, the AIP tripping time increased significantly due to the second inverter which was simply operating at unity power factor. This is understandable since the amount of reactive power fed by the inverter should be doubled when the active power production in the islanded circuit doubles in order for the frequency to deviate as much as in the case where one inverter equipped by the Q-f droop was sustaining the island alone (7). However, the AIP performance still deteriorated to a significantly lower level when the inverter, which was equipped with the Q-f droop, was paralleled with the SG based DG unit which was operating at unity power factor (red curve). In fact, the islanding could not be detected in 2.0s even by increasing the value of the parameter k to 4.0. The dark blue colored curve represents a case where the SG based DG unit was operating at unity power factor in parallel with two inverter based DG units that were equipped by the Q-f droop. In this case, islanding could be detected in 2.0s when the parameter k was set to a value greater than 2.4. Note that the ratio of inverter to SG based DG was 2/1 in this case. The last case respectfully represents a case where the SG was set to operate in parallel with three inverter based DG units (light blue curve), i.e., the ratio of inverter to SG based DG was 3/1. As it can be seen from the graph, the AIP performance increases along with the increase in inverter to SG based DG ratio. The load was set to match the production in each of the cases. The parameter k was varied from 1.0 to 4.0 by 0.1 steps.

It can be seen from Fig. 6 that there were few cases where increasing the value of the k increased the AIP trip time when the SG based DG unit was present. The reason for these cases was that the increase in the parameter k intensified the initial swing of the SG speed which, however, was not large enough

for reaching the UFP/OFP threshold. Now, the reactive power fed/absorbed by the inverters caused a deviation in voltage which resulted to a change in the consumption of the load. This, in turn, caused the P_e in (3) to change which caused the SG speed to swing to another direction. However, increasing the parameter k sufficiently lead to a situation where the first swing in frequency already reached the UFP/OFP limit which again shortened the AIP trip time.

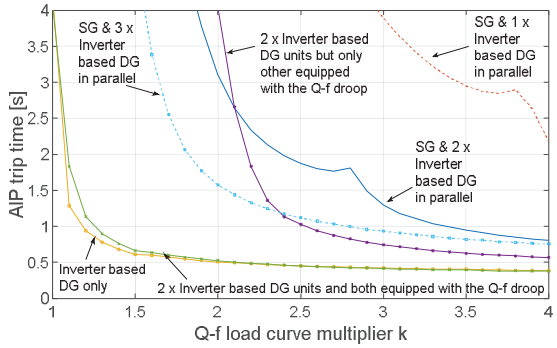

Figure 6. The effect of the Q_{ref}-f droop multiplier k on AIP

Fig. 7 illustrates how the inertia constant of the SG affects the AIP performance with different values of the parameter k. In this case, there were two inverter based DG units in parallel with the SG. Together with the graphs in Fig. 6, the curves in Fig. 7 can be used to get a rough idea of how significantly the Q-f droop based AIP performance is degraded when a SG is connected in parallel with inverters. Fig 6 gives an idea to what extent the ratio between inverter and SG based DG affects the AIP performance, whereas, Fig. 7 can be used to evaluate the impact of the inertia constant value.

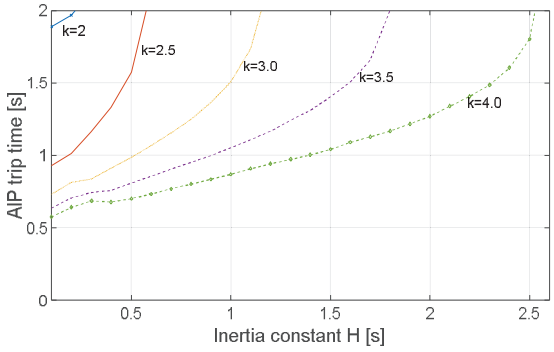

Figure 7. The effect of inertia constant H on islanding detection

An NDZ map which was formed by conducting a large number of simulations where the SG was operating in parallel with two of the inverter based DG units is shown Fig. 8. The layers marked by different colors in the figure refer to different AIP operation times. The various power imbalance situations where created by varying the consumption of the load. This NDZ map reveals that the most challenging power imbalance combinations from the AIP point of view may not located in the origin. The NDZ also gives an idea of how large power imbalances can still lead to problems with the AIP. However, the size of the NDZ is dependent on the applied voltage and frequency protection thresholds.

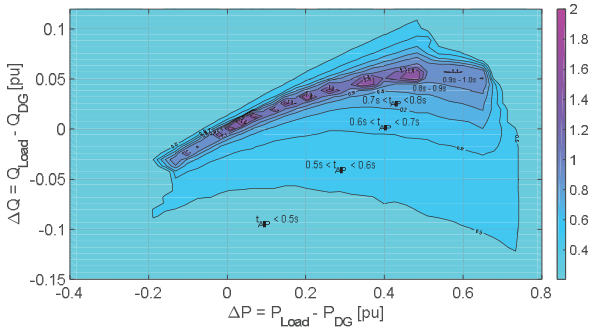

Figure 8. The NDZ of the Q-f droop based AIP when two inverter based DG units and one SG are connected in parallel. The k constant is set to 2.0.

V. Conclusions

This paper analyzed how the presence of SG affects the performance of a Q-f droop based AIP. It was shown that the Q-f droop based AIP is highly effective when the islanded circuit contains only inverter based DG. However, when SG is present in the islanded circuit, frequency cannot be manipulated as strongly anymore as in a case where the island is sustained by only inverter based DG. Nevertheless, reactive power injection still indirectly affects the frequency by changing the voltage and thereby also the active power load. It was also analyzed how the ratio of between inverter based DG and directly coupled SG affects the AIP performance. The effect of the inertia constant of the SG on AIP performance was also studied in the paper.

References

[1] *IEEE Std. for Interconnecting Distributed Resources with Electric Power Systems*, IEEE Standard 1547, 2003

[2] H. H. Zeineldin, "A Q-f droop curve for facilitating islanding detection of inverter-based distributed generation", *IEEE. Trans. Power Electron.*, vol. 24, pp. 665-673, March 2009

[3] Y. Zhu, D. Xu, N. He, J. Ma, J. Zhang, G. Shen and C. Hu, "A novel RPV (Reactive Power Variation) antiislanding method based on adapted reactive power perturbation, "*IEEE Trans. Power Electron.*, vol. 28, pp. 4998-5012, Nov. 2013

[4] Z. Ye, "Study and Development of Anti-Islanding Control for Synchronous Machine-Based Distributed Generators," GE Global Research Center, Niskayuna, New York, Subcontract report NREL/SR-560-38018, March 2006

[5] C. Mouw, M. Ropp, B. Enayati and R. Eastham, "Simulation study of islanding in two synchronous generator DG applications, in Proc. 2014 IEEE PES General Meeting

[6] O. Raipala, A. Mäkinen, S. Repo and P. Järventausta, "The Effect of Different Control Modes and Mixed Types of DG on the Non-Detection Zones of Islanding Detection", in *Proc. CIRED 2012*

[7] D. P. Kothari and I. J. Nagrath, "Power system stability," in Modern Power System Analysis 3rd. ed., New Delhi; Tata McGraw-Hill, 2004

[8] L. Jiang, W. Cai, B. Liu and S. Duan, "Parameter design and impacts on power quality of a Q-f droop curve based islanding detection method", in *Proc. IEEE ECCE 2013*

[9] *ENTSO-E Network code for "Requirements for grid connection applicable to all generators"*, March 2013

[10] O. Raipala, S. Repo and P. Järventausta, "Network information system based loss of mains risk managent", in Proc. CIRED 2013

[11] A. S. Mäkinen and H. Tuusa, " Impact of strength of fault current path on the operation of decoupled double synchronous reference frame phase locked loop", *in Proc. ICREPQ'13*

Publication 8

O. Raipala, A. S. Mäkinen, S. Repo and P. Järventausta, ”An anti-islanding protection method based on reactive power injection and ROCOF” *IEEE Trans. Power Delivery*, vol. 32, pp. 401-410, February 2017

Available at: https://doi.org/10.1109/TPWRD.2016.2543503

An Anti-islanding Protection Method Based on Reactive Power Injection and ROCOF

O. Raipala, *Student Member, IEEE*, A. S. Mäkinen, *Student Member IEEE*, S. Repo, *Member, IEEE* and P. Järventausta, *Member, IEEE*

***Abstract*—All Distributed generation (DG) units need to be equipped with an anti-islanding protection (AIP) scheme in order to avoid unintentional islanding. Unfortunately, most AIP methods fail to detect islanding if the demand in the islanded circuit matches with the production in the island. Another concern is that many active AIP schemes cause power quality problems. This paper proposes an AIP method which is based on the combination of a reactive power versus frequency droop and rate of change of frequency (ROCOF). The method is designed so that the injection of reactive power is of minor scale during normal operating conditions. Yet, the method can rapidly detect islanding which is verified by PSCAD/EMTDC simulations.**

***Index Terms*—Distributed power generation, islanding, power system protection.**

I. Introduction

The rapidly increasing amount of distributed generation (DG) is raising concerns related to the functioning of distribution network protection. Especially challenges related to the functioning of anti-islanding protection (AIP) have been studied actively in recent years. Unintentional islanding is prohibited due to the associated safety hazards and it is thus mandatory to equip all DG units with an AIP protection scheme. Islanding should be detected and ceased within 2 seconds according to many international standards such as the IEEE 1547 [1]. However, faster detection times are needed if fast automatic reclosing is used on feeders that contain DG.

AIP protection methods can be divided into passive, active and communication based methods. Passive methods are based on locally measuring certain system quantities, such as voltage magnitude, frequency or rate of change of frequency (ROCOF). The idea behind these methods is that some changes in the measured quantities usually occur during the transition to islanding. The downside of these methods is that most of these methods fail to detect islanding in case if the production in the islanded circuit closely matches with the load in the islanded circuit. The problematic active- and reactive power imbalance combinations which lead to non-detected islanding are referred to as the non-detection zone (NDZ). Active AIP methods, which are based on drifting voltage magnitude or frequency out of the predefined thresholds by deliberate injection of perturbations, are usually characterized by a smaller NDZ in comparison with the passive methods. However, the better islanding detection performance of active methods comes at the cost of degraded power quality. Communication based methods are immune to the NDZ problem but they tend to be costly.

Active AIP methods have received significant attention due to their high performance in the last years. Especially frequency drift based AIP methods have been highlighted [2], [3]. Reactive power variation (RPV) based AIP schemes are one of the effective ways of drifting frequency during islanding. RPV based AIP methods are favorable in the sense that they do not cause current distortion unlike many other active AIP schemes [4]. Controlling the reactive power output of the DG unit is also more reasonable in comparison to manipulation of the active power output of the DG unit due to economic reasons. That is, DG is desired to feed all the available power provided by the utilized energy source such as photovoltaic cells or wind turbine. Reference [5] presented a Q-f droop based AIP method which pursued to drift the frequency out of the utilized over- or underfrequency (OUF) thresholds. However, islanding detection can be fairly slow using this method if the utilized OUF thresholds specify a relatively wide normal operation frequency range such as many European grid codes [6]. Reference [7] presented an intermittent bilateral RPV method in which there is also a zero period in the RPV pulse in addition to the maximum and minimum values ±5% of the active power output. Reference [8] improved this bilateral RPV method by [7] by only injecting intermittent unilateral RPV pulses. The method seemed to be fit for Chinese OUF thresholds 49.5 Hz and 50.5 Hz. However, this method would cause very large disturbances during normal operating conditions if the method was tuned for a system with broader OUF thresholds, such as Continental Europe where the utilized OUF thresholds are 47.5 Hz and 51.5 Hz [6]. Reference [9] presented an AIP method which is based on constantly injecting a RPV pulse consisting of three parts of equal duration. The two first parts of the RPV pulse form a symmetric triangular shape, whereas, the reactive power reference is kept at zero in third part. During islanding, the absolute value of ROCOF will be constant during the first two parts of the RPV pulse. This can be used as a criterion to detect islanding. However, different approach has to be used in multi-inverter case unless the RPV pulses happen to be synchronous. In such a case, the periodically changing

The authors are with the Department of Electrical Engineering, Tampere University of Technology (TUT), Tampere, Finland (e-mail: ontrei.raipala@tut.fi).

frequency is used as a criterion to detect islanding. This approach is innovative in the sense that frequency is not drifted outside the utilized OUF thresholds which facilitates the transition to intentional microgrid. However, the method still causes a constantly injected disturbance which may be harmful during normal grid connected state especially if large amount of DG units are equipped with this AIP scheme.

This paper presents an active AIP method for inverter connected DG units which is based on forcing the frequency to drift at such a rate during islanding that the utilized ROCOF threshold is exceeded. This is achieved by using a dedicated reactive power versus frequency droop (Q-f droop). The use of the ROCOF function improves the performance of the AIP method in terms of islanding detection time in comparison with the existing RPV based AIP methods. The proposed method is especially advantageous in comparison with existing RPV based AIP methods if the utilized DG interconnection standard defines relatively wide OUF thresholds. Moreover, the islanding can be detected by smaller injection of reactive power in comparison with most existing RPV based AIP schemes. In addition, the performance of the proposed method does not degrade when multiple inverter based DG units are equipped with the same method.

This paper is organized as follows. Chapter II introduces the basic principles behind the proposed method. After this, the simulation model which is used for verifying the functioning of the proposed method is presented in chapter III, whereas, the actual simulation results are presented in chapter IV. Finally, conclusions are drawn in chapter V.

II. Reactive power variation based AIP

A. The Q-f load curve

Most AIP methods are based on detecting the changes in system quantities such as voltage and frequency. These changes, which usually take place when islanding occurs, are mainly caused by the imbalance between the production and consumption of real- and reactive power in the island. The relations between active- and reactive power with voltage and frequency can be understood by examining a case where an inverter is feeding a parallel load connected to the circuit as shown in Fig. 1.

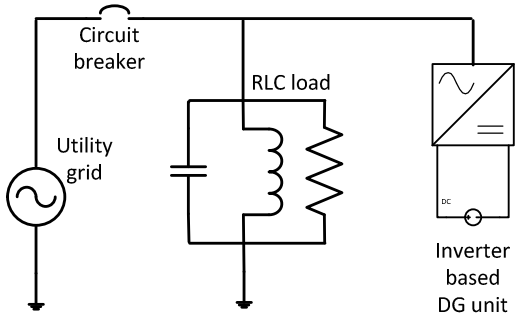

Fig. 1. A simple circuit for islanding detection analysis

When the circuit breaker in Fig. 1 is closed, the difference between the local production and consumption of active and reactive power is being imported or exported by the utility grid. However, when the circuit breaker is open and the studied system is thus islanded, the active- and reactive power consumed by the load have to match with the production of the inverter as expressed in (1) and (2), where V refers to phase voltage of the circuit and the subscripts INV and Load refer to inverter and load. Thus, from (1) it can be seen that voltage is proportional to active power. Consequently, assuming that voltage is determined by P_{INV} and load resistance R, a clear relation between reactive power and frequency can be seen from (2). Frequency f will deviate to such a value that the reactive power consumed by the load matches with the production of the islanded DG in the island. This can be expressed as in (2).

$$P_{INV} = 3\frac{V_{ph}^2}{R} = P_{Load} \qquad (1)$$

$$Q_{INV} = 3V_{ph}^2\left(\frac{1}{2\pi fL} - 2\pi fC\right) = Q_{Load} \qquad (2)$$

If the inverter is operating at unity power factor and thus produces no reactive power, then the frequency has to deviate to such a value that the load consumes no reactive power either. This is the resonance frequency f_r of the load.

$$f_r = \frac{1}{2\pi\sqrt{LC}} \qquad (3)$$

Let us now define (2) with the help of the resonance frequency and the quality factor of the load. The quality factor Q_f of a parallel RLC load can be expressed as follows

$$Q_f = R\sqrt{\frac{C}{L}} = 2\pi f_r RC = \frac{\sqrt{Q_L Q_C}}{P_{Load}} \qquad (4)$$

Where Q_L refers to the inductive- and Q_C to the capacitive reactive power consumed by the load. Now the inductance L and capacitance C of the RLC load can be expressed with the help of (3) and (4) as follows

$$L = \frac{R}{2\pi Q_f f_r} \qquad (5)$$

$$C = \frac{Q_f}{2\pi R f_r} \qquad (6)$$

And using (5) and (6), (2) can be written as in (7) [8]

$$Q_{Load} = P_{Load} Q_f\left(\frac{f_r}{f} - \frac{f}{f_r}\right) \qquad (7)$$

Despite the non-linear nature of the Q_{Load}-f curve (7), the curve is approximately linear within the typical frequency variation range determined by the utilized OUF thresholds. Three Q_{Load}-f load curves with different resonant frequencies expressed by (7) are shown in Fig. 2 (Qf=1.0 and P_{Load}=500 kVA). If the circuit in Fig. 1 is islanded while the reactive power reference Q_{ref} of the inverter is zero, i.e. the DG unit operates at unity power factor, frequency will settle to the resonance frequency of the load. If a scenario like this occurs and the resonance frequency of the load lies within the OUF limits, then islanding cannot be detected by frequency relays.

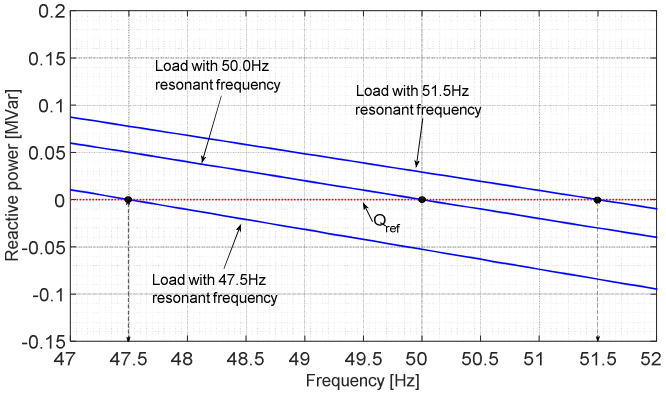

Fig. 2. Load curves with different resonant frequencies

B. *The proposed AIP method*

The idea behind the Q-f droop based AIP method is to equip the protected DG unit with a Q_{ref}-f droop curve, which is steeper than the load curves and that has a negative slope [5]. This principle is illustrated in Fig. 3.

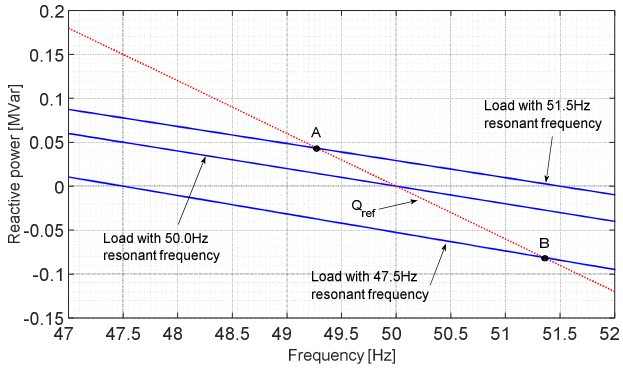

Fig. 3. The principle of Q-f droop based AIP

Looking at the point marked by A in Fig. 3, for a small change in frequency towards the UFP threshold, the reactive power reference of the inverter is larger than the consumption of the load. Thus, the frequency has to drop in order to increase the reactive power consumption of the load as it can be seen from (2). This trend continues until the frequency drops below the utilized UFP threshold. The point A is thus an unstable state for the frequency. Similarly, looking at the point marked with the letter B, for a small change in frequency towards the OFP threshold, the reactive power reference of the inverter is lower than the reactive power of the load. Consequently, the frequency has to rise in order to bring the reactive power consumption of the load to be equal to the reactive power produced by the inverter. Thus the point B is similarly an unstable state for the frequency. Refer to [5] for more information on the Q-f droop based AIP.

It can be ensured that the Q_{ref}-f droop curve of the AIP method is steeper than the Q-f load curve by multiplying the equation (7) by a suitable constant k, which obviously has to be larger than one. This can be expressed as in (8). One can see from (8) that the larger the value of the quality factor, the steeper the load curve, and thus the steeper the Q_{ref}-f droop has to be in order to guarantee that frequency cannot stabilize within the OUF thresholds during islanding.

$$Q_{ref} = kP_{ref}Q_f\left(\frac{f_r}{f} - \frac{f}{f_r}\right) \qquad (8)$$

In practice this curve is predetermined based on the desired level of performance. The utilized quality factor value depends on the applied national or international standard. For instance, in the UK, a quality factor value above 0.5 has to be applied [10], whereas, the IEEE 1547 standard specifies a quality factor value 1.0 for AIP testing [1]. The resonance frequency f_r in (8) should be chosen to be equal to nominal frequency and the value of the parameter k has to be larger than 1.0. The distribution network protection engineers would thus only set the parameter k to a desired value for obtaining a desired level of performance. Note that the reactive power reference Q_{ref} depends on the active power reference P_{ref} for avoiding excessive feeding of reactive power.

However, instead of waiting for the frequency to drift out of the utilized UFP/OFP limits, the intention of the proposed method is to cause the frequency to drift at a desired rate so that the utilized df/dt threshold is exceeded. In this paper, the ROCOF index is calculated as a moving average of five consecutive 20 ms measuring windows from the frequency measured by the phase locked loop (PLL).

$$ROCOF_{100ms} = \frac{\sum_{i=5}^{5} ROCOF20ms_i}{5} \qquad (9)$$

The idea behind the proposed method is to cause the utilized ROCOF threshold to be exceeded for a time T_{tar} which is larger than the utilized tripping delay. For ensuring the proper functioning of the method, the desired ROCOF level ($ROCOF_{tar}$) should exceed the utilized threshold during islanding by a suitable margin. The slope of the Q_{ref} curve can be obtained by differentiating (8) and setting the frequency equal to the resonant frequency, that is f=f_r.

$$\frac{dQ_{ref}}{df} = -2kP_{ref}\frac{Q_f}{f_r} \qquad (10)$$

However, if (10) is directly used as the slope of the Q_{ref}-f curve, the inverter could feed more reactive power than what is needed for causing the measured ROCOF index to exceed the utilized threshold. This disadvantage can be avoided by rate limiting the reactive power reference so that the ROCOF index only reaches the desired level and does not exceed it. Rate limiting the reactive power reference to the desired level naturally reduces the injection of reactive power during short lasting grid disturbances. Equation (11) expresses the appropriate reactive power per second rate limitation:

$$Q_{Rate,\lim} = \pm \frac{\Delta Q_{ref}}{\Delta t} = \pm \frac{Q_{tar}}{T_{tar}} \qquad (11)$$

where the reactive power at target frequency, Q_{tar}, is calculated by using equation (7) at the frequency f_{tar}:

$$f_{tar} = f_{nom} - T_{tar} ROCOF_{tar} \qquad (12)$$

The ROCOF function is claimed to have caused nuisance tripping in certain conditions [11]. In order to alleviate this risk, an additional criterion checking whether the frequency has actually reached the target value, is used together with the ROCOF criterion in the proposed scheme. That is, the method only trips in case if the ROCOF threshold is exceeded at the same time while either the lower target ($f_{tar,low}$) or higher target ($f_{tar,high}$) value of frequency has been reached as illustrated in Fig. 4. The thresholds $f_{tar,low}$ and $f_{tar,high}$ are calculated by subtracting the product of the ROCOF target value and the utilized tripping delay. This causes no significant delay since the f_{tar} is designed to be reached anyway for reaching the desired ROCOF level. Yet, at the same time this additional criterion enhances the protection security of the proposed method.

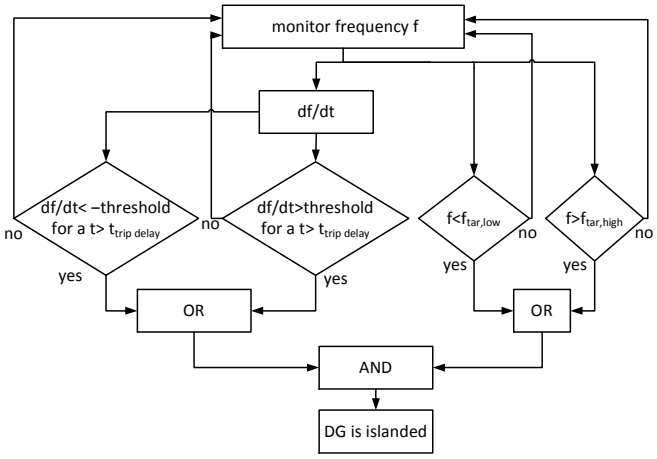

Fig. 4. The islanding detection process in the proposed AIP scheme

The ROCOF threshold and ROCOF target value $ROCOF_{tar}$ should be selected to be relatively high for avoiding unwanted tripping. This does not jeopardize the protection sensitivity of the AIP because the injected reactive power causes the ROCOF target to be reached during islanding as long as the Q_{ref} curve and rate limitation (11) are chosen so that the chosen ROCOF target level can be reached.

III. Simulation Model

The DG unit used in these simulation studies was a 500 kVA rated full power converter connected wind turbine which is based on the model presented in [12]. This DG unit was connected to the 20 kV section of the circuit via a step up transformer whose ratio was 0.69 kV / 20 kV as shown in Fig. 5. The purpose of these simulation studies is to analyze the functioning of the proposed anti-islanding protection. The modelling of the mechanical parts of the wind turbine was thus not taken into account because the mechanical time constants are considerably larger than time constants related to the proposed anti-islanding protection. The mechanical parts, the generator and generator side converter were thus modelled as a current source i_{WT} in the DC-link of the frequency converter whose value can be obtained as follows:

$$i_{WT} = \frac{p_{gen}}{u_{dc}} \qquad (13)$$

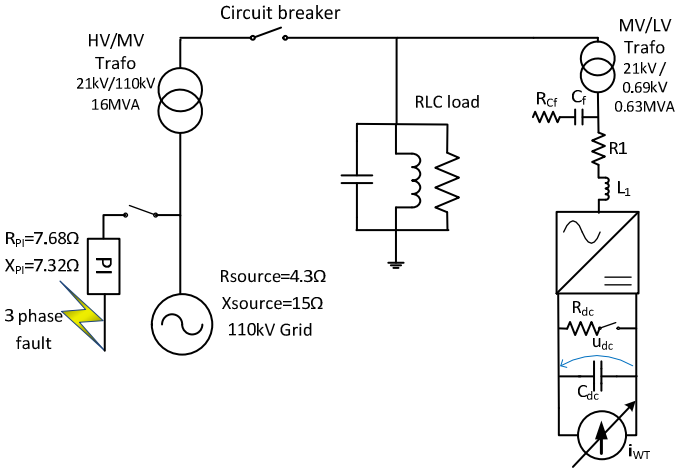

Fig. 5. The simulation model

The control system is shown in Fig. 6. The vector control the grid side converter was established in a reference frame synchronized to the connection point voltage of the DG unit by using a PLL component from the PSCAD master library. The output of the dc-link voltage controller is the d-component of the inverter converter current. The aim of the dc-link voltage controller is to maintain constant dc-link voltage and thereby ensure that the generated active power is fed into the network. The reference value for the reactive power is given according to (8) which, however, is rate limited as expressed in (11). The q-component of the current was limited to 194.5 A which corresponds to 0.95 power factor at rated power, whereas, the d-component of the current was limited to 900 A. The parameters of the utilized simulation model and control system are shown in table I. Note that the symbols in table I refer to Fig. 5 and Fig. 6.

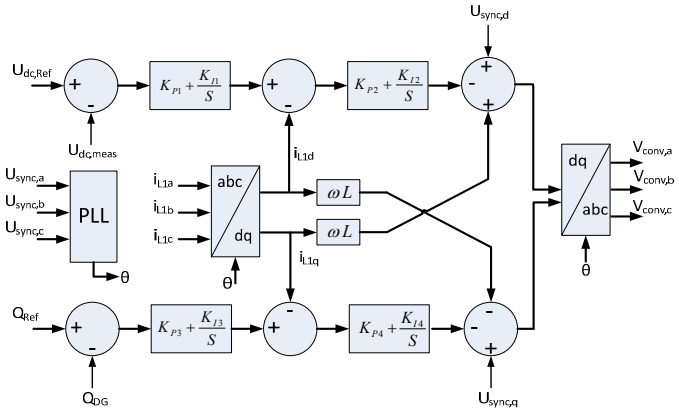

Fig. 6. The control system of the inverter

TABLE I
Parameters of the utilized simulation model

DG inverter controller parameters			
K_{p1} = 4.0	K_{p2} = 0.6	K_{p3} = 0.01	K_{p4} = 0.6
K_{I1} = 0.025s	K_{I2} = 0.003s	K_{I3} = 6.0s	K_{I4} = 0.003s
110 kV Grid parameters			
f_{nom} = 50Hz	grid resistance = 4.3Ω		grid reactance = 15Ω
HV / MV transformer (110 kV / 21 kV)			
S_n = 16MVA	copper losses = 0.0052pu		$X_{leakage}$ = 0.103pu
DG transformer (21 kV / 0.69 kV)			
S_n = 0.63MVA	copper losses = 0.0026pu		$X_{leakage}$ = 0.038pu
Filter parameters			
L_1=300 µH	R_1 = 2.4mΩ	C_f = 0.2mF	R_{cf} = 0.25Ω
DG unit parameters			
S_{nom} = 0.5MVA	C_{dc} = 22mF	R_{dc} = 2Ω	$U_{dc,nom}$ = 1100V
Load parameters at power balance (Pload = 498.7kW, Q = 0Mvar)			
R=801.85Ω	L=2.56H	C=3.97µF	Q_f=1.0

The 0.69 kV / 20 kV transformer forms the grid side inductance part of the LCL filter. The switching action was not taken into account in this study. A braking chopper is connected to the dc-link of the inverter as shown in Fig. 5 for protecting the dc-link from overvoltages. The switch connecting the resistance R_{dc} to the dc link is closed if the dc-link voltage should exceed the value 1250 V.

A fault branch, which is shown in Fig. 5, is also included in the model. This branch is only used in the simulation concerning the stability of the proposed AIP method. In other simulations, this fault branch is always disconnected.

IV. Simulation Results

This chapter presents simulation studies for verifying the functioning of the method presented in chapter II. The simulations are performed by using the PSCAD/EMTDC and the model presented in chapter III. The utilized simulation time step was 50 µs. The ROCOF index was calculated by passing the frequency measured by the PLL to a low pass filter whose output was then sampled by a 1000 Hz sampling frequency. The threshold used for the ROCOF protection function was 2 Hz/s and the tripping delay was assumed to be 200 ms. The rate limitation of the reactive power droop was set to correspond to 3 Hz/s by using (11). The quality factor of the load was assumed to be 1.0 as these values are considered appropriate for testing anti-islanding protection in the IEEE 1547 standard. The OUF thresholds were assumed to be 47.5 Hz and 51.5 Hz, which is in line with the OUF thresholds used in most of the Europe [6].

A. AIP performance during balanced islanding

A simulation case, where islanding is set to occur at time 25.0 s by opening the circuit breaker between the grid and the studied circuit, is shown in Fig. 7. The consumption of the load was set to match the power produced by the inverter. The Q–f droop was disabled in this case.

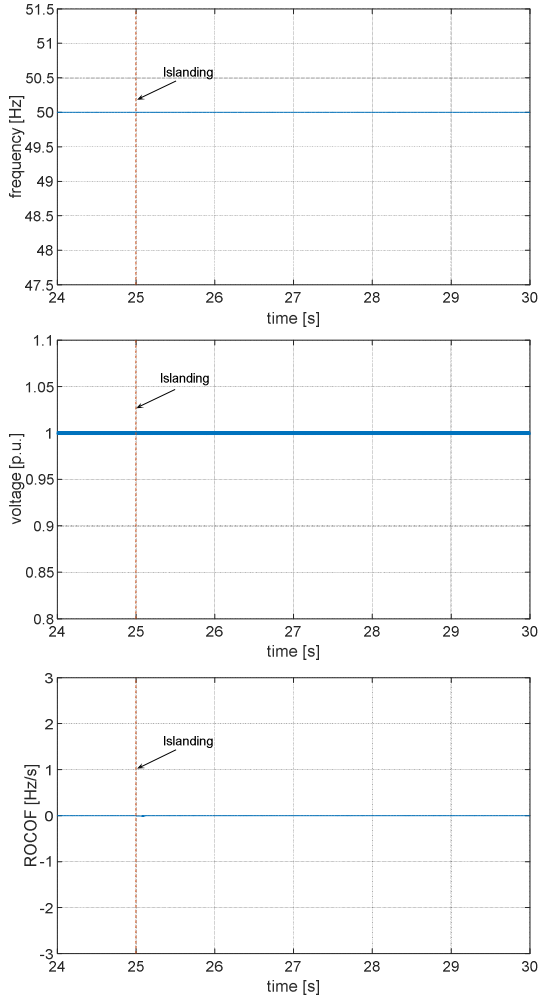

Fig. 7. The frequency, voltage magnitude and the ROCOF index when islanding occurs at time 25.0 s

The top most graph in Fig. 7 depicts the frequency. This is obtained by low pass filtering the output of the PLL component. The cut off frequency of the filter was 25 Hz. The graph below this respectively shows the voltage magnitude and the lower most graph represents the ROCOF index. The load was set to match the production of the utilized inverter based

DG unit. The DG unit was set to operate at its nominal power at unity power factor and the resonant frequency of the load was set to 50.0 Hz. As it can be seen from Fig. 7, the voltage magnitude, frequency and ROCOF index stay very close to their nominal values due to the non-existent power imbalance between production and consumption. Islanding could thus not be detected by these passive AIP methods under these circumstances.

In the following, the Q – f droop was enabled and the previous simulation was repeated. The multiplier constant k in (8) was set to 2.0. By utilizing the proposed AIP, islanding is detected in 433 ms as it can be seen from Fig. 8.

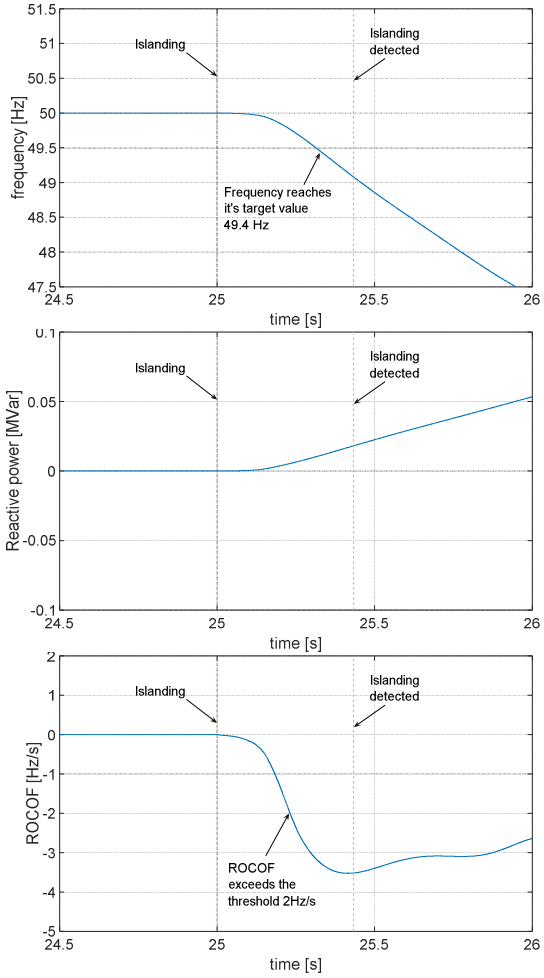

Fig. 8. The reactive power fed by the inverter, frequency of the studied circuit and the ROCOF index when islanding occurs at time 25.0 s.

Starting from the top, the graphs in Fig. 8 represent frequency, the reactive power fed by the DG unit and the ROCOF index. One can observe from the graphs that reactive power fed by the DG unit causes the frequency to drift towards the UFP limit. The proposed protection function trips after the ROCOF index has remained over 2 Hz/s for 200ms while the frequency falls below the target frequency 49.4 Hz ($f_{tar,low}$ in Fig. 4). As it can be seen from Fig. 8, the utilization of ROCOF reduces the islanding detection time considerably in comparison to a case where islanding would only be detected by using the OUF thresholds 47.5 Hz < f < 51.5 Hz. Moreover, the required amount of reactive power fed by the inverter for detecting islanding is significantly lower when using the proposed method in comparison to the case where frequency would be drifted to 47.5 Hz by feeding reactive power. One can also observe from Fig. 8 that the AIP method does not cause disturbances to the grid during normal operating conditions as long as the frequency stays at nominal. This is a considerable benefit in comparison with most active AIP schemes which constantly inject perturbations to the grid.

The following case shown in Fig. 9 illustrates how the value of the multiplier constant k affects the performance of the proposed AIP scheme in three different scenarios. In the first scenario, there was only one inverter operating in parallel with the load, whereas, two inverters were connected in parallel in the second scenario and three inverters in the third scenario. The relay tripping time is displayed on the vertical axis of Fig. 9, whereas, the value of the constant k is shown on the horizontal axis.

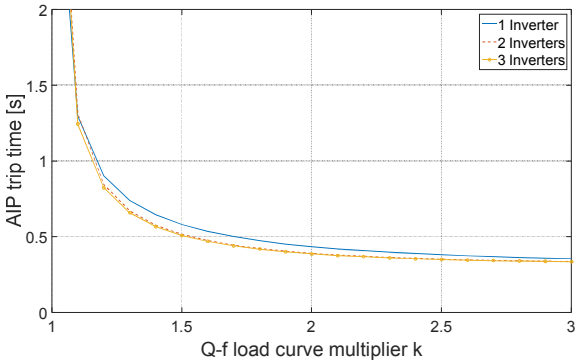

Fig. 9. The effect of the utilized multiplier k value on AIP performance

The figure is based on similar simulations as what is presented in Fig. 8 with the exception that the parameter k is varied from 1 to 3. That is, the quality factor of the load was set to 1.0, the resonant frequency of the load was 50.0 Hz and the consumption of the load was set to match with production of the inverter. One can observe from the graph that the islanding detection time increases considerably if the constant k is smaller than 1.5. On the other hand, one can also see that increasing the value of the multiplier from 2.5 brings no significant improvement to the performance of the AIP scheme. One can also see that the number of inverters operating in parallel hardly has any effect on the performance of the proposed AIP scheme. This shows that the AIP scheme is suitable for multi-inverter operation.

B. Power imbalance versus tripping time

The previously presented simulation cases analyzed the performance of the proposed AIP scheme only in the case when the consumption of the load matched with production of the DG unit. In the following, a tripping time map is shown in a coordinate system where the active power imbalance before the islanding is shown on the horizontal axis, whereas, the vertical axis represents the reactive power imbalance before the islanding event. The under- and overvoltage protection

thresholds were set to be 0.8 pu and 1.1 pu. The tripping delay for the voltage protection was set to 200ms. The innermost areas in Fig. 10 which are indicated by pink color refer to the power imbalance combinations where it took from 500 ms to 550 ms to detect the islanding. Similarly, the following areas surrounding these pink areas refer to operation times between 450ms to 500ms, 400ms to 450ms and 350ms to 300ms. All the other power imbalance conditions which are marked by the white color led to an operation time less than 300ms. The map was composed by making a series of simulations, where the active power imbalance was varied by changing the consumption of the load by 0.005 pu steps, whereas, the reactive power load was varied by 0.000625 pu steps. The inverter was always set to operate at nominal power and unity power factor. The constant k in (8) was kept at 2.0 in all of the simulations and the quality factor of the load was 1.0. The axes in Fig. 10 are given in per unit quantities. One can see from Fig. 10 that the proposed AIP scheme is able to detect islanding within 300 ms in most cases. The detection of islanding only took longer than 300 ms in cases where the reactive power imbalance was approximately within ±1 percent of the active power fed by the inverter.

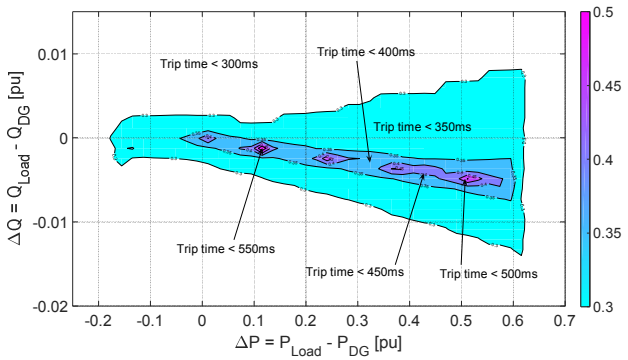

Fig. 10. A tripping time map in a ΔP versus ΔQ coordinate system

The undervoltage protection (UVP) threshold used in the previous simulations was 0.8 pu. However, if the utilized grid code requires DG units to have low voltage ride through (LVRT) capability, the UVP has to be set to allow the LVRT. In the following, the UVP settings were changed so that they were in line with the grid code of the Finnish transmission system operator Fingrid [13]. The UVP settings were given as a simplified 6 step curve which was in line with the LVRT requirement curve meant for generating units whose rated capacity is between 0.5 MW and 10 MW. This is illustrated in Fig. 11. Now, the same procedure that was used for composing Fig. 10 was used for obtaining the tripping map in the case where the UVP settings were those shown in Fig. 11. The obtained tripping map is shown in Fig. 12. The active power consumption of the load was varied by 0.05 pu steps, whereas, the reactive power consumption of the load was varied by 0.00125 pu steps. As it can be seen from Fig. 12, the performance of the AIP method degraded due to the change in UVP settings. That is, the areas where it took more than 300ms increased significantly. However, the islanding detection times were still always considerably faster than the 2.0s detection time requirement in [1].

When looking at Fig. 10, one can see that the UVP threshold 0.8 pu caused the regions where it took more than 300 ms to detect islanding to be cut when the ΔP was approximately larger than 0.62 pu. This is because voltage was always less than 0.8 pu above this ΔP value. However, in Fig. 12 the UVP threshold was not even reached. That is, more simulations where the value of ΔP was increased further would have been needed for reaching the UVP limit due to the LVRT compatible UVP settings. The regions where it took more than 300ms to detect islanding would thus extend even further than what is shown in Fig. 12.

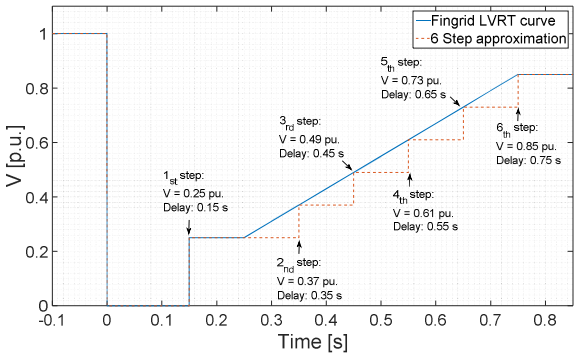

Fig. 11. The LVRT compatible UVP settings used for obtaining the tripping map shown in Fig. 12.

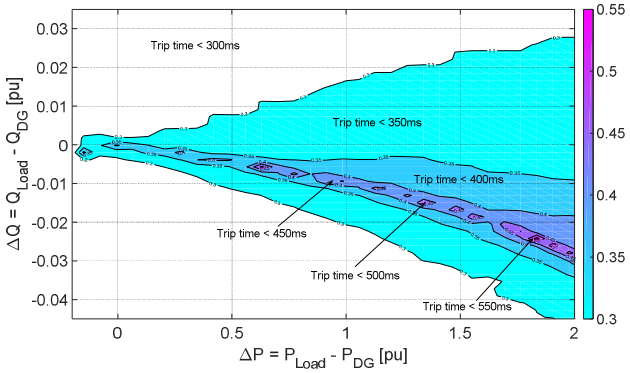

Fig. 12. The tripping time map of the proposed method when the UVP settings were changed to be LVRT compatible

It is noteworthy that some grid codes may require DG units to support the power system during LVRT by injecting reactive power. If this is required, additional coordination logic is needed between the LVRT support and AIP. This type of logic is needed for such a case where a voltage dip occurs while the frequency is greater than nominal, and the grid code requires DG units to support the system by injecting reactive power. In such case, the DG unit should feed reactive power for supporting the system while the AIP method orders the DG unit to absorb reactive power. This conflict could be avoided by making a logic which would order the AIP method to inject reactive power when voltage drops below a predefined value and thereby aim to reach the negative ROCOF threshold instead of the positive ROCOF threshold. Another noteworthy issue is that some grid codes may require DG units to operate

at non-unity power factor for regulating local voltage. If DG units equipped by this AIP scheme are required to operate at non-unity power factor, some amount of reactive power capacity should be reserved for the proposed AIP scheme.

C. The stability of the proposed AIP scheme

In the following, the fault branch depicted in Fig. 5 was connected to the circuit for testing the stability of the proposed method. The external grid fault was set to occur at time 25.0 s and last for 500 ms. The UVP was disabled. This simulation case is shown in Fig. 13.

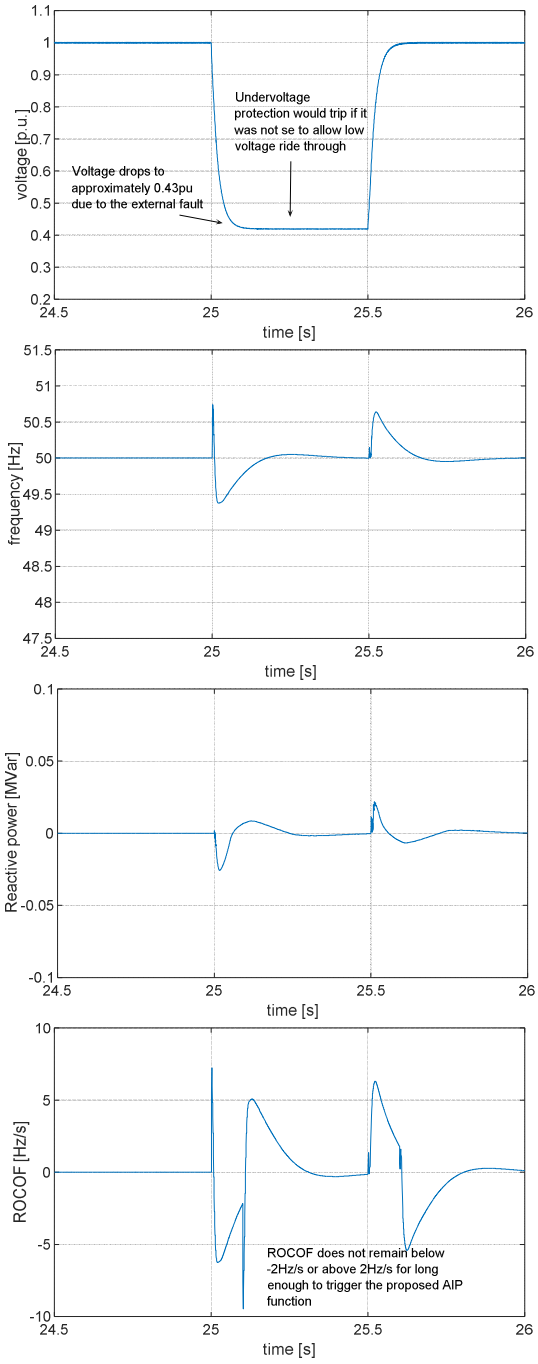

Fig. 13. Voltage, frequency, reactive power and ROCOF when a 500ms lasting external fault occurs

After the voltage dip, it takes approximately 150 ms for the PLL to synchronize to the network voltage. During this time, there are uncontrolled deviations in the reactive power output of the inverter. After proper synchronization, the reactive power is controlled again by the current q – component control of the inverter. This phenomenon is thus not caused by the Q–f droop, that is, the inverter would behave in a very similar manner even though the Q–f droop was disabled. The measured ROCOF oscillates significantly due to the sharp changes in frequency. However, the ROCOF does not stay above the upper threshold 2 Hz/s or below the lower threshold -2 Hz/s long enough to trigger the AIP function. Moreover, the additional frequency checking criterion which was illustrated in Fig. 4 also reduces the risk of unwanted tripping. Thus, the method does not trip the DG unit unintentionally due to the external grid fault.

The braking chopper in the DC link is activated during the fault once the DC link voltage rises to its upper limit 1250 V_{DC}. The DC link voltage rises during the fault because the inverter is not able to feed all the generated power to the network during the voltage dip as it can be seen from Fig. 14.

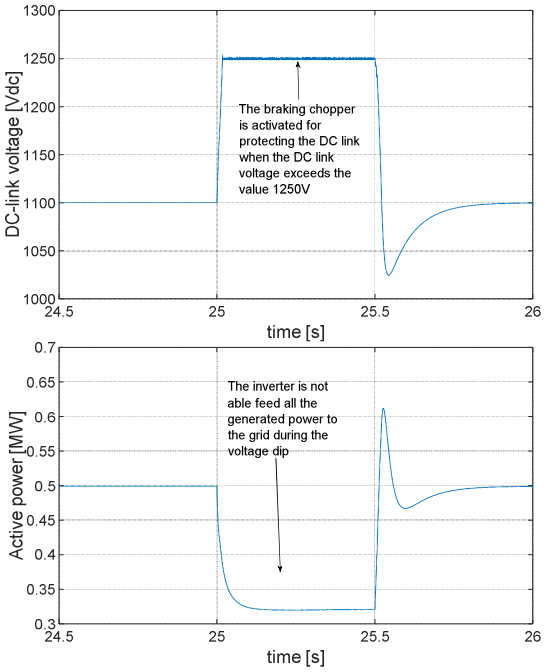

Fig. 14. Active power fed by inverter and the DC link voltage during the 500ms lasting external fault

The previous simulation case showed that a symmetric three phase fault did not cause major difficulties for the proposed AIP scheme. However, unsymmetrical faults may cause the frequency detected by the PLL to fluctuate considerably more than in symmetrical faults. This issue is demonstrated in the following simulation case which is shown in Fig. 15. At time 25.0 s a two phase short circuit lasting for 0.15 s occurs while the system is not islanded. This causes the frequency detected by the PLL to oscillate, which in turn causes the Q-f droop to respond accordingly by ordering the DG unit to feed/absorb reactive power. However, due to the rate limited reactive

power reference, the injected disturbance is reduced. The ROCOF index oscillates largely but there is no danger of nuisance tripping because the frequency does not deviate even close to its target value.

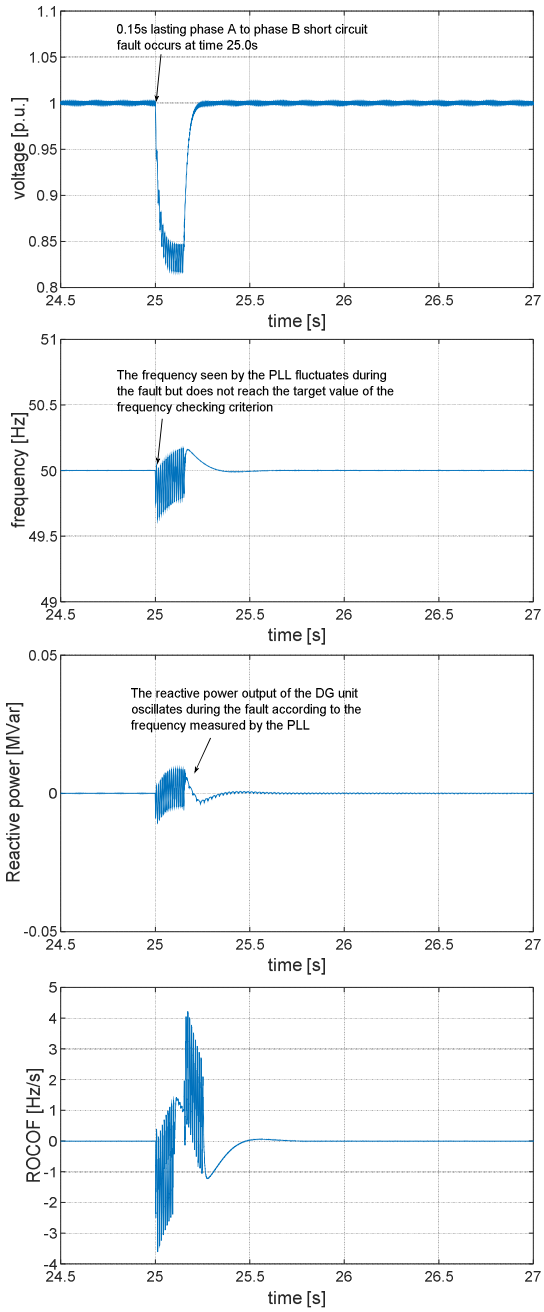

Fig. 15. Voltage, frequency, reactive power fed by the DG unit and the ROCOF index when a 0.15s lasting phase A to B short circuit fault occurs.

The following simulation case analyses the stability of the proposed protection scheme when a large load is switched on for a one second period of time. The parameters of the RLC load shown in Fig. 5 are selected so that the nominal apparent power of the loads is 10 MVA. Three different scenarios are simulated with three different power factors of the load. The load was initially switched off, and at time 25.0 s, the load is switched on for a one second period after which it is disconnected again. The voltage, frequency and ROCOF during these load switching cases are shown in Fig. 16. It can be seen that large oscillations in the measured ROCOF occur especially when the load is switched on at time 25 s. However, these oscillations are short lasting and they do not cause unwanted tripping. Moreover, the frequency target criterion illustrated in Fig. 4 is not fulfilled either, that is, frequency does not fall below 49.4 Hz or above 50.6 Hz.

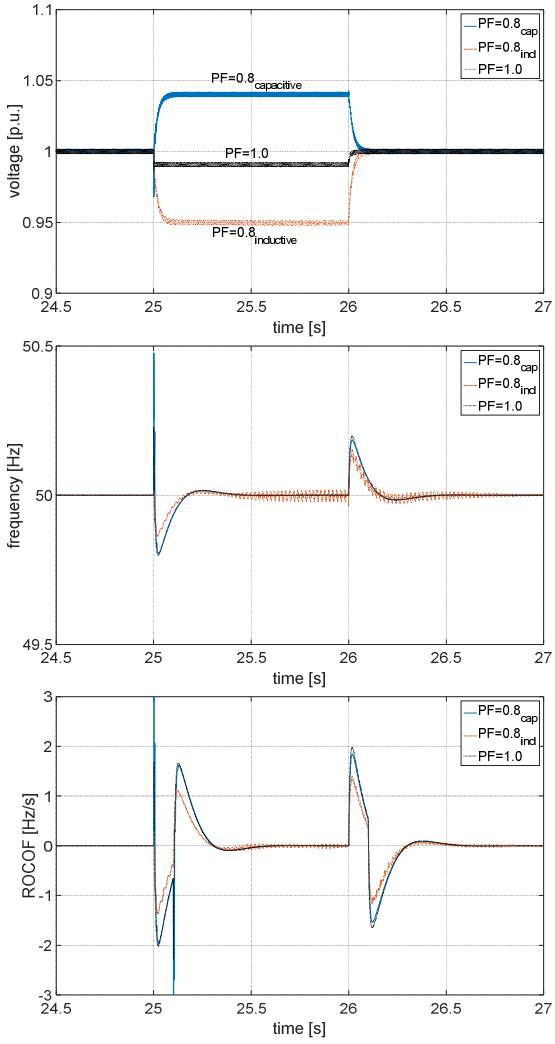

Fig. 16. Voltage frequency and ROCOF when a 10MVA rated load is switched on at time 25.0 s and off at time 26.0 s

V. Conclusions

This paper presents an AIP method based on the combination of a dedicated Q-f droop, ROCOF function and frequency checking. The proposed method provides secure and rapid islanding detection while having a minor impact on the grid during normal operating conditions. The method is especially advantageous if the utilized frequency protection thresholds specify a large normal operation frequency variation range for DG units, which is typical in Europe. Another benefit of this method is that no continuous pulse is being injected when frequency is at its nominal value. The fact that no continuous pulse is being injected makes the method inherently suitable for multi inverter operation. Due to the rate

limitation of the reactive power reference that is used in the proposed method, the reactive power injection is reduced in comparison to traditional Q-f droop based AIP.

VI. References

[1] *IEEE Std. for Interconnecting Distributed Resources with Electric Power Systems*, IEEE Standard 1547, 2003.

[2] P. Mahat, Z. Chen and B. Bak-Jensen, "Review of Islanding Detection Methods for Distributed Generation" *in Proc. DRPT 2008*, pp. 2743-2748

[3] R. Theodorescu, M. Liserre and P. Rodriquez, *Grid Converters for Photovoltaic and Wind Power Systems*, West-Sussex, UK, Wiley

[4] Y. Jin, Q. Song and W. Liu, "Anti-islanding Protection for Distributed Generation Systems Based on Reactive Power Drift", *in Proc. 2009 IEEE Industrial Electronics conf., pp. 3970-3975*

[5] H. H. Zeineldin, "A Q-f Droop Curve for Facilitating Islanding Detection of inverter-based Distributed Generation", *IEEE Trans. Power Electron.,* vol. 24, pp. 665-673, March 2009

[6] ENTSO-E Network code for "Requirements for grid connection applicable to all generators", March 2013

[7] J. Zhang, D. Xu, G. Shen, Y. Zhu, N. He and J. Ma, "An Improved Islanding Detection Method for a Grid-Connected Inverter with Intermittent Bilateral Reactive Power Variation" *IEEE Trans. Power Electron.,* vol 28, pp. 268-278, January 2013

[8] Y. Zhu, D. Xu, N. He, J. Ma, J. Zhang, Y. Zhang, G. Shen and C. Hu, "A novel RPV (Reactive-Power-Variation) Antiislanding method based on adapted reactive power perturbation," *IEEE Trans. Power Electron.*, vol. 28, pp. 4998-5012, Nov. 2013.

[9] X. Chen and Y. Li, "A Nondestructive Islanding Detection Method Based on Adaptive and Periodic Disturbance on Reactive Power Output of Inverter-Based Distributed Generation", *Journal of Applied Mathematics*, vol. 2014, pp. 1-11, July 2014

[10] A. Woyte, R. Belmans and J. Nijs, "Testing the Islanding Protection Function of Photovoltaic Inverters"*, IEEE Trans. Energy Convers.,* vol. 18, pp. 157-162, March 2003

[11] W. Freitas, W. Xu, C. M. Affonso and Z. Haung, "Comparative analysis between ROCOF and vector surge relays for distributed generation applications", *IEEE Trans. Power Del.*, vol. 20, pp. 1315-1324, Apr. 2005

[12] A. S. Mäkinen and H. Tuusa, "Impact of strength of fault current path on the operation of decoupled double synchronous reference frame – phase locked loop", in *Proc. ICREPQ'13*

[13] Fingrid Plc. (Sep. 2013). Specifications for the Operational Performance of Power Generating Facilities VJV2013. [Online]. http://www.fingrid.fi/en/customers/Customer%20attachments/Connection/2013/Specifications%20for%20the%20Operational%20Performance%20of%20Power%20Generating%20Facilities%20VJV2013.pdf

VII. Biographies

Ontrei Raipala received his M.Sc. degree from Tampere University of technology in 2009. He is currently a PhD student at the department of electrical engineering in Tampere University of technology. His research interests include integration of DG, real-time simulation and distribution network protection issues.

Anssi Mäkinen received his M.Sc. degree from Tampere University of technology in 2008. He is currently a PhD student at the department of electrical engineering in Tampere University of technology. His research interests include control systems and fault ride through behavior of wind turbines.

Sami Repo received his M.Sc. and Dr.Tech. degrees in Electrical Engineering from Tampere University of Technology in 1996 and 2001 respectively. At present he is a Professor at the Department of Electrical Engineering of Tampere University of Technology. His main interest is the management of active distribution network including distributed energy resources.

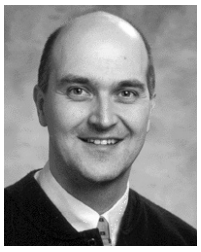

Pertti Järventausta received his M.Sc. degree in Electrical Engineering from Tampere University of Technology in 1990 and his Dr.Tech. degree in Electrical Engineering from Lappeenranta University of Technology in 1995. At present he is a professor at the Department of Electrical Engineering of Tampere University of Technology. The main interest focuses on the electricity distribution and electricity markets.

Tampereen teknillinen yliopisto
PL 527
33101 Tampere

Tampere University of Technology
P.O.B. 527
FI-33101 Tampere, Finland

ISBN 978-952-15-4104-9
ISSN 1459-2045